

DOCUMENTATION REPORT

**Development and Application of an Integrated Hydrologic Model
to study the Effects of Climate Change
on the Chuitna Watershed, Alaska**



**By
Robert H. Prucha, PhD, PE**

Integrated Hydro Systems, LLC, P.O. Box 3375, Boulder CO 80307



And

Jason Leppi, MS, Stephanie McAfee, PhD and Wendy Loya, PhD

The Wilderness Society, 705 Christensen Dr., Anchorage AK 99501

April 2012

DISCLAIMER STATEMENT

This report was prepared under a cooperative agreement with the U.S. Fish and Wildlife Service, an agency of the United States Government. Neither the United States Government nor the USFWS make any warranty, express or implied, or assumes any legal liability or responsibility for use, or the results of such use of any information contained herein. The views and opinions of authors expressed in this document do not necessarily state or reflect those of the United States Government or the USFWS.

Table of Contents

Table of Contents	iii
List of Tables	v
List of Figures	v
1.0 Introduction	1-8
1.1 Study Objectives	1-9
1.2 Summary Report Available.....	1-9
1.3 General Approach	1-9
1.3.1 Study Area	1-11
1.3.2 General Approach and Report Organization.....	1-11
2.0 Characterization of System Hydrology.....	2-1
2.1 Data Types and Sources.....	2-1
2.2 GIS/database Design.....	2-3
2.3 Topography/DOQQ	2-1
2.4 Geology.....	2-5
2.4.1 Faults and Synclines and Tectonic Setting	2-5
2.4.2 Stratigraphy.....	2-9
2.4.3 Soil Distribution.....	2-11
2.4.4 Surface geology	2-14
2.4.5 Subsurface Geology	2-17
2.5 Hydrology	2-24
2.5.1 Climate Data	2-24
2.5.1.1 Precipitation Data.....	2-24
2.5.1.2 Snow Course Data.....	2-31
2.5.1.3 Air Temperature.....	2-31
2.5.1.4 Reference Evapotranspiration	2-31
2.5.2 Surface Water.....	2-35
2.5.2.1 Watershed and Stream Drainage System	2-35
2.5.2.2 Surface Water Bodies/Wetland Areas	2-37
2.5.2.3 Stream Flow Data	2-39
2.5.3 Groundwater	2-42
2.5.3.1 Groundwater Aquifers	2-42
2.5.3.2 Subsurface Hydraulic Properties.....	2-43
2.5.3.3 Springs/Seeps.....	2-44
2.5.3.4 Groundwater wells.....	2-45
2.5.3.5 Groundwater Depths and Elevations	2-45
2.6 Vegetation	2-50
3.0 Conceptual Integrated Hydrologic Flow Model	3-1
3.1 Conceptual Flow Models	3-1
3.1.1 Snowmelt Conceptual Flow Model	3-2
3.1.2 Unsaturated Zone Conceptual Flow Model	3-2
3.1.3 Hillslope Conceptual Flow Model.....	3-3
3.1.4 Watershed-scale Conceptual Flow Model	3-5

3.2	Summary of Data Gaps	3-7
4.0	Integrated Hydrologic Model Development	4-10
4.1	Integrated Hydrologic Numerical Flow Code.....	4-10
4.1.1	Code Selection	4-10
4.1.2	MIKE SHE/MIKE 11 Capabilities	4-12
4.2	Numerical Model Development.....	4-14
4.2.1	Model boundary and grid discretization	4-14
4.2.2	Unsaturated Zone Flow	4-15
4.2.3	Saturated Zone Flow	4-16
4.2.4	Overland Flow	4-17
4.2.5	Streamflow	4-18
4.2.6	Climate.....	4-26
4.2.6.1	Precipitation and Air Temperature.....	4-26
4.2.6.2	Snowmelt	4-26
4.2.6.3	Reference Evapotranspiration and Plant Transpiration	4-27
5.0	Integrated Hydrologic Model Calibration.....	5-29
5.1	Available Calibration Data	5-29
5.2	Calibration Approach.....	5-30
5.3	Calibration Results (1980 to 2000).....	5-32
5.3.1	Comparison of Simulated and Observed Data.....	5-32
5.3.2	Other Simulated Hydrologic Responses - Basecase	5-42
6.0	Future Scenario Simulations	6-1
6.1	Definition of Future Scenarios.....	6-1
6.2	Results of Future Scenario Simulations.....	6-3
6.2.1.1	Changes in Snowpack.....	6-3
6.2.1.2	Changes in the Unsaturated Zone	6-7
6.2.1.3	Changes in the Saturated Zone	6-13
6.2.1.4	Changes in Surface Flows.....	6-15
7.0	Summary and Conclusions	7-1
8.0	References.....	8-1
	Appendix A - USDA National Resources Conservation Service (Soils Dataset Download Information).....	1
	Appendix B - Long-term Monthly NARR Precipitation Data Comparison to Available Site Data.....	1
	Appendix C - Additional Hydrologic Response of Basecase Model.....	1

List of Tables

<i>Table 2-1. Summary Statistics of Annual Precipitation by Elevation.....</i>	2-29
<i>Table 2-2. Summary of Seasonal Event Intensity, Precipitation and Duration.....</i>	2-29
<i>Table 2-3. REFET FAO56PM RET Values by Elevation (in/yr)</i>	2-33
<i>Table 2-4. Drainage Area.....</i>	2-35
<i>Table 2-5. Available days of average daily streamflow at gaged streams from 1981 to 2006.</i>	2-40
<i>Table 2-6. Summary of Hydraulic Properties for Hydrostratigraphic Units.....</i>	2-43
<i>Table 2-7. Areal coverage of vegetation types</i>	2-50
<i>Table 4-1. Summary of Soil Hydraulic Properties (Basecase Model).....</i>	4-15
<i>Table 4-2. Lengths (meters) of Simulated Streams.....</i>	4-22
<i>Table 4-3. Simulated Stream Leakage Values (Basecase Model).....</i>	4-25
<i>Table 4-4. Summary of Model Climate Input Parameters (Basecase)</i>	4-27
<i>Table 4-5. Summary of Vegetation Parameters.....</i>	4-28
<i>Table 5-1. Summary of Average Annual Water Balance Components - Basecase</i>	5-46

List of Figures

<i>Figure 1-1. Location of Proposed Chuitna Coal Mine, Alaska.....</i>	1-10
<i>Figure 1-2. Study Area and Basemap Features for Chuitna River watershed</i>	1-14
<i>Figure 1-3. General Approach for Model Development and Application.....</i>	1-15
<i>Figure 2-1. General Approach to Convert Data into GIS, GIS design and Basic GIS Analyses.</i>	2-4
<i>Figure 2-2. ASTER Topography (~ 23 m spatial resolution, and ~3 m vertical accuracy).....</i>	2-2
<i>Figure 2-3. 3-D Perspective of Watershed and Topography.....</i>	2-3
<i>Figure 2-4 High Resolution DOQQ of Mined part of watershed (http://edcns17.cr.usgs.gov/NewEarthExplorer/)</i>	2-4
<i>Figure 2-5. Tectonic Setting - Bruin Bay and Clark Lake Faults.....</i>	2-6
<i>Figure 2-6. Faults mapped through the watershed.</i>	2-8
<i>Figure 2-7. Generalized Stratigraphy for Cook Inlet Basin and Chuitna Watershed.</i>	2-10
<i>Figure 2-8. Spatial Soil Distribution (U.S. Department of Agriculture, Natural Resources Conservation Service).....</i>	2-12
<i>Figure 2-9. Soil distribution of USDA-NRCS soil hydrologic types.....</i>	2-13
<i>Figure 2-10. Surficial Geology (digital GIS coverage).....</i>	2-15
<i>Figure 2-11. 3-dimensional View of Surface Geology and Structure draped over Surface Topography.</i>	2-16
<i>Figure 2-12. Isopachs of Regional Kenai Formation (Oil Well data) of Minable Coal Sequence (Layer 2)2-18</i>	
<i>Figure 2-13. Isopach of Quaternary (Unconsolidated) Glacial Deposits/Alluvium.....</i>	2-19
<i>Figure 2-14. Locations of N-S and E-W Sections Through the Chuitna Watershed.....</i>	2-20

Figure 2-15. Northwest-Southeast section through the proposed mine area.	2-21
Figure 2-16. West-East Surface Profiles (looking North).	2-23
Figure 2-17. Local Climate Stations (NARR, PacRim, NCDC locations, snow course locations).	2-25
Figure 2-18. Annual Precipitation (in/yr) NARR Dataset (2_1)	2-27
Figure 2-19. Distribution of Annual Precipitation (in/yr) based on NARR data and Lapse Rate.	2-28
Figure 2-20. Storm Characteristics (non-elevation adjusted NARR dataset at 2_1).	2-30
Figure 2-21. Average Monthly Air Temperatures – NARR data (point 21).	2-32
Figure 2-22. Average Daily Air Temperature, Net Radiation, Reference Evapotranspiration, Wind Speed and Precipitation (Example year 1980).	2-34
Figure 2-23. Sub-Watershed Scale Watersheds, Simulated Streams and Streamflow Gage Locations.	2-36
Figure 2-24. Surface Water Bodies (from USGS quadrangle, DOQQ inspection).	2-38
Figure 2-25. Long-Term Surface Water Daily Discharge (cfs) for gage (230, 180, 220, 110, 45).	2-41
Figure 2-26. Groundwater wells and simulated water levels (Arcadis, 2007). Yellow dots are historical wells, red are 2006.	2-46
Figure 2-27. Available Groundwater Depths for Quaternary Deposits (Wells in Alluvium and Glacial Deposits).	2-48
Figure 2-28. Modeled Vegetation Distribution	2-51
Figure 3-1. Conceptual Snowmelt Model.	3-1
Figure 3-2. Conceptual Flow Model – Unsaturated Zone	3-2
Figure 3-3. Conceptual Hillslope Flow Model.	3-4
Figure 3-4. Conceptual Watershed-scale Flow Model.	3-6
Figure 4-1. Comparison of Traditional Groundwater Model and a Fully Integrated Hydrologic Model. ..	4-11
Figure 4-2. Hydrologic Processes Simulated in the MIKE SHE/MIKE 11 Code.	4-13
Figure 4-3. Saturated Zone Hydraulic Conductivity Values (Unconsolidated Deposits = Layer 1 – Basecase Model).	4-19
Figure 4-4. Selected Stream Profiles.	4-23
Figure 4-5. Cross-Sections.	4-24
Figure 4-6. Leaf Area Index and Root Depth.	4-28
Figure 5-1. Comparison of Simulated and Observed Snowmelt.	5-36
Figure 5-2. Comparison of Daily Simulated and Observed Streamflow – Chuitna - Gage 230 and Stream 2003 - Gage 180.	5-37
Figure 5-3. Comparison of Daily Simulated and Observed Streamflow – Lone Creek (2002) - Gage 220 and Stream 2004 - Gage 110.	5-38
Figure 5-4. Comparison of Simulated and Observed Streamflow – Stream 2003 at Gage 140 and Lone Creek (2002) at Gage 195.	5-39
Figure 5-5. Groundwater Residuals (m). Positive values indicate observed head > simulated head.	5-41
Figure 5-6. Sub-watershed Water Balance Areas	5-45
Figure 6-1. Climate Change Scenarios for 2080-2099 for Alaska (Christensen et al, 2007)	6-2

<i>Figure 6-2. The A1B scenario refers to a future where global population peaks mid-century, there is rapid economic growth and a balanced portfolio of energy technologies is rapidly adopted that includes fossil fuels and high efficiency technologies. (Climate Impacts Group, 2009)</i>	6-2
<i>Figure 6-3. Simulated Average Daily Snow Depth (mm SWE).</i>	6-4
<i>Figure 6-4. Simulated Baseline Snowpack (every 2 days).</i>	6-6
<i>Figure 6-5. Change in Average End Date and Reduction in Days of Snowpack.</i>	6-7
<i>Figure 6-6. Simulated Average Monthly Surface (Top 5 cm) Soil Moisture for Mine and Upper Chuitna Areas.</i>	6-9
<i>Figure 6-7. Simulated Soil Moisture at 1 cm and 1 m depth at Locations A and B (previous figure).</i>	6-10
<i>Figure 6-8. Average monthly Flow or Accumulation (Recharge, Baseflow, Overland flow, AET, Precipitation and Snow Storage) for Upper and Lower Chuitna sub-watersheds.</i>	6-11
<i>Figure 6-9. Simulated percent change in mean annual Actual Evapotranspiration (AET) for five climate change scenarios relative to the historical baseline, by sub-watershed.</i>	6-12
<i>Figure 6-10. Average Daily AET by month for the Basecase (1980 to 2000) and TmaxPmax Scenario (2080 to 2100) for the Upper Chuitna sub-watershed.</i>	6-12
<i>Figure 6-11. Change in Groundwater Recharge Relative to the Basecase</i>	6-13
<i>Figure 6-12. Upper Chuitna sub-watershed average monthly change in Recharge for climate scenarios on lower plot.</i>	6-14
<i>Figure 6-13. Change in Groundwater Baseflow to Streams Relative to the Basecase</i>	6-15
<i>Figure 6-14. Change in Overland Flow to Streams Relative to the Basecase</i>	6-16
<i>Figure 6-15. Annual and Seasonal Changes in Streamflow Relative to the Basecase.</i>	6-17
<i>Figure 6-16. Average Monthly Streamflow based on simulated flows every 2 hours at Gage 230 in Lower Chuitna.</i>	6-19
<i>Figure 6-17. Simulated Average Seasonal Change in Streamflow Relative to the Basecase by Sub-Watershed.</i>	6-20

List of Figures – Appendices

<i>Figure B-1. Comparison of NARR data to Local Data.</i>	B-1
<i>Figure C-1. Simulated Average of Annual Actual Evapotranspiration - 1980 to 2000 (mm/yr).</i>	C-2
<i>Figure C-2. Simulated Average of Annual Soil Evaporation - 1980 to 2000 (mm/yr).</i>	C-3
<i>Figure C-3. Simulated Average of Annual Plant Transpiration - 1980 to 2000 (mm/yr).</i>	C-4
<i>Figure C-4. Simulated Average of Annual Groundwater Recharge - 1980 to 2000 (mm/yr).</i>	C-5
<i>Figure C-5. Simulated Average of Annual Groundwater Baseflow (mm/yr) to Streams (1980 to 2000)</i> ...	C-6
<i>Figure C-6. Simulated Average of Annual Overland Flow (mm/yr) to Streams (1980 to 2000)</i>	C-7
<i>Figure C-7. Simulated Average Annual Snowpack (mm/yr).</i>	C-8

1.0 Introduction

The Chuitna (Chuit River) Watershed is located about 45 miles west of Anchorage on the northwestern side of Cook Inlet near the Native Village of Tyonek and the community of Beluga (Figure E-1). It is an important ecosystem that supports five species of Pacific Salmon, several species of resident fish and a variety of wildlife such as moose, brown and black bears, wolves, beavers, bald eagles and numerous other species of migratory birds. The watershed consists of a large network of nearly 200 miles of streams that drain about 150 square miles into Cook Inlet. Factors affecting streamflow within this ecosystem are complex and strongly influenced by seasonal changes in climate and dynamic interaction with the groundwater flow system. Groundwater flows are critical to salmon habitat because they cool surface waters in warm months and heat them in cold months. Salmon spawn, rear and overwinter in areas with groundwater upwelling or downwelling which provide oxygenated water at temperatures conducive to development and survival of eggs and juvenile fish (Groot and Margolis, 1991). Because of climate change associated impacts in Alaska, such as wetland drying, rapid glacial retreat, increased bark-beetle infestations and fires, concerns are mounting about similar impacts of climate change on these sensitive hydrologic systems that are fundamental to the integrity of the entire watershed ecosystem.

By the end of 2100, global climate models project that both air temperature and precipitation will increase significantly in southcentral Alaska. The magnitudes of projected changes however depend on many factors and vary seasonally. For example, air temperatures during winter periods are projected to increase between 4°C and 10°C, while precipitation may increase from 6% to greater than 50% over present day conditions based on global climate model results for a “moderate” greenhouse emissions scenario (Christensen et al., 2007). Projected changes in climate will translate into hydrologic changes through alteration of rain and snowfall timing and intensity, evapotranspiration and groundwater and surface flows.

Land-use changes are also expected to change the hydrology of the Chuitna watershed. In the 1960s, oil companies explored the Tyonek Formation of the Kenai Group within the lower watershed area for hydrocarbons. By the mid-1970s coal companies began exploring the extensive coal seams along the middle of the watershed, in the southern part of the Beluga Coal Fields. The PacRim Coal, LLC mining company (PacRim) is currently pursuing a permit to extract approximately 300 million tons of coal from what would be Alaska’s largest open-pit coal mine (~5,000 acres). Part of PacRim’s proposed plan involves removing about 11 miles of salmon spawning and rearing habitat during a 25-year mining operation. PacRim conducted local baseline characterizations of surface and groundwater hydrology around the proposed mine area, but has not yet develop an integrated understanding of how the surface and groundwater interact within the watershed. This is important because to fully understand how climate change or mining/mine reclamation impacts the system hydrology, especially downstream of the mine, the integrated hydrologic flow system must be well understood. While we do not

explore mining impacts in this investigation, our model provides an approach for such future analyses.

This report documents steps in the development and application of a fully-integrated, distributed-parameter, hydrologic code of the Chuitna Watershed to assess effects of climate change on system hydrology. Another report by Prucha et al, 2011 titled “Integrated Hydrologic Effects of Climate Change in the Chuitna Watershed, Alaska” summarizes key findings in this report.

1.1 Study Objectives

The primary objective of this study is to assess the range of hydrologic impacts within the Chuitna Watershed due to future climate changes predicted by current global climate modeling using an integrated hydrologic modeling tool. This research can also be used to understand how an integrated hydrologic model can be used to explore scenarios of climate change or land use change and the types of data that are needed to develop a site-specific model.

1.2 Summary Report Available

A summary of the work presented in this full documentation report is available. Please see:

Prucha, R.H., Leppi, J., McAfee, S., Loya, W., 2011. Integrated Hydrologic Effects Of Climate Change in the Chuitna Watershed, Alaska.

1.3 General Approach

Integrated Hydro Systems, LLC (IHS) in Boulder, Colorado was contracted by The Wilderness Society (TWS) in Anchorage, Alaska (www.wilderness.org) to assess current and future hydrologic conditions within the Chuitna Watershed for the United States Fish and Wildlife Service. IHS has considerable experience characterizing, conceptualizing and conducting mathematical modeling of natural and modified hydrologic flow systems impacted by development (www.integratedhydro.com).

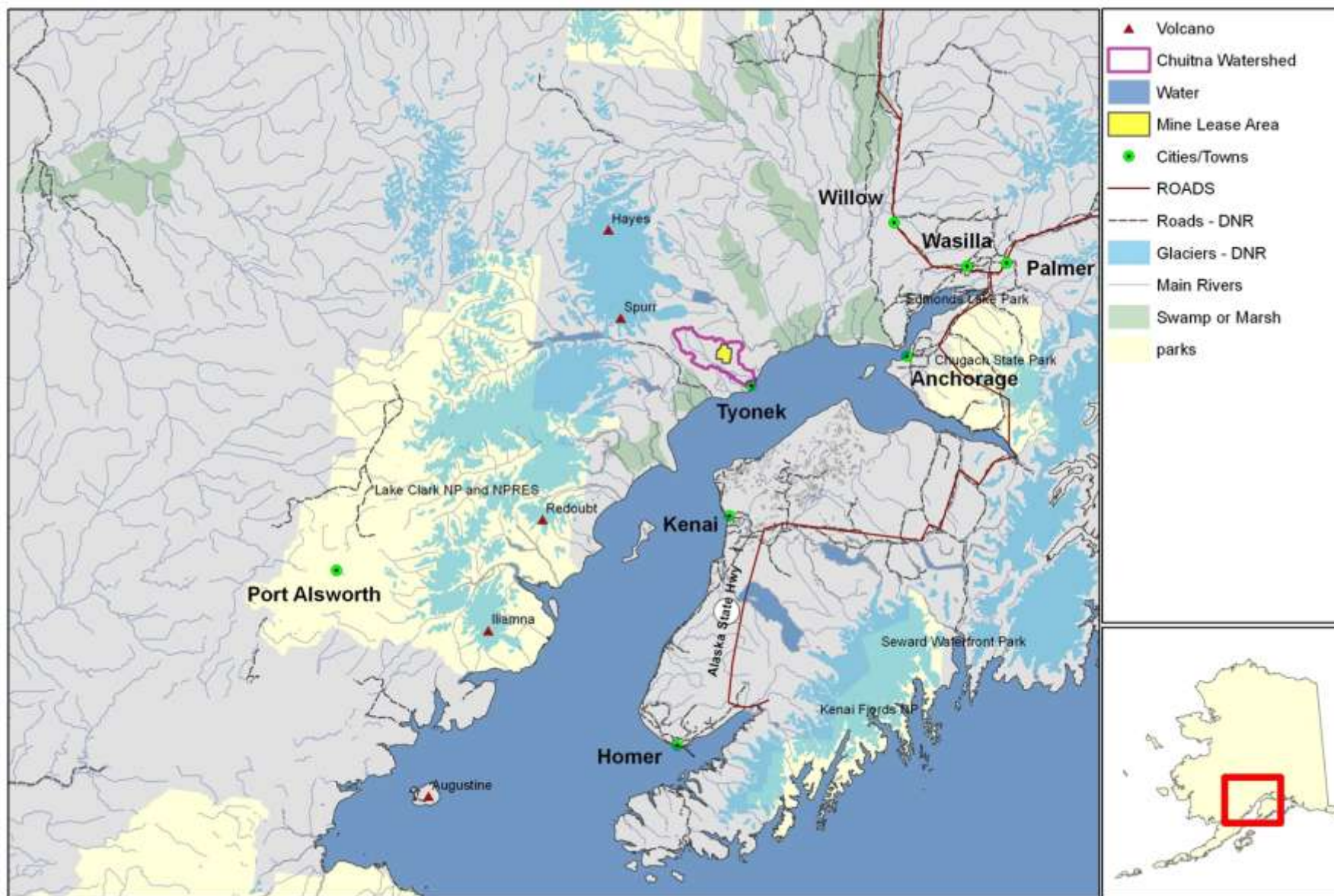


Figure 1-1. Location of Proposed Chuitna Coal Mine, Alaska.

1.3.1 Study Area

The entire Chuitna surface watershed area (“Chuitna Watershed”), shown on Figure 1-2 was selected as the study area for two reasons. Future mining may occur in the upper watershed and the modeling tool developed for the entire watershed could be used to evaluate land-use changes in this area, in addition to the proposed PacRim mining area (see purple line on Figure 1-2). The entire Chuitna Watershed was also selected because groundwater boundary conditions along the perimeter of smaller sub-watershed boundaries shown on Figure 1-2 would not be appropriate due to the significant slope of surface topography from northwest to southeast. For example, although surface water may be constrained to flow within the sub-watershed boundaries, groundwater flow is dictated by the slope and configuration of subsurface hydrostratigraphy, which may not coincide with surface topography. Eight sub-watersheds are also shown on the Figure 1-2 that are useful later in describing the hydrologic behavior in different areas of Chuitna Watershed.

1.3.2 General Approach and Report Organization

A general approach used to meet the study objectives is outlined on Figure 1-3. Developing the model predictions of hydrologic impacts due to future climate changes required several steps. These are briefly described here and references are provided to sections where the steps are described in more detail. The report is generally organized following these steps, with additional references to Appendices.

- Data Review - publically available data were obtained and reviewed (see Section 2.1). Much of this data is from studies conducted by PacRim, though additional information had to be obtained outside of the proposed mine area, for example in the upper Chuitna Watershed area.
- Characterization (Section 2.0) - To facilitate spatial analysis of the different available datasets over the Chuitna Watershed, available data were input into digital databases and linked to a geographical information system (GIS) described further in Section 2.2. Detailed characterizations, following industry standards (ASTM D5979-2002), are provided for key areas of the surface-subsurface integrated hydrologic system, including topography (Section 2.3), Geology (Section 2.4), Hydrology (Section 0) and Vegetation (Section 2.6). The characterization step involves first reviewing raw data, such as geologic information from a borehole, and then combining such information from multiple boreholes to develop system-wide interpretations of geologic conditions.
- Flow Conceptualization (Section 3.0) – The most important step in developing a successful mathematical model of an integrated hydrologic system is conceptualizing flow into, out of and within the system, and describing the processes that control these flows. Flows in an integrated hydrologic system like the Chuitna Watershed are complex; the subsurface geology is highly faulted and multiple aquifers communicate

with each other and with surface waters in a complex way over time due to seasonal changes in climate. One cannot hope to accurately define flows conditions within the system over time, especially given the sparseness of data, much of which is localized around the proposed PacRim mine in the mid-watershed area. However, attempts are made to describe the important conceptual flow processes, and flows within the system in Section 3.1 following industry standards (ASTM D5979 – 2002, Kolm, 1993). It is commonly accepted in the hydrologic community that the chief source of uncertainty in hydrologic models comes from inadequate description of conceptual flow models (Neuman and Weiranga, 2003). As a result, gaps in data and implications to the conceptual flow model are also described in Section 3.2.

- Numerical Model Development (Section 4.0) – The numerical (or mathematical) integrated flow model of the Chuitna Watershed is developed based on the conceptual flow model. Details of the software code used to develop the integrated flow model are described in Section 4.1, while details of the actual model processes, inputs, boundary conditions and assumptions are described in detail in Section 4.2. Key processes in the integrated flow model include:
 - Snowmelt using a modified degree-day snowmelt model,
 - Full 1-dimensional unsaturated zone flow using Richard’s equation,
 - Actual Evapotranspiration (AET) is calculated using the Kristensen and Jensen method based on a Reference Evapotranspiration (RET, see Section 2.5.1.4), soil evaporation and plant transpiration as a function of time-varying leaf area index and root depth,
 - Streamflow using a fully hydrodynamic flow equations that allow for wave propagation and backwater effects,
 - Fully 3-dimensional groundwater flow, and
 - Two-dimensional diffusive-wave overland flow to streams.
- Model Calibration (Section 5.0) – Once developed, the numerical model is calibrated against historical data to demonstrate its ability to simulate historical hydrologic conditions. The process of calibration is iterative and involved several steps. Initial model simulations are run using a specific set of model input parameter values and external boundary conditions, including climate conditions with time. Simulated output is then compared against observed data, such as streamflow over time at different gage locations, and if the simulated flows do not reproduce observed flows within a target range, model inputs are adjusted and the model rerun. Although somewhat subjective, the model is deemed calibrated when simulated results compare well with observed data. The calibrated model represents the Basecase mode, or baseline conditions. Basecase is used interchangeably in this report with baseline.
- Future Scenario Simulations (Section 6.0) – Five future climate change scenarios were defined based on the average seasonal climate changes determined from 21 global climate models (GCM) (IPCC 2007) for the A1B mid-level CO2 emissions

scenario for the period 2080 to 2100. Results of the climate scenario simulations were compared against the Basecase to determine a relative change in the hydrologic conditions, rather than attempting to predict the new state of the system (i.e., streamflow, or groundwater levels at a specific point in the system). The model developed in this study is more appropriate for predicting the relative change in state rather than predicting the actual state of the system. The predicted state of the system is sensitive to the accuracy of various model input (i.e., surface topography, subsurface information) which are limited.

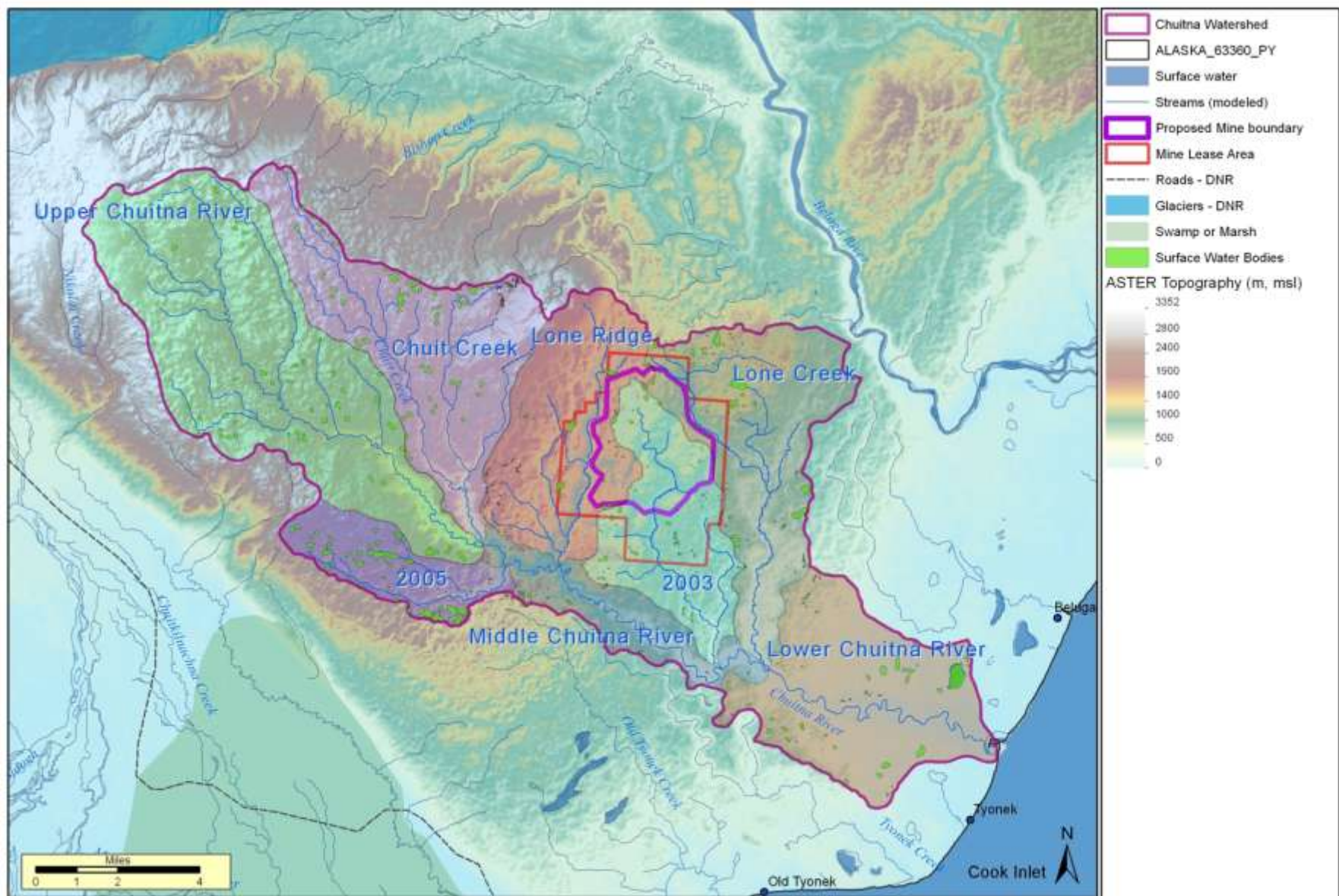


Figure 1-2. Study Area and Basemap Features for Chuitna River watershed

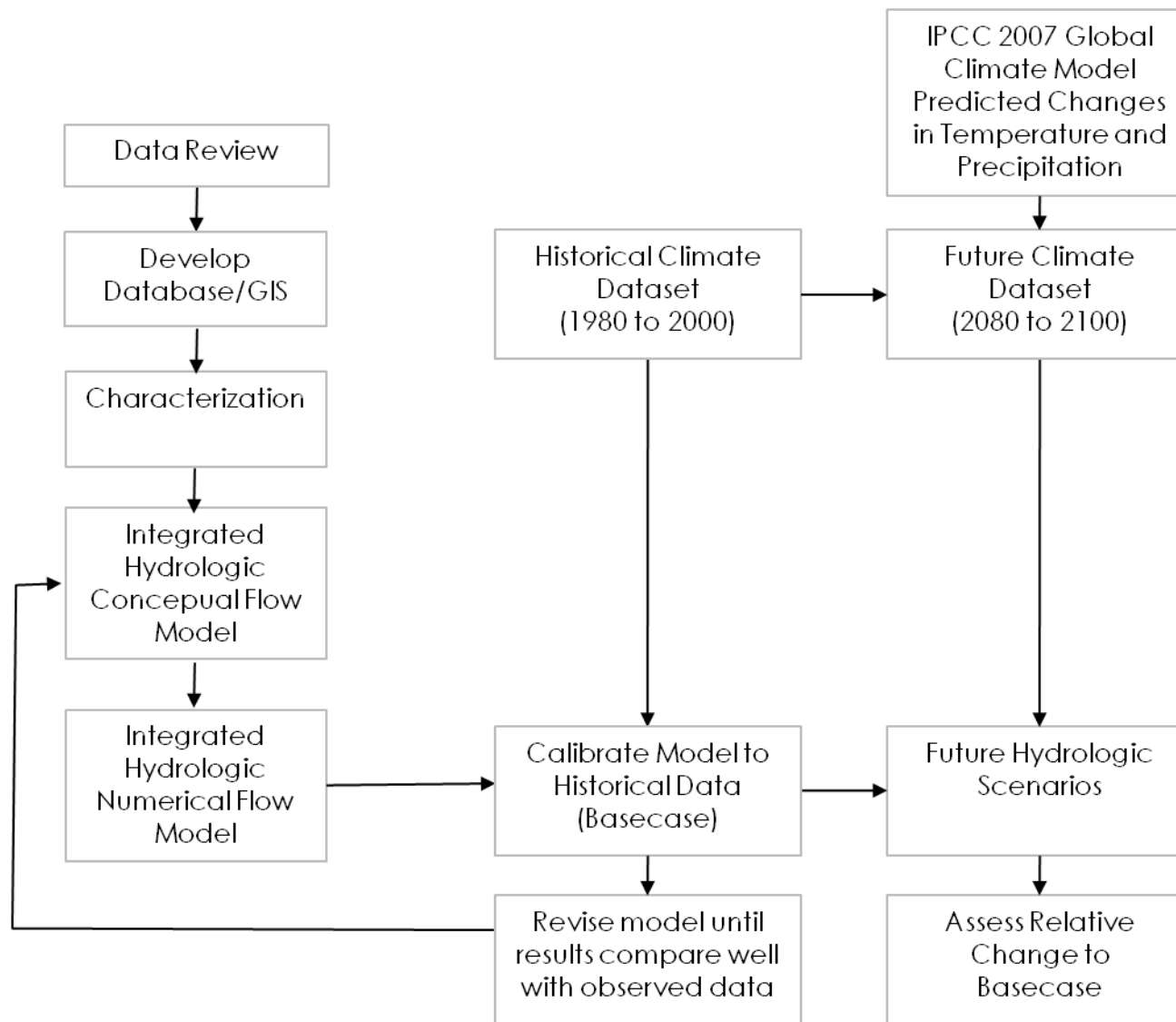


Figure 1-3. General Approach for Model Development and Application

2.0 Characterization of System Hydrology

The characterization of system hydrology is a critical step required in developing sound conceptual and numerical flow models. For an integrated hydrologic flow model, both the surface and subsurface flow systems must be characterized. Characterization generally involves two key steps. First raw data are analyzed; for spatial analyses, this is typically done using GIS tools and techniques, and for temporal analyses, data is often plotted in time using standard spreadsheet software such as Microsoft Excel. The use of GIS provides a powerful way to spatially correlate different types of data (i.e., mapped surface geology compared to geologic information obtained from boreholes) in a consistent coordinate system. The second step in characterization involves developing interpretations based on analysis of the raw data. These steps are standard practice in hydrogeology as defined by ASTM D5979 (2002) for characterizing groundwater systems, but they are also applicable to fully integrated hydrologic systems.

Surface and subsurface flow systems are characterized in this section. Data types relevant to developing a fully integrated hydrologic flow model and the source of these data are described first in Section 2.1. A brief description of the GIS and databases developed for this study is provided next in Section 2.2. The data and characterizations of both the surface and subsurface flow systems are described in Sections 2.3 through 2.6.

2.1 Data Types and Sources

Only data useful in the development of the integrated numerical model are described in this section. A more detailed description is presented the description of the numerical model input in Section 4.0.

Much of the data available within the Chuitna Watershed is from PacRim studies and only within the proposed PacRim mine lease area or in the eastern-central watershed area (see lease area on Figure 1-2). Data outside this area were obtained from mainly through GIS web-portals online or other studies conducted by the Alaska DNR. The main sources of data are summarized below by type. Though attempts were made to obtain several specific digital datasets from PacRim (i.e., high-resolution surveyed topography, their geologic model and lithologic information from more than 430 geologic boreholes), they chose not to provide these for this study. As a result, the characterization and conceptual understanding of the subsurface and the ability to simulate surface flows at a high-level of accuracy is limited in this study. This also prevents direct comparison of results from the integrated flow model developed here against results from groundwater flow modeling by a mine consultant (Arcadis, 2007). Despite these data limitations, sufficient data exist across the Chuitna Watershed to allow development of an integrated numerical flow model.

Key PacRim Reports reviewed:

- Reports generally found here: <http://www.chuitnaseis.com/project-support-documents.html>
- <http://dnr.alaska.gov/mlw/mining/largemine/chuitna/index.htm>

Hydrologic Data

- Arcadis, 2007. Chuitna Coal Project Addendum D12-B Groundwater Model for Mine Engineers, Inc.
- Riverside (Riverside Technology, Inc.), 2006. Chuitna Coal Project Hydrology Component Baseline Report Historical Data Summary. June 2006.
- Riverside, 2007. Chuitna Coal Project Hydrology Component Baseline Report Historical Data Summary. Including Appendices A through D. March 2007.
- Riverside 2010. Chuitna Coal Project Groundwater Baseline Report – Draft 1982 through 2010. April 2010.
- Oasis Environmental Inc. (Oasis) 2010. Investigation of Seeps and Hydrologic Exchange between Surface Waters and the Hyporheic Zone for Selected Sections of Streams 2002 and 2004. Draft Rev. 5 dated February 2, 2010.

Climate Data

- McVehil-Monnet Associates, Inc. 2006. Site Climatology for the Chuitna Coal Project prepared for: Mine Engineers, Inc., June 2006.
- NOAA <http://www.ncdc.noaa.gov/oa/ncdc.html>
- NARR dataset: <http://www.esrl.noaa.gov/psd/data/gridded/data.narr.html>

Geologic Data

- Mine Engineers, Inc., 2007. Geology Report Chuitna Coal Project, Beluga, Alaska, May 2007. Includes Appendices.
- Alaska DNR – oil wells/lithology.
- Alaska Department of Natural Resources, Division of Geological and Geophysical Surveys (<http://www.dggs.dnr.state.ak.us/index.php>)
- USGS geologic mapping: <http://pubs.usgs.gov/of/2009/1108/>

Soils

- Chien-Lu Ping, Brown, Terry, 2007. Soil Resources of Chuitna Coal Mine, Alaska, Report to DRven, Anchorage, Alaska

- NRCS-USDA: <http://soildatamart.nrcs.usda.gov/>

Vegetation

- HDR Alaska, Inc., 2007. Chuitna Coal Project Baseline Report for Vegetation and Wetlands Prepared for Mine Engineers, Inc. May 2007.
- Kenai – GIS <http://www.borough.kenai.ak.us/gisdept/>

2.2 GIS/database Design

Figure 2-1 shows the general approach used to convert available data into a GIS project file and basic GIS analyses. The GIS for the Chuitna Watershed was prepared using ESRI's latest version of ArcGIS version 10 (May 2010). An ArcMAP project document file was created and allows definition of a hierarchical directory structures, similar to windows explorer.

Most data used in this study were obtained from digital reports, typically in digital tables. The coordinate system used in this study is NAD83, UTM Z6N. These data were imported into an Excel spreadsheet and then imported into the GIS project file. Other data were also available in the form of GIS files (i.e., polygons, lines, or points) and were directly incorporated into the GIS. In several cases, spatial data found on hardcopy maps were scanned, imported into GIS and then georeferenced so that the information could be converted into digital GIS coverages. Once the GIS was created, basic analyses were performed on the data, such as calculating areas, distances, cross-sections, or interpolations on for example geologic surfaces. Model input was also created using the GIS.

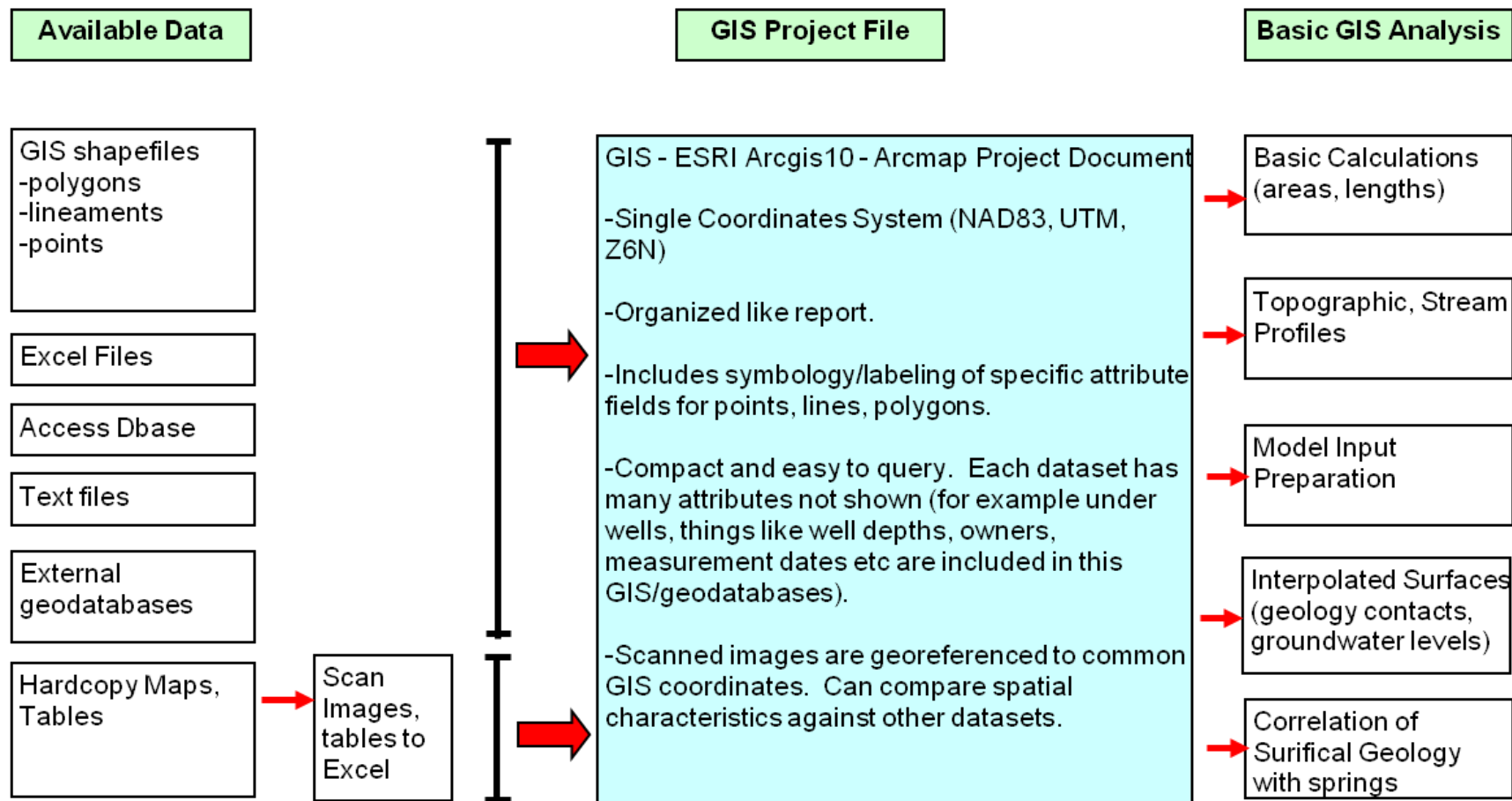


Figure 2-1. General Approach to Convert Data into GIS, GIS design and Basic GIS Analyses.

2.3 Topography/DOQQ

Perhaps the single most critical dataset required to construct an integrated hydrologic model is the surface topography. The accuracy and resolution of the topographic dataset directly affects the accuracy of the simulated output. This is especially true near streams, where the streambed elevations relative to adjacent surfaces controls how much overland flow and groundwater baseflow flow into, or out of the streams. The resolution of the topography also dictates how well, sub-grid scale features, such as continuous drainages are captured in the model. For example, if the resolution of the topographic dataset is coarse compared to (i.e., 30 meters) the width of small, extensive drainages (i.e., 10-meters wide), the model may incorrectly promote infiltration over surface drainage because the topography is not refined enough to capture the smaller drainage features.

The topographic dataset used in this study was obtained from the Advanced Spaceborne Thermal Emission and Reflection Radiometer (ASTER) Global Digital Elevation Model (GDEM) State Wide Mapping Initiative: http://browse.alaskamapped.org/#browse/available_data.

Within the Chuitna Watershed, surface elevations rise to over 800 meters along the upper watershed boundary (Chuitna Plateau area). Average sub-watershed topographic surface slope aspects (direction that ground surface slopes) range from 142 to 165 degrees from north (clockwise), suggesting the overall topography slopes southeast (90) to south (180). A GIS zonal statistical analysis of the 23 m resolution ASTER topography within each of the 8 sub-watersheds shows that slopes range from 3.4 to 7.3 degrees. Slopes are highest in the upper elevation watersheds, and lowest in lower watersheds.

Figure 2-4 shows the extent of a digital orthophoto quadrangle (DOQ) imagery also used in this study to help refine locations of streams and surface water bodies. It only covers the lower half of the watershed and was obtained from <http://edcsns17.cr.usgs.gov/NewEarthExplorer/>. This information was useful in revising digital surface water drainages (Section 4.2.5) and defining surface water bodies (Section 2.5.2.2).

These two coverages (the DEM and DOQQ) are critical high-resolution datasets used to develop the groundwater flow model. The topography represents the upper surface of the model. The 10-meter resolution is adequate for the modeling because important hydrologic features (i.e., stream drainage areas) are much larger than 10-meters. The topography is also used to determine the streambed elevations in the model, which are used to calibrate the model.

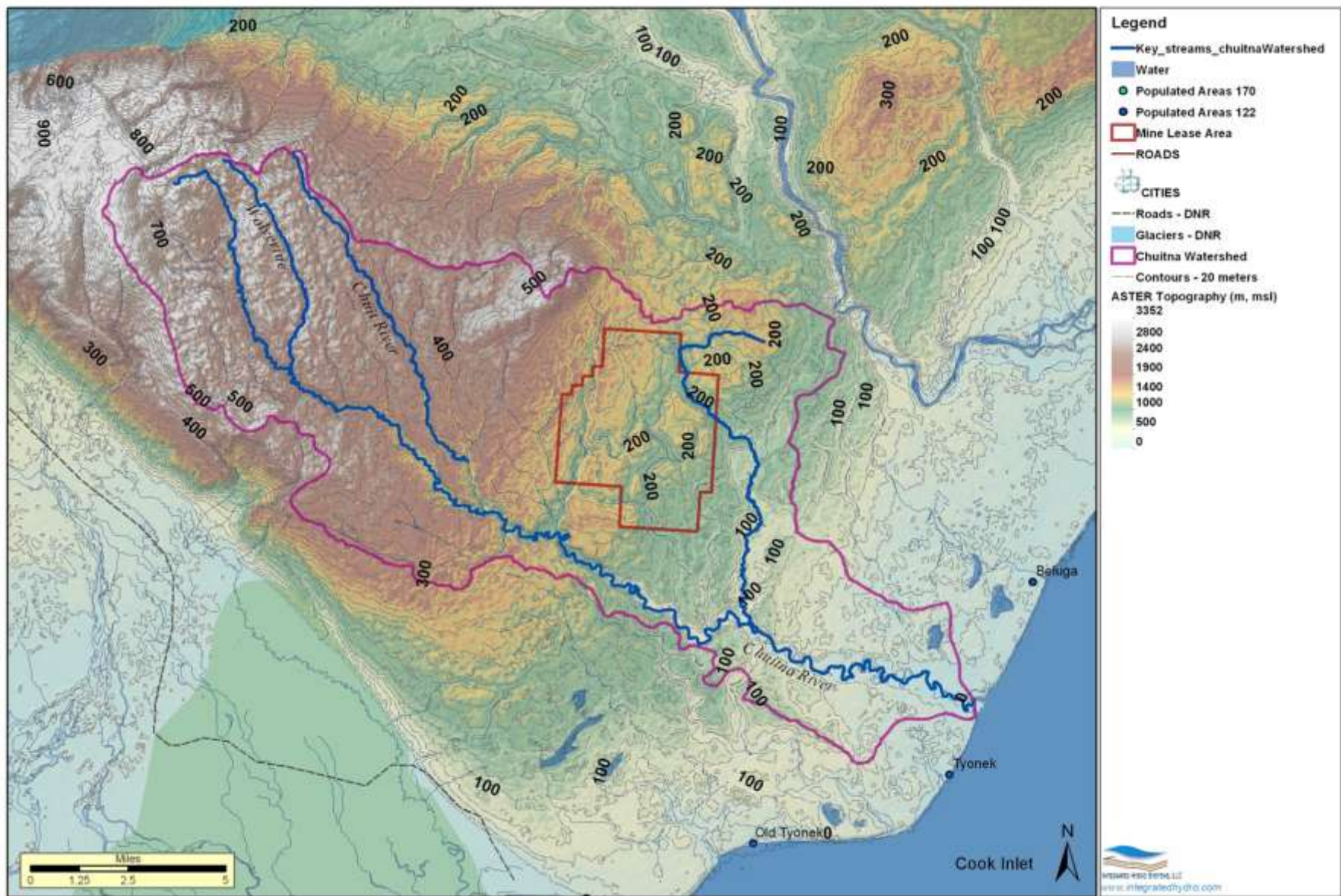


Figure 2-2. ASTER Topography (~ 23 m spatial resolution, and ~3 m vertical accuracy)

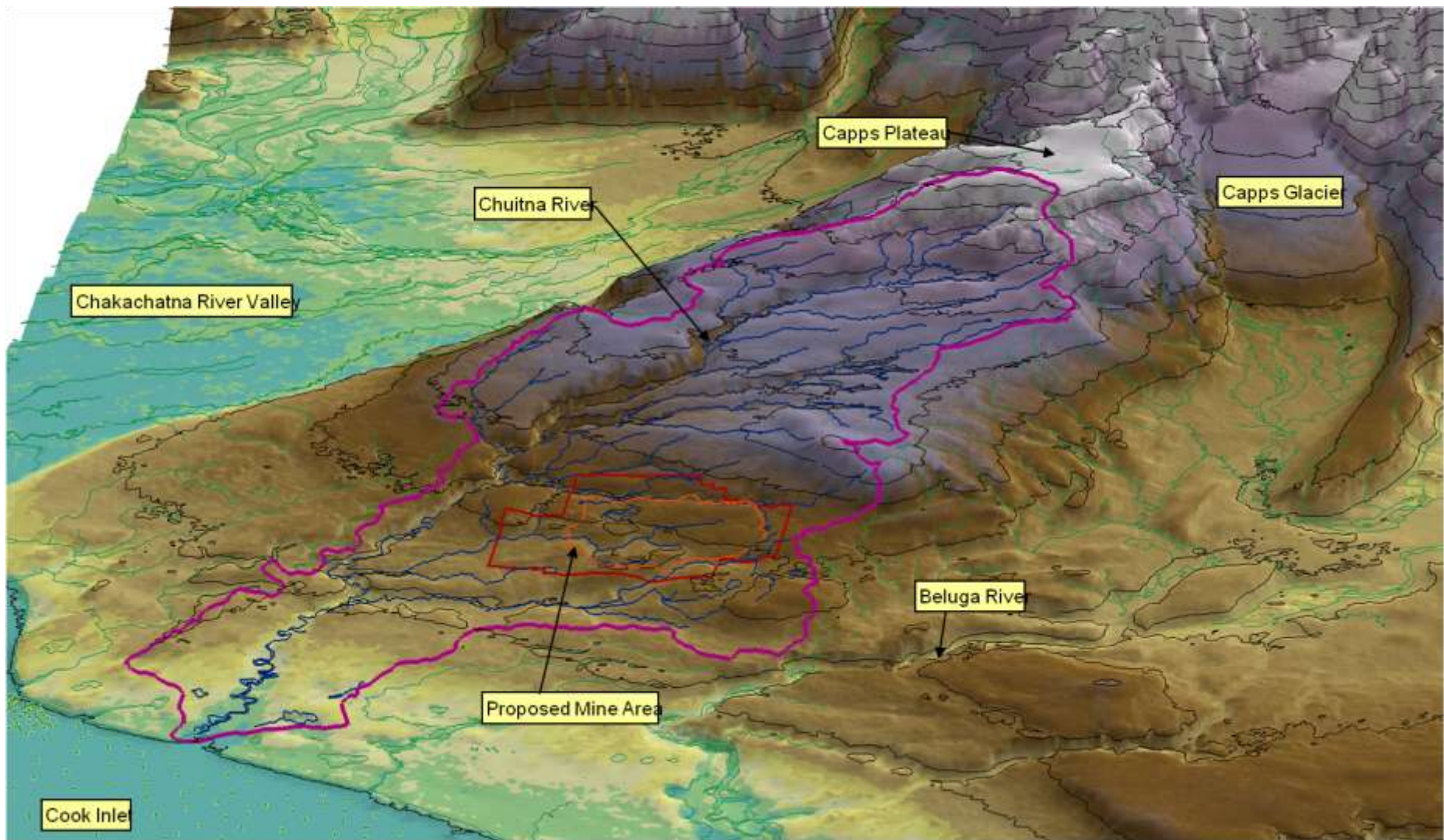


Figure 2-3. 3-D Perspective of Watershed and Topography

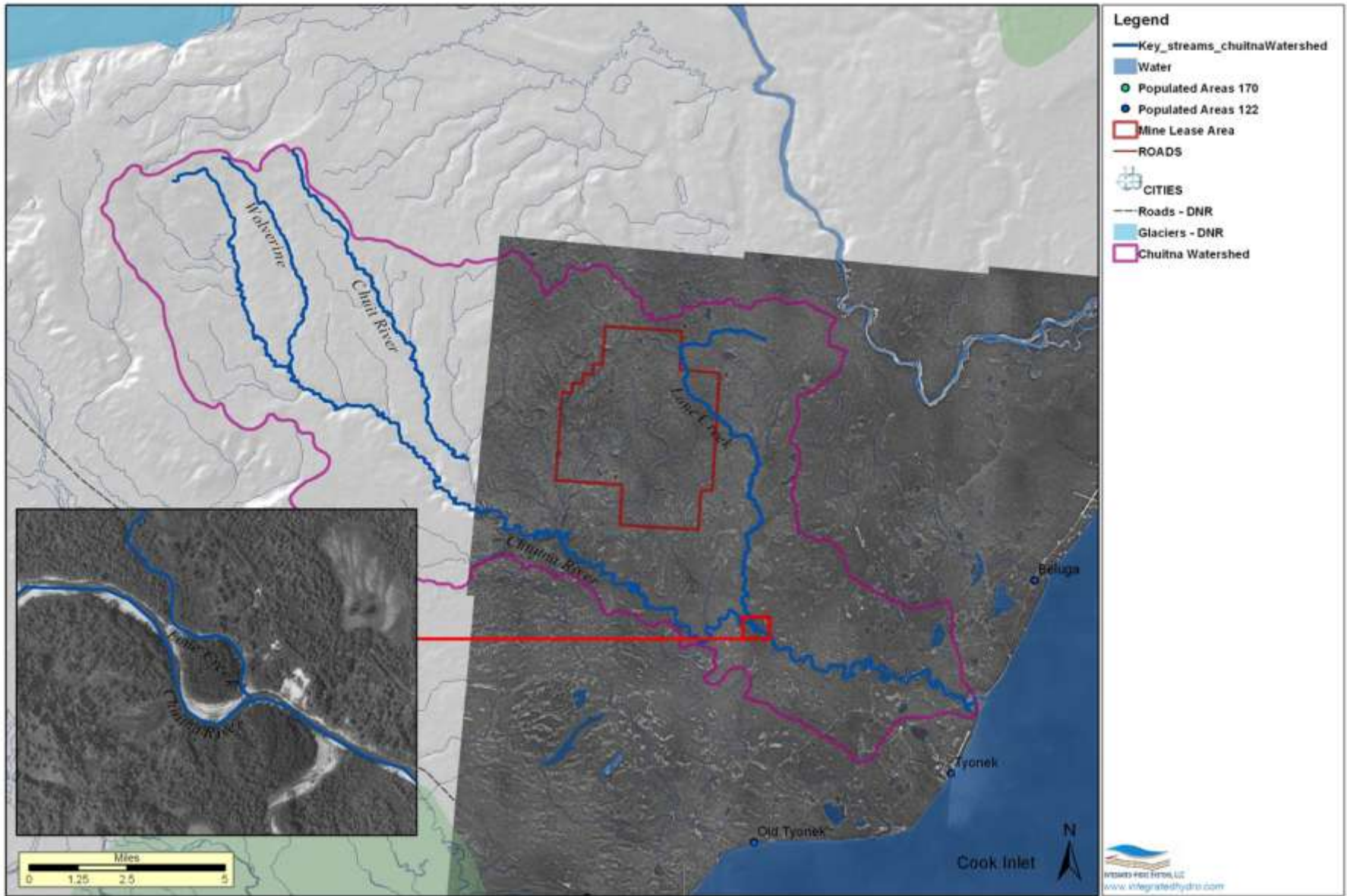


Figure 2-4 High Resolution DOQQ of Mined part of watershed (<http://edcsns17.cr.usgs.gov/NewEarthExplorer/>)

2.4 Geology

The subsurface hydrologic flow system is strongly controlled by the types of geologic material and their configuration material within a watershed. Integrated hydrologic models require that the geology be described from the ground surface to some point below the extent of an aquifer of interest to account for infiltration of precipitation at the surface and eventually recharging the lower aquifer. A geologic model is typically prepared, which describes how the geologic material varies both vertically and spatially within the watershed. Despite the lack of data outside of the proposed PacRim mine area, adequate published information was available from published information, mainly from the Alaska DNR website (<http://www.dggs.dnr.state.ak.us/index.php>).

This section describes the following available information and subsequent interpretations:

- Section 2.4.1 – Faulting,
- Section 2.4.2 – Stratigraphy,
- Section 2.4.3 - Soils Distribution – (Shallow),
- Section 2.4.4 - Surface Geology (outcrop) and
- Section 2.4.5 - Subsurface Geologic Units (from PacRim).

2.4.1 Faults and Synclines and Tectonic Setting

The tectonic setting typically has a profound effect on the geologic conditions within hydrologic systems. The Chuitna Watershed is located within a very active tectonic region, where the Pacific plate is subducting beneath the North American plate (lower plot on Figure 2-5). The upper plot on Figure 2-5 shows the approximate location of the Chuitna Watershed (yellow rectangle) on the northern part of a northeast trending, intermountain trough (Cook Inlet Basin), also referred to as Cenozoic forearc basin. The basin is flanked on the northwest by the southern Alaska Mountain range and on the south by the Chugach Mountains and extends about 200 miles and is about 60 miles wide. Typical of subduction zones, a number of volcanoes (i.e., Redoubt Volcano (3108 m), Iliamna Volcano (3053 m), and Mount Douglas (2140 m), and Mount Spurr (3383 m)) occur further from the near-surface subduction point, or northeast of the basin (lower plot on Figure 2-5).

Two major steep, reverse/ strike-slip faults, the (no. 3 on upper plot) Castle Mountain – Lake Clark Fault (LCF) and (no. 4) Bruin Bay Fault (BBF) are part of the tectonic subduction system cross the Chuitna Watershed (Figure 2-6). As the Pacific plate subducts beneath the North American plate, blocks on the south side of these faults are dragged down relative to blocks on the north side. The Border Ranges Fault (no. 5) bounds the southern Cook Inlet Basin, but the block on the north side is thrown down relative to the southern side. This action caused the Cook Inlet Basin to drop, and fill with a deep sedimentary sequence (Orange and light yellow shaded area).

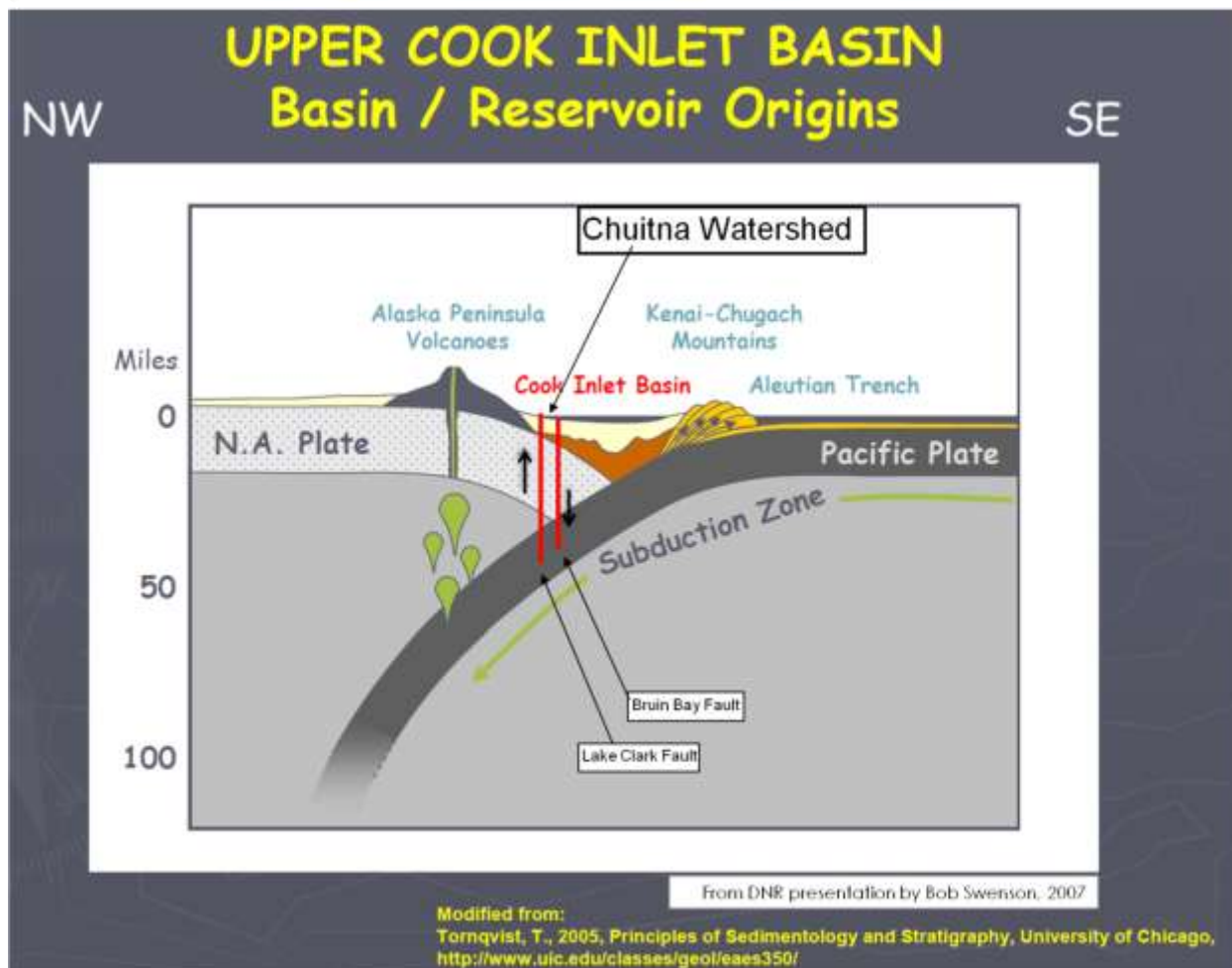
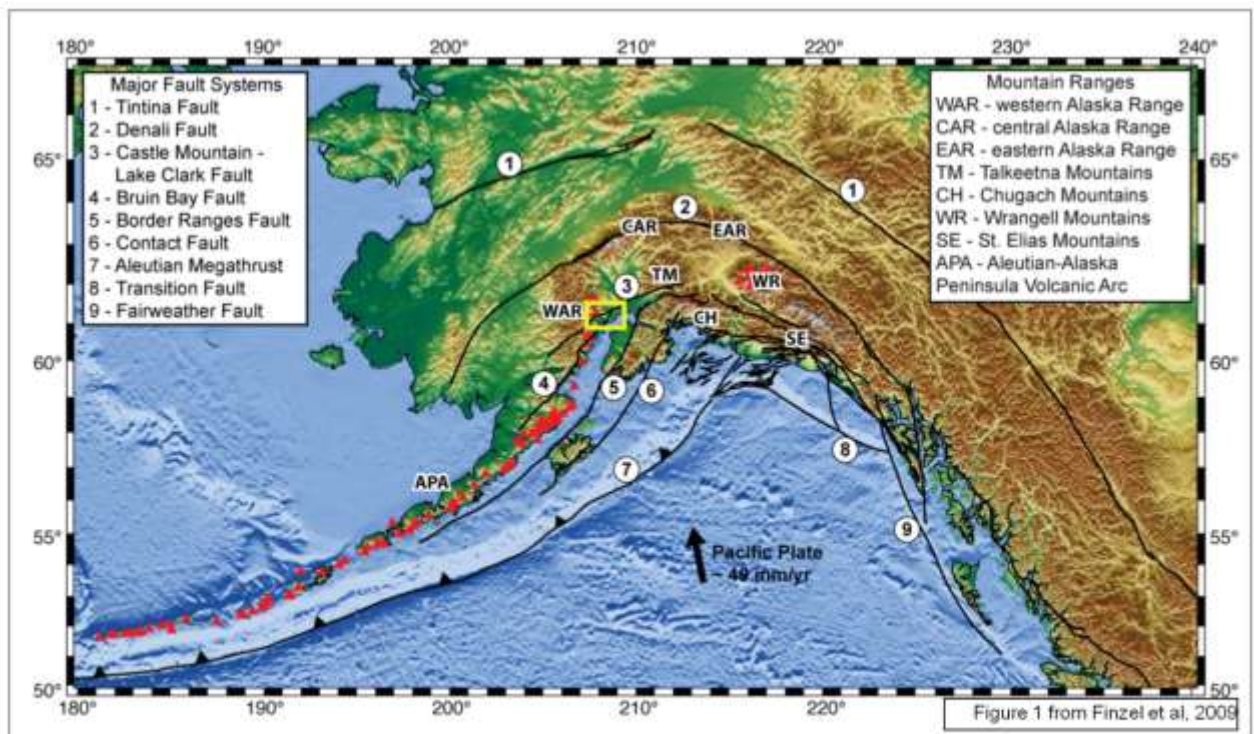


Figure 2-5. Tectonic Setting - Bruin Bay and Clark Lake Faults

Traces of several faults identified within the watershed are shown on Figure 2-6 (Hackett, et al, 1977, Wilson et al, 2009, Mine Engineers, 2007, and Flores et al, 1997). The “U” indicates the side of the fault that has been upthrown, and the “D” indicates the downthrown side. The arrows indicate the side and direction of lateral fault movement. Lateral displacements on the LCF in the Chuitna watershed area (Beluga Plateau) range from 5 to 26 km (Kohler and Reger, 2011), and though lateral displacement on the BBF is unknown, displacements along the southern extent range from 19 to 65 km (Finzel et al, 2009). Vertical displacements are believed to range from 500 to 1000 meters on the LCF based on stratigraphic offsets on the western flank of the Beluga Plateau (Kohler and Reger, 2011). Although the vertical offsets along the BBF within the watershed area are also unknown (i.e., due to lack of boreholes in this area and heavy vegetation), vertical displacements in the southern Cook Inlet are up to 3 km.

2.4.2 Stratigraphy

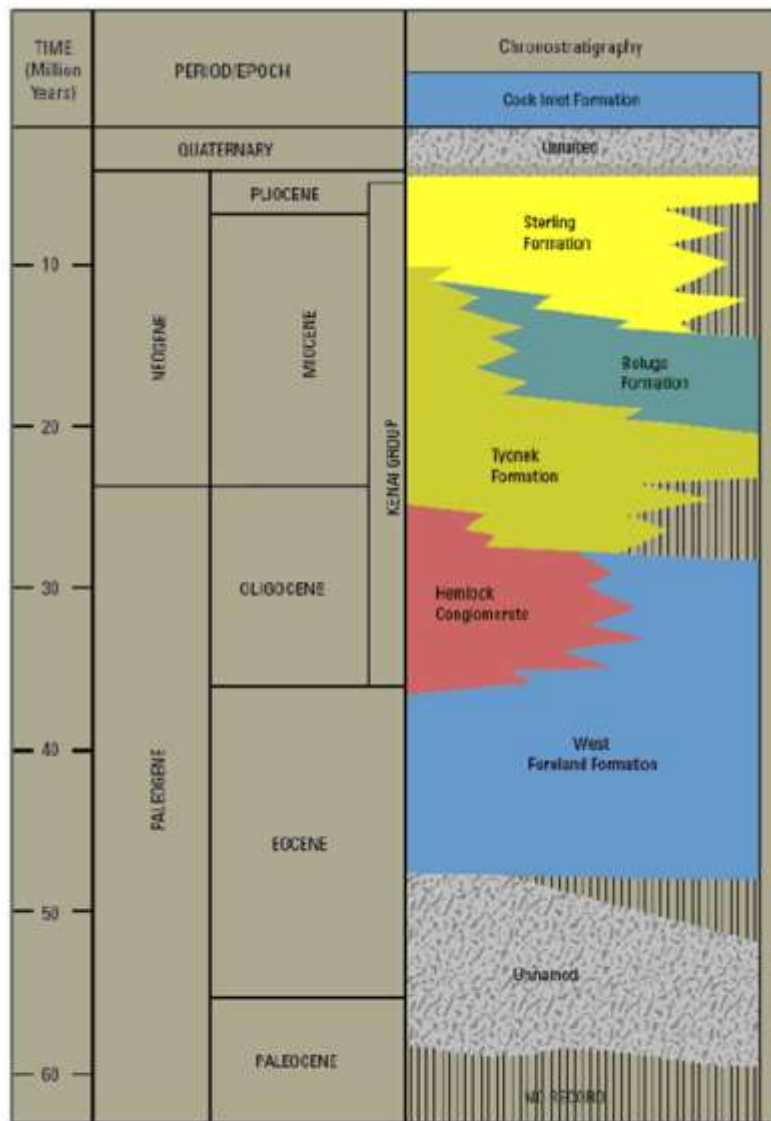
Generalized stratigraphic information for the Cook Inlet Basin (left plot) and for the local Chuitna Watershed Mined Coal Sequence (right plot) are summarized on Figure 2-7. The Tertiary-age (1.8 to 65 million years) sequence of five sedimentary rock formations (Kenai Group) are more than 25,000 feet thick in the center of Cook Inlet Basin and thin at the basin margins, for example near the LCF (Hartman et al, 1972). The Kenai Group is thickest beneath the lower, or southeastern edge of the Chuitna Watershed (>15,000 ft, Hartman et al, 1972). All formations shown on Figure 2-7 occur beneath the Chuitna Watershed, though the large regional faults (LCF and BBF) dictate which formation outcrops at the surface due to the significant lateral and vertical offsets. For the purposes of this study, the bedrock formations of most interest, or that directly influence shallow groundwater within overlying unconsolidated Quaternary deposits within the watershed, include:

- Lower Chuitna Watershed: Beluga Formation (>5300 ft) – Nonmarine, interbedded, weakly lithified sandstone, siltstone, mudstone, shale, coal and minor volcanic ash
- Middle Chuitna Watershed: Tyonek Formation (>7000 feet in the mine area, Harman et al, 1972) – Carbonaceous nonmarine conglomerate and subordinate sandstone, siltstone, and coal (Wilson et al, 2009)
- Upper Chuitna Watershed: West Foreland Formation (thickness is unknown, but likely > 2900 ft based on an oil well on the southern side of Upper Chuitna River, Hartman et al, 1972) – cobble conglomerate interbedded with lesser sandstone, laminated siltstone, and silty shale.

Detailed, near-surface stratigraphic information is mostly from boreholes drill logs in the PacRim geology report and only for the area of the proposed mine (Mine engineers Inc., 2007 and Riverside, 2010). Some information from deep oil wells in the area suggest the combined Kenai Group formations in the watershed are many thousands of feet thick, and thicknesses increase towards Cook Inlet. The general stratigraphy in the mine area includes:

- Holocene Muskeg (0 to 23 ft)
- Holocene Alluvium (0 to 40 ft)
- Pleistocene Glaciofluvial Deposits - Major moraine and kame deposits, Wilson et al, 2009) and Glacial Deposits
- Tyonek Formation

Although the Tyonek coal seams (i.e., Brown coal bed on Figure 2-7) within the proposed coal mine area are topographically higher than the 13 km of the Tyonek formation exposed along the middle Chuitna (between the LCF and BBF), they are actually stratigraphically lower (older) due to the 1 to 4 southwestern slope of the beds.



from Riverside, 2010 (originally from Flores et al, 2004)

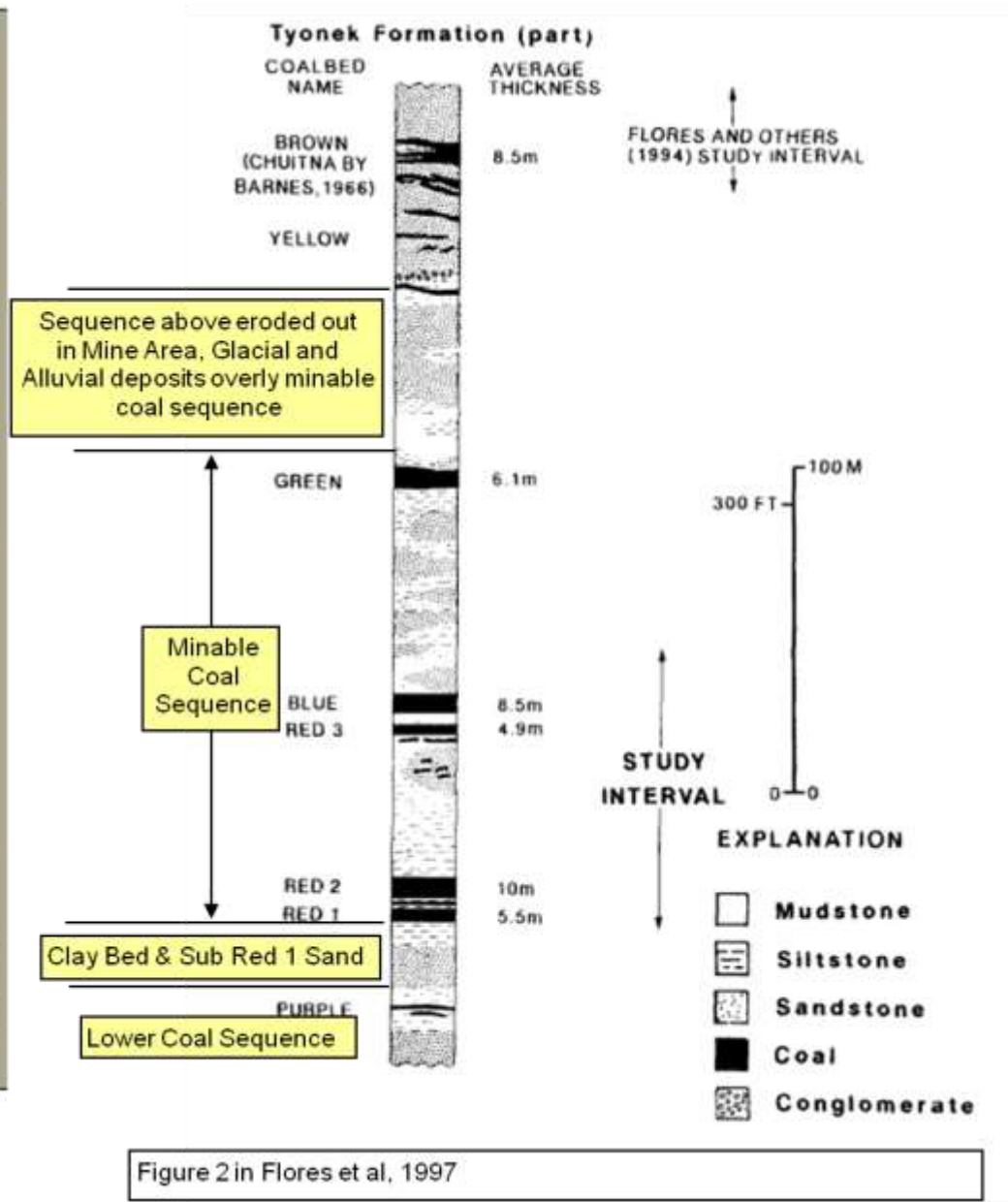


Figure 2 in Flores et al, 1997

Figure 2-7. Generalized Stratigraphy for Cook Inlet Basin and Chuitna Watershed.

2.4.3 Soil Distribution

A detailed 2007 Soil Survey Geographic (SSURGO) database for Yentna Area, Alaska for the Chuitna Watershed was obtained from the U.S. Department of Agriculture, Natural Resources Conservation Service weblink: <http://SoilDataMart.nrcs.usda.gov/>. The downloaded survey information includes both tabular information in a Microsoft Access database and associated spatial information as GIS shapefiles. The soil information is a critical dataset used in the hydrologic modeling because it controls the rate of infiltration, groundwater recharge and overland flows. If precipitation intensities exceed soil hydraulic conductivity values, overland runoff will be generated. Although a PacRim soil survey in 2006 was reviewed (Ping and Brown, 2007) for this study, it only covered the area around the proposed mine.

The SSURGO spatial distribution on soils across the Chuitna Watershed, shown on Figure 2-8, is complex and strongly influenced by topographic slope. Dominant soils within a group are summarized into SSURGO hydrologic soil groups (A to D) on Figure 2-9, where “D” soils represent soils with very low infiltration and high runoff potential, and “B” soils are soils with high infiltration and low runoff. There were no “A” soils within the Watershed and few “C” soils. The distribution shows that the upper, steeper watershed areas are predominately “D” soils and lower areas are “B” soils, which suggests the potential for surface runoff is greater in upper watersheds.

Information on the vertical hydraulic properties of the soil is also provided in the SSURGO database, but only to 5 feet depth. Example soil profiles and saturated hydraulic conductivity values are summarized in Appendix A - . Typically, the first 3 to 6 inches of soil are described as either peat, or slight to moderate decomposed organic matter. A silt loam/loam material occurs beneath this to about 2 to 3 feet. Depending on the soil type and location, the material from 2 to 3 feet to 5 feet is variable and ranges from coarse cobbly sand to muck, or bedrock. Hydraulic conductivity values in the SSURGO database range from 1.4e-4 to 4.2e-6 m/s.

A review of the 20 available borehole logs (Mine Engineers, 2007) provided in the PacRim geology baseline report show that the thickness of peat (or Muskeg) ranged from 2 to 23 feet (average of 9.3 ft) and occurred in all boreholes. This seems contrary to information in the SSURGO database that suggests peat only occurs from 3 to 6 inches. This is also at odds with the following statement (Riverside, 2010): *“Peat deposits occur in depressions on the glacial deposits. Drilling indicates that the peat is up to 23 ft thick and covers portions of the proposed mine area (Map 3, Mine Engineers, 1998).”* This suggests peat only occurs in depressions, yet all 20 borehole logs show peat and with thicknesses much greater than the 3 to 6 inches indicated in the SSURGO database. The geology report also states that surficial deposits (peats, alluvium) are 30 to 45 inches thick in upland areas. Because the borehole logs are site-specific and prepared by professional geologists, it is likely that the organic soils (peat) effectively occur throughout the entire watershed rather than just within depressions, and average about 9 feet in thickness.

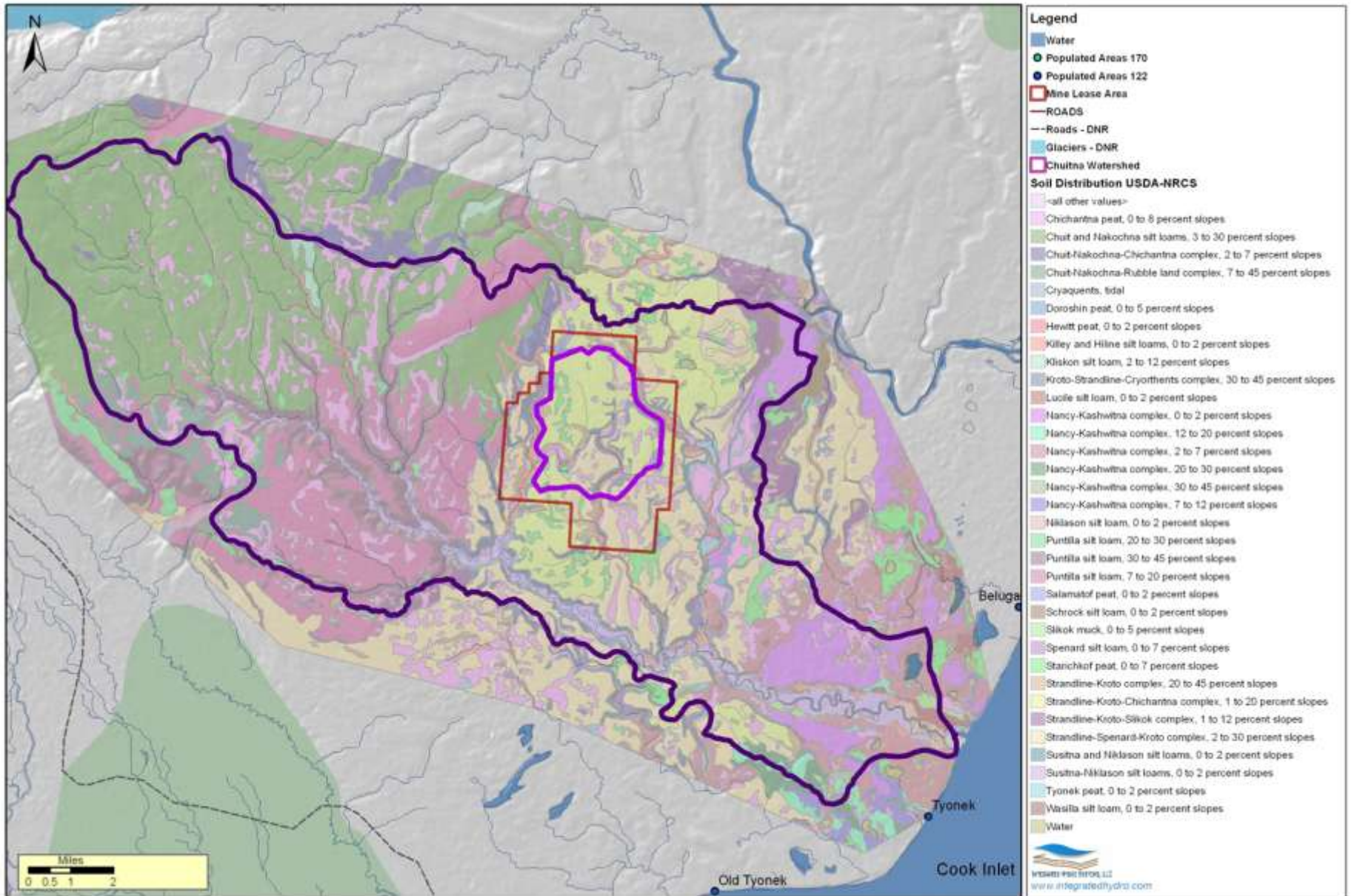


Figure 2-8. Spatial Soil Distribution (U.S. Department of Agriculture, Natural Resources Conservation Service)

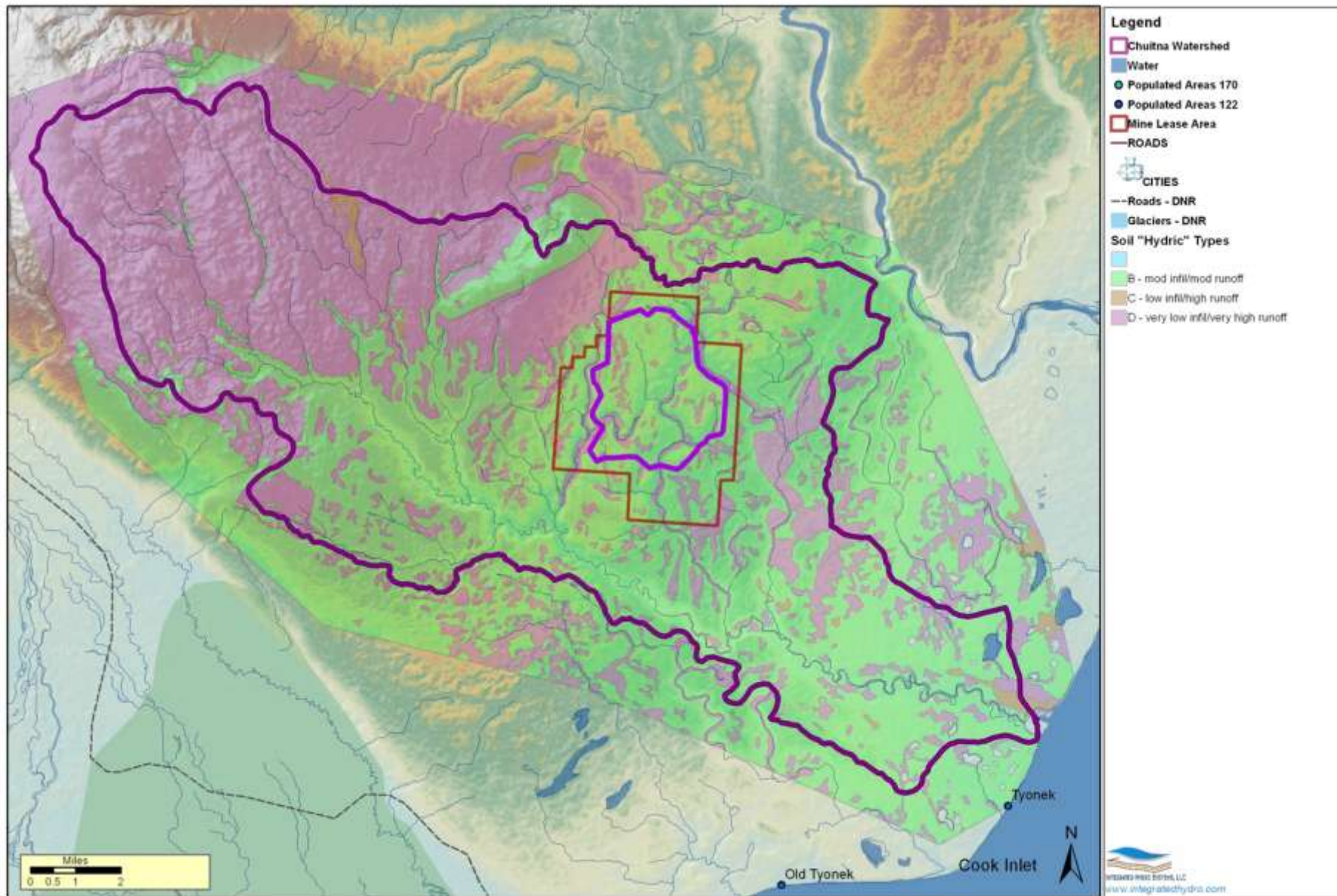


Figure 2-9. Soil distribution of USDA-NRCS soil hydrologic types.

2.4.4 Surface geology

Surface geology was obtained from a recent USGS effort (<http://pubs.usgs.gov/of/2009/1108/>) by Wilson et al (2009) to compile historical surface geology surveys from the early 1960s to present into a single set of GIS coverages (Figure 2-10). Three key areas occur within the watershed. The upper watershed, northwest of the LCF shows outcrops of the West Foreland Formation of the Kenai Group (Blue – Twf) along more steeply incised streambeds. Some Tyonek occurs in this area as well (orange – Tkt) immediately overlying the West Foreland and represents the bottom of the Tyonek formation and top of the West Foreland formations. In a 3-dimensional perspective view of the surface geology, draped over the surface topography (Figure 2-11), the West Foreland formation lying adjacent to the Tyonek formation on the northwestern flank of the Beluga Plateau is a clear indication of the substantial lateral and vertical displacement that have occurred along the LCF. The Tyonek outcrops along the entire length of the Chuitna River from the LCF to the BBF. Odum et al, 1986) believe this outcrop represents the upper part of the Tyonek formation based on radiometric age dating. Southeast of the BBF, the Beluga formation outcrops for a few kilometers, but is then overlain by thousands of feet of Quaternary Deposits (and Sterling formation) at the edge of Cook Inlet (Hartman et al, 1972).

Quaternary glacial deposits (drift) cover the majority of the watershed (Qg), though volcanics (Qtw) occur in the western uppermost watershed area and a granitic intrusion occurs in the area known as Lone Ridge (TKg), in the eastern part of the upper watershed. Glacioalluvium deposits (Qgc), are well-sorted, stratified sands and gravels that occur primarily in the middle watershed area, near the proposed mine area and primarily in present-day surface drainages. Lower watershed areas, near Cook Inlet, are characterized by glacioestuarine (Qge) or glacial outwash deposits (Qgo) which are both well-bedded and sorted gravel and sands within beds. Though not shown on Figure 2-10, Riverside (2007) indicates that Holocene alluvium (sands and gravels) is restricted to only major active surface drainages (i.e., Lone Creek, 2003 and 2004) and associated floodplains (finer-grained deposits), though alluvial areas seem to extend to nearly all drainages near the mine (Map 5.2.4 in Riverside, 2007). No discussion was presented in the Riverside (2007) report on how the map of the Holocene alluvium was constructed, but it is assumed here that the distribution shown was only inferred. This seems to be supported by the fact that subsequent groundwater modeling did not follow this alluvium distribution very closely (i.e., Figure 4 in Arcadis, 2007).

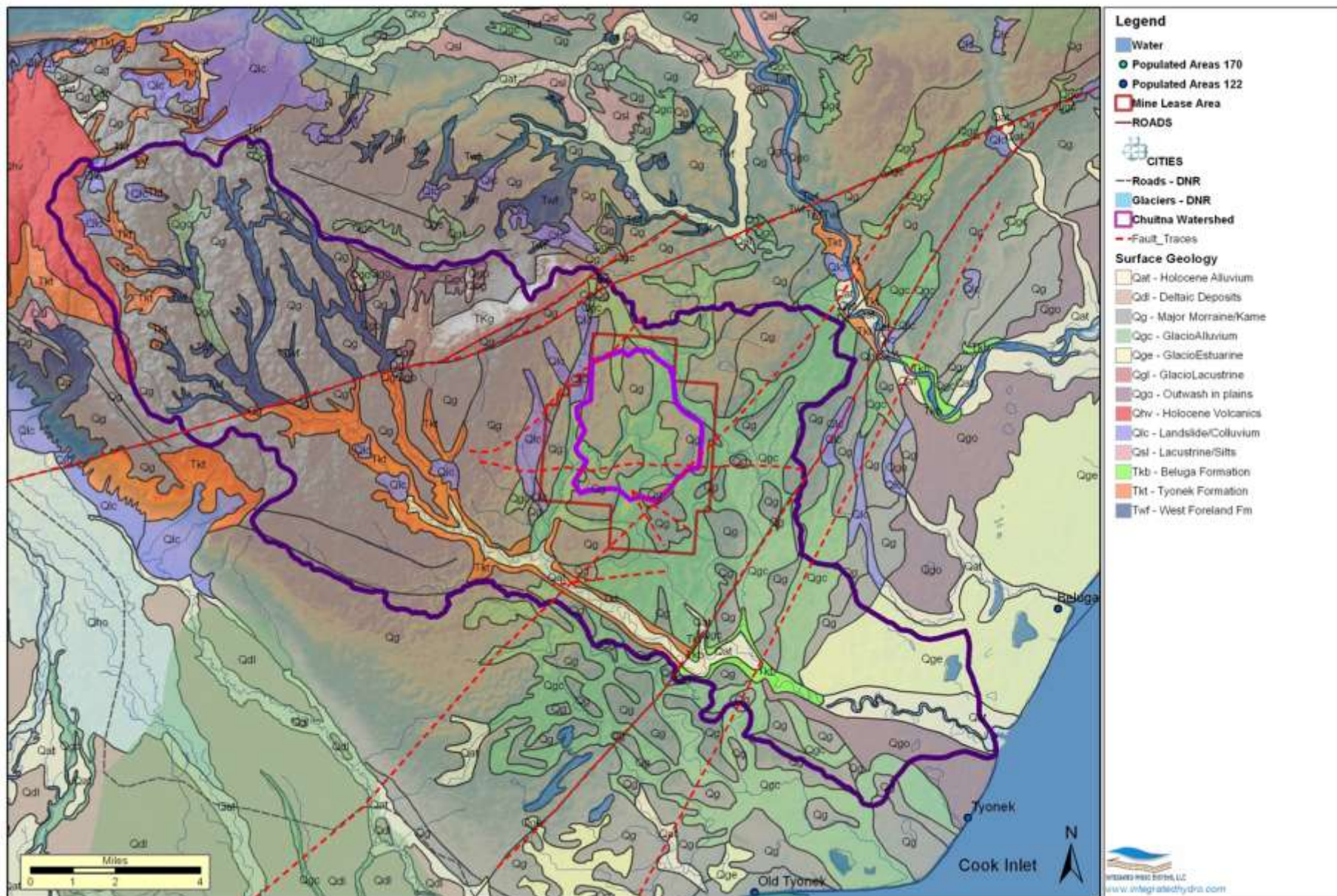


Figure 2-10. Surficial Geology (digital GIS coverage).

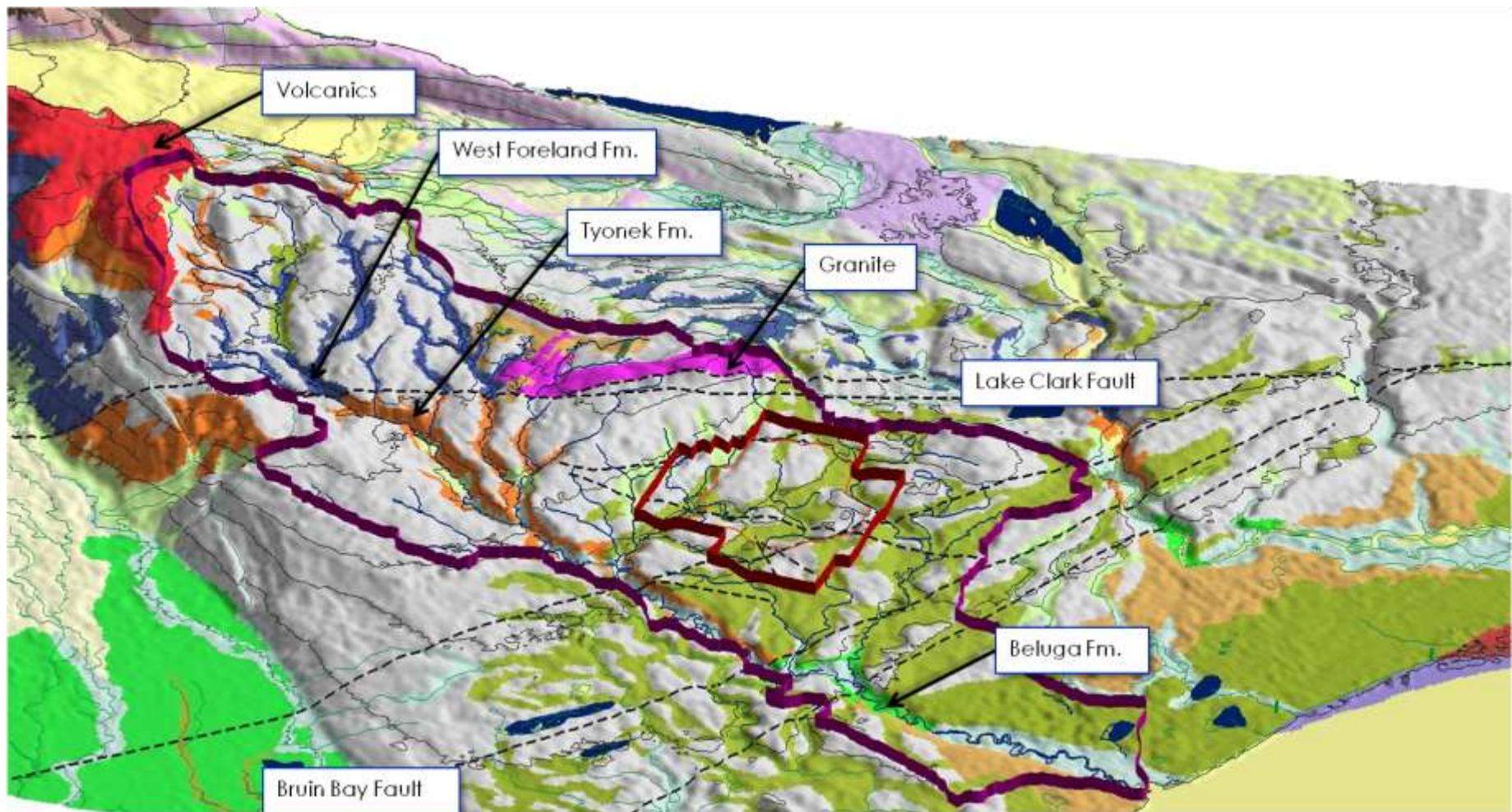


Figure 2-11. 3-dimensional View of Surface Geology and Structure draped over Surface Topography.

2.4.5 Subsurface Geology

A description of the subsurface geology within the Chuitna Watershed described in this section is based on several sources of information. Regional-scale subsurface geologic information is from oil well information compiled by the Alaska DNR (Hartman et al, 1972), and to a lesser extent from USGS boreholes in the region (Odum et al, 1986, Odum et al, 1988). Figure 2-12 shows bedrock isopach contours for the Kenai Group and Quaternary Deposits developed based on a series of available oil well borehole information (Hartman et al, 1972), mostly drilled in the 1960s. Isopach maps of other Kenai formations were also created from the oil well borehole information including for the West Foreland, Hemlock, Tyonek, Beluga, and the combined Sterling and Quaternary deposits. In addition to the oil well data, local borehole data also provide subsurface geologic information, but only down several hundred feet and only within the proposed PacRim coal mine area.

The thickness of unconsolidated deposits (overburden), or the combined glacial deposits and peat/alluvium (also known as Quaternary deposits) is a critical dataset in the hydrologic model. Shallow groundwater that collects in this material effectively perches over the lower permeability bedrock. As a consequence, much of the baseflow in streams is contributed by groundwater discharge from this zone. Based on a review of the trends in thickness of overburden from available PacRim boreholes, and from observations by Odum et al (1986), an isopach map of the Quaternary deposits over the entire watershed was developed (see Figure 2-13). Thicknesses shown were iteratively determined through initial hydrologic modeling. The general trend imposed on the distribution involves assigning approximately 30 meters thickness in non-stream areas, and 1 to 5 meters thickness in stream areas. Near Cook Inlet, the thickness of the Quaternary deposits increases dramatically based on the Quaternary isopach map in Hartman et al (1972).

Figure 2-14 and Figure 2-15 show cross-section locations and a northwest-southeast cross-section through the long axis of the Chuitna Watershed (roughly aligned with the Chuitna River), respectively. Figure 2-16 shows five sections oriented southwest to northeast, or perpendicular to the long axis section on Figure 2-15. The sections were constructed using the 3D Analyst extension within the ArcGIS environment and the ASTER digital surface topography. The thickness of the Quaternary deposits shown on Figure 2-15 is consistent with Quaternary deposit isopachs shown on Figure 2-13. The thickness of the Kenai Group formations beneath the watershed is large, exceeding 1000 feet in the upper, middle and lower Chuitna areas. Similar sections have been drawn along the same northwest-southeast alignment (Flores et al, 1994, Hackett, 1976, Hackett, 1977, McGee, 1973, Finzel et al, 2009) but these have been largely inferred from the surface geology and faulting. Near faults, the dips of stratigraphic layering within the Kenai formations appear to be folded based on the vertical offset direction (i.e., Finzel et al, 2009, Detterman, 1976). This is further supported by stratigraphy depicted in sections constructed by the PacRim consultant Mine Engineers, Inc. (Map 4, 2007) and in Flores et al, 1997.



Figure 2-12. Isopachs of Regional Kenai Formation (Oil Well data) of Minalse Coal Sequence (Layer 2)

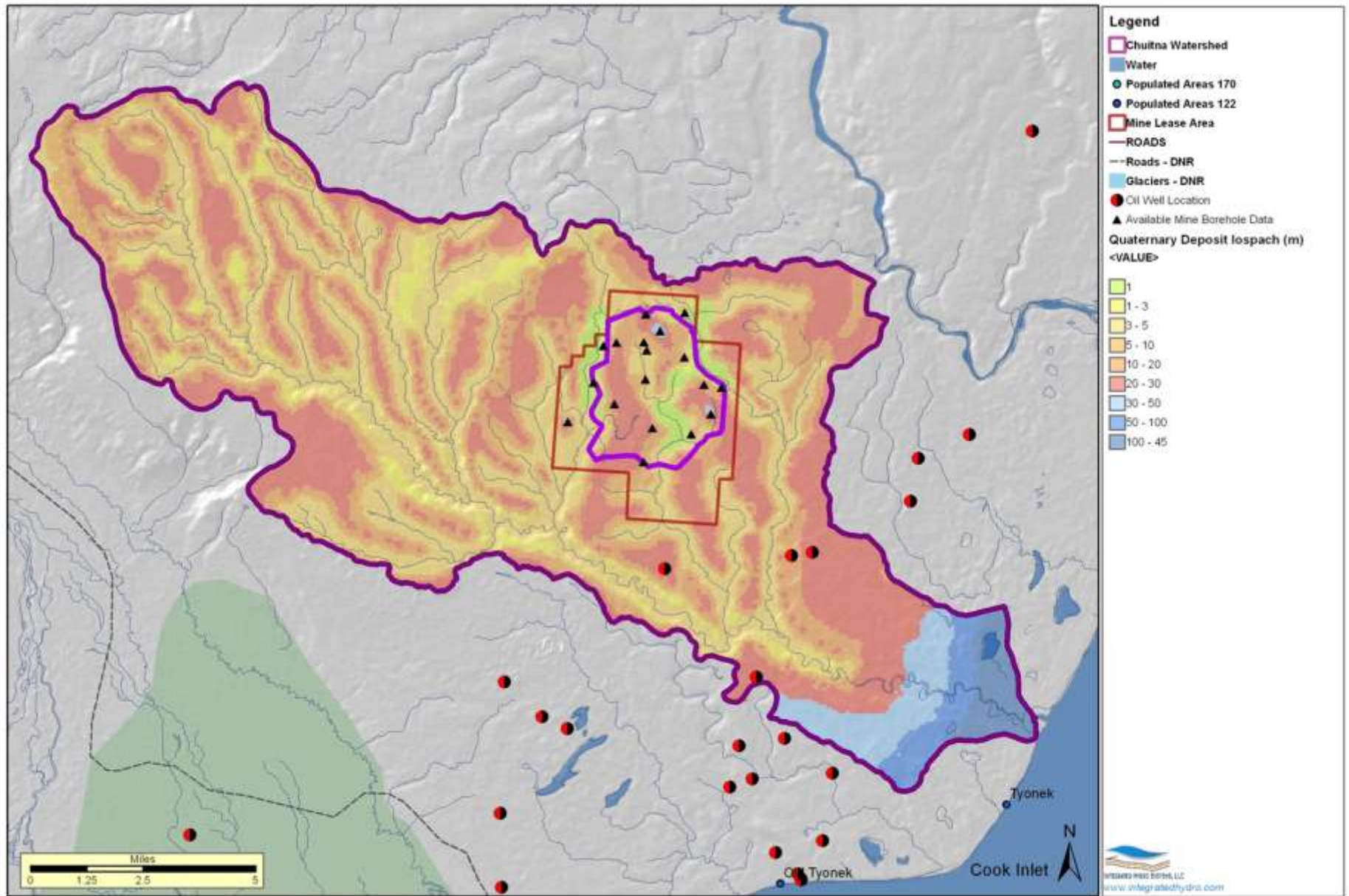


Figure 2-13. Isopach of Quaternary (Unconsolidated) Glacial Deposits/Alluvium

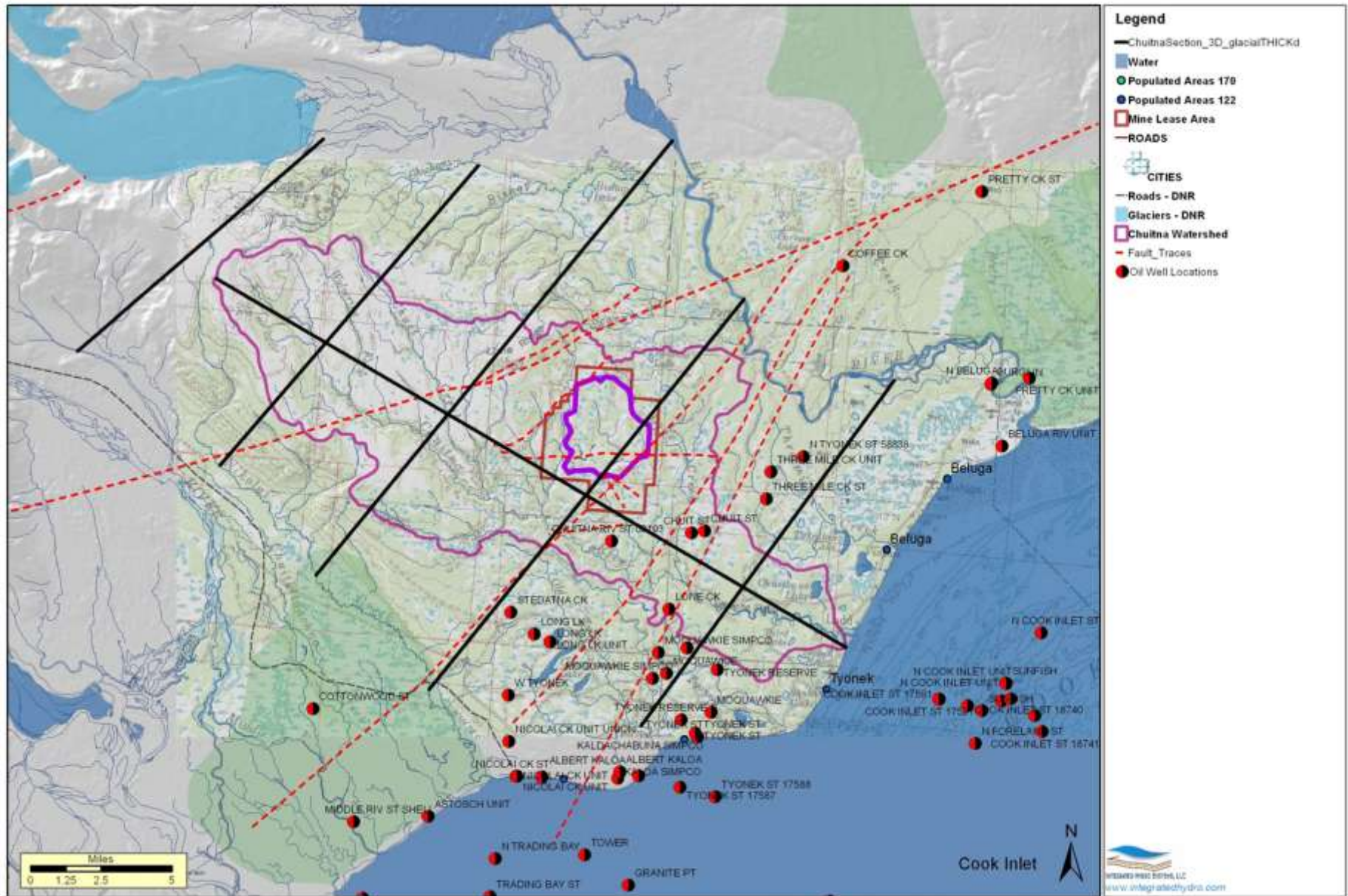


Figure 2-14. Locations of N-S and E-W Sections through the Chuitna Watershed.

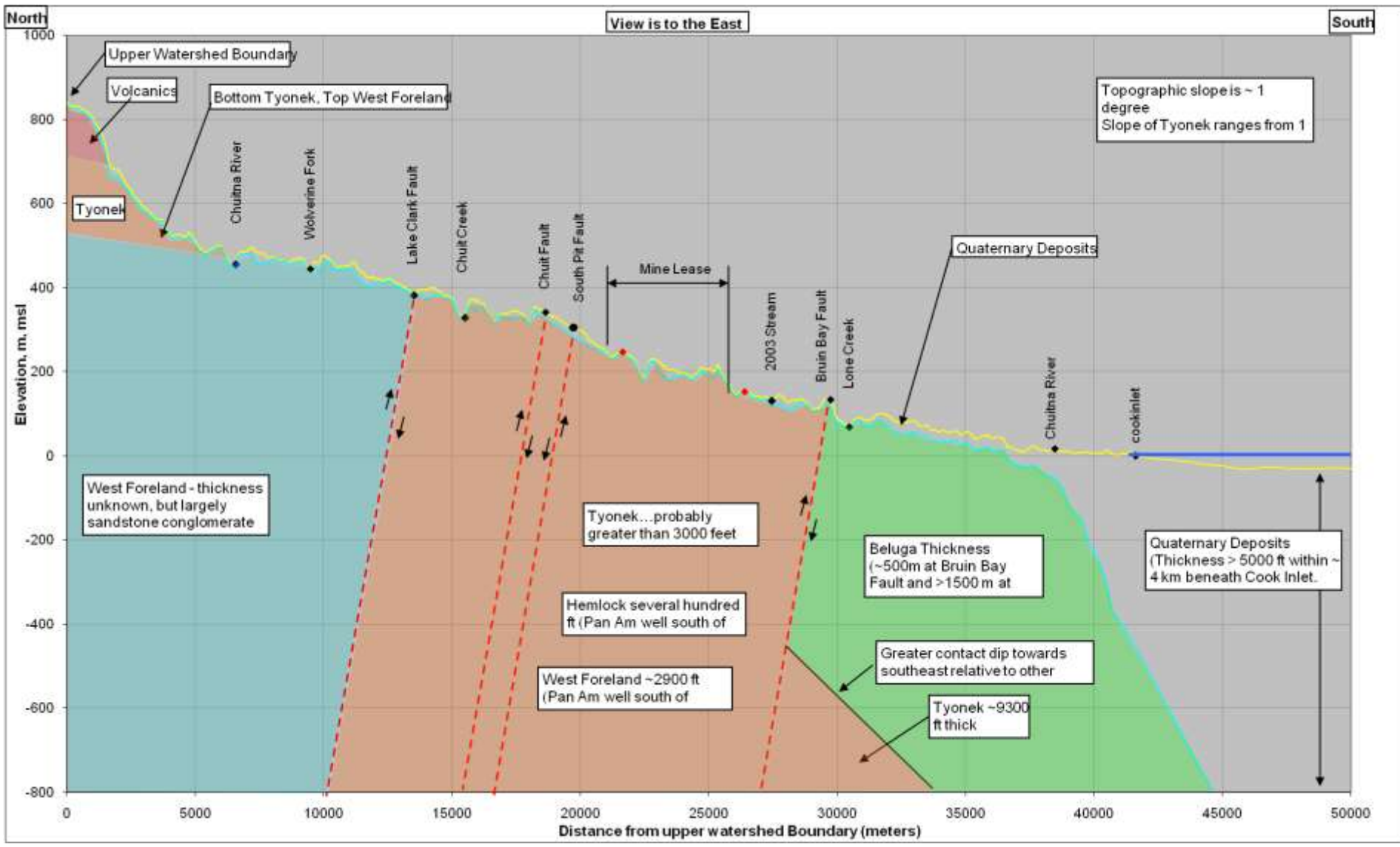


Figure 2-15. Northwest-Southeast section through the proposed mine area.

Neither the geologic database, more than 430 borehole logs, nor digital sections were made available by PacRim for this study, so details of the layering within the Tyonek formation, or other Kenai formations is largely only pictorial. Stratigraphy described in Flores et al (1994) and Flores et al (1997) along the middle Chuitna River and in the southern proposed mine area, respectively, indicate lateral facies change in the 1 to 4 degree sloping bedrock layers within the Tyonek formation. For example, significant sandstone conglomerate (>50%) occurs along the middle Chuitna area and also increases towards the southern proposed mine area, where a fluvial channel likely existed (i.e., along Lone Creek). Recent borehole logs (SR34-11, SR35-11, SR36-11) drilled to through the Sub-Red 1 Sand seem to support this (PacRim, 2011). The Tyonek beds also dip to the south, along a southward dipping anticlinal axis (averaging 1 to 6 degrees), which is slightly greater than the average dip of the ground surface towards the south.

The lateral changes in facies likely promote increased deeper drainage of groundwater to the south and west of the proposed mine, but it is difficult to define this accurately without detailed borehole information. Drainage to the west is further complicated because the layers dip below the extent of erosion in the Chuit River; Flores et al, (1994) indicates exposed bedrock along the Chuit River is younger than the minable coal sequence in the proposed mine. Therefore, lateral drainage of groundwater within the minable coal and underlying Sub-Red 1 Sand strata may continue beneath the Chuitna towards the western flank of the Chuitna Watershed, though this is unknown due to a lack of subsurface characterization in this area.

The faults and relatively large displacements are important to understanding how groundwater flows through the subsurface. Fault offsets cause abrupt changes in the permeability of aquifers, which also appear to cause abrupt changes in groundwater pressures (and therefore flows) across these features. For example, artesian pressures (where groundwater levels rise above ground surface) are reported in Sub-Red 1 Sand wells near the South Pit fault (Riverside, 2010), located in the southern area of the proposed mine. This suggests that fault offsets limit lateral flow in permeable strata, which increase pressures as the groundwater effectively ‘backs-up’ and cause artesian conditions.

Based on the overall topographic slope of the Chuitna Watershed from northwest to southeast, and a similar bedrock slope direction (though slightly steeper), artesian pressures should buildup on the north/northwestern sides of faults and drop on the south/southeastern sides. Riverside (2006) indicates well 26F2 located south of the fault and screened in the minable coal sequence has notably lower heads than wells north of the fault in the same stratigraphic zone. However, recent boreholes drilled in the Sub-Red 1 Sand (PacRim, 2011) south of the South Pit fault show artesian pressures (nearly 40 feet above ground). This suggests other fault offsets south of the South Pit fault (i.e., see ‘Unknown’ fault identified by Hackett, 1977, north of BBF on Figure 2-6) probably also contribute to the strongly confined artesian conditions in this area.

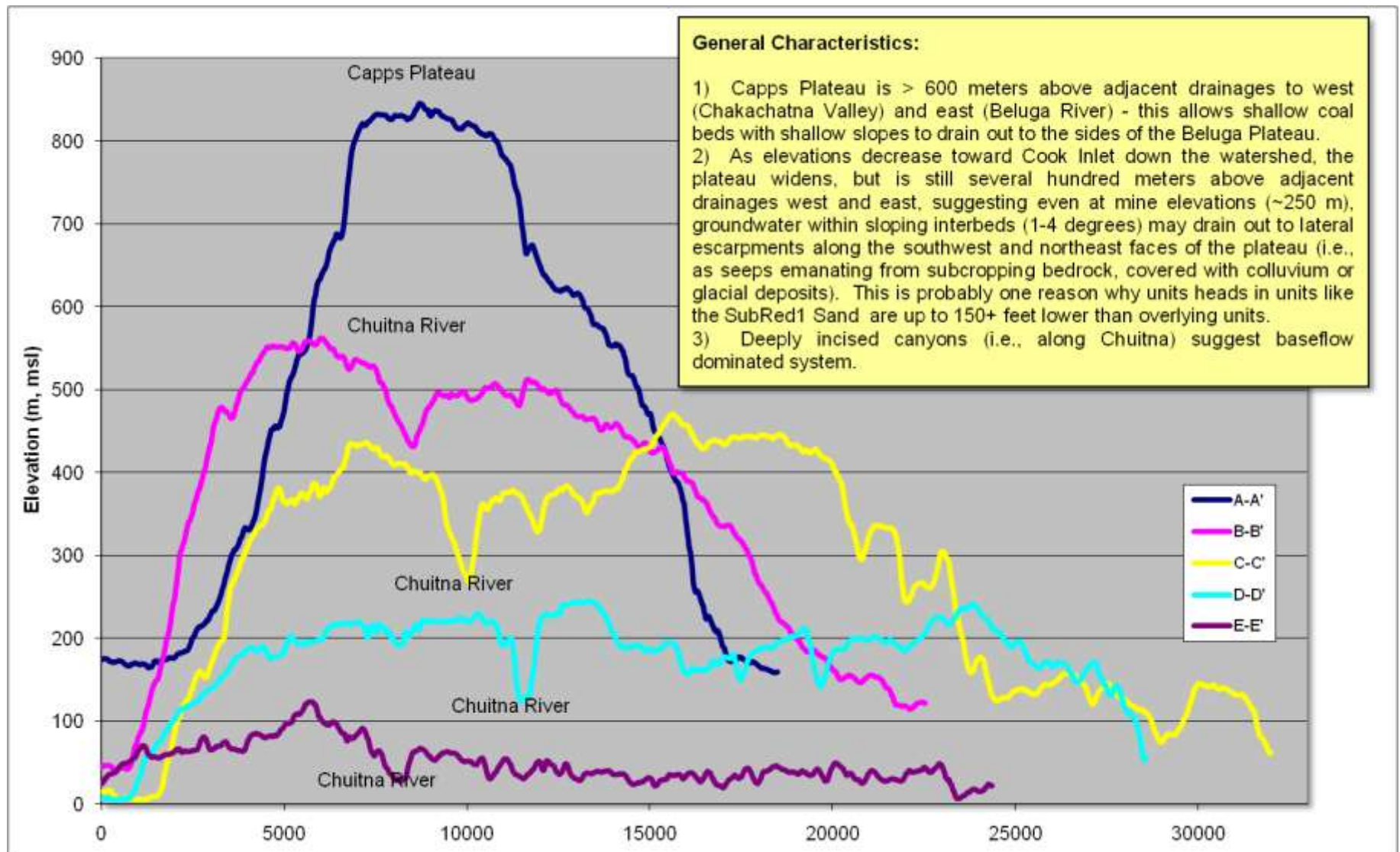


Figure 2-16. West-East Surface Profiles (looking North). Dimensions for X-Axis are meters.

Along the LCF, linear springs have been identified (Detterman, 1976), for example along the Lone Ridge Scarp, suggesting groundwater may flow along these features from depth and discharge to the ground surface, rather than just increasing pressures in lower strata.

Faults are also believed to have strongly influenced sedimentation within the basin (Finzel et al, 2009). Therefore, to fully understand how sediments were deposited within the Chuitna Watershed, one needs to fully understand where faults occur, how they were displaced and the timing of this displacement. This determines the depths and configuration of the overlying unconsolidated deposits.

2.5 Hydrology

2.5.1 Climate Data

Alaska climate is characterized by four main zones; maritime, transition, continental and arctic. The majority of Alaska falls within the continental zone (extreme temperatures and low precipitation), while the Chuitna Watershed is located within the transition climate zone (PacRim consultant: McVehil-Monnett Associates, Inc., 2006), which is between the maritime (coastal) and continental (inland) zones. In this zone, summer temperatures are higher than those in the maritime zone, while winter temperatures are colder and more similar to those in the continental zones. The climate zones are heavily influenced and bounded by large mountain ranges that control how shallow air masses flow between the zones. Proximity to coastal waters helps moderate (fewer extremes) weather in maritime/transition zones because water temperatures change very slowly.

This section describes climate data needed to support hydrologic modeling of the Chuitna Watershed. Input data to the hydrologic model includes precipitation, air temperature and a reference evapotranspiration (RET). The RET depends on other climate data including dew point temperature (used instead of vapor pressure), wind speed, net solar radiation, air temperature and precipitation. The spatial and temporal distributions of these data are described below.

2.5.1.1 Precipitation Data

The primary source of precipitation data used in this study is from the North American Regional Reanalysis (NARR). NCEP Reanalysis data are provided by the NOAA/OAR/ESRL PSD, Boulder, Colorado, USA, from their Web site at <http://www.esrl.noaa.gov/psd/data/gridded/data.narr.html>. The NARR dataset is a long-term (1979 to 2009), consistent, high-resolution (every 32-km) climate dataset for the North American domain, output every 3-hours, as a major improvement upon the earlier global reanalysis datasets in both resolution and accuracy. A number of consistent climate output variables are provided every 3-hours, which was useful in calculating RET values every 3-hours (http://www.emc.ncep.noaa.gov/mmb/rreanl/narr_archive_contents.pdf). Figure 2-17 shows the locations of NARR data points within the vicinity of the Chuitna Watershed, snow depth measurement sites and regional climate stations.

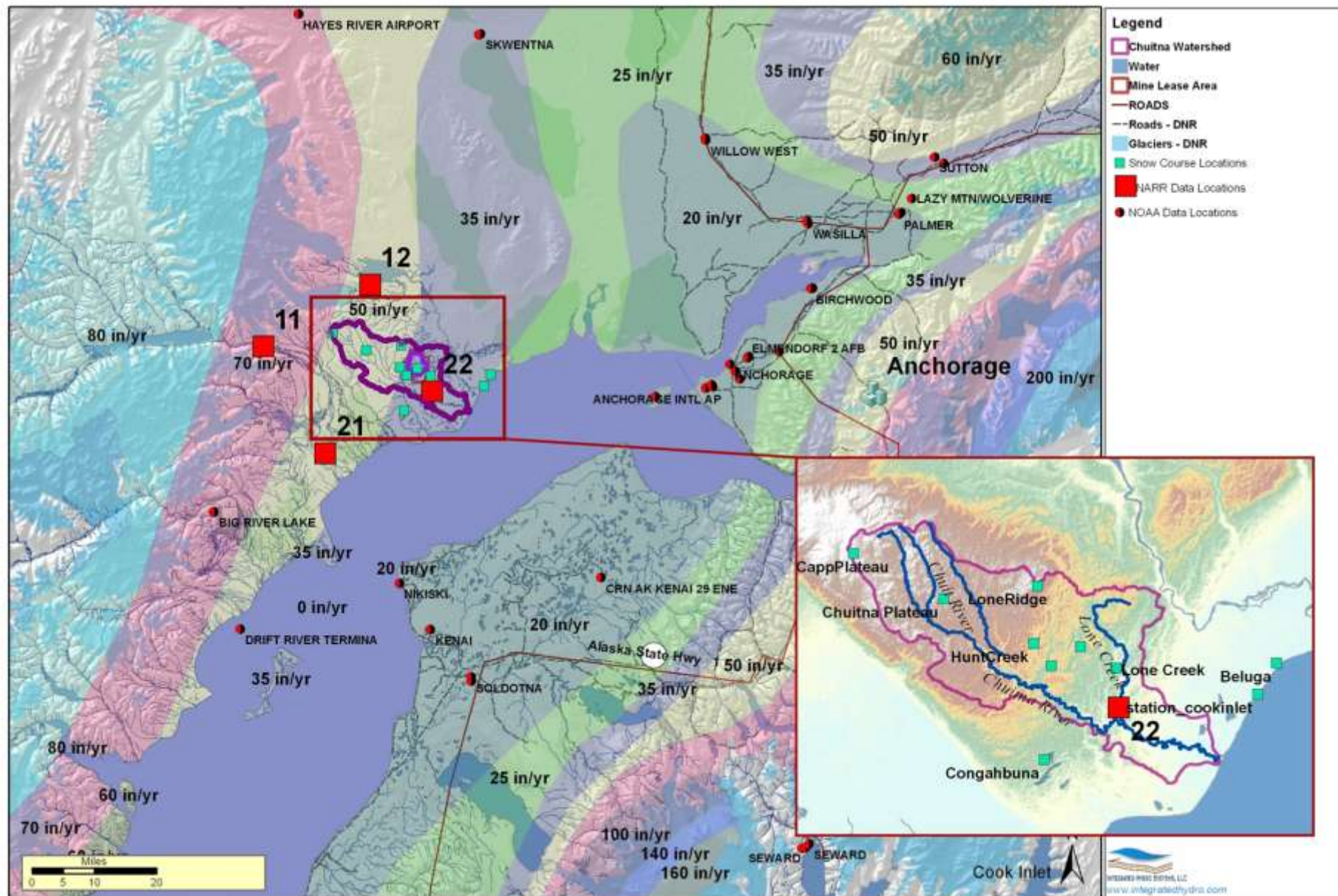


Figure 2-17. Local Climate Stations (NARR, PacRim, NCDC locations, snow course locations).

Available precipitation data within the Chuitna Watershed is limited. Eleven unheated, non-recording and 2 tipping bucket rain gages installed within the vicinity of the mining area in the early 1980s and generally at stream gage locations were reported to have issues (Riverside, 2007). As a result, no usable (i.e., sub-daily and accurate data at multiple locations) long-term data (i.e., years) exist within or near the watershed, except at the NCDC Beluga Station. Two new gages installed in December 2005 are heated, but only one is located near the mine and the other near Ladd Landing along the coast. This limits any long-term assessment of the spatial variability of precipitation at the site.

Annual estimates of precipitation based on the limited site data are also uncertain. Riverside (2007) states the following: “*Estimates of precipitation during the 13-month baseline period from the original baseline study (ERT, 1984) range from 38 inches at the coast (Shirleyville and Beluga) to 65 inches on Capps Plateau and 50 inches on the mine area. The average annual precipitation (September 1982 through August 1983) for the Chuit River Basin was estimated to be 48 inches. RTi used the average precipitation records at Beluga (about 20 years of record) and the snow course data (4 to 9 years depending on the site), to generate precipitation estimates. The average annual estimate range from 66 inches on the Capps Plateau, 44 inches on the mine area, to 28 inches at Beluga.*” These results suggest both significant variation in the spatial precipitation amounts and notable uncertainty in these values due to the lack of site-specific, long-term, spatially distributed climate data.

The long-term annual precipitation determined by Riverside (2007) at the Beluga station (75 feet elevation) and the mine site (800 feet), 28 and 44 in/year, respectively, were used to determine a lapse rate of 17% change in precipitation per 100 meters elevation. These values were iteratively tested using the integrated flow model and resulted in good correlation between observed and simulated surface flows, and snowmelt amounts and timing (described further in Section 5.3).

Annual precipitation values for four vertical elevation zones were developed using the calculated lapse rate. Annual precipitation is shown on Figure 2-18 for the original unmodified NARR data point 21 (on Figure 2-17) and an adjusted time-series for the 100 m elevation. The spatial distribution of average annual precipitation is shown on Figure 2-19. Summary statistics are summarized in Table 2-1. Average annual precipitation amounts range from 37.6 to 95.7 in/year for 100 m and 700 m elevations, respectively. The average 95.7 in /year of precipitation at 700 m elevation is higher than the 65 to 66 in/year estimates reported in the Riverside (2007) report, however estimates at the mine (800 feet) and Beluga elevation (75 feet) are reproduced well with this lapse rate. Data is unavailable in the upper Chuitna Watershed to confirm the higher precipitation amounts, but results of the hydrologic modeling (Section 5.3) suggests the model and these climate assumptions are able to capture long-term time-varying streamflow, baseflows and snow depths throughout the model well. Long-term monthly precipitation for the NARR data point 21 appear to compare well against the NCDC Beluga and Hayes River stations (Appendix B -).

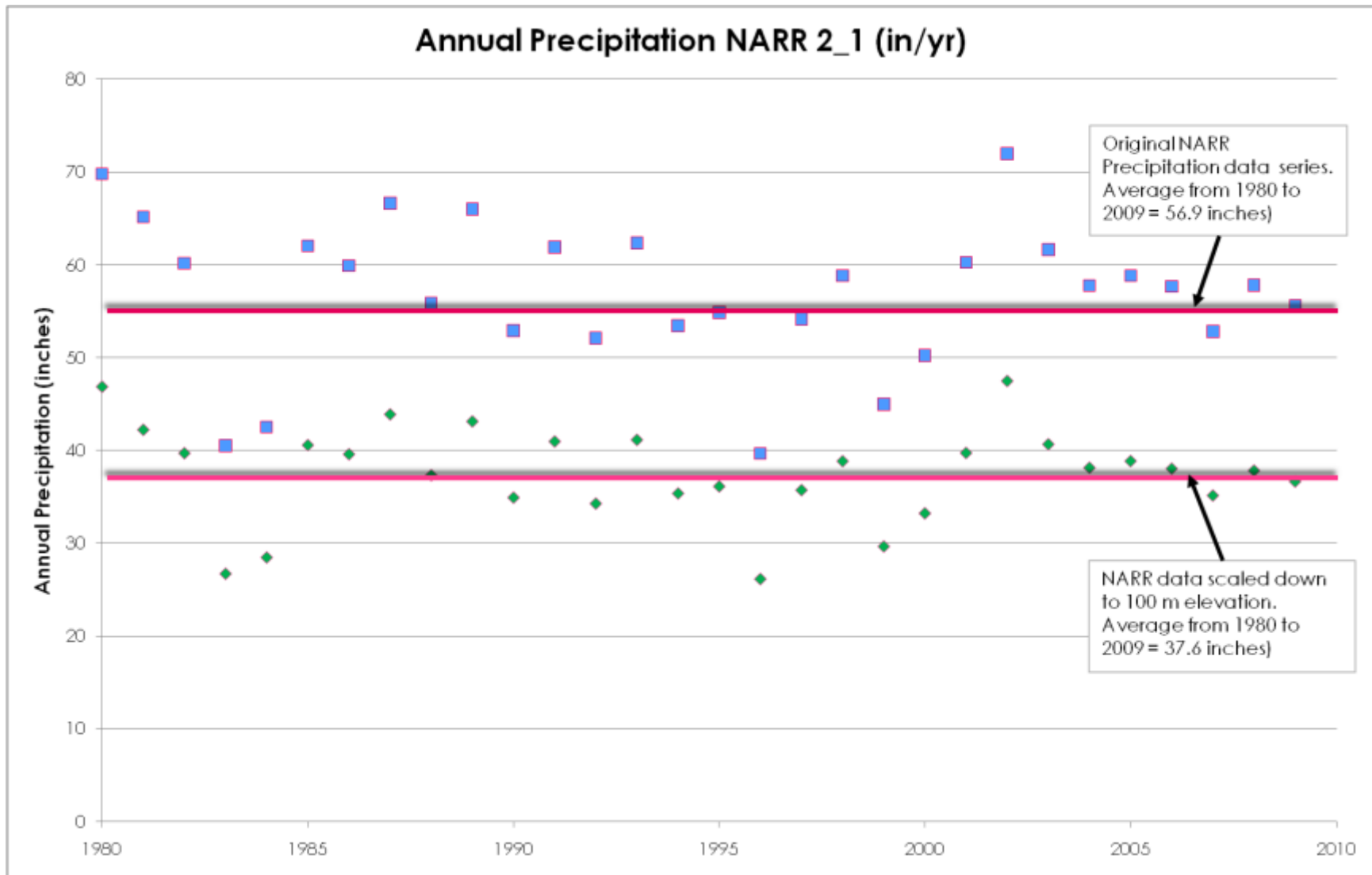


Figure 2-18. Annual Precipitation (in/yr) NARR Dataset (2_1)

Table 2-1. Summary Statistics of Annual Precipitation by Elevation

	100m	300m	500m	700m
Average	37.6	56.9	76.3	95.7
Maximum	47.5	71.9	96.4	120.8
Minimum	26.2	39.6	53.1	66.6
Standard Deviation	5.2	7.9	10.6	13.2

Seasonal statistics calculated for 1980 through 2009 for the NARR data point 21 precipitation dataset are summarized in Table 2-2. Average event intensities, average maximum event intensities, average event precipitation amounts and average event durations by season are included in the table. Results show relatively low average event precipitation intensities (0.5 to 0.6 mm/hr) with little seasonal variation, except slightly lower spring intensities. Average maximum intensities are highest in the fall (1.0 mm/hr) and lowest in the spring (0.6 mm/hr). Event durations average between 12.1 hours in spring to 14.7 hours in fall. Because these data are only provided at 3-hour intervals, it is likely they under-predict shorter-term event intensities, particularly during warmer months. Despite this, these data indicate that over the watershed precipitation, regardless of the season are generally characterized as low intensity and long duration.

Table 2-2. Summary of Seasonal Event Intensity, Precipitation and Duration

Season	Avg Event Intensity (mm/hr)	Avg of Max Event Intensity (mm/hr)	Avg Event Precipitation (mm)	Avg Event Duration (hrs)
fall	0.6	1.0	13.5	14.7
spring	0.5	0.6	9.4	12.1
summer	0.6	0.8	10.5	12.3
winter	0.6	0.8	12.2	14.2

Storm characteristics for the unadjusted NARR 21 data point from 1980 through 2009 are summarized graphically on Figure 2-20. Net precipitation and the number of storm events greater, where more than 0.01 inches falls in a 3-hour period (i.e., the measurement accuracy of recording devices) are shown in the left two graphs by season. The number of events varies by year, typically ranging from about 90 to 140 events. Fall and summer seasons have slightly more events, but are generally similar across seasons (25 to 35 events per season). The two graphs on the right show histograms of event durations and maximum intensities. The histogram indicates that 90% of the events last less than 30 hours and do not exceed 1.6 mm/hr maximum intensities. This is important because it confirms the low intensity, long-duration storm intensities and suggests, along with hydraulic properties of soils (Section 2.5.3.2) that infiltration is promoted over runoff throughout the watershed.

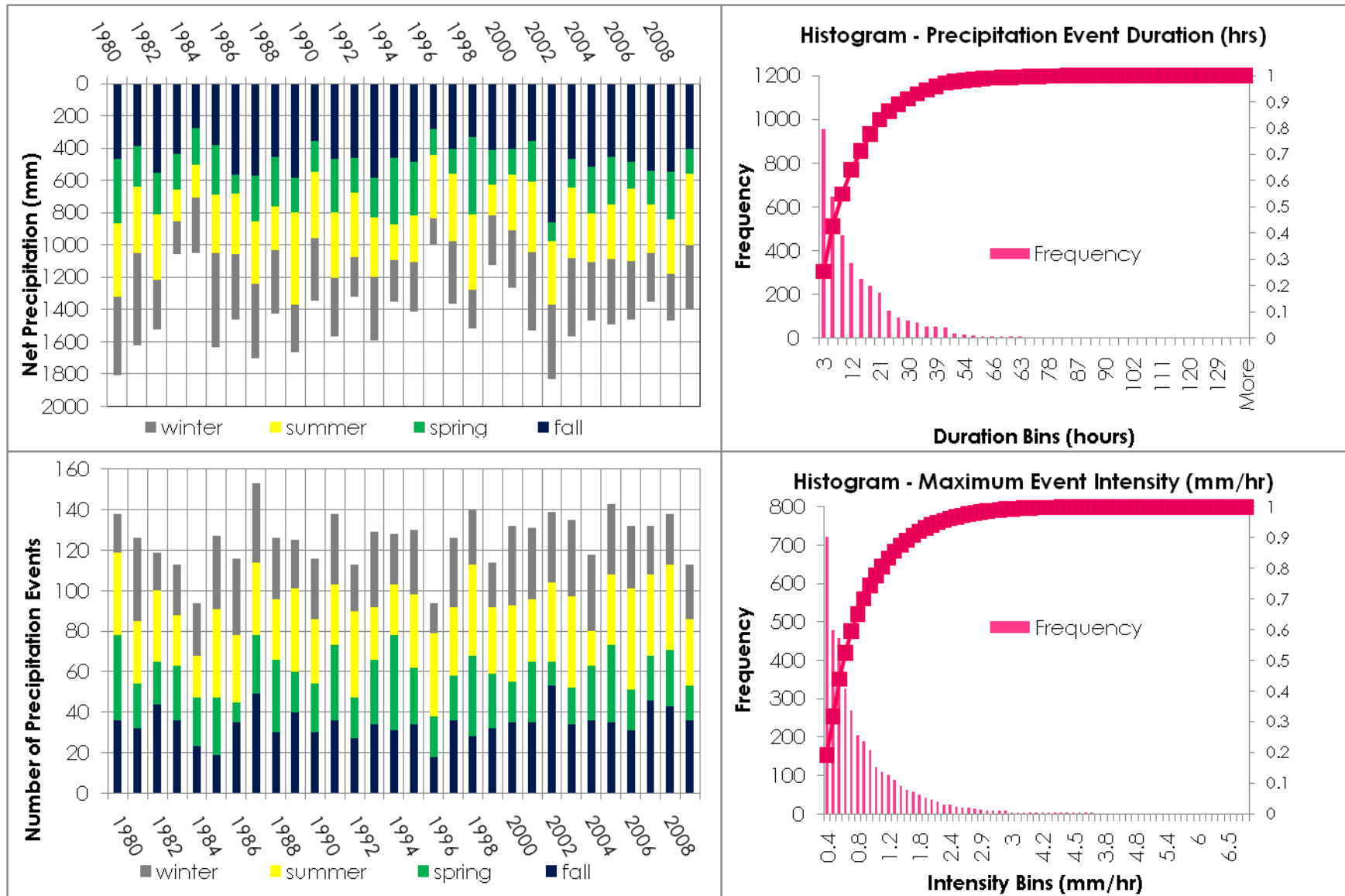


Figure 2-20. Storm Characteristics (non-elevation adjusted NARR dataset at 2_1).

2.5.1.2 Snow Course Data

Measured snow depths in time at different locations throughout the watershed are important data used in this study to calibrate the hydrologic model. Snow depths, in snow water equivalent (SWE), were measured at eight locations (see Figure 2-17) over the extent of the Chuitna Watershed (Riverside, 2007). Depths were recorded at the first of months for February through May. It is unclear whether attempts were made to estimate the snowpack for other months, such as June and November through January, when snow cover exists. Average annual depths were provided from about 1982 through 2006, but the actual number of years varies for each gage. In addition, measurements were also provided for all gages for 1983.

Data indicate that snow depths increase with elevation and melt-out sooner at lower elevations (i.e., Granite Point). Depths generally increase to a maximum in either April 1st, or May 1st. It is not possible from the available data to determine the exact date of complete melt-out, but the rapid increase and peak in spring streamflow suggests it melts relatively quickly, for example around June 1st or within a few weeks after. At Granite Point (lowest elevation, near Cook Inlet), melt-out in 1983 occurred prior to April 1st. All other stations showed significant SWE May 1st.

2.5.1.3 Air Temperature

Like the NARR precipitation data, air temperature also varies with elevation. As a result, an elevation lapse rate ($^{\circ}\text{C}/\text{meters elevation}$) had to be determined using the single NARR time-series at point 21 (Figure 2-17). Using the first of month snow depths at different locations, the integrated hydrologic code was used to iteratively determine an appropriate lapse rate for the air temperature. Details on the lapse rate are described further in Section 4.2.6.1.

Monthly average air temperatures for the NARR data point 21 are shown for the 4 elevation zones on Figure 2-21. Temperatures at 700 meters elevation exceed those at 100 meters by about 4 degrees. This is an important characteristic of the climate within the watershed hydrology and is a key reason (in addition to solar radiation) why snowmelt starts earlier in the spring at lower elevations and lasts longer in upper elevations. Standard deviation values are also shown on the plot for the 100 meter elevation band to illustrate how variability in monthly temperatures increases during the winter. This is an important characteristic because future climate changes are greatest during winter months and increase the potential snowmelt (temperatures $> 0^{\circ}\text{C}$), especially at lower elevations. This is one reason why it was important to develop spatial distributions of both precipitation and air temperatures.

2.5.1.4 Reference Evapotranspiration

The process of evapotranspiration is a critical component of the watershed hydrology. It controls the transfer of water from the land to the atmosphere. It includes water loss from

open water bodies, snow (sublimation), unsaturated soil moisture, plant transpiration and plant canopy. It is a complex process that depends on several climate variables, including air temperature and precipitation. Reference evapotranspiration, or RET is amount of water that is removed from a hypothetical crop where water is not limited.

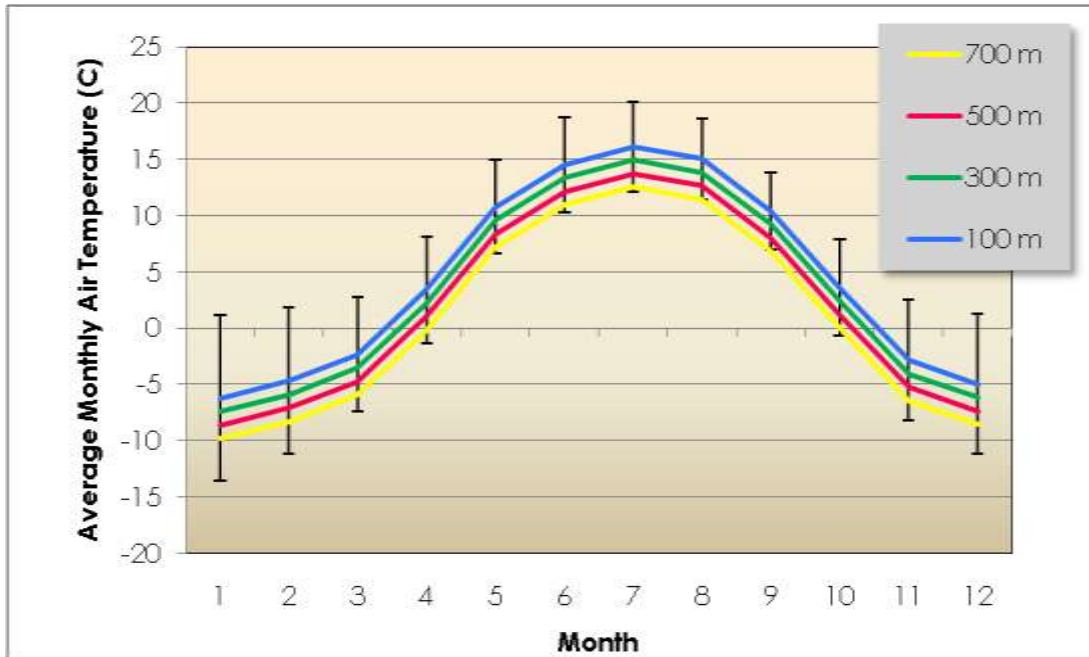


Figure 2-21. Average Monthly Air Temperatures – NARR data (point 21)

RET values for the Chuitna Watershed were calculated based on the FAO56 Penman-Monteith method outlined by Allen et al, 1998 for an Alfalfa reference crop. The Alfalfa reference was chosen because it is more similar to the vegetation within the watershed than a short reference like grass. The REFET code, developed at the University of Idaho, Reference Evapotranspiration Calculator Version - Windows 3.1

July 2008 by Dr. Richard G. Allen <http://www.kimberly.uidaho.edu/ref-et/> was used to calculate the RET values from 1980 to 2000 based on the following NARR climate data every 3-hours:

- Net Radiation
 - Summarize short- and long-wave radiation data (from NARR).
 - Summarize Net Radiation calculation (SW-LW).
- Dew Point (instead of vapor pressure)
- Wind speed (10 m height from NARR dataset)
- Air Temperatures
- Precipitation

The precipitation and air temperature time-series were varied by elevation (4 elevation zones including 100 m, 300 m, 500 m and 700 m) as described in Sections 2.5.1.1 and 2.5.1.3 to account for variations in RET with elevation. Effects of slope and aspect on RET were not considered in this study.

Annual average, maximum and minimum calculated FAO56 Penman-Monteith RET values for different elevations from the REFET code are shown in Table 2-3. Average RET values range from 25.8 in/year at 100 meters elevation to 21.2 in/year at 700 meters. The values drop with elevation because of the changes in temperature and precipitation with elevation. Newman and Branton (1972 report similar, though slightly lower average values (~19 to 20.5 in/year) for potential evapotranspiration values at the Matanuska agricultural station based on 40 years of data. Riordan et al (2006) reported potential evapotranspiration values ranging from 19.7 to 21 at Talkeetna and 22 to 23 in/year at Bettles using mean monthly temperatures and the Thornthwaite method.

Table 2-3. REFET FAO56PM RET Values by Elevation (in/yr)

	100m	300m	500m	700m
Average	25.8	25.5	25.2	25.0
Minimum	20.4	20.2	19.9	19.7
Maximum	28.9	28.6	28.3	28.0

Average daily RET values for 1980 are shown on Figure 2-22 (lower plot). The two upper plots show that the RET is strongly influenced by, and similar to daily air temperatures and net solar radiation (incoming long- and short-wave). Daily RET values are much higher in the summer due to increased air temperatures and radiation and can exceed 8 mm/day. During the winter, RET values drop to nearly 1 mm/day. RET is less influenced by the daily fluctuations in precipitation and wind speed shown on the upper and lower plots, respectively. During summer precipitation events, air temperatures cool, increasing cloud cover reduces the net radiation and RET values decline. As a result, during summer months, RET variability is much greater than during winter months. During winter months, the upper plot shows that the air temperature actually increases during precipitation events. This is likely due to the moderating effects of the maritime climate zone.

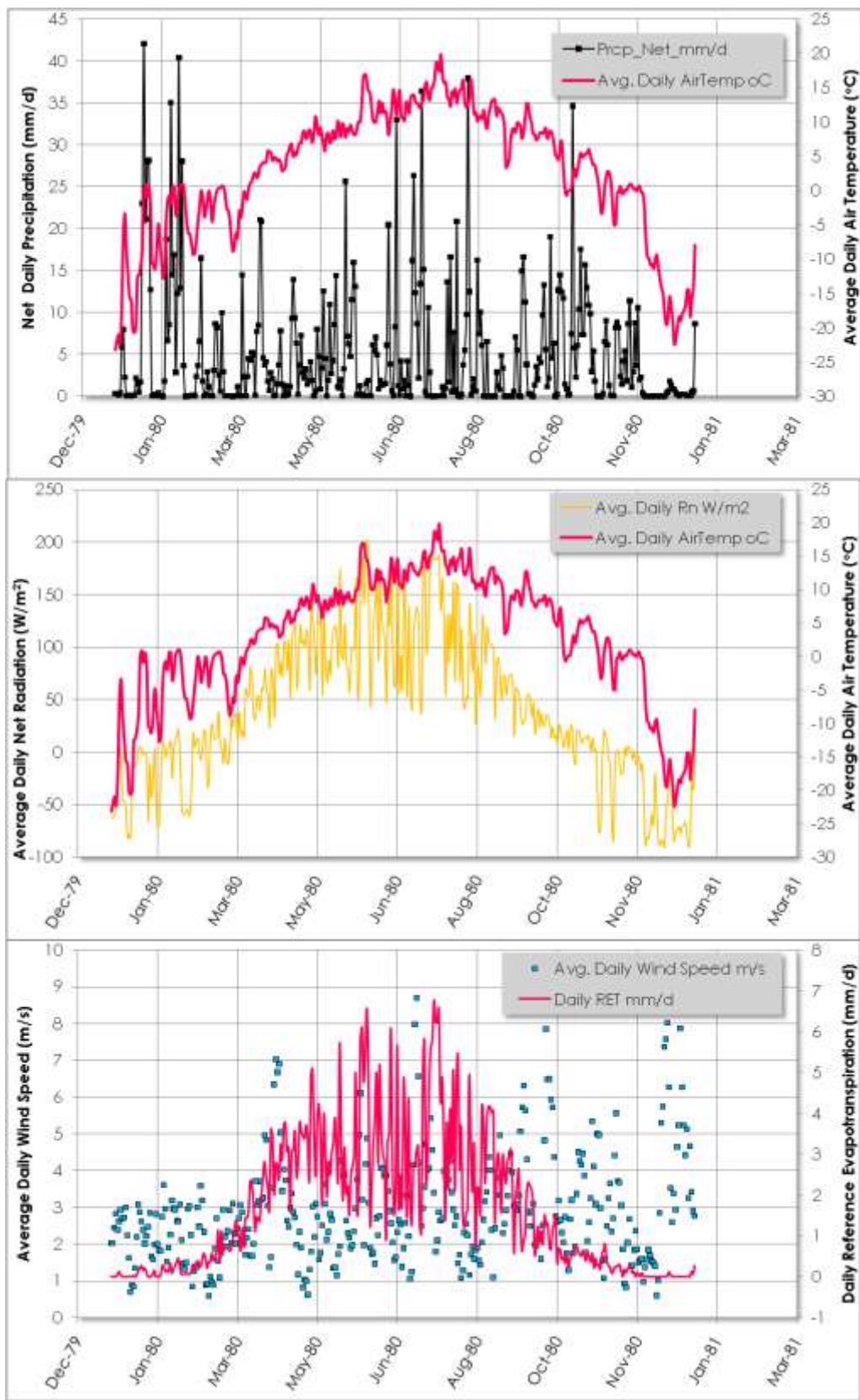


Figure 2-22. Average Daily Air Temperature, Net Radiation, Reference Evapotranspiration, Wind Speed and Precipitation (Example year 1980).

2.5.2 Surface Water

The following characteristics of the surface water flow system within the Chuitna Watershed are described in this section:

- Watershed areas and stream drainage network (Section 2.5.2.1),
- Pondered water areas (Section 2.5.2.2) and
- Stream flow data (Section 2.5.2.3).

2.5.2.1 Watershed and Stream Drainage System

GIS shapefiles of 12-digit Hydrologic Unit watershed boundaries for the Chuitna Watershed were downloaded from the U.S. Department of Agriculture, Natural Resources Conservation Service, National Cartography and Geospatial Center (<http://www.ncgc.nrcs.usda.gov/products/datasets/watershed/index.html>). Figure 2-23 shows eight 12-digit boundaries within the Chuitna Watershed, herein referred to as “sub-watersheds”. The boundaries were further refined in the sub-watershed areas so that they aligned with surface water gages also shown on Figure 2-23. The surface water flow gages shown are related to the proposed mining and were obtained from Table 3.1 in the surface water baseline study (Riverside, 2009). A USGS gage (15294450) originally located near Gage 230 in the Lower Chuitna sub-watershed monitored flows from 1975 to 1986, but was discontinued. Although no gages are located in the upper reaches of the Upper Chuitna River, Chuit Creek and 2005 sub-watersheds, flows are gauged at the lower ends of these drainages. Table 2-4 summarizes the drainage areas in square miles for the eight sub-watersheds. Approximately (Table 2-4) 185 miles of streams drain these sub-watersheds, or a total of about 150 square miles.

Table 2-4. Drainage Area

Drainage Name	Area (mi²)
Upper Chuitna River	37.7
Middle Chuitna River	7.9
Lower Chuitna River	21.1
Lone Creek (2002)	20.8
Lone Ridge (2004)	17.8
Chuit Creek	22.8
2003	14.0
2005	7.8

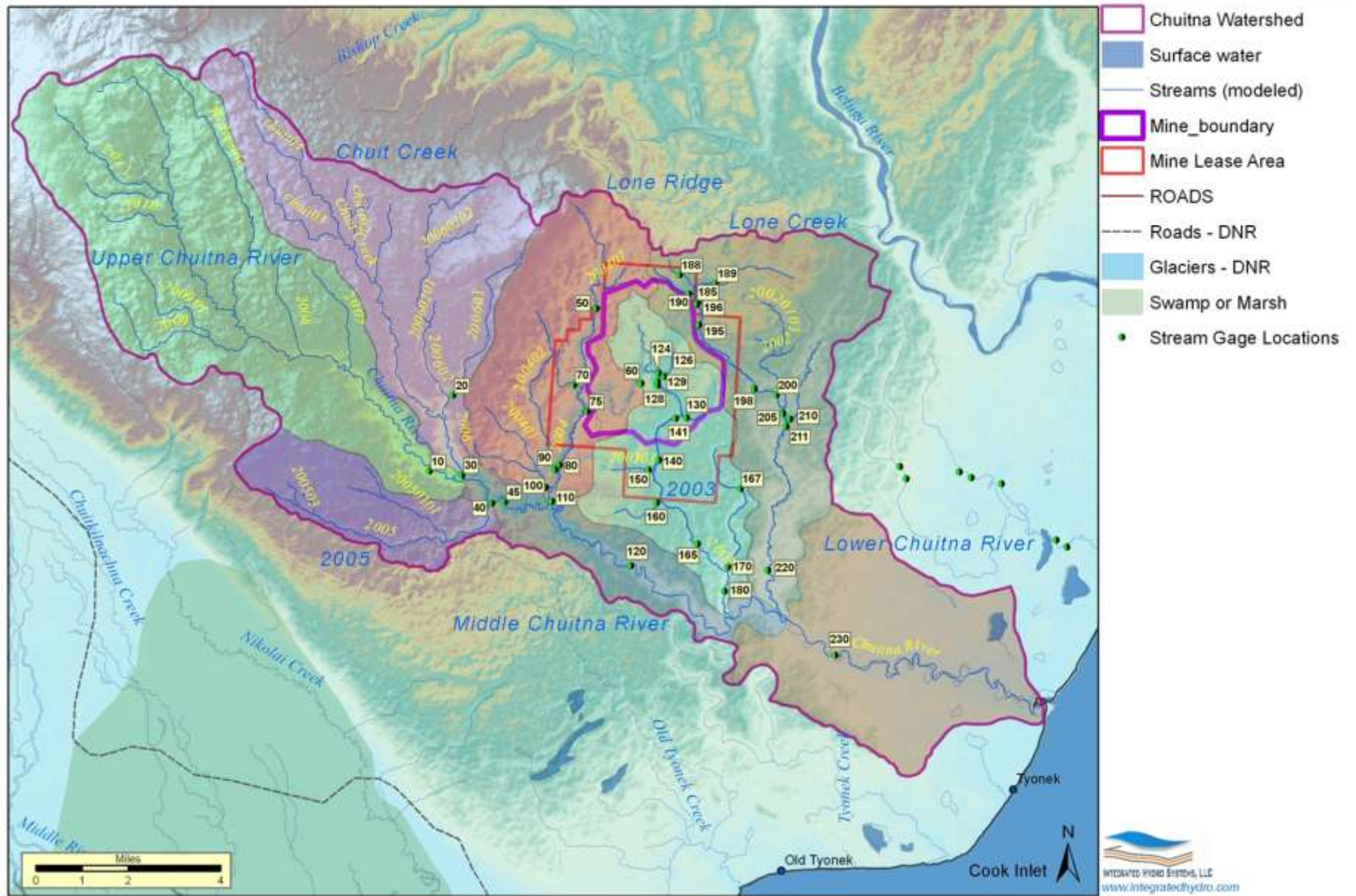


Figure 2-23. Sub-Watershed Scale Watersheds, Simulated Streams and Streamflow Gage Locations.

Note: Not all gages shown have data.

2.5.2.2 Surface Water Bodies/Wetland Areas

Figure 2-24 shows the approximate locations of surface water bodies identified based on review of DOQ review (Section 2.3) and USGS topographic quadrangle maps (250K and 7.5k). More than 700 surface water bodies occur throughout the Chuitna Watershed (about 2% of the total area) in local depressions where overland runoff accumulates and possibly groundwater. Riverside (2007) states “*surface of the glacial drift in this area is dotted with numerous small ponds, lakes, and bogs that are poorly drained. However, the water level data indicate that the depth to groundwater in the glacial drift ranges from 8 to 76 ft beneath the surface. These data suggest that in general, the surface water features are not directly connected to the water table. The numerous surface water features are presumably perched on low-permeability soils that mantle the surface of the glacial drift over most of the mine area. Most infiltration likely occurs in the better-drained wooded areas where soil conditions are more amenable to percolation.*”

No boreholes were drilled through surface water bodies, nor were shallow piezometers installed to test whether low permeability soils (relative to non-ponded areas) are present, or whether the surface water bodies are hydraulically connected with shallow groundwater. Monitoring the elevation of the surface water body over time could have also confirmed that surface water bodies develop and are maintained primarily by surface runoff, but this was not performed. Review of available groundwater levels (Appendix C1, Riverside, 2007) indicates that groundwater levels are at, or very near ground surface at many well locations within the proposed mine area, suggesting the surface water bodies are likely sustained at some level by groundwater discharge. A wetland functional assessment (HDR Alaska, Inc, 2008) seems to confirm this, particularly for wetland areas located at the toe of slopes. The exact hydrogeologic configuration that produce and maintain the surface water bodies cannot be determined due to lack of data in these areas, but several types of wetlands occur within the proposed mine area, including fens, bogs, beaver ponds, and vegetated wetlands. Bogs are wetlands where groundwater discharge into surface water is not significant. Fens are wetlands sustained by groundwater discharge. The wetland survey did not provide information on the relative degree of inflows from surface water runoff and groundwater discharge.

Ultimately this lack of data prevents describing these surface water bodies in the hydrologic model and predicting impacts due to climate change in them with a high level of accuracy. These are important hydrologic features that have been studied in Alaska because they may already show signs of climate impacts (Klein et al, 2005, Riordan et al, 2006, Klein et al, 2011).

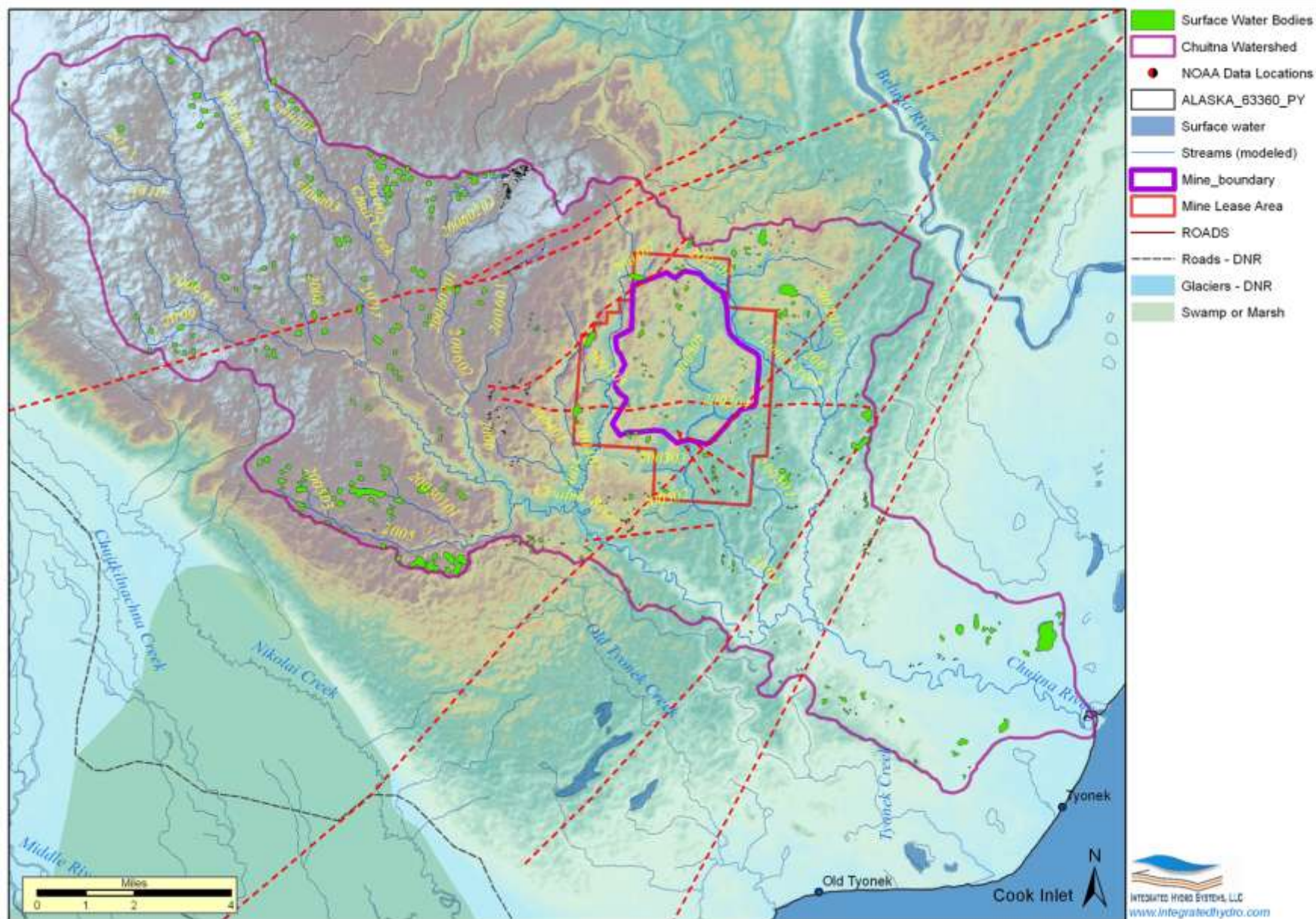


Figure 2-24. Surface Water Bodies (from USGS quadrangle, DOQQ inspection).

2.5.2.3 Stream Flow Data

Long-term daily streamflow data (water discharge records) were obtained for a number of flow gages shown on Figure 2-23 from Appendix B-5 in the Hydrology Component Baseline Study (Riverside, 2007). Data are available from 1982 through 2006, but availability is variable as seen in Table 2-5. The best period of overlap with the most gages occurs from 1982 to about 1985. From 1985 to 2006, streamflow data are only available along the lower drainages of 2003, Lone Creek (2002), 2004 and the Lower Chuitna. Instantaneous flow measurements are also provided for many of the gages in Appendix B-3 in the same Riverside report.

Mean daily streamflow (cfs) is plotted from mid-1982 to mid-1985 on Figure 2-25 for seven gage locations. The upper plot shows the vertical axis of streamflow ranging from 0 to 4000 cfs, while the lower plot shows the range from 0 to 500 to emphasize lower flow characteristics. Streamflow hydrographs at the different gage locations share similar characteristics. For example:

- Two main runoff events occur each year; spring snowmelt (April to June) and fall rainfalls (August to October).
- Based on instantaneous flow measurements, flows are typically lowest during the April-May time period; less than 0.5 cfs in small tributaries, less than 5 cfs in larger streams, and less than 50 cfs in the lower Chuitna.
- Streamflow generally increases downstream due to continuous baseflow contributions upstream. Flow contributions from 2003 (gage 180) and 2004 (gage 110) streams are typically 5% to 15% of the flow in the lower Chuitna (gage 230), while flows from Lone Creek (2002) are 10% to 20%. Flow in the Chuitna above stream 2004 (gage 45) contributes 40% to 75% of the lower Chuitna flow, depending on the time of year. For example, it is 40% in April 1st, when maximum snowmelt in the upper watersheds have not peaked. It is 75% by early June, when runoff from upper watersheds peak.
- Peaks streamflow typically occur during fall runoff (September and October)
- Peak streamflow volumes occur during spring runoff period (typically in May)
- Streamflow increases relatively rapidly during spring and fall runoff periods, but recede more slowly.
- Long recession curves are important characteristic of flow system caused mostly by groundwater baseflow, which is slow discharge (weeks to months) of groundwater held in storage within the unconsolidated deposits (or glacial/alluvium aquifer system).

The accuracy of streamflow measurements is hard to determine based on information provided in the baseline reports (Riverside, 2009). For example, streamflow measurements have been impacted in many gage locations by increased stages behind active beaver dams. In addition, ice formation also influences streamflow measurements. Riverside (2009) reports “*River ice formation and subsequent melting drastically affected stage discharge relationships*”.

Year ↓	Gage																
	230	20	45	50	80	128	120	110	129	140	141	180	195	196	198	200	220
1981																	
1982	153	157	163		153		156	159		159		159				166	158
1983	365	327	273	92	365		365	243		365		365	116			365	365
1984	187	218		57	217		188			144		207	189			346	60
1985	365						92	365		243		92	365		92	255	
1986	365						365	365				365	365		365		
1987	365						365	365				365	365		365		
1988	366						366	366				366	366		366		
1989	365						365	365				365	365		365		
1990	365						365	365				365	365		365		
1991	365						365	365				365	365		365		
1992	366						366	366				366	366		366		
1993	365						365	365				365	365		365		
1994	365						363	365				365	365		365		
1995	310						310	310				310	310		310		
1996	67							67									
1997	247							247									
1998												81					
1999	173							173				92	174				
2000	366							366				366	366				
2001	365							365				365	365				
2002	365							365				365	365				
2003	273							273				273	273				
2004								113				267					
2005												145		44			
2006									80	136		137	365		92		92

Table 2-5. Available days of average daily streamflow at gauged streams from 1981 to 2006.

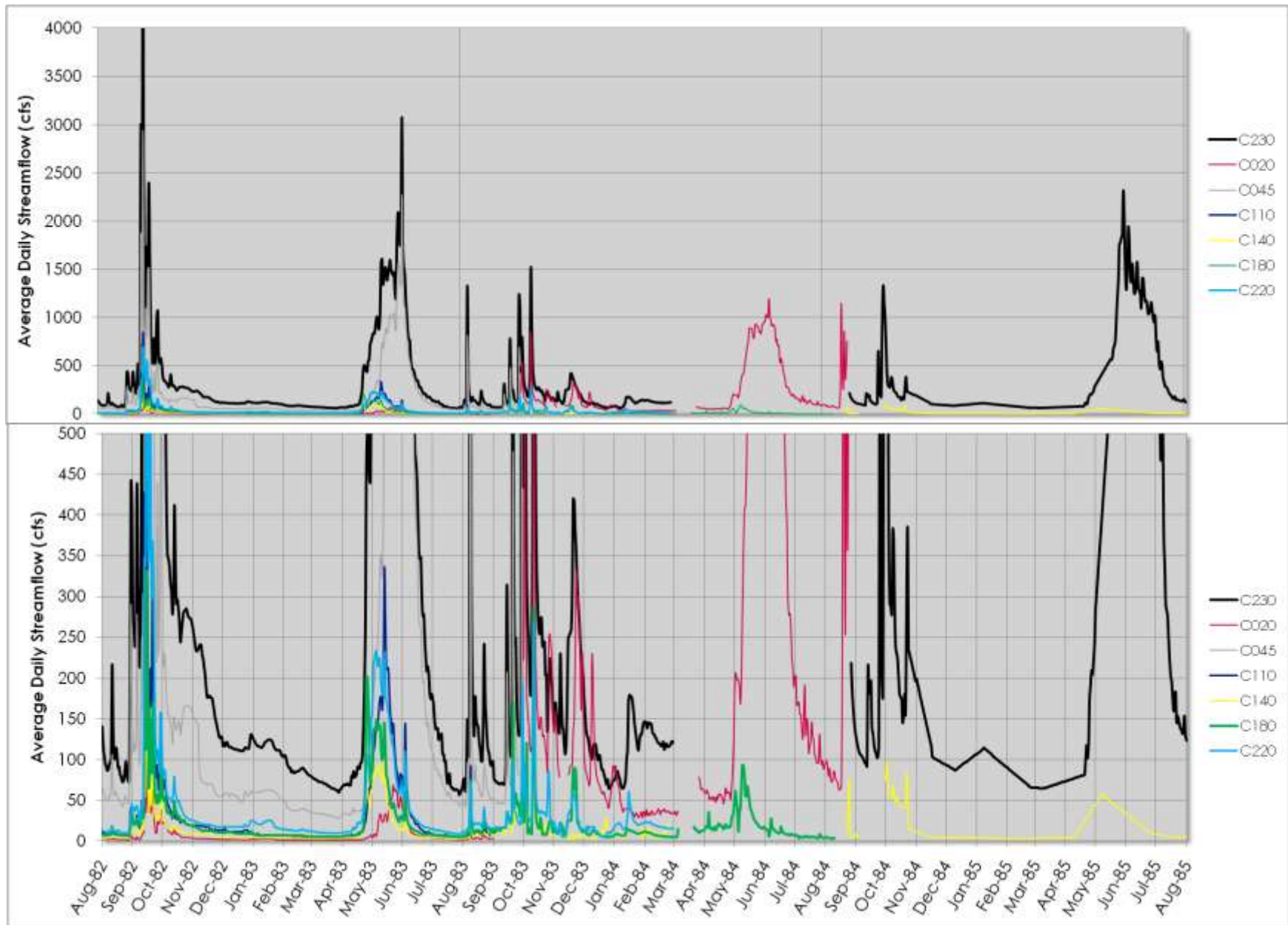


Figure 2-25. Long-Term historical Surface Water Daily Discharge (cfs) for gages 230, 180, 220, 110 and 45.

2.5.3 Groundwater

Characteristics of the groundwater flow system are described in this section. Groundwater aquifers and associated hydraulic properties are described in Sections 2.5.3.1 and 2.5.3.2, respectively. Areas where groundwater discharges to the surface as springs or seeps are described in Section 2.5.3.3. Groundwater wells screened through these aquifers are described next in Section 2.5.3.4. Finally groundwater depths and potentiometric surfaces are described in Section 2.5.3.5.

2.5.3.1 Groundwater Aquifers

Four hydrostratigraphic units (HSU) described in the area of the proposed mine in the groundwater baseline report (Table 4-2 in Riverside, 2010) make up an upper and lower aquifer zone within the Chuitna Watershed. The unconsolidated deposits, alluvium and glacial drift, represent the upper flow system, and a minable coal sequence and underlying Sub-Red 1 Sand represent the lower bedrock flow system. A description of HSUs beneath the Sub-Red 1 Sand is not provided in the Riverside report, probably because the proposed mining will not extend into the Sub-Red 1 Sand HSU. Descriptions of HSUs within the West Foreland and Beluga Kenai Group bedrock formations underlying glacial deposits in the upper and lower Chuitna Watershed areas, north of the LCF and south of the BBF, respectively are also undefined. However, because these bedrock formations share similar stratigraphies (i.e. interbedded conglomerates, siltstones etc) as the Tyonek formation beneath the proposed mine, they are assumed to have characteristics similar to the Tyonek HSU. All bedrock HSUs are therefore expected to exhibit limited hydraulic communication with overlying glacial units, due to the alternating beds of low and high permeability bedrock (i.e., coal/siltstone vs. sandstones). As a result, groundwater in HSUs below the Sub-Red 1 Sand probably contributes little to the upper HSU flow system.

PacRim geologists used more than 430 boreholes to construct a 3-dimensional geologic model of the subsurface. Because this model was not provided and only 20 of these boreholes were available, it is impossible to reproduce details of the separate coal beds and interbeds and overburden thickness. As a result, the minable coal sequence, like the PacRim groundwater consultant Arcadis (2007), this HSU is simply modeled as a single unit with a low vertical permeability.

The Sub-Red 1 Sand HSU is separated from the overlying minable coal sequence by a low permeability clay/silty clay bed that is up to 30 feet. Riverside (2010) states *“In most areas, a clay or silty clay bed (that is up to 30 ft. thick) separates the sub red 1 sand from the overlying minable coal sequence. The clay bed is assumed to behave as an aquitard separating it from the overlying hydrostratigraphic units.”* Even within the proposed mine area, the confining clay layer can be absent, providing a way for groundwater to flow between the minable coal sequence and the Sub-Red 1 Sand aquifer. No information was provided on the location and extent of the missing clay, or its thickness within the mine area.

The minable coal sequence in the proposed mine area ranges from 60 to 300 feet and consists of alternating beds of coal (0 to 25 feet) and interbed material consisting of loosely consolidated siltstones, mudstones, sandstones and conglomerates of highly variable thickness (5 to 180 feet). The southeastern area of the proposed mine area probably corresponds to the source channel for overbank deposits (interbeds of lower permeability) that occur between coal seams. In the southeastern area, the interbeds are coarser, and likely represent higher permeability zones of continuous sandstones/conglomerate (Flores et al, 1997). Flores et al 1994 also point out that significant sandstones/conglomerate occur along the entire length of the Chuitna between the LCF and BBF, suggesting permeability of the minable coal sequence increases from the mine area towards the west, or Chuitna (down dip).

The Quaternary deposit HSU (or Overburden aquifer) consisting of the distributed Holocene alluvium and peats overlying glaciofluvial and glacial deposits represents the uppermost aquifer zone that occurs throughout the Chuitna Watershed. It is assumed to occur in the upper Chuitna and lower Chuitna watershed areas based on the extent of glacial deposits mapped in the surficial geology (Section 2.4.4). Within the mine area, thicknesses range from 0 to 200 feet for the glacial deposits and 0 to 40 feet for the alluvium (Riverside, 2010). Outside of the proposed mine area, no information is available on the variability in thickness of these deposits.

2.5.3.2 Subsurface Hydraulic Properties

Hydraulic data for the difference HSUs identified throughout the Chuitna Watershed are sparse, and only available within the proposed mine area. Table 2-6 summarizes available hydraulic information based on testing and modeling.

Table 2-6. Summary of Hydraulic Properties for Hydrostratigraphic Units

Hydrostratigraphic Unit	Low Kh (ft/d)	High Kh (ft/d)	Low Kv (ft/d)	High Kv (ft/d)	Source
Peat (sapric to fibric)	0.03	79.3			Lett et al, 2000
Alluvium - assuming 40 ft thick	10	167			Riverside, 2010
Alluvium - streambed testing	0.0007	68			Oasis, 2010
Alluvium - observed	0.25	4.2			Arcadis, 2007
Alluvium - modeled	20	300	3	5	Arcadis, 2007
Glacial Deposits	10	60	0.1 - 1	0.6 - 6	Riverside, 2010
Glacial Drift	1.5	50	0.2	1	Arcadis, 2007
Intrusive Granodiorite - modeled	0.05		0.01		Arcadis, 2007
Coal Sequence - observed	0.00028	14			Arcadis, 2007
Coal Sequence - modeled	0.01		0.0009		Arcadis, 2007
Coal beds*	0.0028	14.2			Riverside, 2010
Interbeds (packer tests)*	0.00028	1.4			Riverside, 2010
Sub-Red 1 Sand - observed	1.3	8			Arcadis, 2007
Sub-Red 1 Sand - modeled	1	20	0.00002		Arcadis, 2007

*Values are likely higher by an order of magnitude because testing was done using packers.

In general, permeability decreases with depth. Alluvial material appears to be the most permeable material of the HSUs, though the local presence of clean gravels and sands within the glacial deposits can also be very permeable. Peats have variable hydraulic conductivities, but they typically are high in shallow layers (fibric) and decrease in deeper soil layers (sapric), where decomposition is greater (Letts et al, 2000). Although the peat is too shallow to really constitute a separate, continuous aquifer unit within the system, the hydraulic properties of this material are very important in controlling surface infiltration, groundwater recharge and overland runoff to streams.

By contrast, glacial deposits are much more permeable than the underlying minable coal sequence. This contrast is the primary reason why groundwater levels in the glacial deposits are higher than in the underlying minable coal sequence in the proposed mine area. Groundwater flow from the glacial deposits into the minable coal sequence is limited. No information was found on the vertical hydraulic conductivity of the coal seams themselves, but they are believed to be related to fractures (Riverside, 2010). The modeled vertical conductivity values for the Sub-Red 1 Sand are very low (0.00002 ft/d) because this reflects the presence of the clay layer mostly present within the mined area.

Rubblized zones along faults can represent either permeable conduits or impermeable barriers to groundwater flow. Because of vertical offsets along faults and artesian aquifer conditions (where groundwater levels are above ground surface) in wells near these faults within the proposed mine area, the faults are believed to act as impermeable conduits (Riverside, 2010, Arcadis, 2007). This may not be true however, along the LCF, in the Lone Ridge area, where a granitic intrusion is present (north side). In this area, Detterman et al (1976) reports the presence of a series of springs along the fault alignment. The fault plane in this area may represent a permeable zone, rather than a barrier. No hydraulic testing was performed to confirm fault permeability, and the vertical and lateral offsets, lateral extents of the smaller faults are quite uncertain due to the thick vegetation.

Specific yields of the different HSU material range from 0.13 to 0.2, except for the coal and granitic intrusion (0.01) based on groundwater modeling (Arcadis, 2007). Confined aquifer storage (specific storage) values were specified as $1e-5$ for all HSUs, except the coal sequence was specified at $1e-4$ based on modeling.

2.5.3.3 Springs/Seeps

Riverside (2009) in their Surface Water Baseline study state “*Stream reaches with significant inflow from springs or seeps were not evident in the immediate vicinity of the mine lease area*”. However, in a detailed spring and seep survey conducted in stream 2003 during their 2007 Piezometer study, Oasis Environmental (Appendix A, 2010) reported a different finding: “*The headwaters of stream 2003 contained a high concentration of spring seeps that cumulatively resulted in substantially lower stream temperatures relative to downstream locations.*” They also state “*Spring seeps were frequently observed along both banks longitudinally throughout this section of the river.*”

Oasis Environmental also states in their 2010 seep study along the 2002 and 2004 streams: *“Springs and seeps were identified in the field based on substantially cooler water temperatures relative to the mainstem channel. Dense vegetation as well as solar radiation on side channels and mixing with surface waters may have caused field staff to miss springs and seeps while traversing the reach. Consequently, this was not a comprehensive mapping of springs and seeps in portions of stream 2002 and 2004.”*

Based on the above findings, springs occur throughout the drainages and not just in the headwaters. Upwelling areas do not occur continuously along streams, but are distributed intermittently based on local landforms. Oasis reported 21 and 30 springs/seeps along 8 km segments of streams 2002 and 2004, respectively. Because no spring or seep flows were reported in this study, it is impossible to determine the net flow contribution of springs to streamflow. In addition, no effort seems to have been made to assess spring flow in the vicinity of faults.

2.5.3.4 Groundwater wells

Groundwater monitoring wells are only available within the proposed mine area. The number of wells decreases sharply with depth as shown on Figure 2-26. Only 5 wells are available in the Sub-Red 1 Sand, 11 in the minable coal sequence and 70 in the Quaternary deposits (overburden aquifer) were identified. Water level data is only available for some of these wells because coordinates were only provided for some of the wells. Although more wells have been installed in this area, many have been omitted from further analysis because of various problems (Riverside, 2010). Only the historical wells (yellow dots) shown on Figure 2-26 are believed valid and used in the groundwater modeling (Arcadis, 2007).

2.5.3.5 Groundwater Depths and Elevations

This section describes available groundwater depth and elevation information in the Chuitna River watershed. Groundwater elevations (and depths) measured over time are a critical dataset for calibrating the groundwater flow portion of the integrated hydrologic flow model. Two groundwater baseline studies were conducted, one in 2007 (Riverside, 2007) and one in 2010 (Riverside, 2010). Appendices summarizing the groundwater data were only available in the 2007 baseline study. Groundwater level data are available from 1983 to 1993 and in 2006 in Appendix C-1 (Riverside, 2007). Time-averaged (steady state) water levels were found in the groundwater modeling report (Arcadis, 2007).

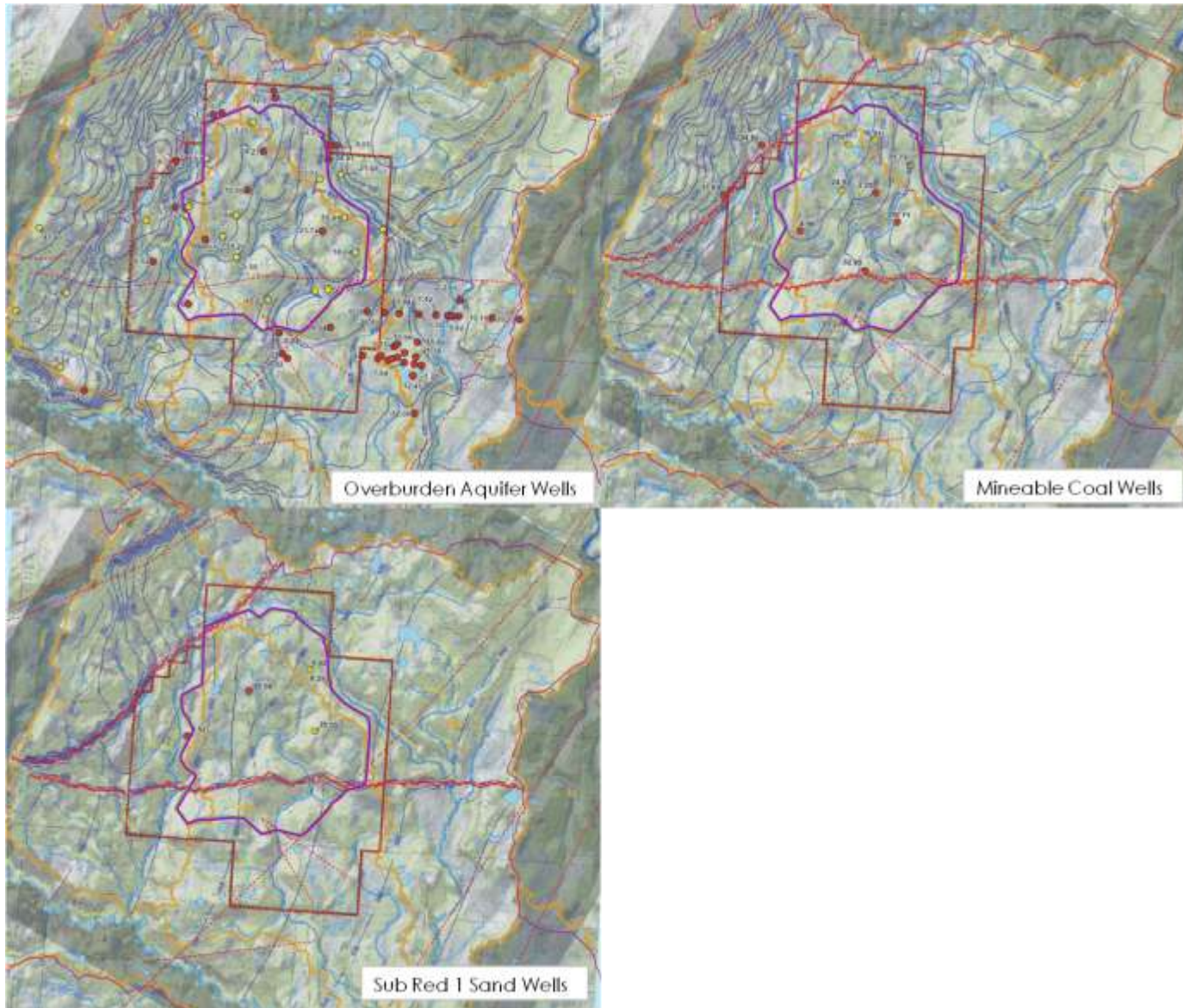


Figure 2-26. Groundwater wells and simulated water levels (Arcadis, 2007). Yellow dots are historical wells, red were measured in 2006.

A significant number of the wells within the proposed mine area appear to have uncertain water level measurements (1983 to 2009). Of the 106 monitoring wells listed in Table 4-5 in Riverside (2010), 29 were installed during or after 2006. Water levels were measured in 77 historical monitoring wells (1983 to 1993) within the proposed mine area. Only 58 of the 106 wells are used in the 2010 baseline characterization because of a number of problems. The 2010 groundwater baseline report (Riverside, 2010) states *“During the June 2006 site reconnaissance, 70 of the original 83 wells were relocated in the field. However, a number of the wells suffered from frost damage to the PVC casing that restricted access to the well for down hole measurements or sampling. A number of wells with water level data were excluded from the 2007 baseline characterization for reasons that included multiple zone completions and a lack of seal between zones.”* The basis used for determining that a well was damaged due to frost heave is unclear. This raises questions about the validity and uncertainty of water levels from all wells included in the baseline characterization.

The problem with wells screened across multiple zones with no seal is that, in the Chuitna Watershed groundwater flow system, pressures typically differ significantly across adjacent aquifer zones. Since individual aquifer zone water level measurements are needed to assess flow within the 3-dimensional groundwater system, wells screened across multiple zones do not allow measurement of a representative water level for individual aquifers. In fact, over time, wells open to multiple zones can significantly change local groundwater conditions, making it nearly impossible to understand the natural flow system, for example how faults impact flows, or the locations and rates of discharge. Another danger in using uncertain data is that models can be incorrectly calibrated to questionable data, yielding uncertain results. For example, some wells (i.e., 23C1, 26B2) excluded from both Riverside 2007 or 2010 baseline reports were included as calibration targets in the Arcadis (2007) model calibration.

In a related issue, given the cross-zone screening and lack of seals in many wells between zones in historical monitoring wells, long-term equilibration between zones may have also occurred between the Sub-Red 1 Sand, minable coal and Quaternary deposit HSUs via the more than 430 boreholes which would likely have penetrated all units (mostly exploratory holes). If these boreholes were not carefully backfilled with cement, it is possible that inter-borehole flow between the HSUs could have taken place, changing the natural state of the system over the proposed mine area. Over time (decades) this could have caused the long-term changes observed in many wells between the 1983 to 1993 and 2006+ monitoring periods (i.e., wells 06A2, 14A1, 15T, 20B1 etc).

Reported depths to groundwater range from approximately 8 to 76 ft below ground (Riverside, 2010), yet a number of wells have levels at, near, or even above ground surface (25J, 24L, 21K, 20C1, 25U, 26S, 27A1, 27H1, 28H2, 28M, 25A1, 35G1, A03A, A15A, G01B, G14A, G15A, G28A, G33A). Groundwater depths at wells where coordinates could be determined (42) were averaged over time and are shown on Figure 2-27. For wells shown, average depths are 8.3 m, and the minimum and maximum depths are 0 to 63.7 m. The plot clearly indicates a trend where groundwater depths are shallow in stream areas, and generally deepen with distance from streams (upland areas),

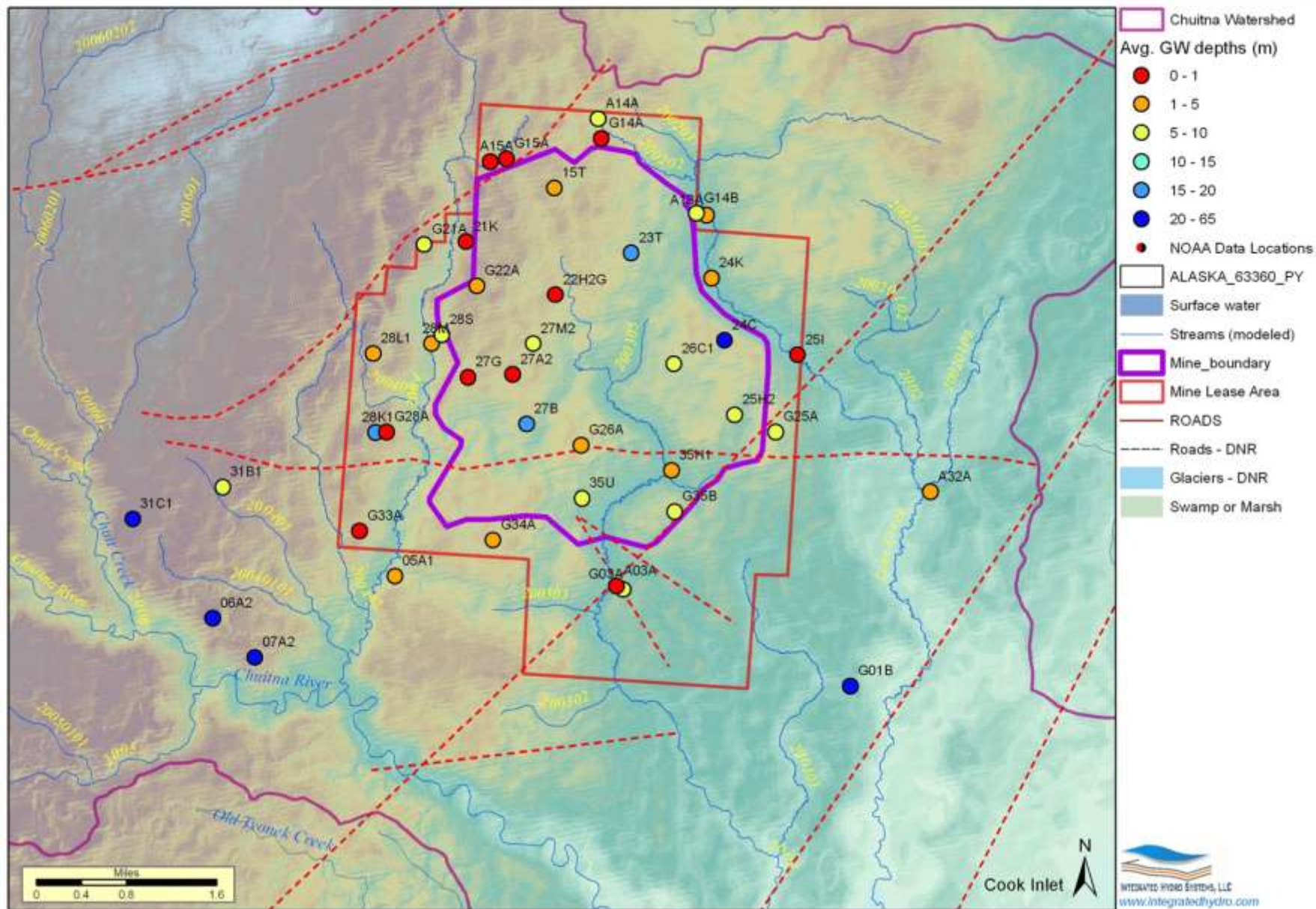


Figure 2-27 . Available Groundwater Depths for Quaternary Deposits (Wells in Alluvium and Glacial Deposits)

but this is not always the case. Groundwater depths in upland areas can actually also be very shallow (< 1 m), for example due to locally lower hydraulic conductivities. Time-averaged groundwater depths are greatest (20 to 65 m) near the Chuitna and in southern Lone Creek, possibly because interbed material within the minable coal sequence transition into more permeable sandstones and conglomerate in these areas.

Riverside (2010) states “*With the exception of well 06A2, all wells show an increase in water levels for the 2006-2010 period compared to the 1983-1993 period.*” They also state “*The water levels in the glacial drift exhibited variations ranging from less than one foot to 22 feet over the monitoring period in individual wells.*” Groundwater depths (Appendix C-1, Riverside, 2007) in some wells (even those included in the baseline report) however, show greater changes, such as 06A2 (~17.4 m) and 24B2 (~44.5 m) during the monitoring period. Although 24B2 wasn’t included in the baseline report, this may be an example where the significant increases in groundwater depths are caused by re-equilibration of the aquifer system to cross-screened aquifer zones. The change in groundwater depths over the monitoring period appears to be less in alluvial wells, probably because of the moderating effects of the nearby relatively steady stream stage elevations.

Arcadis (2007) reported that seasonal groundwater level variations in the Quaternary deposits range from less than 1 foot to up to 5 feet. However, time-varying groundwater depths in Appendix C-1 show that measurements have not been collected at a frequency necessary to capture true extent of seasonal variation (intermittently and monthly to quarterly at best). It is likely that variations in levels are greater than reported over key recharge events such as spring runoff and fall rains. Modeling results (Section 5.3) also seem to support this. Screened across the blue coal, well 19A1 shows a 7.3 m change from June to July 1983. Other wells show greater seasonal variations than 5 feet, such as wells 21J, 22D3, 26C3, 35A2, 35A3 (10s of feet).

Head differences in well pairs screened through the unconfined Overburden aquifer (above the minable coal) and the Sub-Red 1 Sand are significant in the proposed mine area. Only three well pairs were found, but heads in the upper aquifer exceed those in the Sub-Red 1 Sand by 93 to over 180 feet. This strong downward gradient implies that the Sub-Red 1 Sand aquifer is strongly confined, or hydraulically disconnected from the upper aquifer. Data are insufficient to determine a flow direction in this lower aquifer, or what role faults play in controlling the flows.

No potentiometric or water table maps were prepared in the baseline studies. This is a standard step in characterizing groundwater flow systems and is used as the basis for inferring groundwater flow directions. The only groundwater surfaces prepared were based on groundwater modeling (Arcadis, 2007) and are shown as contours on Figure 2-26. Because the surface contours are simulated, they do not exactly match observed data and reflect assumptions imposed in the modeling. Potentiometric surfaces could not be prepared in this study using the depths to groundwater in Appendix C-1 (Riverside, 2007) because available top of casing (TOC) elevations did not line up well with the available ASTER Topography dataset. As a result, it is difficult to determine the true

direction of groundwater flow within the glacial deposits, minable coal and Sub-Red 1 Sand HSUs. Based on available data, at a watershed-scale, groundwater generally flows in an east-southeast direction, similar to the overall topographic gradient, and locally it flows towards surface streams in the shallower units in most locations, and in deeper units where they are eroded (i.e., Upper Lone Creek).

2.6 Vegetation

A GIS shapefile distribution of vegetation types (2000 to 2003) across the Chuitna Watershed was obtained from the U.S. Geological Survey’s National Land Classification Database (Homer et al, 2004) at <http://www.mrlc.gov/>. Although this original dataset included 16 vegetation classifications, including open water and perennial ice/snow, for the purposes of the modeling conducted in this study, these were combined into the 7 categories shown on Figure 2-28. The final 7 vegetation zones and their areal coverage within the Chuitna Watershed are summarized in Table 2-7. The two predominate types of vegetation are Shrub/Scrub <5 m height (53%) and Deciduous Forest (38%). The Shrub/Scrub occurs almost exclusively in the upper Chuitna Watershed, while the Deciduous Forest is distributed throughout the middle and lower Chuitna watershed areas. Open water areas correlate well with those identified on the basis of DOQ imagery and USGS quadrangle maps.

Table 2-7. Areal coverage of vegetation types

Type	square miles	%watershed
Deciduous Forest	56.5	38%
Evergreen Forest	1.5	1%
Emergent Herbaceous Wetlands	9.0	6%
Shrub/Scrub (<5 m height)	79.3	53%
Dwarf Scrub (<20 cm height)	2.9	2%
Barren Land	0.1	0%
Open Water	0.8	1%

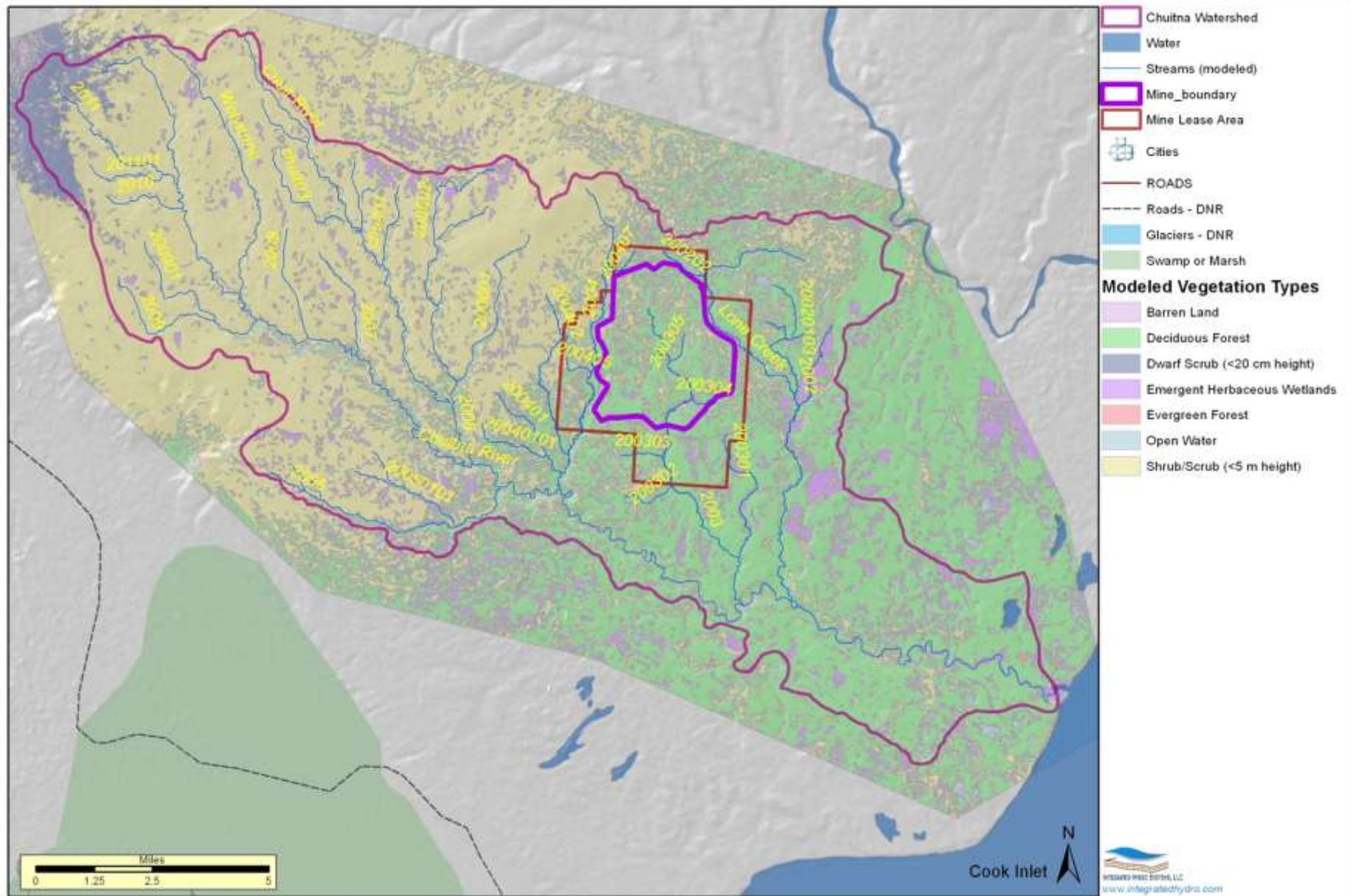


Figure 2-28. Modeled Vegetation Distribution

3.0 Conceptual Integrated Hydrologic Flow Model

In a basic sense conceptual flow models are used to describe both the processes and pathways associated with how water flows into, through and out of the watershed. These models are critical to the successful development of subsequent mathematical flow models and are typically the primary source of uncertainty introduced in numerical model predictions. If underlying processes or flow paths are poorly understood, the numerical model typically fails to predict hydrologic responses. Nueman and Wieranga 2003 (<http://www.nrc.gov/reading-rm/doc-collections/nuregs/contract/cr6805/cr6805.pdf>) summarize characterization and conceptualization of hydrologic systems in detail and point out the need to assess multiple conceptualizations, especially in systems where data are sparse. This accounts for our lack of information and understanding of flow paths and processes. Often alternative conceptual flow models are omitted from further consideration, when one out performs the other. The process of testing alternative conceptual models is iterative with the integrated numerical modeling as described earlier on Figure 1-3. Conceptual flow models for the Chuitna Watershed hydrologic system are described first in Section 3.1. This is followed by a brief description of data gaps in Section 4. It is useful to point out gaps in data after developing conceptual models, because implications of the data gaps translated to later numerical modeling become more apparent.

3.1 Conceptual Flow Models

The conceptual integrated hydrologic flow model developed in this study differs from the groundwater conceptual model developed for the local proposed mine area (Arcadis, 2007). For the integrated model, all of the hydrologic processes that influence the hydrologic responses observed in the system, for example streamflow or groundwater levels must be described. This is more challenging than developing a conceptual model for just the groundwater system, but it is also essential because it forms the framework for developing the fully integrated numerical model described in more detail in Section 4.0. The conceptual flow models are described similar to how the integrated flow code operates (see Section 4.0).

Conceptual models are described in the following sequence to illustrate how the local-scale processes and pathways translate into the more complex and cumulative hydrologic responses observed at the full watershed-scale.

- Snowmelt
- Unsaturated zone flow processes, including evapotranspiration,
- Hillslope hydrologic processes
- Watershed-scale hydrologic processes

Typically water quality and temperatures are described, but this is outside the scope of this study.

3.1.1 Snowmelt Conceptual Flow Model

Snowpack and subsequent melting of the snow represent important processes and a large source of water in the Chuitna Watershed hydrologic system. As such, it is important to describe how snowpack develops, is converted to snowmelt, or lost to the atmosphere. A generalized watershed hillslope section along with various snowmelt processes is illustrated on Figure 3-1.

When air temperatures fall below freezing, precipitation occurs as ‘dry’ snow on the ground surface, or canopy. If temperatures remain below freezing, continued precipitation will add to what is referred to as snowpack. During the course of a day and depending on the specific climate conditions, several different (USACE, 1998) energy processes can act individually, or together to reduce the snowpack (ablation). These include:

- Net radiation (net short- and long-wave radiation),
- Sensible heat flux (air convection) between the snow surface and the air,
- Latent heat flux associated with vapor evaporation (loss to atmosphere) and condensation (gain to snowpack),
- Conductive energy flux between the ground surface and subsurface and
- Advective energy contained in rain (i.e., rain on snow).

Net radiation, sensible heat and latent heat are the largest sources of heat in melting snow. The relative degree to which one dominates varies widely, and depends on many factors (USACE, 1998). When enough heat is added to the snowpack, liquid water (snowmelt) forms and infiltrates to the base of the dry snowpack and becomes ‘wet’ snow. Once the storage capacity of the wet snow is exceeded, snowmelt can either re-freeze, infiltrate, or runoff. Gray and Prowse (1992) state that the single most important factor that determines whether snowmelt runoff, or infiltrates is the ability for the water to infiltrate frozen soils. Generally, the ground remains unfrozen beneath deep mountain snowpack and frozen in areas of shallow snowpack with extended periods of sub-freezing temperatures. Even where frozen, snowmelt can still infiltrate into the ground (Sutinen et al, 2009), through cracks, or macropores, though the rate depends on a number of factors, including amount of ground cover, soil hydraulic properties and depth of freeze. Surface runoff increases the more frozen the soils are.

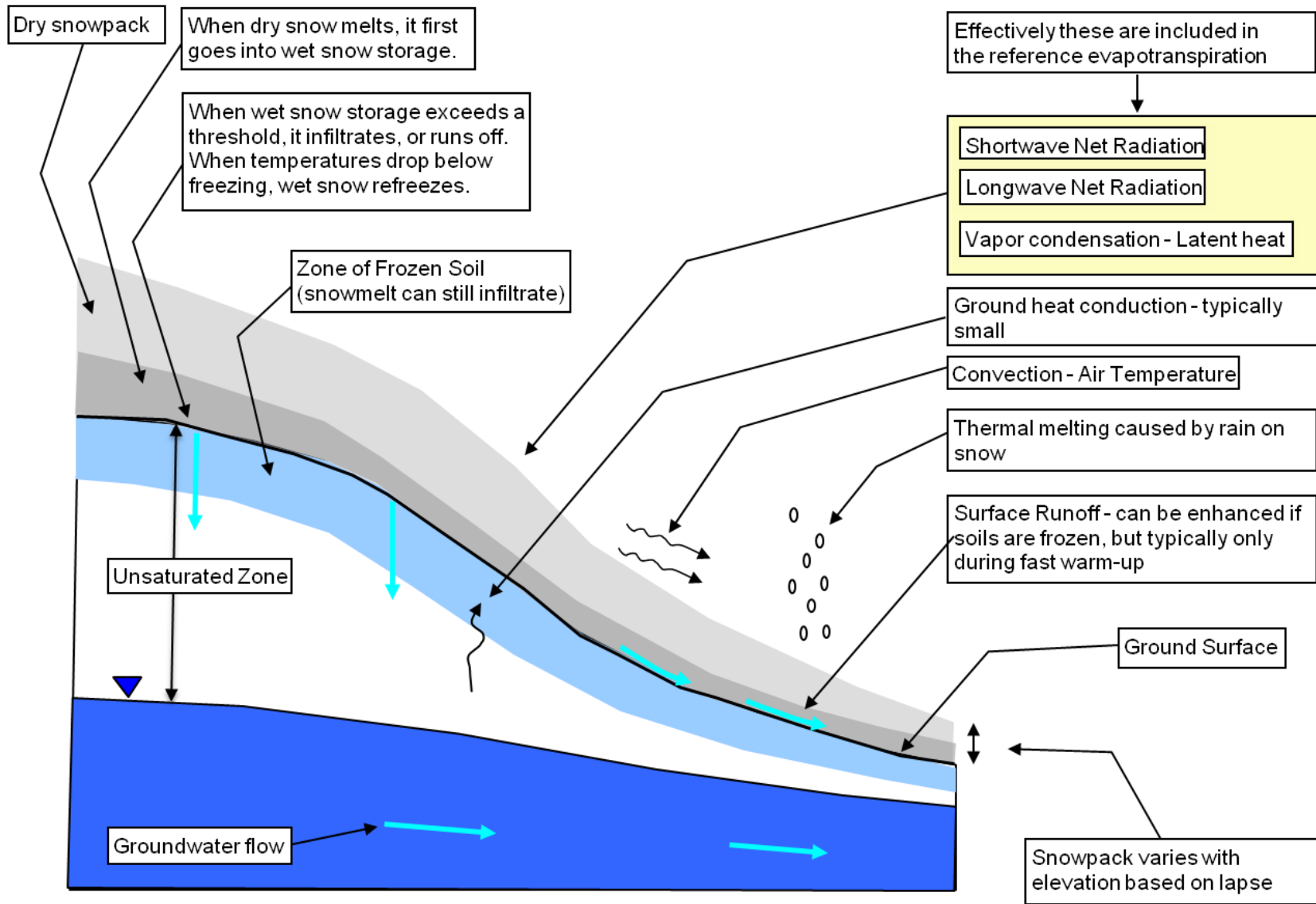


Figure 3-1. Conceptual Snowmelt Model

3.1.2 Unsaturated Zone Conceptual Flow Model

A generalized unsaturated zone column extending from ground surface down to the groundwater table is shown on Figure 3-2. Shallow peat soils cover much of the surface of the Chuitna Watershed (based on the occurrence in the proposed mine area) and become increasingly decomposed with depth, for example, fibric (slightly), hemic (moderate) and sapric (strong). Soils typically transition from the peats into permeable Quaternary glacial or glaciofluvial deposits that overlie the minable coal sequence.

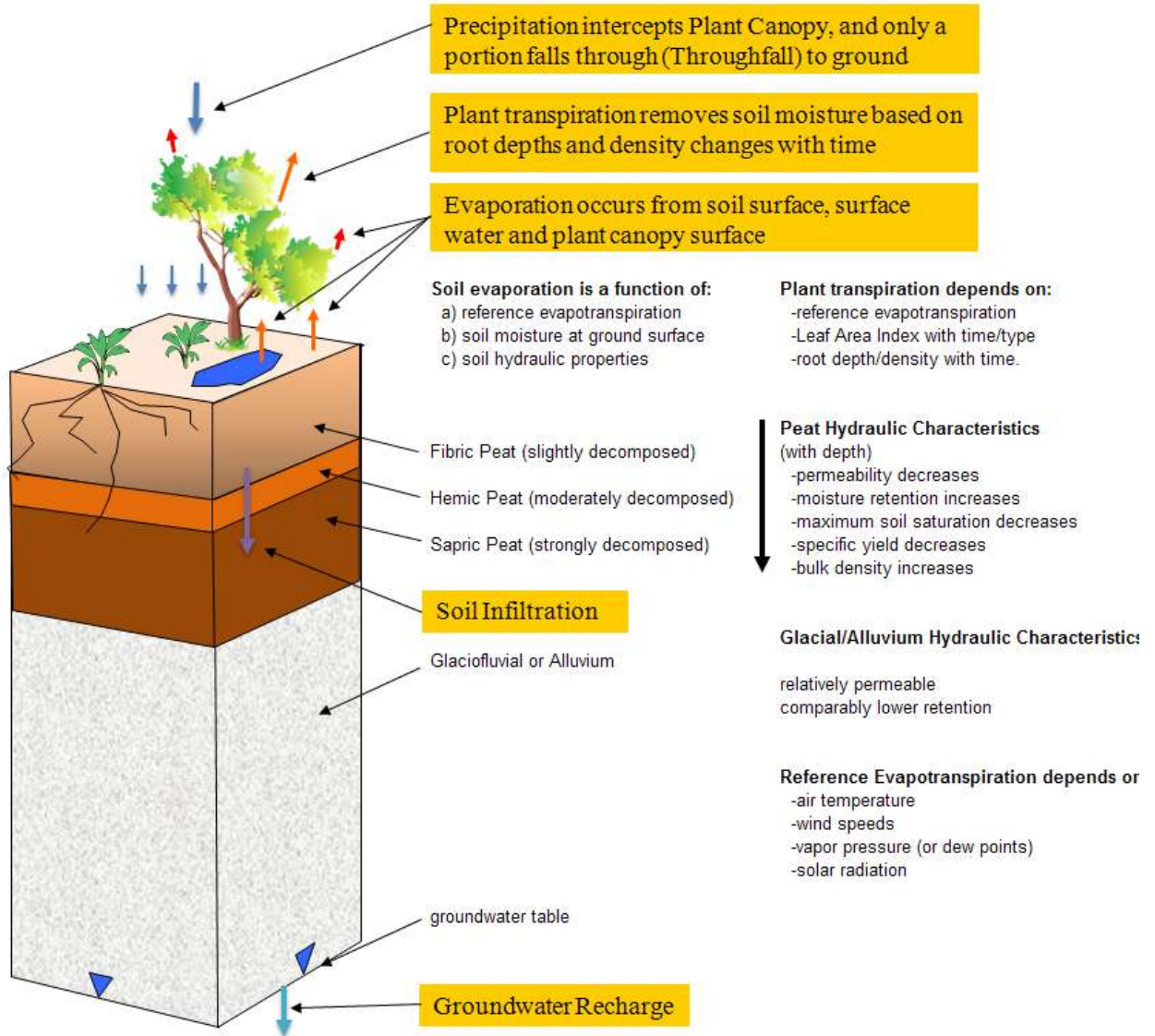


Figure 3-2. Conceptual Flow Model – Unsaturated Zone

As precipitation reaches the land surface, a portion of it is intercepted by the vegetation canopy, where it is eventually evaporated back into the atmosphere. The rest falls through to the ground surface as ‘throughfall’. The throughfall then begins to infiltrate

the ground surface, increasing soil moisture while the precipitation continues. At the soil surface, a portion of the water available to infiltrate is lost via soil evaporation to the atmosphere. A portion of water is also removed to the atmosphere as it infiltrates downward, past the root zone, via plant transpiration. The combination of soil evaporation and plant transpiration is termed 'evapotranspiration'. The portion of infiltrating water that remains past the root zone continues to flow through the unsaturated zone and eventually recharges the shallow aquifer (Quaternary deposits).

The soil moisture content in the unsaturated zone is directly affected by the infiltration, groundwater recharge and evapotranspiration processes. These processes and soil moisture are dynamically linked to changes in climate and strongly related to the spatial variability of hydraulic properties of soils across the Chuitna Watershed. Results of integrated modeling show that the hydrologic response of the system to annual variations in climate is strongly influenced by the broad coverage of organic/peat soils across the watershed (Section 2.4.3). The organics' high soil retention maintains high saturations in the root zone and also helps produce the long streamflow recession curves that follow spring melt and fall rains.

3.1.3 Hillslope Conceptual Flow Model

Perhaps the most important conceptual flow model developed for this study is of the hillslope illustrated on Figure 3-3. Hydrologists have long used hillslope models as the basis for understanding hydrologic flow conditions at the watershed-scale (Kirkby, 1978). Watershed catchments can be viewed as a series of hillslopes that vary in length, soils, vegetation, slopes and so on. They are typically defined with a hilltop area (which represents a surface-water divide) which slopes down in a convex-concave form, transitioning into a riparian stream system at the bottom. Hillslopes are typically characterized by unconsolidated deposits (Quaternary glacial deposits) overlying bedrock formations (minable coal sequence). Unconsolidated deposits are generally more permeable than the bedrock, which causes saturations to buildup at the interface between the unconsolidated deposits and bedrock. Groundwater flows downhill in the unconsolidated deposits and into the stream as 'baseflow'. It can also discharge to the ground surface as a contact seep, or spring that is formed where the minable coal sequence outcrops at the surface. In these locations, groundwater flowing in the overlying Quaternary deposits is forced to discharge at the ground surface.

Despite the number of studies conducted on hillslope hydrology, flow dynamics associated with subsurface lateral flows remain poorly understood (Graham et al, 2010). Hortonian flow can cause surface runoff to streams when precipitation intensities exceed the soil's infiltration capacity, but in the Chuitna Watershed, the precipitation rates are low (see 2.5.1.1) compared to average permeability of peat soils, or the underlying glacial deposits. In forested catchments, it is more recently generally believed that groundwater stormflow dominates runoff (streamflow) McGuire and McDonnell, 2010. Anderson and Burt (1990) indicate that steeper slopes, deep soils and narrow valleys promote subsurface stormflow, while Horton overland flow really only occurs in areas with little vegetation and low permeability soils. Subsurface stormflow, or baseflow entering the

stream associated with a storm event, can dominate the streamflow response to the storm, rather than overland runoff processes. The degree to which baseflow dominates the streamflow response is complex and depends on many factors associated with the hillslope model illustrated on Figure 3-3, such as:

- climate conditions (intensity, duration, snow/rain),
- unsaturated soil hydraulic properties (hydraulic conductivity-pressure soil moisture retention characteristics),
- preferential flow paths (i.e. macropores),
- saturated and residual moisture contents,
- saturated zone hydraulic properties (spatial distribution of hydraulic conductivity and storage coefficients),
- bedrock surface configuration,
- vegetation coverage (vegetation types, root depths, leaf area index with time),
- streambed hydraulic properties,
- slope of streambed, and
- width and topographic configuration of streambed, and stream flow conditions).

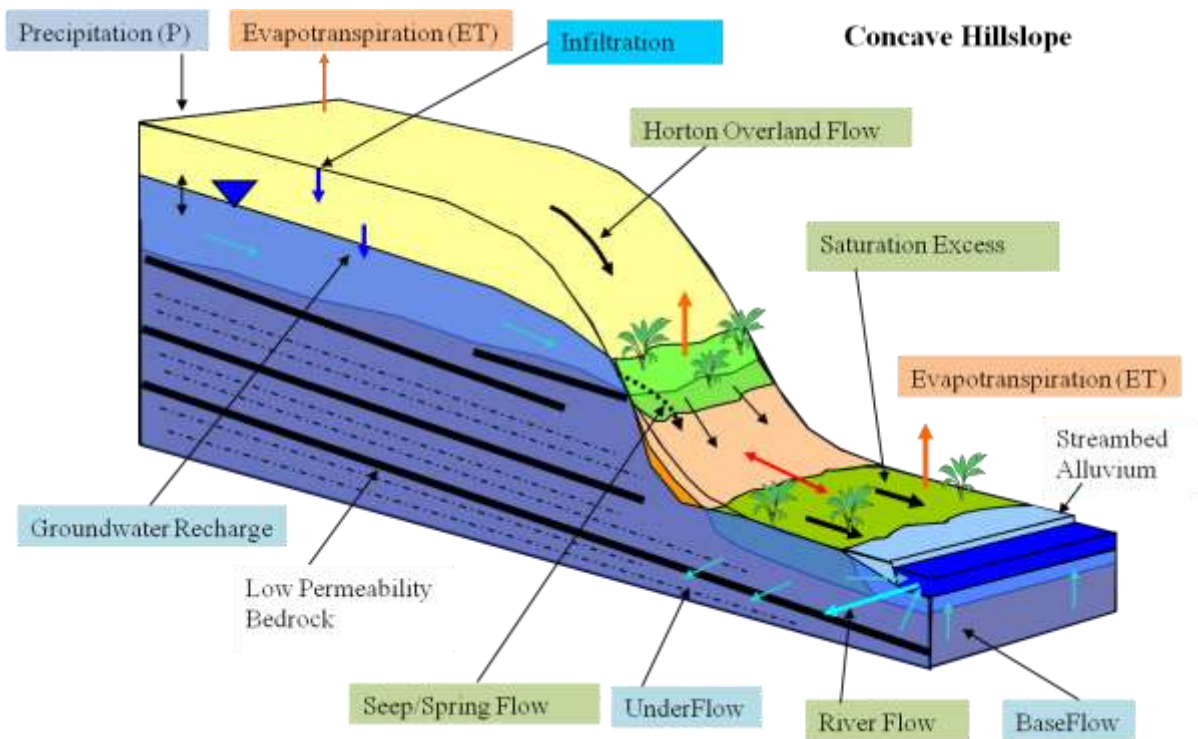


Figure 3-3. Conceptual Hillslope Flow Model

Where hillslopes transition into the stream riparian area, storm events can cause shallow groundwater to rise up and saturate the ground surface. This causes ‘saturation excess’, or saturation overland flow, which contributes surface runoff to streamflow. The areal extent of surface saturation increases with storm duration and intensity and then contracts after the storm passes. The saturated areas are referred to as variable source areas (VSA)

(Chow et al, 1988) and are likely an important process within the Chuitna Watershed, though hillslopes have not been instrumented to verify this.

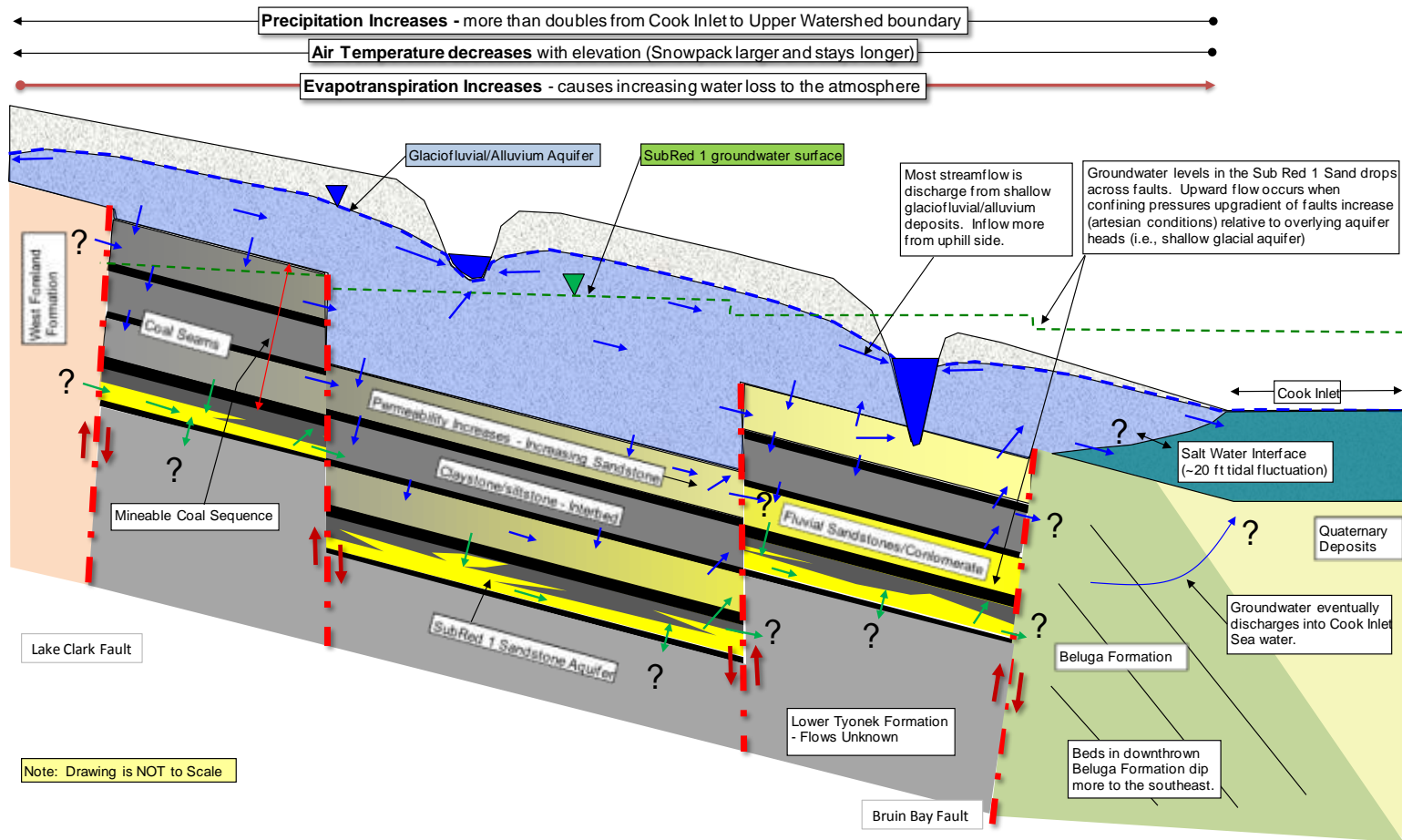
In mid- and upper-hillslope areas groundwater levels are generally deeper and exhibit more damped response to storm events than the lower hillslope areas because infiltration of precipitation takes longer to reach the groundwater table as recharge. This increases storage of groundwater in uphill areas relative to lower hillslope areas that takes time to travel downhill to eventually discharge to streams as baseflow. This lag is what causes the continuous, but gradual recession of streamflow to baseflow conditions during winter periods, or mid-summer. Results of more recent hillslope hydrology research indicates that isotopic data suggest event streamflow is primarily from older groundwater (up to several years), suggesting that it is derived primarily from hillslope contributions, and to a lesser degree from riparian groundwater (i.e. flowing beneath the stream) and saturation excess (Kirchner, 2003, McGuire and McDonnell, 2010).

3.1.4 Watershed-scale Conceptual Flow Model

Figure 3-4 illustrates the conceptualization of flow over the entire Chuitna Watershed. Key points include:

- Over the extent of the watershed, the surface topography and upper bedrock surface dip towards the southeast. While this likely dominates the overall direction of groundwater in deeper bedrock units, shallow groundwater in the Quaternary deposits are dictated more by the topography and streams in the local sub-watershed drainages (see Figure 2-23). For example, the Lone Creek (2002), 2003, and 2004 sub-watershed drains towards the southwest into Chuitna drainage.
- Significant fault offsets likely strongly influence groundwater flow within bedrock units, but it remains unclear whether flows in the overlying Quaternary deposits are influenced by these. Groundwater levels near the faults in the proposed mine area have been reported to be artesian. If the faults are in fact impermeable (no real hydraulic evidence found), then modeling showed that artesian (or elevated heads) conditions would be expected to occur on the uphill (or northern/northwestern) side of faults, and lower levels would occur on the downhill sides. If faults act as permeable conduits, heads would likely be elevated within the fault zone. But no clear evidence exists in hydrologic data (i.e., changes in streamflow across faults) to conceptualize flow across, or within identified faults.
- Across the watershed, from Cook Inlet to Capps Plateau (uppermost boundary), precipitation, temperature and RET vary with elevation. Precipitation more than doubles with elevation (Section 2.5.1.1), air temperatures decreases about 4°F with increasing elevation (Section 2.5.1.3) and RET decreases with elevation (Section 2.5.1.4). These spatial variations help explain the time to peak spring streamflow and subsequent slow (month) recession curves. This also probably helps explain differences in vegetation types in lower vs. upper elevations (i.e., long growing season at lower elevations).

Figure 3-4. Conceptual Watershed-scale Flow Model



- In upper watershed areas, lower infiltration soils (Section 2.4.3) promotes greater surface runoff than in lower, flatter sub-watershed areas.
- Groundwater inflow to the Chuitna Watershed is believed to be largely from direct recharge from precipitation and snowmelt. Because the watershed narrows to a topographic high along the upper watershed boundary, no lateral inflows of groundwater are expected in the upper area. Groundwater discharges from the unconsolidated Quaternary deposits primarily to streams. Discharge may also occur across localized lower watershed boundaries, that represent surface water divides, but due to a lack of geologic data in these areas and the regional slope towards Cook Inlet. Discharge in the Lower Chuitna area is into the Cook Inlet for both the Quaternary deposits and underlying bedrock formations (i.e., Sterling, and Beluga). Discharge amounts and locations within bedrock units underlying the Quaternary deposits (i.e., West Foreland in Upper Chuitna, Tyonek in middle Chuitna and Beluga in lower Chuitna) remain uncertain due to the combined effects of faults and dips of the bedrock. Within the proposed mine area, bedrock units dip southward along an anticlinal axis and also to the west and east at angles that appear to somewhat exceed the general surface slope. Flows within more permeable bedrock units may drain to east and west escarpments faces of the Chuitna Watershed or simply leak up through fault zones in over-pressured pathways (i.e., near the south pit fault).
- The combination of vegetation and soil hydraulic properties within the watershed promotes infiltration rather than surface runoff. Vegetation coverage is high throughout the watershed; more than 50% is short shrub/scrub (upper drainages) and nearly 40% is deciduous (lower drainages), and 6% are wetlands. More than 700 surface water bodies cover about 2% of the entire Chuitna Watershed and represent local areas where overland runoff accumulates and possibly interacts with groundwater, though this hasn't been confirmed by field testing. High amounts of organic matter (i.e., peat) in surface soil also promote infiltration of snowmelt or rainfall due to their high soil water retention characteristics.

3.2 *Summary of Data Gaps*

Several gaps in knowledge were identified and their implications to modeling:

- 1) **Surface Topography:** An accurate, high resolution topography over the entire watershed is unavailable. Although a hydrologic model can be simulated using the available ASTER topographic dataset, inaccuracies in stream profiles, cross-sections and use of groundwater elevations limit the model's ability to simulate accurate stream depths, velocities and groundwater surface elevations. Review of a higher resolution PacRim topographic survey of the mine area shows the presence of smaller-scale streams not indicated in the ASTER topographic dataset. The result of this actually causes the model calibration developed in this study to produce lower than observed streamflows from, for example, the Stream 2003 drainage (streamflows from the smaller-scale streams is not simulated without more accurate topography). Unfortunately, even if the PacRim surveyed topographic dataset were available, it does not cover the extent of the entire Chuitna Watershed, only the proposed mine

area. This is a critical dataset required for more accurate hydrologic modeling. A higher resolution topography would also help better define wetland and pond areas.

- 2) **Borehole Information:** Thickness of Quaternary deposits (glacial + alluvium + peat) is only known around the mine area and only from 20 available boreholes. More than 430 borehole logs are available, but this was not publically available. This is also an important dataset essential for understanding the subsurface hydrogeology and its relation to the surface flow system. It directly influences the storage and movement of groundwater from upland areas to streams and influences baseflows. The depth to bedrock (thickness of Quaternary deposits) is also an important factor controlling subsurface flows within the system. Limited information on the depth to bedrock across the entire Watershed increases uncertainty in the hydrologic model because this surface has to be estimated from the 20 boreholes located within the proposed mine area.
- 3) **Soil Hydraulic Data:** Hydraulic properties of soils data are limited to generalized soil properties in the USDA NRCS soils database. However, modeling conducted in this study show that the hydraulic properties of the soils, and their spatial distribution is critical to simulating the amount of surface runoff to streams (saturation excess), the amount lost to AET and the amount and dynamics of groundwater recharge, which eventually influences the magnitude and timing of baseflows to streams.
- 4) **Faults:** The location, extent and hydraulic properties of faults over the Chuitna Watershed, let alone in the proposed mine area is poorly understood. As a result, the effect of faults on subsurface and surface flows is also not well understood. Although faulting is believed to largely influence only groundwater flows within the bedrock, localized groundwater flow conditions between the bedrock and overlying glacial deposits, or influence of faulting on streamflow is uncertain.
- 5) **Wetlands:** Wetlands are assumed to not be in direct hydraulic communication with the groundwater system (Riverside, 2010). However hydraulic testing of the communication was never performed and these important hydrologic features that occur throughout the Chuitna Watershed that will be affected by changes in climate and land-use.
- 6) **Climate Data:** Site-specific, spatially-distributed, accurate, long-term, continuous climate data is lacking over the watershed. The NARR dataset is a good reasonable alternative and includes consistent climate variables to calculate RET, but it will not account for local-scale variations over the watershed. Continuous (i.e., sub-hourly) climate data, especially during the warmer months is unavailable to describe the short-term, high-intensity precipitation events and associated climate changes that are necessary to translate this into an accurate hydrologic response in the system. Distributed climate data over the entire watershed at time interval that allows resolution of short-term, high intensity events (i.e., every 15-minutes, or at a minimum, hourly) combined with spatially distributed hourly streamflow measurements would allow better understanding of the timing and magnitude of groundwater baseflows, AET and overland flows.

- 7) **Snowpack:** Full-season snow depth measurements should be collected to more accurately calibrate snowmelt parameters in the integrated flow model.
- 8) **Groundwater data:** Available groundwater data appear to be quite uncertain, due to problems with cross-aquifers screens, poor seals, freeze impacts, and surveying problems. Groundwater levels should be collected continuously (hourly) using dataloggers and pressure transducers over at least 1 year at all locations. Measurements should be monitored at a time interval similar to stream/climate data measurements (i.e., hourly) to provide snap-shots of how the system responds to specific climate events. It is especially important in model calibration, to capture the dynamics of relatively rapid variable source area saturation buildup near streams (i.e., groundwater table reaches the surface quickly). Better spatial distribution of shallow groundwater wells (Quaternary deposits), especially across hillslope profiles at in different sub-watersheds. For example, data should be collected in upland area, mid-slope and along streams to better understand the water table slope. Spatially distributed well-pairs are essential in this system, especially on both sides of known faults and through all hydrostratigraphic units, but are severely lacking.
- 9) **Streamflow data:** Only mean daily stream discharge data are available, and only in intermittently in gages near the proposed mine. This should be collected hourly and throughout the watershed at numerous gages. Even one year's data across the watershed and concurrently with spatially distributed hourly climate and groundwater data would provide invaluable insight into how the system responds to climate variability.

4.0 Integrated Hydrologic Model Development

This section describes the selection of the numerical hydrologic code and its capabilities (Section 4.1), and the development of the model input and associated assumptions (Section 4.2).

4.1 Integrated Hydrologic Numerical Flow Code

4.1.1 Code Selection

The integrated hydrologic flow conditions outlined in the conceptual models (Section 3.1) require a code that is able to account for the spatio-temporal variation in climate, soils, vegetation and geologic properties across the Chuitna Watershed. Additionally, the code must also simulate coupled surface runoff, channel flow, unsaturated zone flow and groundwater flow to account for the dynamic and integrated nature of the hydrologic system. Traditional single-process codes such as groundwater or surface water do not meet these needs.

Figure 4-1 illustrates the difference between single-process codes, like the USGS code MODFLOW (<http://chl.erdc.usace.army.mil/gms>), MODFLOW-Surfact code used by Arcadis, (2007) or the USACE HEC surface flow codes (<http://www.hec.usace.army.mil/>) and fully integrated hydrologic codes, which are capable of simulating the hydrologic conditions in the Chuitna Watershed. Hydrologic flow conditions in integrated codes are driven by external climate data, while in single-process codes, processes such as recharge must be specified, with considerable uncertainty. The integrated codes simulate all of the hydrologic processes, whereas in single-process codes assumptions about boundary conditions must be specified.

Kimley-Horne (2002) reviewed 15 hydrologic models and selected the MIKE SHE/MIKE 11 code to use in everglades restoration projects. James et al (2000) at the University of Florida under contract through the Saint Johns River Management District reviewed 153 hydrologic and recommended use of the MIKE SHE code to simulate integrated surface/groundwater flows in Volusia County, Florida. CDM (2001) reviewed seventy-five models during an extensive literature review and considered MIKE SHE, HMS, FHMFIPIR, SWATMOD, MODFLOW, DYNFLOW, MODBRANCH, SWMM, AND HSPF for further evaluation. They gave MIKE SHE the highest scores considering various criteria such as regulatory acceptance, ease of use, GIS integration, model limitations and expandability.

Illangasekare et al, 2001 reviewed a number of distributed hydrologic codes and selected the MIKE SHE code for use in a US DOE former nuclear weapons plant environmental project, Rocky Flats Environmental Technology Site (RFETS) in Golden Colorado (<http://www.integratedhydro.com/CodeSelectionRFETS.pdf>). Illangasekare et al, 2001b also performed a code verification and validation for the RFETS project (http://www.integratedhydro.com/MSHEVerification_summary.pdf).

The MIKE SHE/MIKE 11 software code, developed by the Danish Hydraulic Institute (DHI) was selected for use in this study because of its broad use world-wide and application in similar northern snowmelt-driven environments (Borden et al, 2010, <http://www.obwb.ca/wsd/about/project-reports>).

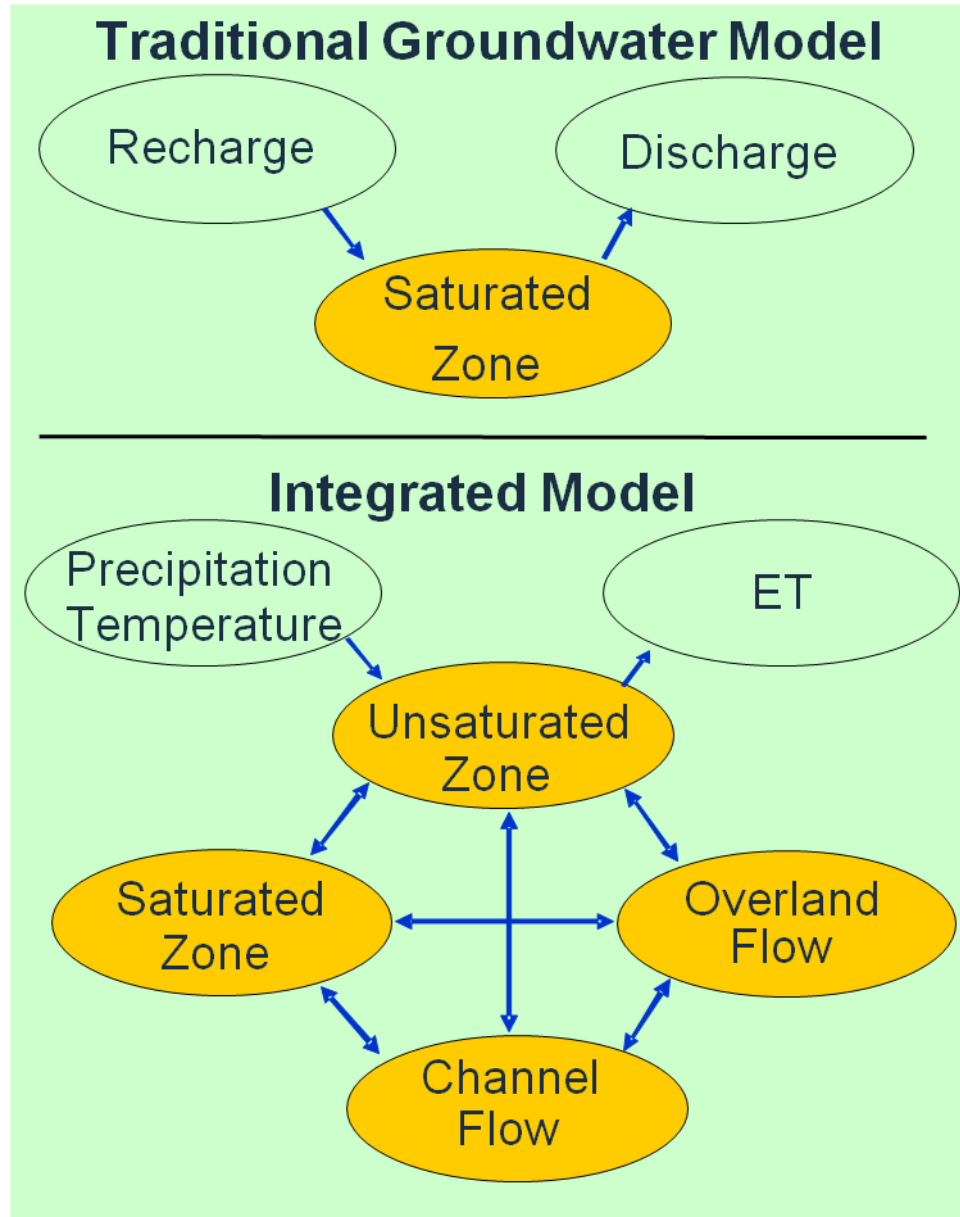


Figure 4-1. Comparison of Traditional Groundwater Model and a Fully Integrated Hydrologic Model.

4.1.2 MIKE SHE/MIKE 11 Capabilities

Graham and Butts (2005) summarize the use and capabilities of the MIKE SHE software (http://www.dhisoftware.com/upload/dhissoftwarearchive/papersanddocs/waterresources/MSHE_Book_Chapter/MIKE_SHE_Chp10_in_VPSinghDKFrevert.pdf). Key capabilities are shown on Figure 4-2 and summarized here:

- MIKE SHE/MIKE 11 is a physically-based, spatially-distributed, finite difference, hydrologic code that simulates fully coupled flows including surface flows (overland flow, channelized flow) and subsurface flows (saturated and unsaturated zone).
- MIKE 11 is a one-dimensional, fully-dynamic hydraulic and hydrology model for simulating river channel flows and water levels. Flows are calculated using a choice of fully dynamic Saint-Venant open channel flow equations, or simplifications (kinematic, diffusive, and dynamic). MIKE 11 is dynamically linked with the MIKE SHE portion of the code that simulates the remaining hydrologic processes.
- Overland flow is simulated using the 2-D Diffusive Wave finite difference approximation of the Saint Venant equations. Digital elevation models can be used directly by the model to route overland flow.
- Using the Kristensen and Jensen method (Kristensen and Jensen, 1975) actual evapotranspiration (AET) is calculated based on soil evaporation and plant transpiration as a function of time-varying leaf area index and root depth,
- Saturated zone flow – simulated using a 3-dimensional Darcy equation and solved numerically by an iterative implicit finite difference technique,
- Unsaturated zone is simulated using a full 1-dimensional unsaturated zone flow using Richard's equation (Graham and Butts, 2005),
- Climate – precipitation, air temperature and RET are specified spatially and temporally at any time-step of interest, and
- Snowmelt – Simulated using a modified degree-day model that allows wet/dry snow specification, elevation lapse rates and melting by shortwave radiation, convective air flow and advective heat from rain on snow.

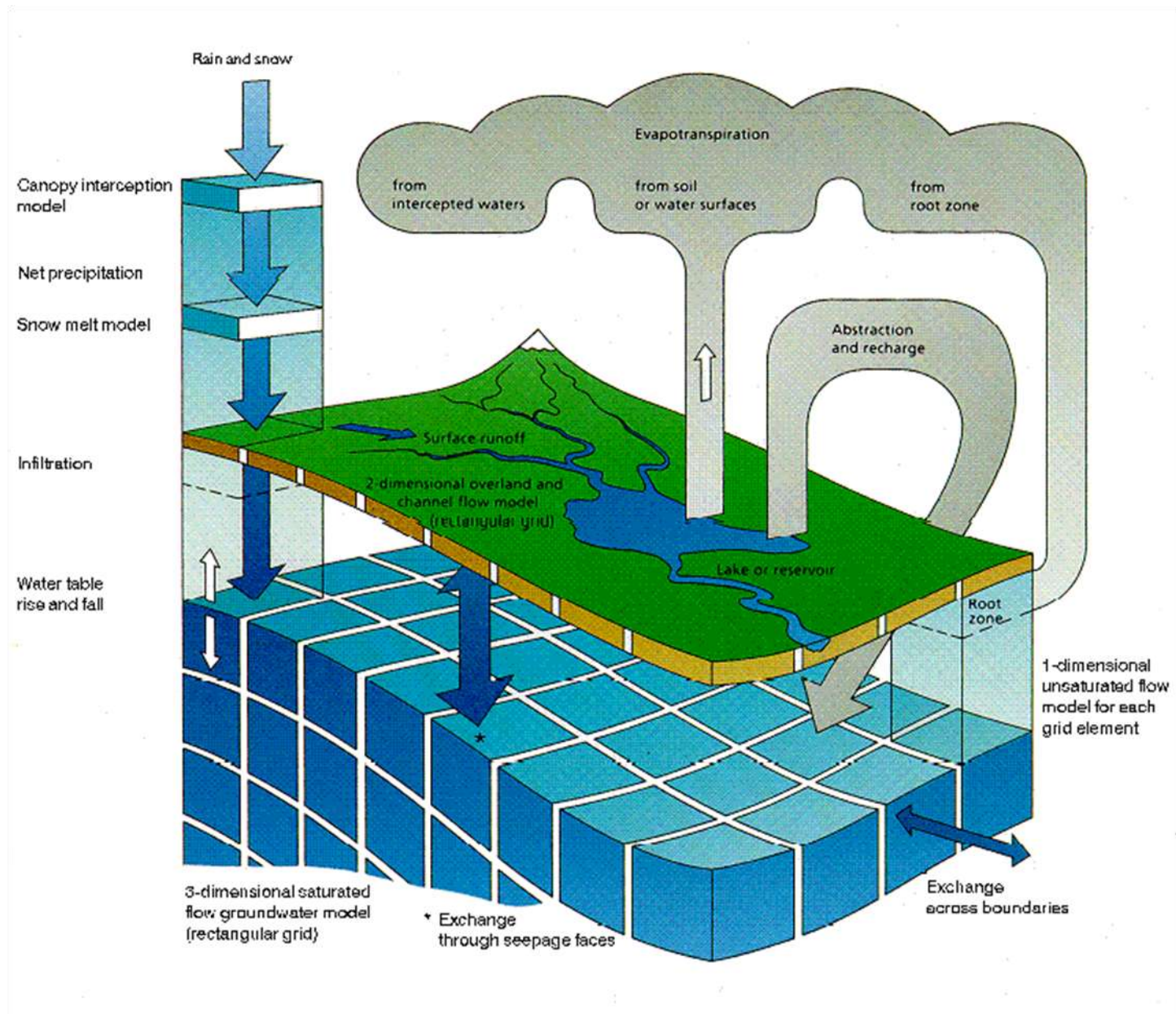


Figure 4-2. Hydrologic Processes Simulated in the MIKE SHE/MIKE 11 Code.

Some examples of where MIKE SHE/MIKE 11 has been used include:

1. DHI Website:
<http://mikebydhi.com/Applications/WaterResources/WaterManagement.aspx>
2. Everglades Restoration - Kissimmee Basin. The Kissimmee Basin Hydrologic Assessment, Modeling, and Operations Planning Study (KB MOS), a component of the Kissimmee River Restoration Project, is a South Florida Water Management District (SFWMD or District) initiative to identify alternative structure operating criteria to meet the flood control, water supply, aquatic plant management, and natural resource operations objectives of the Kissimmee Basin and its associated water resource projects. To evaluate alternative structure operating criteria, evaluation performance measures and evaluation performance indicators have been developed and will be used in conjunction with hydrologic and hydraulic modeling tools to predict future performance of alternative plans.)
<https://projects.earthtech.com/sfwmd-kissimmee/>
3. Rocky Flats, Golden, Colorado. The integrated models developed for this 10-square mile area were thoroughly peer-reviewed by national experts. The site is similar size to that of the Chuitna site, though it was industrialized. The focus of this modeling project evaluated how, like the proposed mining, the integrated surface/subsurface flow system changed due to changes in landsurface/subsurface. This model was run for years using hourly/sub-hourly timesteps and spatially distributed precipitation as rainfall/snowfall. ([www.integratedhydro.com/rfets/SWWB Main Report.pdf](http://www.integratedhydro.com/rfets/SWWB_Main_Report.pdf))

4.2 Numerical Model Development

The development of the MIKE SHE/MIKE 11 model datasets and associated assumptions are presented in this section.

4.2.1 Model boundary and grid discretization

The MIKE SHE/MIKE11 model boundary coincides with the study area boundary (see Figure 1-2). This boundary was selected because it represents a surface water divide based on topography. This boundary is also generally valid as a groundwater divide given the structure of the entire watershed. Surface and groundwater divides represent good boundaries in integrated models because no flows are expected across them.

Simulation of subsurface and overland flows requires specification of a regularly-spaced, square finite difference grid across the model domain. A 200-meter grid was selected as a compromise between trying to use the finest grid possible to better simulate smaller-scale features (i.e., streams) and minimizing the model run times. The total number of grid points is 206 (x-direction) and 86 (y-direction), or 10244. The number of active cells is 9709.

4.2.2 Unsaturated Zone Flow

Actual hydraulic properties for soils within the watershed were unavailable. Instead, standard unsaturated zone soil properties, based on published data (Leij et al, 1996) for a silt loam were used as an initial starting soil for the two soil zones defined in the UDSA NRCS soil distributions (see Figure 2-9) for hydrologic codes B (moderate infiltration) and D (low infiltration). Soil parameters were adjusted during model calibration and the final values are summarized in Table 4-1. Although various sets of soil parameters were considered in the modeling, such as two soil layers to represent the shallow high organic material (i.e., peat) overlying quaternary soils (i.e., silt loam), this combination could not reproduce the long, slow spring streamflow recession curve. A single soil type was found to reproduce the streamflow response best.

The vertical discretization of each soil column is the same throughout the model and starts with 1 cm cells at ground surface to account for the non-linear soil evaporation and transpiration in this top cell. Vertical cells were smoothly increased in size to a constant 0.5 m to below the groundwater table. A total of 106 vertical cells define the unsaturated zone at every active cell in the model (9709 cells). Initial conditions are automatically specified as an equilibrium moisture distribution at field capacity.

Table 4-1. Summary of Soil Hydraulic Properties (Basecase Model)

Parameters	Silt Loam ("B" Hydrologic Group)	Silt Loam ("D" Hydrologic Group)
<i>Retention Curve</i>		
Saturated Moisture Content	0.45	0.41
Residual Moisture Content	0.1	0.1
Field Capacity Moisture Content	0.32	0.24
Wilting Point Moisture Content	0.12	0.11
Van Genuchten (Alpha, 1/cm)	0.005	0.005
Van Genuchten (n)	1.66	1.66
m	0.398	0.398
<i>Hydraulic Conductivity Curve</i>		
Saturated Hydraulic Conductivity (m/s)	8.0E-06	4.0E-06
Van Genuchten Alpha (1/cm)*	0.067	0.067
Van Genuchten n*	1.45	1.45
shape factor, l	0.365	0.365

*Note: Different alpha and n values were used because these improved simulation of baseflow/streamflow during calibration and reflect the high

4.2.3 Saturated Zone Flow

The saturated zone is represented by only two layers, the unconsolidated Quaternary deposits and the minable coal layer. The Sub-Red 1 Sand layer was not simulated because of very limited data, a high degree of confinement with overlying layers (Section 2.5.3.5), localized occurrence in Tyonek formation between the LCF and BCF (Section 2.4.4) and in the proposed mine area, apparent compartmentalization of the unit between other faults (i.e., South Pit and Chuit) in the mine area and an overall uncertainty in its lateral extent and recharge/discharge areas.

The bottom surfaces of the unconsolidated Quaternary deposits and the minable coal sequence were specified in the model. The estimated spatially-varying thickness of Quaternary deposits (Figure 2-13) was subtracted from the surface topography (Figure 2-2) using GIS techniques (ESRI Spatial Analyst software). The bottom of the minable coal sequence was calculated as 100 m below the spatially variable Quaternary deposits based on the approximate thickness within the mine area. The bottom of the minable coal sequence could not be determined from available consultant or DNR reports. Because the thickness of all of the Kenai formations (West Foreland, Tyonek and Beluga) underlying the Quaternary deposits appear to be thousands of feet thick beneath the watershed an effective thickness of the bedrock aquifer (i.e., minable coal sequence in proposed mine area) is somewhat arbitrary. The hydraulic properties play a more important role in how this layer affects the stream and groundwater flows in the overlying Quaternary deposits. Ultimately, because of the low permeability relative to the Quaternary deposits, assumptions about the thickness of this aquifer layer are not critical to calibrating the model.

Although interbed deposits within the mineable coal appear to transition into more permeable sandstones/conglomerate towards Lone Creek and towards the Chuitna, hydraulic properties for the minable coal sequence were assigned values similar to those used in the Arcadis (2007) groundwater flow model. The local Arcadis model in the mine area did not show this transition zone, but did assign different hydraulic properties for the granitic intrusion in the Lone Ridge areas. Horizontal hydraulic conductivity values specified for the granitic zone and minable coal in this study are $1.7e-7$ m/s and $3.5e-8$ m/s, and vertical hydraulic conductivities are $3.9e-9$ m/s and $3.5e-8$ m/s, respectively. Similar hydraulic values assumed for the minable coal sequence in the West Foreland and Beluga bedrock formations, north and south of the LCF and BCF, respectively. Variable hydraulic properties for the interbed transition zones in the minable coal sequence were not simulated due to a lack of information on lateral extent and actual hydraulic properties. There was also a desire to assess whether similar water levels and baseflows would be simulated using similar hydraulic properties in the minable coal. Using similar hydraulic values for the minable coal sequence also allows for more direct future comparison of reclamation conditions between the Arcadis groundwater model and the integrated flow model. Specific yields and confined storage values are 0.01 and 0.0001 for all units. These are similar to those specified in the Arcadis model

Three saturated hydraulic conductivity zones were defined for the unconsolidated Quaternary deposits (Figure 4-3). This distribution is based on the recent surface geologic mapping (Section 2.4.4). Highest horizontal:vertical hydraulic conductivities are assigned to the glacioalluvium ($1.7\text{e-}4$ m/s : $3.0\text{e-}6$ m/s), and lower values for the glacial drift ($3.0\text{e-}5$ m/s : $1\text{e-}6$ m/s) and colluviums, glacio-estuarine deposits and glacial outwash ($5.5\text{e-}6$ m/s : $1.0\text{e-}6$ m/s). The horizontal/vertical anisotropy specified in this study is within the range specified in the Arcadis report. Initial values specified for each of these zones were close to those specified in the Arcadis model, but then adjusted to the above values during calibration against available groundwater depths. Specific yields and confined storage values are 0.2 and 0.0001, respectively for all unconsolidated deposits. These are similar to those used in the Arcadis model.

Lateral boundary conditions were specified as no-flow over the entire extent of the Chuitna Watershed, except for a relatively small length near the outlet of the Chuitna into Cook Inlet. This boundary condition was specified as a constant head boundary with a head of 0 ft, mean sea level. This allows groundwater in both aquifer layers to discharge to Cook Inlet.

Initial conditions were obtained by running the integrated model with an initial groundwater surface equal to a depth of 10 m below ground surface. After cycling the model through a few years, relatively steady groundwater surfaces for the two aquifer layers were obtained at the starting date of the model runs and used as the initial conditions for actual calibration simulations.

In the minable coal sequence aquifer layer, all faults (Figure 2-6) are simulated as barriers by using limited leakage values across them. This is accomplished in MIKE SHE by using the 'sheet pile' module and assigning a leakage coefficient of $3.5\text{e-}11$ 1/s. These leakage coefficients were assigned to the fault such that the hydraulic conductivity of the simulated faults is similar to those in the Arcadis model for the Chuit and South Pit faults.

4.2.4 Overland Flow

Surface resistance controls the rate of runoff from overland plains. A single surface resistance value (Manning M) is specified for the entire Chuitna Watershed. Although site-specific data were unavailable the value was set to $10\text{ m}^{(1/3)}/\text{s}$ based on dense brush in summer or a heavy stand of trees with a few down trees (Chow, 1959) in floodplains. System hydrologic response is not very sensitive to this parameter. As a result, it was not considered a calibration parameter and therefore not varied during the simulations.

Another parameter affecting overland flow is a threshold value controlling the amount of surface depression storage. In the model, this was set at 2 mm depth. Once ponding depths exceed this depth, overland flow can occur. The parameter accounts for small variations in the surface topography typical in catchments. This value was determined through initial calibration simulations.

Boundary and initial conditions also need to be specified in the model for overland flow. Because overland flow is a rapid process relative to subsurface flows, initial depths of overland water were set at 0 mm. This was also justified because of the long simulation time periods (i.e., 1980 to 2000). Boundary conditions simply assume that no overland flow occurs along any of portion of the Chuitna Watershed boundary.

The model developed here has a grid resolution too large to capture individual springs, but instead simulates the combined effect of these inflows to streams as ‘groundwater baseflow’. In reality, there is little difference in streamflow response if groundwater discharges near streams as spring/seep flow versus occurring as a more diffuse and distributed inflow to streams from underlying alluvium (which likely intercepts localized groundwater inflows from fractures, faults and where bedrock units sub-crop the alluvium). However, in terms of the net effect on stream temperatures, distinguishing between the two will be more important due to the radiation heating of spring/seep discharge prior to entering the streams (increased heat inflows compared to baseflows).

4.2.5 Streamflow

Streamflow is simulated in 45 streams included in the Chuitna Watershed shown on Figure 2-23. A summary of simulated stream names, lengths and cross-section location intervals are included in Table 4-2. Forty five total stream segments are simulated, including the Chuitna. Four stream order levels occur within the simulated network. Typically the first 3 Strahler stream levels are considered headwater streams and are located in upper, steeper reaches of the Chuitna Watershed. Streams extend a total of 185 miles (297 km) and segment lengths range from 0.5 to over 40 miles (Chuitna). The Chuitna River is considered a 4th-order Strahler stream, whereas the Mississippi River is a 10th order.

The portion of the integrated code that simulates stream hydraulics (MIKE 11) requires the geographical locations of streams, the connections between streams, cross-sections along each segment and hydraulic properties. A critical model input for streamflow is defining the stream profile, from top to bottom. A comparison of initial GIS streamline delineation (Section 2.5.2.1) against available DOQ imagery and the digital topographic surface (Section 2.3) showed notable errors in location. This resulted in considerable streambed profile variations, where elevations both increased and decreased downstream. This required that stream locations be remapped using the higher-resolution DOQ imagery, available in the lower Chuitna Watershed area, and manual smoothing of the profiles so that elevations decreased smoothly downstream. Stream profiles for selected streams are shown on Figure 4-4. The original and smoothed profiles are shown for the Chuitna. The smoothed profiles generally honor low points in the original streambed because inaccuracies in the original profile tend to over-estimate elevations (i.e., incorrect stream lines always cut across higher elevation areas, adjacent to actual stream locations).

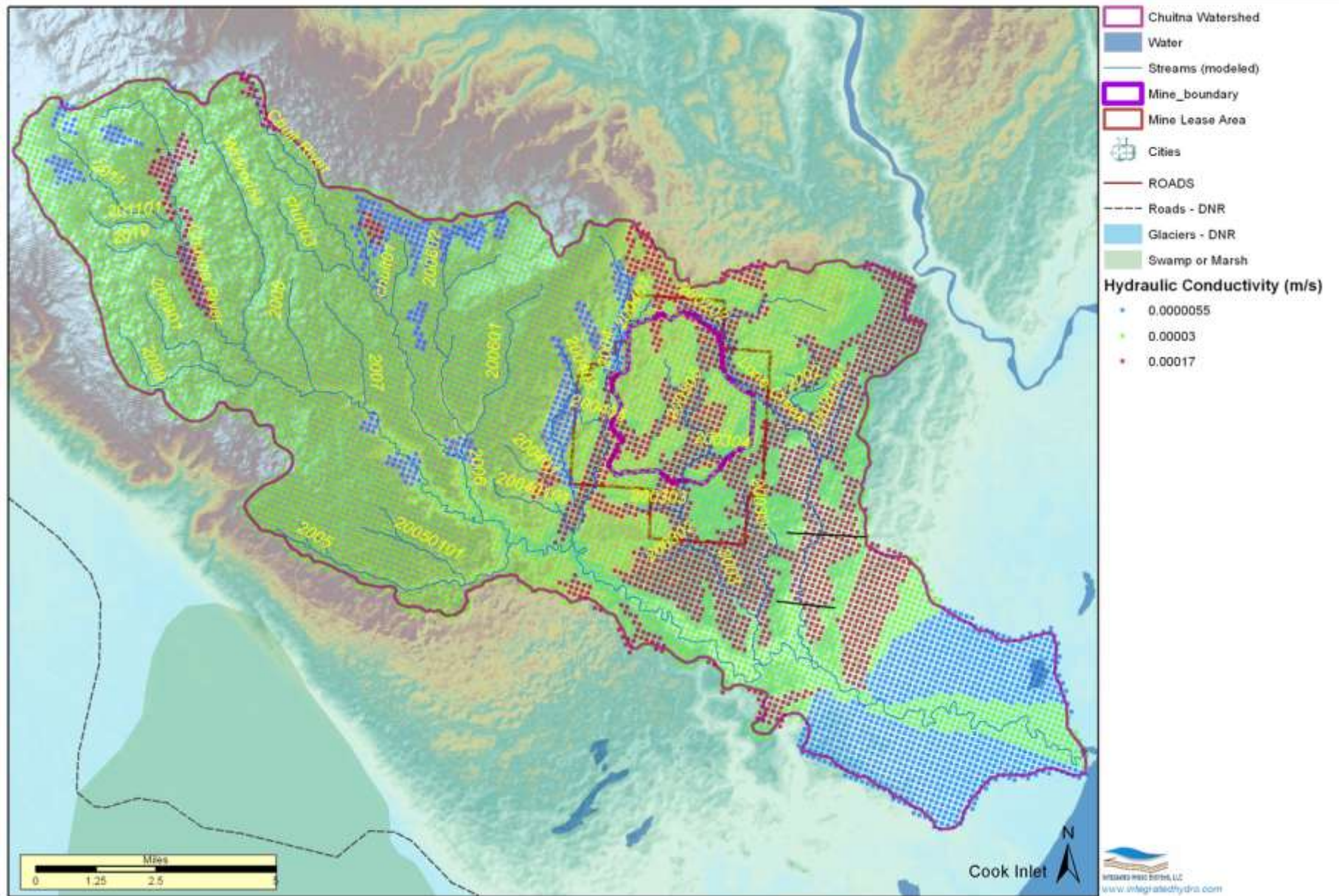


Figure 4-3. Saturated Zone Hydraulic Conductivity Values (Unconsolidated Deposits = Layer 1 – Basecase Model).

Once streambed profiles were constructed for all 45 streams, cross-sections along each stream could be developed. The MIKE 11 code required sections at the beginning and end of each segment, and one every 0.5 to 2.0 km to capture topographic variations in profiles. The larger intervals were specified for longer streams, like the Chuitna. At each cross-section, the MIKE 11 code calculates a stage (depth) based on the cross-sectional area and a specified minimum distance between calculations nodes (dx). Because detailed surveyed cross-sections for each simulated stream were not available and the digital ASTER topographic dataset is too coarse to resolve sections for most simulated streams, generic profiles had to be constructed (see Figure 4-5). This is appropriate for simulating volumetric flows within the system, but not for simulating stage and stream velocities,



which are sensitive to the accuracy of cross sections. Wider stream sections (50 m) were specified for lower, larger streams, including the Chuitna and narrower sections (30 m) were used for upper (headwater) reaches. These sections were determined by examining simulated streamflow from initial simulations to ensure that maximum flows did not exceed the section dimensions.

Reports and photos reviewed suggest most streambeds are characterized by cobbles, gravel and are heavily vegetated, or have dense brush, though no estimates of Manning M values were identified. Streambed resistance was therefore set $20 \text{ m}^{(1/3)}/\text{s}$ for all streams. For mountainous streams, Chow (1959) indicates resistance values do not vary much (i.e., 20 to 25). As a result this parameter was not considered a calibration parameter (i.e., not varied).

The rate of flow between surface flows and underlying groundwater is determined by adjusting streambed leakage coefficients (1/s). Leakage values are summarized on Table 4-3 and were determined through model calibration. The calibration was sensitive to

these values. Higher values increase the rate of flow between surface flows and groundwater (i.e., Stream 2003).

Upstream boundary conditions in all streams were set as no-flow and the only downstream boundary condition required was along the Chuitna at Cook Inlet. Although this boundary varies with tide, no streamflow or groundwater level data were identified within this tidal zone which the model could be calibrated against. The surface water elevation was set at mean sea level, which is reasonable over a 20-year period and because the focus of hydrologic impacts due to climate change is upstream of the Chuitna Gage 230 (last gage location on the Chuitna). Because the Chuitna Watershed drains into Cook Inlet, tidal fluctuations in the Chuitna will not affect hydrology above the high tide elevation.

Flows were simulated using the fully hydrodynamic option in MIKE 11 (i.e., using St. Venant equations) so that backwater effects and flows in steeper slopes could be modeled. An option to use automatic time-steps was also specified. This feature helps optimize the numerical time-step required to solve the set of surface flow equations. When precipitation events occur and rapid changes in streamflow occur, the code automatically decreases the time-step to account for the shorter-term dynamics.

Table 4-2. Lengths (meters) of Simulated Streams

Mike11 Stream	Total Stream Length		Cross Section Interval (meters)
	(meters)	(miles)	
Chuitna River	64573	40.1	2000
Lone Creek	25415	15.8	2000
Chuit River	18646	11.6	1000
2003	18476	11.5	1000
2004	17438	10.8	1000
Wolverine	11546	7.2	1000
200602	10764	6.7	1000
2005	10102	6.3	1000
200402	7962	4.9	1000
2009	7122	4.4	1000
200301	6975	4.3	1000
200601	6808	4.2	1000
2011	6736	4.2	1000
2002	5605	3.5	1000
200901	4755	3.0	500
20020101	4667	2.9	500
chuit03	4419	2.7	500
20050101	4271	2.7	500
2007	4229	2.6	500
20040101	4146	2.6	500
2008	4077	2.5	500
2006	3366	2.1	500
2010	3177	2.0	500
200401	3148	2.0	500
chuit01	3095	1.9	500
201101	3056	1.9	500
chuit02	2550	1.6	500
20020103	2412	1.5	500
200405	2379	1.5	500
20060202	2365	1.5	500
200202	2350	1.5	500
201102	2326	1.4	500
chuit04	2202	1.4	500
200302	2093	1.3	500
200407	1970	1.2	500
20020102	1577	1.0	500
200303	1530	1.0	500
200203	1462	0.9	500
200501	1424	0.9	500
200305	1280	0.8	500
200503	1045	0.6	500
200304	1028	0.6	500
200502	883	0.5	500
20060201	832	0.5	500
chuit0201	813	0.5	500
Total Distance	297	185	

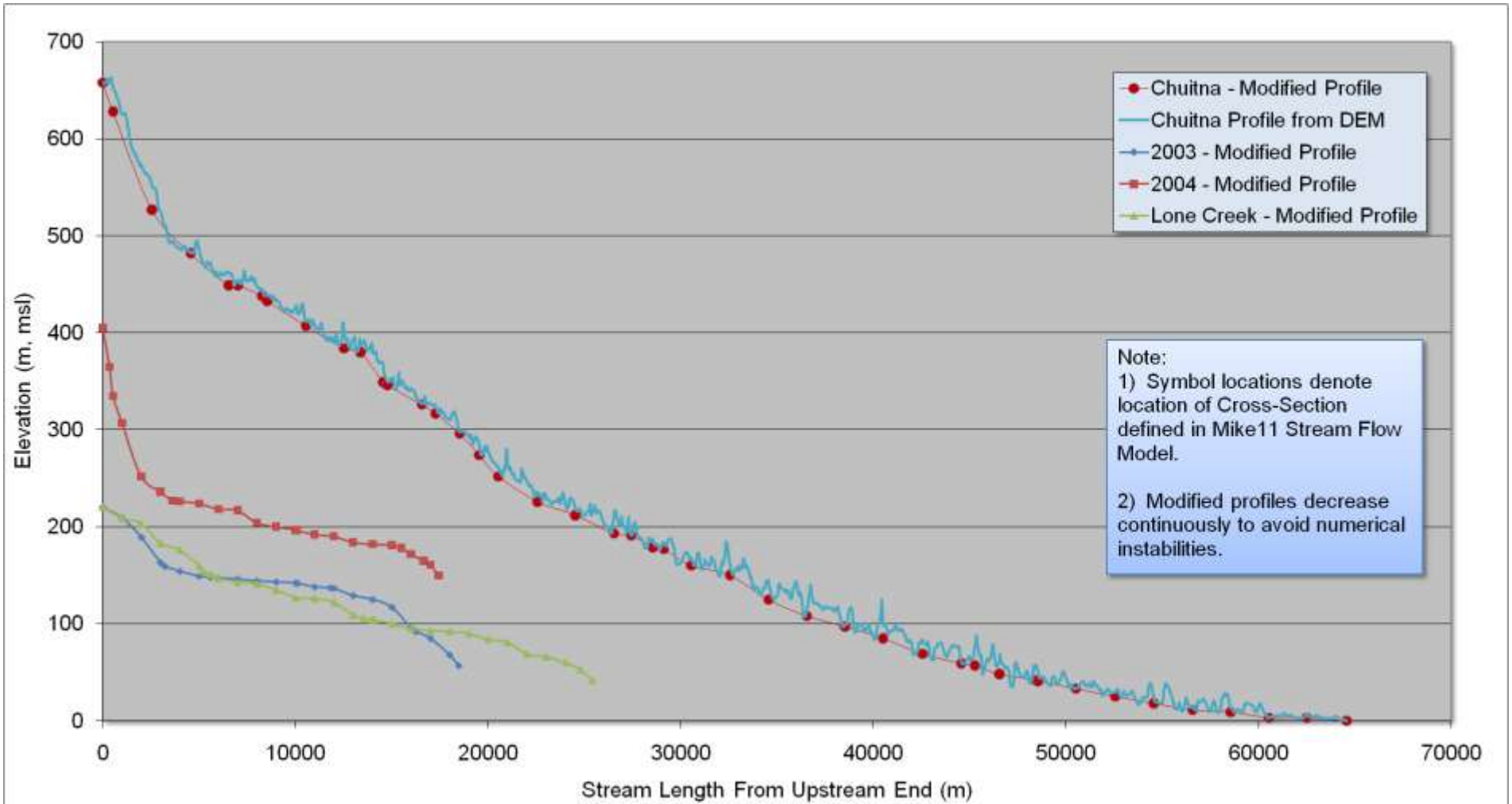


Figure 4-4. Selected Stream Profiles

The original Chuitna stream profile from the ASTER DEM is shown in light blue. The modified profile is shown with the thin red line with red circles.

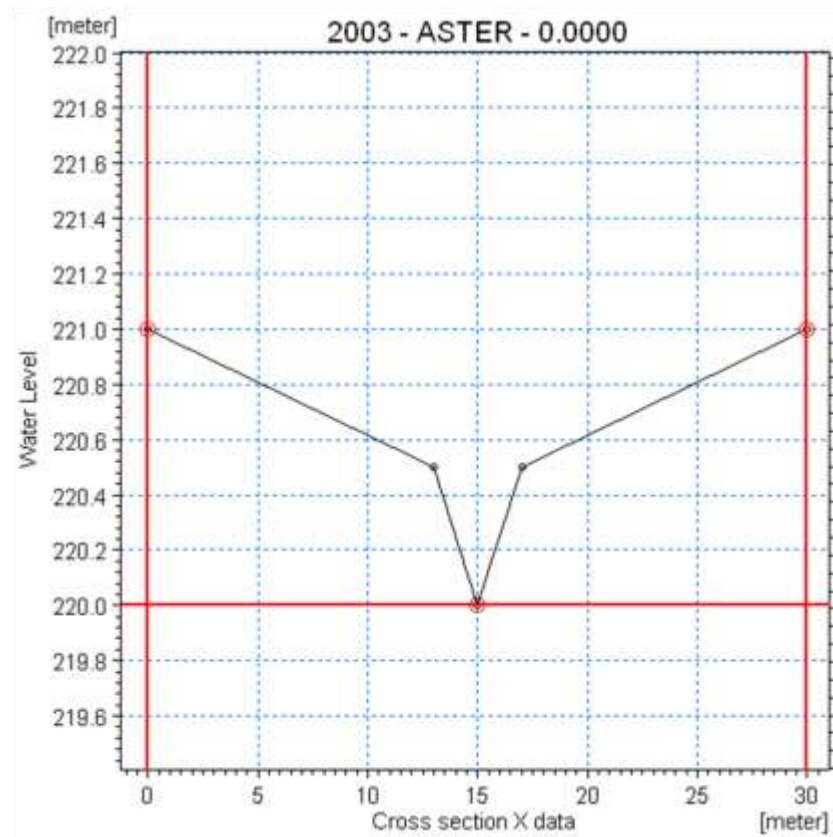
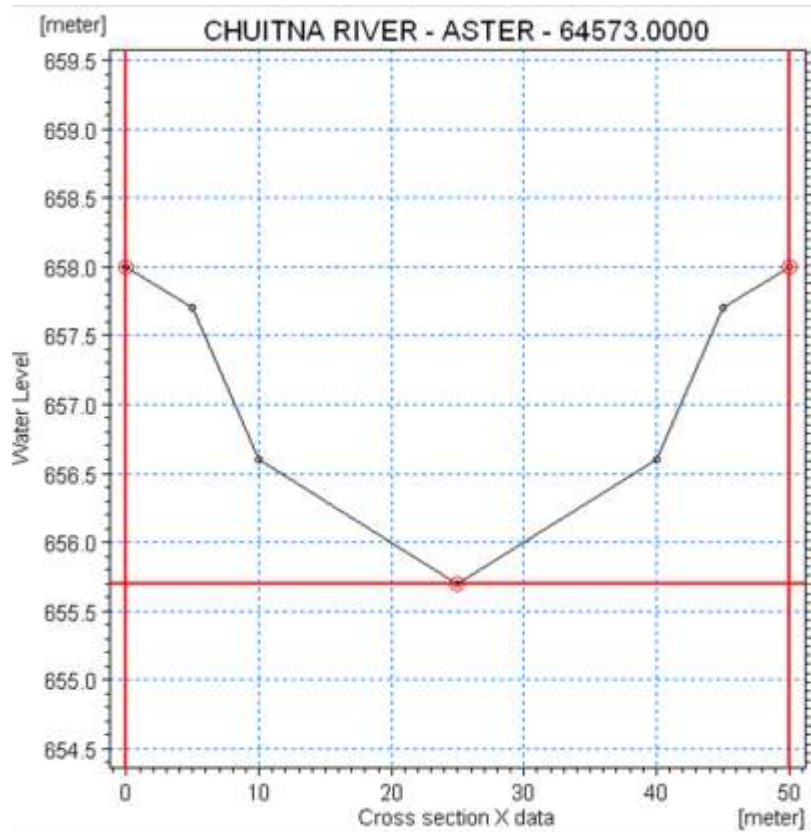


Figure 4-5. Cross-Sections.

The left plot shows a wider (50 meters) and taller (2.25 meters) section for the lower Chuitna River and a narrower (30 meters) section for Stream 2003 (1 meter high).

Table 4-3. Simulated Stream Leakage Values (Basecase Model). Stream branches identified as 2004 are part of the Lone Ridge sub-watershed and 2002 are part of the Lone Creek sub-watershed.

Stream "Branch"	Starting Chainage (m)	Ending Chainage (m)	Leakage Type	Leakage Value (1/s)
200503	0	1045	Aquifer + Bed	5.0E-05
chuit04	0	2202	Aquifer + Bed	5.0E-05
201101	0	3056	Aquifer + Bed	5.0E-05
chuit03	0	4419	Aquifer + Bed	5.0E-05
2010	0	3177	Aquifer + Bed	5.0E-05
Wolverine	0	11546	Aquifer + Bed	5.0E-05
200901	0	4755	Aquifer + Bed	5.0E-05
2008	0	4077	Aquifer + Bed	5.0E-05
200502	83	883	Aquifer + Bed	5.0E-05
chuit0201	0	813	Aquifer + Bed	5.0E-05
20060202	0	2365	Aquifer + Bed	5.0E-05
chuit01	0	3095	Aquifer + Bed	5.0E-05
20060201	0	832	Aquifer + Bed	5.0E-05
2007	0	4229	Aquifer + Bed	5.0E-05
200601	0	6808	Aquifer + Bed	5.0E-05
Chuitna River	5000	64573	Aquifer + Bed	7.0E-05
Chuitna River	0	5000	Aquifer + Bed	1.0E-08
200602	0	10764	Aquifer + Bed	5.0E-05
2006	0	3366	Aquifer + Bed	5.0E-05
2005	30	9800	Aquifer + Bed	5.0E-05
20050101	0	4271	Aquifer + Bed	5.0E-05
2009	0	7122	Aquifer + Bed	5.0E-05
2011	0	6736	Aquifer + Bed	5.0E-05
chuit02	0	2550	Aquifer + Bed	5.0E-05
Chuit River	0	18646	Aquifer + Bed	5.0E-05
2004	0	17438	Aquifer + Bed	5.0E-05
200407	0	1970	Aquifer + Bed	5.0E-05
200402	0	7962	Aquifer + Bed	5.0E-05
2003	0	18476	Aquifer + Bed	7.0E-04
200305	0	1280	Aquifer + Bed	5.0E-05
200304	0	1028	Aquifer + Bed	5.0E-05
20020103	0	2412	Aquifer + Bed	5.0E-05
20020101	0	4667	Aquifer + Bed	5.0E-05
Lone Creek	0	25415	Aquifer + Bed	5.0E-03
20020102	0	1577	Aquifer + Bed	5.0E-05
200202	0	2350	Aquifer + Bed	5.0E-05
200301	0	6975	Aquifer + Bed	5.0E-05
200405	0	2379	Aquifer + Bed	5.0E-05
200203	0	1462	Aquifer + Bed	5.0E-05
20040101	0	4146	Aquifer + Bed	5.0E-05
200401	0	3148	Aquifer + Bed	5.0E-05
200302	0	2093	Aquifer + Bed	5.0E-05
200303	0	1530	Aquifer + Bed	5.0E-05
200501	0	1424	Aquifer + Bed	5.0E-05
2002	1003	5605	Aquifer + Bed	5.0E-05

4.2.6 Climate

4.2.6.1 Precipitation and Air Temperature

Precipitation and air temperature obtained from the NARR dataset (Section 2.5.1) are input into the model from January 1 1980 to December 31, 1999 every 3-hours. Elevation lapse rates and associated station elevations for the NARR dataset are summarized in Table 4-4. The air temperature and precipitation inputs are both spatially distributed based on the elevation lapse rates. For air temperature, both wet (during precipitation) and dry lapse rates are specified. The dry lapse rates were determined from data measured in 2006 at two PacRim climate stations, one located inland and one along Cook Inlet (Figure 5.0a in McVehil-Monnett Associates, Inc., 2006). Across the entire watershed (~800 m elevation difference), average air temperatures therefore vary nearly 5°C. Wet lapse rates were determined through calibration, but are typically lower than dry air lapse rates because as moist air rises, it does not cool as quickly as dry air due to release of latent heat during condensation (http://rst.gsfc.nasa.gov/Sect14/Sect14_1b.html).

4.2.6.2 Snowmelt

Snowmelt parameters are also summarized in Table 4-4. In a degree-day snowmelt model, air temperatures are used in combination with a specified threshold melting temperature and a degree-day melting coefficient to calculate snowmelt, or conversion of dry snow to wet snow. Typically, threshold melting temperatures use 0°C. Snowmelt simulations were conducted at locations with snowpack measurements (see Section 2.5.1.2 and 5.0) to estimate the 1 mm/°C/day degree day coefficient. Calibration of the model to available snowpack data was most sensitive to the degree day coefficient. The melting coefficient for the thermal energy of rain and the factor for reducing sublimation of dry snow (takes more energy than ET from water) were also both adjusted during calibration, but snowmelt is not as sensitive to these.

As dry snow melts, liquid water infiltrates down to the ground surface and is subject to loss to evapotranspiration as a surface water body. The snow's ability to store water is subject to wet snow storage factor, which when exceeded, allows water to be treated as ponded water in the model. As ponded water, the snowmelt can either infiltrate the soils or runoff, depending on soil hydraulic properties and moisture conditions. This factor is calculated as the ratio of wet storage (SWE) to the sum of wet and dry storage and was adjusted to 0.6 during calibration. This factor was used to adjust the rate of melting during spring melt.

A minimum snow storage is also specified that allows the model to melt snow at a reduced rate where only partial areal snow coverage exists, for example beneath trees. Melting, or freezing rates are multiplied by the ratio of the minimum snow storage to the combined dry and wet storage. The value of 0.6 specified in the model was derived through calibration.

Table 4-4. Summary of Model Climate Input Parameters (Basecase)

Climate Parameters	Parameter Values
Precipitation	
Temporal Frequency	every 3 hours
Elevation for Lapse Rate	300 m
Lapse rate (change with elevation)	17%/100 m
Air Temperature	
Temporal Frequency	every 3 hours
Elevation for Lapse Rate	350 m
Wet Lapse Rate	-0.3 °C/100 m
Dry Lapse Rate	-0.6 °C/100 m
Reference Evapotranspiration	
Temporal Frequency	every 3 hours
Spatial distribution	4 Elevation Zones (100 m, 300 m, 500 m, 700 m)
Snow Melt	
Degree-day Coefficient	1 mm/°C/day
Threshold melting temperature	0 °C
Melting Coefficient for thermal energy of rain	0.15 (1/C)
Factor reducing sublimation rate from dry snow	0.5
Maximum wet snow storage fraction	0.6
Minimum snow storage for full coverage	100 mm
Initial total snow storage	0 mm (summer start)
Initial wet snow fraction	0 mm (summer start)

4.2.6.3 Reference Evapotranspiration and Plant Transpiration

Like the air temperature and precipitation inputs, calculated RET values (Section 2.5.1.4) are also specified in the model every 3-hours. Because the RET values were calculated using the air temperature and precipitation, along with other NARR climate variables, the RET varies consistently with changes in climate conditions over the Chuitna Watershed. For example, when it rains, air temperatures drop and increased cloud cover reduces solar radiation, which cause RET values to decline. RET values were calculated at 4 different elevation bands (100, 300, 500 and 700 m).

The model uses the RET values to calculate plant transpiration and evaporation from soil, water bodies (including wet snow), dry snow and water intercepted on vegetation canopy. To calculate plant transpiration, additional parameters associated with the types and state of vegetation throughout the year must be specified in the model. For example, the variation in Leaf Area Index (LAI) and root depths with time must be specified. Peak

LAI values for the six vegetation types (see spatial distribution Figure 2-28) and open water (Table 4-5) were used to define time-varying LAI values (Figure 4-6) similar to those in Fang et al (2008). Mean and maximum root depths are also summarized in Table 4-5, which were assumed to not vary in time.

Table 4-5. Summary of Vegetation Parameters

Cover Class (NLCD)	LAI peak (stdev)	Location	Sources	Root depth cm (mean/max)
Tall Shrub (orange)	2.24	Seward Peninsula	Thompson 2004	69/123
Low Shrub bog (brown)	1.7	Seward Peninsula	Thompson 2004	56/90
Mixed Deciduous Forest (stone)	5.3 (0.46)	Cook Inlet	Verbyla 2005	75/155
	2.6 (0.7)	Boreal sites	Asner 2003(meta)	
		4 North America	Fang et al, 2008	
Herbaceous (bright green)	1.7 (1.2)	grasslands	Asner 2003 (meta)	89/160
		1 grasslands	Fang et al, 2008	
Evergreen Forest (khaki green)	2.7 (1.3)	Boreal sites	Asner 2003(meta)	55/101
		3.2 North America	& Thompson 2004	
Barren Land (open)	1		Fang et al, 2008	10
Water	0		DHI	0

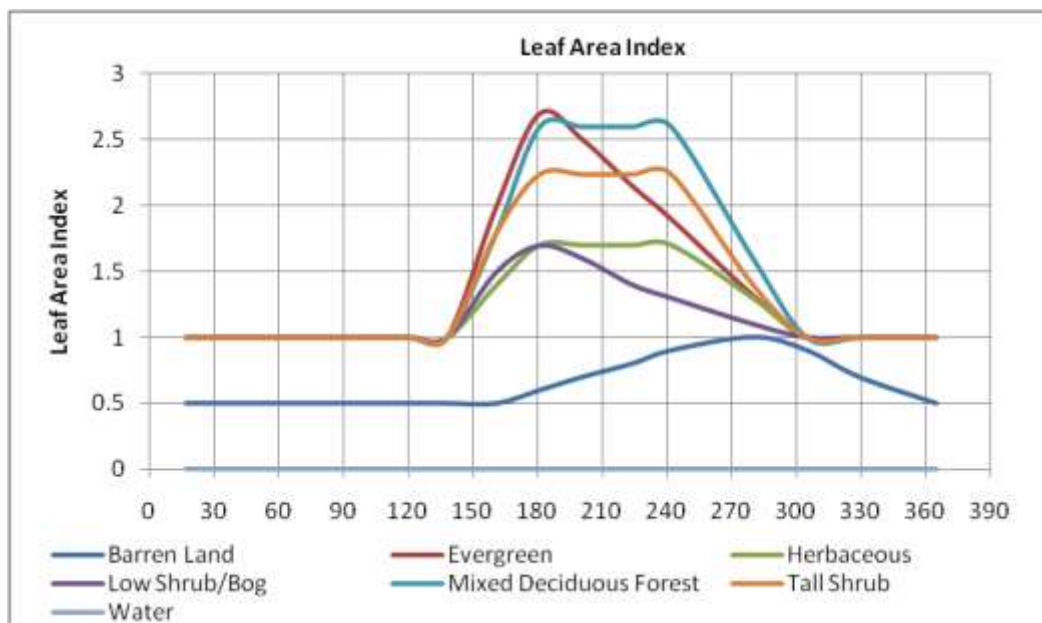


Figure 4-6. Leaf Area Index and Root Depth.

5.0 Integrated Hydrologic Model Calibration

Before the integrated flow model can be used to simulate future conditions, it must be calibrated against hydrologic data that describes the response of the system to variations in climate. For example, following rainfall, streamflow and groundwater levels typically rise and then decline as the precipitation moves through the system. These changes in system hydrology vary in different ways that depend not on the unique characteristics of the rainfall event, but on other factors, such as the spatial variations in aquifer thickness, aquifer or soil hydraulic properties, or vegetation among others. The process of calibration involves adjusting parameter values in the hydrologic model or assumptions in the underlying conceptual flow model so that the model reproduces observed hydrologic response of the system within an acceptable level of accuracy.

This section focuses on describing the approach and results of the model calibration. Available calibration data are described first in Section 5.1. This is followed by a discussion in Section 5.2 on the calibration approach developed for this study considering the following:

- available calibration data (or lack of),
- conceptual flow model complexity and uncertainty, and
- how to achieve the objectives of the modeling.

5.1 Available Calibration Data

Ideally, a fully integrated hydrologic flow model would be calibrated against all hydrologic system responses such as streamflow, groundwater levels, spring flow, soil moisture with depth, pond depths, snowpack measured at a time-scale consistent with sub-daily changes in climate. This would allow the hydrologic response to each climate event, for example the heating and cooling each day, or a short-term precipitation event, to be used as a unique calibration dataset. These data should also be collected across the entire Chuitna Watershed to account for spatial variations in the system response due to changes in system properties and localized climate events and conditions. However, hydrologic systems rarely have enough data to accurately define the aquifer flow system. It is equally rare to find a system where the hydrologic response of the system to climate variability is well monitored. The Chuitna Watershed is no different.

Much of the available data is only available near the proposed mine, and it is generally not well synchronized in time. For example, mean daily streamflow is estimated for various gages throughout the Chuitna Watershed from 1982 through present, but the data only overlaps in time for some of the gages over part of this period. Groundwater levels were also collected intermittently (i.e., typically quarterly) with only some overlap. Snowpack information is available, and spatially distributed over the watershed, but only available on the 1st of month from February through May. No information on soil moisture, surface water pond levels, or spring flow rates was available.

Despite the limited calibration data, available information was used to the extent possible to calibrate the model. Three key datasets were used to calibrate the model:

- Mean daily streamflow data (see Section 2.5.2.3):
 - streamflow data is the most useful of calibration data in the Chuitna Watershed because it represents the combined responses of all upstream groundwater discharge and overland runoff inputs to the stream. Several characteristics of this dataset provide useful information on how the system responds to changes in climate. One limitation of the mean daily data is that short-term, or sub-daily streamflow response to for example, short, intense precipitation events cannot be evaluated. Sub-daily gage data would have helped calibration of the model to short-term runoff events. Examples of important calibration characteristics in the mean daily streamflow response include:
 - flow timing:
 - time to peak,
 - duration and shape of ascending/receding hydrograph,
 - start and end of streamflow events, and
 - duration of baseflows.
 - flow rates (peak) and volumes, and
 - baseflows.
- Snowpack (SWE) at 7 snowcourse locations (see Section 2.5.1.2):
 - Available from first of month from February through May 1983, and
 - Average SWE for first of months from February through May (1983 to 1987).
- Groundwater levels (see Section 2.5.3.5):
 - Due to uncertainty in groundwater elevations (i.e., topographic surface uncertainty), measurements issues (i.e., between pre-1990 and post-2006) and locating wells with coordinates, groundwater depths from only 40 wells were used to calibrate the groundwater flow system in the proposed mine area (the locations are shown in Section 5.3.1),
 - Groundwater depths with time were used where available, otherwise steady state values were used (i.e., from Arcadis, 2007 modeling report).

5.2 Calibration Approach

The approach used to calibrate an integrated flow models is similar to calibrating groundwater flow models (Bear et al, 1992, ASTM D5981–96, 2002), but more challenging because significantly more parameters can be adjusted and the flow system is more dynamic than a groundwater system. For example, significant changes in surface flow can occur over a matter of hours, whereas groundwater response is more like days to months. The approach used to calibrate the distributed-parameter integrated hydrologic flow model of the Chuitna Watershed follows the general approach outlined in Refsgaard

(2007). A step-wise, iterative approach to develop and calibrate the hydrologic model developed by Prucha (2002) and Kaiser-Hill (2002) was also used to guide the model calibration.

Refsgaard (2007) describes an iterative approach involving several steps listed below.

- identify calibration targets,
- specify calibration stages,
- select a calibration method,
- define stop criteria,
- select calibration parameters and define values,
- perform model validation and
- conduct an uncertainty analysis.

For this study, the calibration targets are simply those described above in (Section 5.1). The stages in calibration involved the following steps:

1. Conduct initial sensitivity simulations to identify which parameters the modeled hydrologic system response is most sensitive to. Sub-scale flow models, for example of individual-watershed areas, individual or simple coupled process models (i.e., just groundwater, or groundwater and unsaturated zone) or generalized hillslope models were used to systematically build, test and understand the underlying hydrologic behavior of the system based on the conceptual flow models developed in Section 3.0. These initial simulations were also aimed at identifying reasonable ranges of values for sensitive parameters and testing more conceptual-level assumptions (i.e., the sensitivity of the hydrologic system response to different spatial distributions of glacial thickness over the watershed, sensitivity of flow to using only one bedrock layer etc).
2. Using the full-scale Chuitna Watershed model, short-duration model calibration simulations (i.e., 1980 to 1985) were conducted to take advantage of periods of time where more calibration data were available, to minimize the model run times (i.e., ~2.5 hours for every year simulated) and to further refine sensitive calibration model parameters.
3. A full-scale watershed model, defined as the Basecase, was simulated from 1980 to 2000. Because of the long simulation times (50 hours for 20 years), only limited runs could be performed. The focus of these runs was to refine parameterization of the sensitive model parameters.

Manual calibration was used as the calibration method primarily because the model complexity and long run times do not permit using an automated procedure, such as a local or global optimization algorithm (Blasone et al., 2007). Manual calibration involves adjusting a set of parameter values, running the model, assessing how well the model reproduces observed hydrologic system response (i.e., calibration targets) and then repeating the process until stop criteria are met.

Given the model complexity and uncertainty in model structure, model parameters, external climate data (forcing function) and conceptual models (Vrugt et al, 2005, Neuman and Weiranga, 2003), specific stop criteria could not be defined. Typically these are defined by the objectives of the modeling. For example, if the intent of modeling was to guide the design of local surface culverts to route water for specific climate events, the surface flows in the model would have to be calibrated at a high level. As a result a high-level calibration was not possible for this model. Instead, the goal of the calibration was to attain the best calibration possible using the available data. Calibration results obtained for the PacRim groundwater flow model (Arcadis, 2007) was used as a general guide to assessing calibration performance for the groundwater flow portion of the integrated flow model.

Hill (1998) describes a “principle of parsimony”, where a calibration problem is better posed if its dimensionality is limited and, at the same time, the estimated parameters are sufficient to guarantee a satisfactory model fit. Thus, only a few parameters should be chosen for calibration. Only those parameters which affect the hydrologic system most (i.e., most sensitive) were used to calibrate the integrated flow model. These included:

- horizontal and vertical saturated zone hydraulic conductivity for glacial deposits and for underlying bedrock,
- soil hydraulic properties, including:
 - Saturated hydraulic conductivity of bedrock and glacial deposits,
 - Van Genuchten soil retention factors
- Soil layering
- Streambed leakage coefficients
- Thickness of glacial deposits,
- Climate parameters:
 - lapse rates
 - NARR data locations
- Snowmelt parameters (see Section 4.2.6.2)

The long simulation durations used for the model calibration (1980 to 2000) did not require conducting separate validation simulations. The intent of model validation is to test whether the calibrated hydrologic model is capable of simulating flow conditions for a time period different than used for the calibration. Because of the relatively high level of conceptual, numerical model and calibration data uncertainty over the watershed and the long simulation times, no uncertainty analysis was performed.

5.3 Calibration Results (1980 to 2000)

The calibrated MIKE SHE/MIKE11 integrated flow model produces a considerable amount of data for the 20 year period. Simulated output is compared to observed calibration targets and described in Section 5.3.1. Additional simulated output that describes the hydrologic flow system is described in Section 0.

5.3.1 Comparison of Simulated and Observed Data

A description of the comparison between simulated and observed data starts first with snowpack, because the snowpack needed to be calibrated first. Snowpack is not influenced by the other hydrologic processes within the watershed and the MIKE SHE code allows simulation of snowpack at individual locations. Calibration of streamflow is considered more important than calibrating to groundwater levels because the streamflow represents the cumulative effects of both groundwater and surface water runoff. As such, streamflow calibration is described next, followed by a discussion on calibration to groundwater depths.

Snowpack

Simulated snowpack as SWE is compared against observed data on

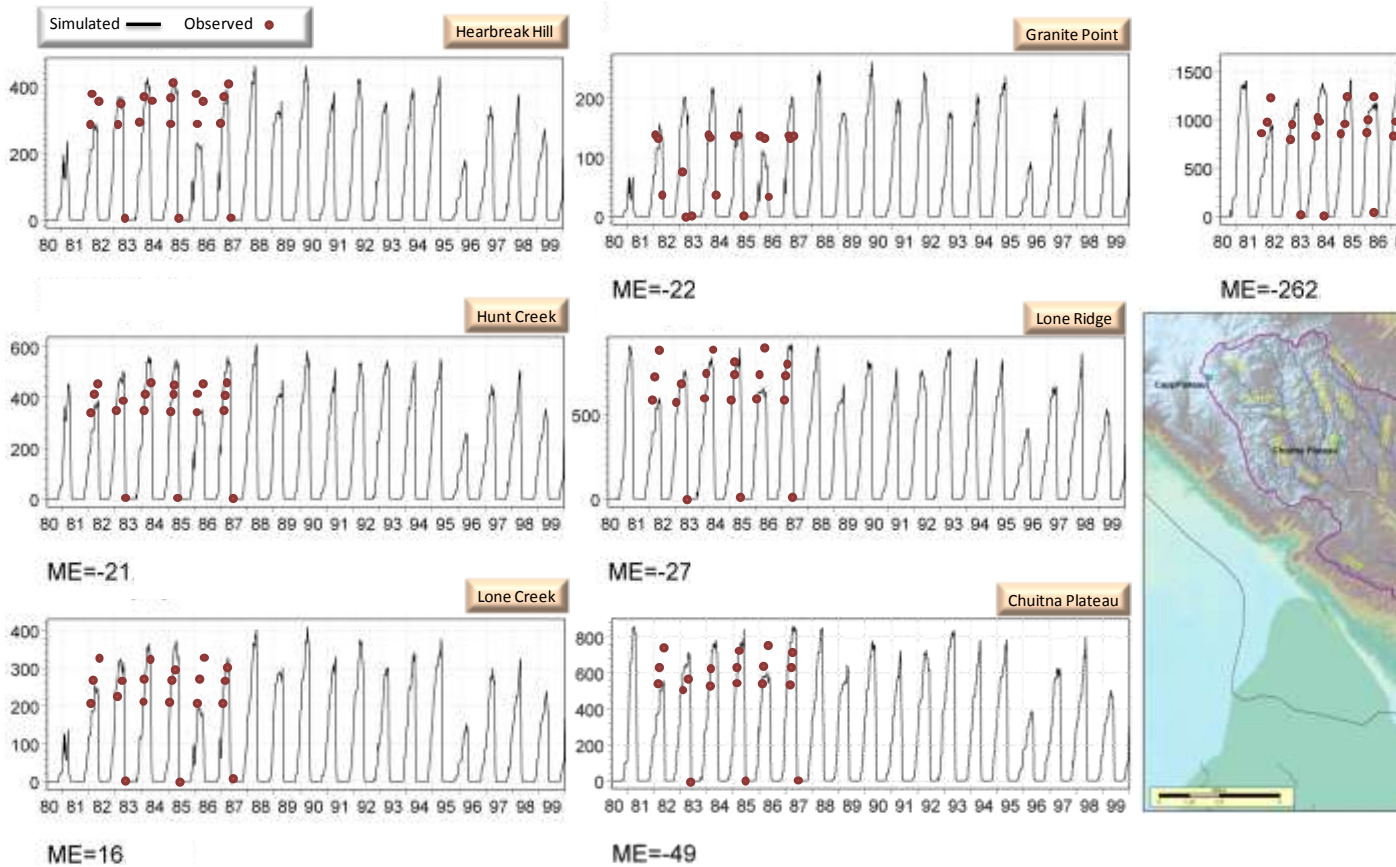


Figure 5-1 for seven snowcourse locations. Although the gage at Granite Point is not within the Chuitna Watershed, the observed data is compared to a point within the watershed at a similar elevation and proximity to Cook Inlet. Traditional calibration metrics such as the mean error, quantify the average error in the calibration process (Anderson and Woessner, 1992). The mean error is also shown for each gage on

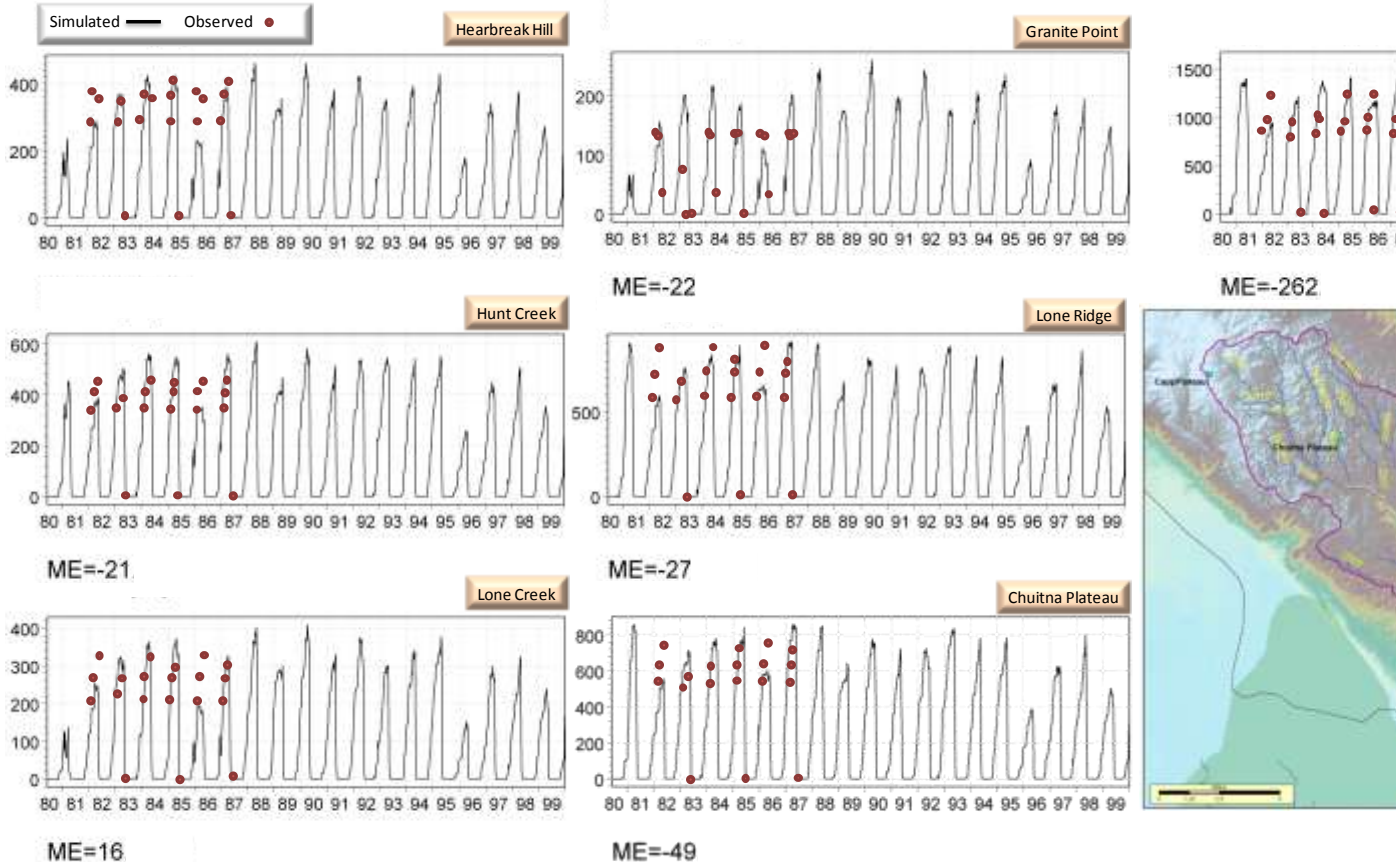


Figure 5-1 and represents the mean of the differences between measured and simulated SWE.

Simulated SWE compared well with observed values, despite using average values (from 1983 to 1987) to compare against simulated SWE. The simulated SWE during this period are quite variable. This is especially true for the 1985-1986 winter periods, where SWE drops to about 50% of the average over the 20 year period. Simulated SWE values during the 1983-1984 winters compare well with observed data over this time period, which represent actual values measured that year. Mean errors are relatively low (ranging from 16 to -262). Correlation coefficients average 71%.

The actual start and end of snowpack at different elevations throughout the Chuitna Watershed cannot be determined from available data. But given the reasonable match obtained for the available time periods, including the gradual increase to a peak in April or May, and the corresponding rapid peak in streamflow in June, it is likely the model simulates a realistic start and end of snowpack at the different elevations.

Streamflow

Simulated mean daily streamflow is compared against observed mean daily streamflow on Figure 5-2 (page 230 and 180), Figure 5-3 (page 220 and 110) and Figure 5-4 (page 140 and 195). Observed data (red dots) are not available at any of the gages for the full 20 year period, though gage 230 (lower Chuitna), gage 180 (lower Stream 2003) and

gage 195 (upper Lone Creek (2002)) have data from the early 1980s through the mid 1990s.

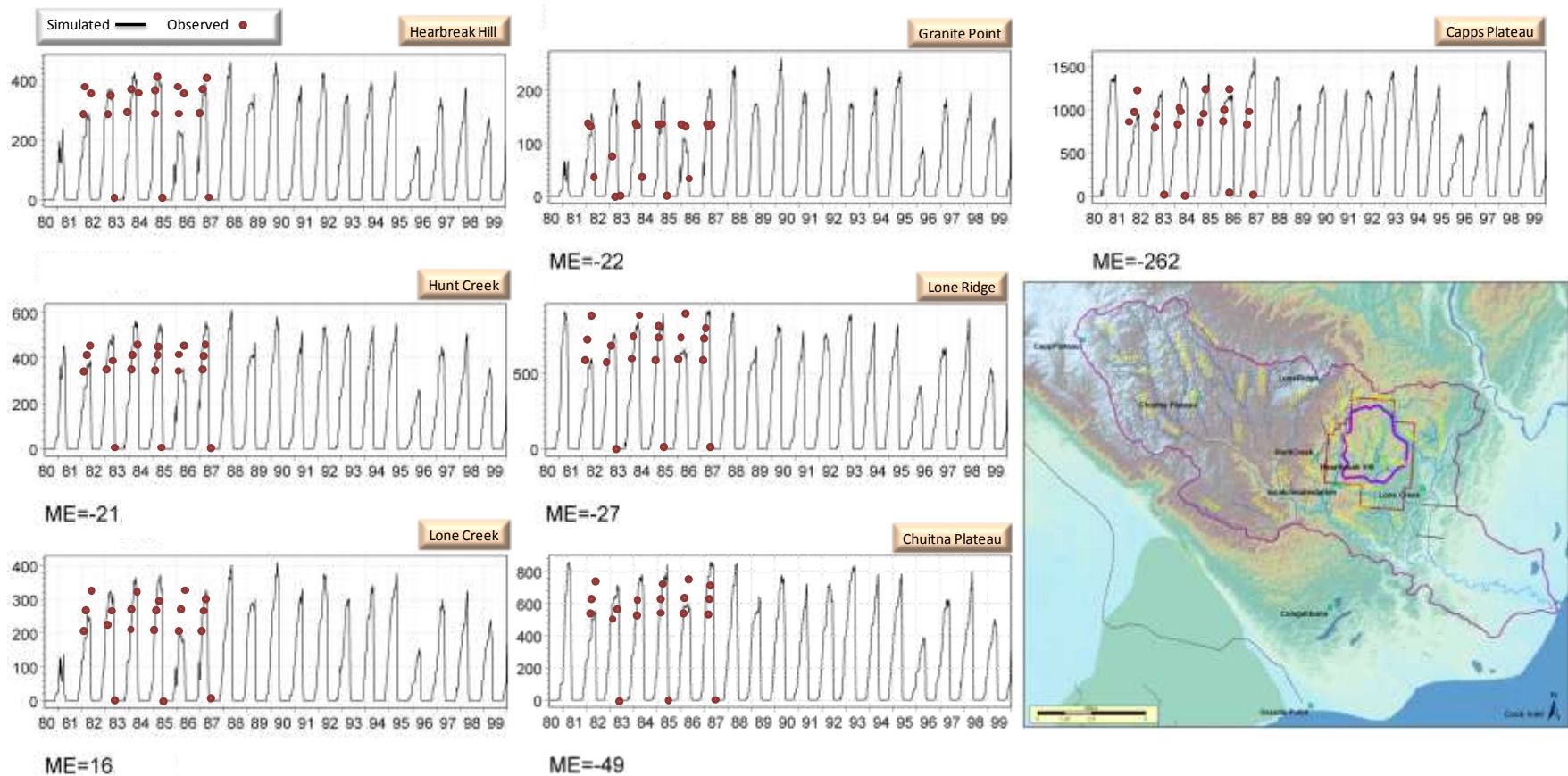


Figure 5-1. Comparison of Simulated and Observed Snowmelt

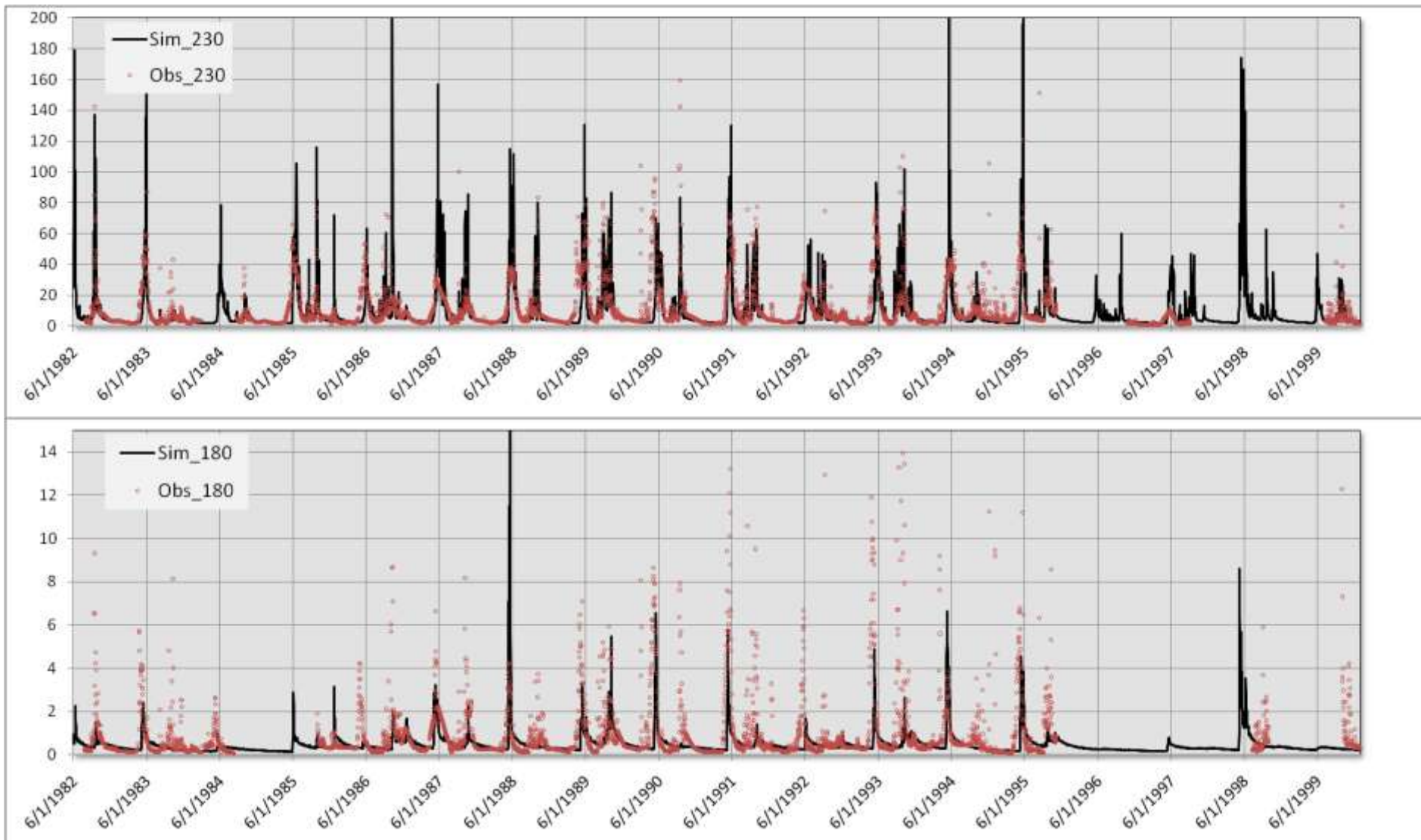


Figure 5-2. Comparison of Daily Simulated and Observed Streamflow – Chuitna - Gage 230 and Stream 2003 - Gage 180.

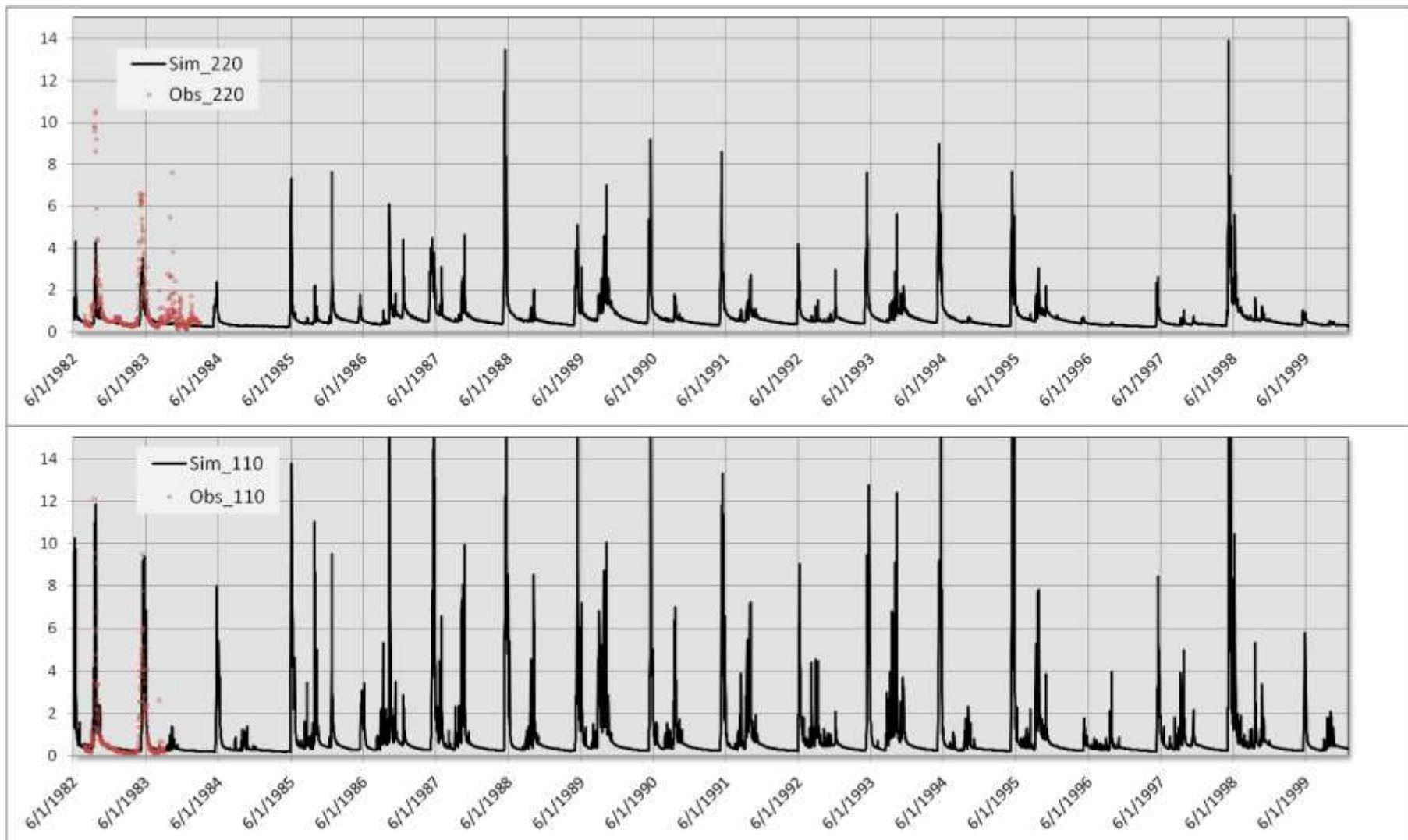


Figure 5-3. Comparison of Daily Simulated and Observed Streamflow – Lone Creek (2002) - Gage 220 and Stream 2004 - Gage 110.

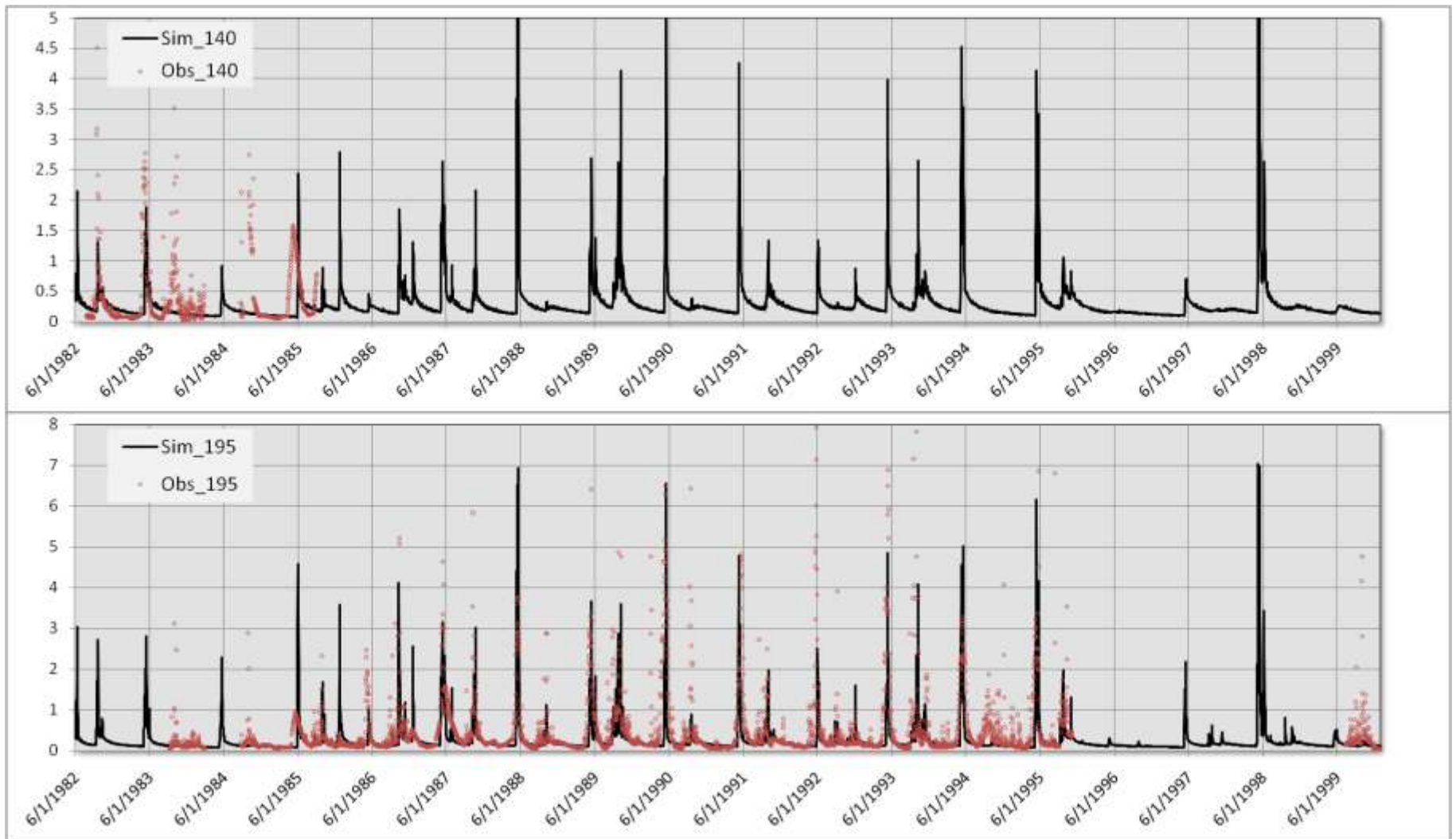


Figure 5-4. Comparison of Simulated and Observed Streamflow – Stream 2003 at Gauge 140 and Lone Creek (2002) at Gauge 195.

Simulated streamflow characteristics at the different gages reproduce those in the observed hydrographs reasonably well. Although higher correlation coefficients are typically required for watersheds that are well gauged, an average correlation of ~55% (range is 6 to 76%, or 45% to 76% excluding gage 180 along Stream 2003). It is unclear why the correlation is poor at gage 180, but simulated flows are lower than observed (peaks and spring runoff). This may be due to errors in streamflow measurements at gage 180, under specifying precipitation, over estimating evapotranspiration, or using a surface topography that does not capture localized lateral surface drainage contributions into the mainstem 2003 stream. Closer inspection of the ASTER topography revealed the existence of two, local stream areas that were not simulated in the MIKE 11 stream network. This could help explain the lower simulated flows in stream 2003. Despite the lower levels, the model is able to reproduce the two key runoff events (spring snowmelt and fall rains), and is also able to simulate the slow recession curves that appear to be generated by baseflow, rather than surface runoff (weeks to months long).

From a semi-quantitative perspective, peak flows are both over- and under-simulated in all gages, except for gage 180 (lower stream 2003) and gage 220 (lower Lone Creek (2002)). This suggests that the NARR climate data series used to drive the integrated flow model may contribute to difference between simulated and observed flows. The bias at gages 180 and 220, however suggest there may be other reasons why streamflow is under-simulated. Other than the reasons mentioned above, the difference may also be due to incorrect spatial variation in thickness of the glacial deposits. The distribution was based on a general trend and use of lithology from only 20 of the more than 430 boreholes in the mine area.

Baseflow is simulated well in all of the gages, which is largely dictated by the slope of hillslope topography and lateral saturated hydraulic conductivity in the glacial deposits. Simulated baseflow decreases with elevation, similar to the observed flows. Once infiltrating precipitation (or snowmelt) enters the shallow aquifer, it is directed laterally in the glacial deposits because of the lower permeability in the underlying bedrock. The streamflow gradually recedes during baseflow periods because of the slow drainage of groundwater from adjacent hillslopes, which is primarily from groundwater storage. Most inter-stream hillslopes within the Chuitna sub-watersheds are on the order of 1 kilometer long, from hilltop to stream.

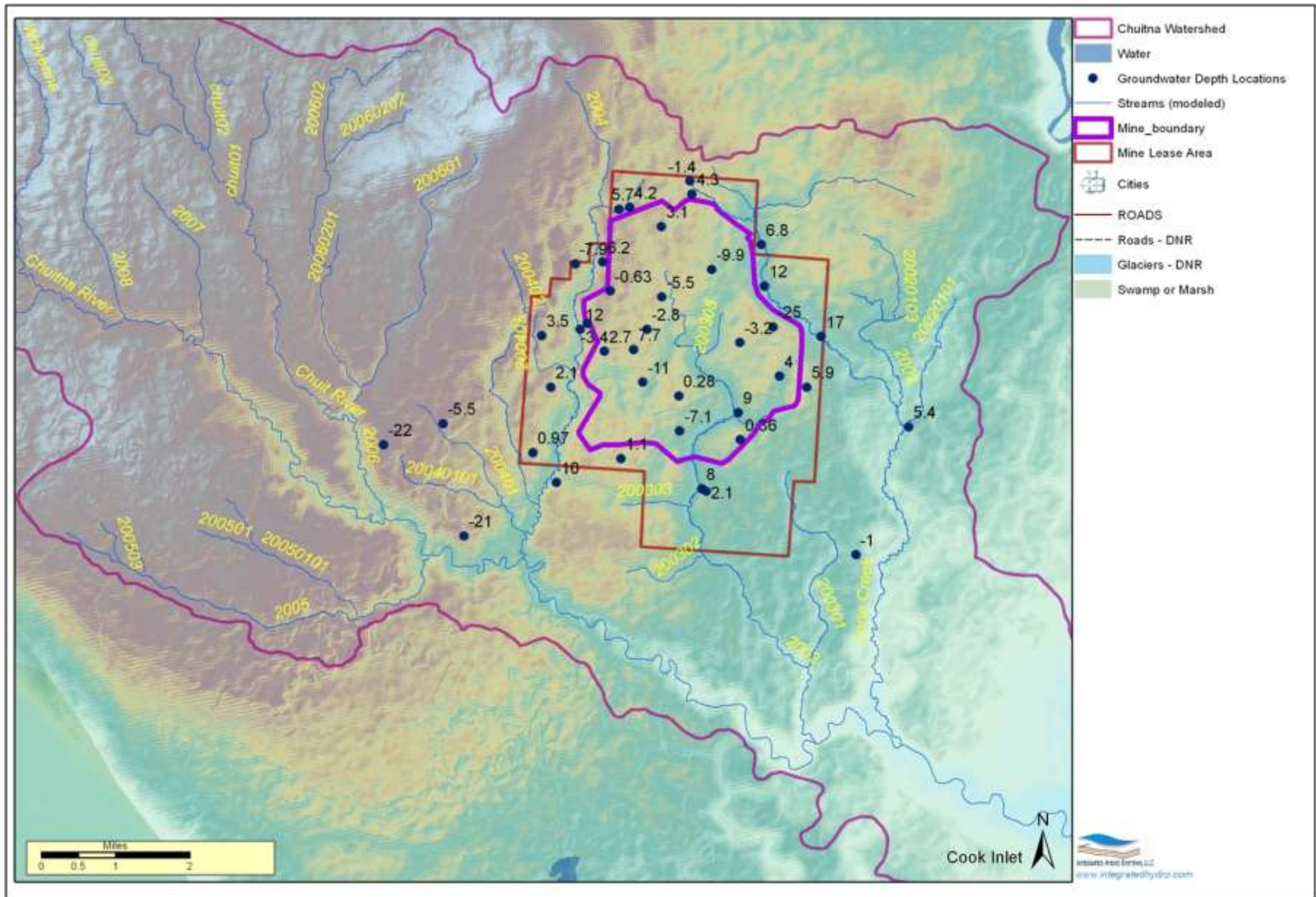


Figure 5-5. Groundwater Residuals (m). Positive values indicate observed head > simulated head.

Groundwater

Figure 5-5 shows the time-averaged difference between simulated and observed groundwater levels for the glacial aquifer. Negative values indicates the model simulates level too high, while positive values indicate simulated levels are too low. The average mean error for all GW well depths considered in this model is less than 1 meter, but the average mean absolute error of all wells is 8.2 m. There are some outliers, but these are actually similar to what Arcadis found in their model. The similarity is partly because saturated hydraulic conductivity values for the two model layers were assigned values similar to those used in the Arcadis model to better compare the results and because no other data were available (i.e., lacking geology, imperfect topography, complete well coverage etc). Results of this calibration show that reasonable results are obtained and appear to be well within 10% of the mean absolute error across the study area. This is a standard typically applied to assess model performance (Hill, 1998). Arcadis (2007) assumes this total 10% head drop to be ~24.0 meters, but this drop extends across their entire model area and not the distance spanned by the wells themselves (more like ~12 m). If 12 meters were used, simulated levels at several wells (the same wells used in the integrated model calibration) would not meet this standard calibration target.

Spatial bias in the simulated water level residuals is low (and similar to Arcadis, 2007), though the model does not simulate the low heads in wells nearest the Chuitna (i.e., -22 and -21 m). The deep observed water levels in this area may reflect increased permeability in the underlying bedrock, due to a transition from siltstone/claystone interbed material to sandstone/conglomerate (Flores, et al, 1994).

The range of simulated groundwater levels in time at wells (12) where coordinates could be identified is greater than observed, however the frequency of measurements is insufficient to capture the complete range of seasonal fluctuations (see Section 5.1). The simulated range of heads in time varies from about 3 to 10 meters, depending on the location.

Although the model simulates water depths for the minable coal layer, they were not evaluated because of the increasing level of uncertainty (lack of geologic model, screened zone, effects of faults etc) and general lack of wells in this unit(s) with coordinates. Observed head data within the minable coal sequence suggests groundwater flow is complicated by lateral facies changes in the interbeds, and leakage between the underlying Sub-Red 1 Sand aquifer and overlying glacial deposits, neither of which is characterized well over the extent of the entire Chuitna Watershed.

5.3.2 Other Simulated Hydrologic Responses - Basecase

The calibrated hydrologic model produces a variety other types of output, for which no calibration data is available, but are useful for describing how the integrated flow system behaves. To understand how the different hydrologic flow processes change across the extent of the Chuitna Watershed, simulated average annual water balances for the different hydrologic components are summarized by eight sub-watersheds shown spatially on Figure 5-6 and in Table 5-1. Water balances in Table 5-1 (upper table) are

provided in mm/m², or mm/year normalized by unit area so they can be directly compared against each other. The lower table provides simulated average annual water balances normalized by annual precipitation. Negative and positive numbers simply follow the adopted water balance procedure in MIKE SHE to assign negative numbers to inflows and positive numbers to outflows. To illustrate how the watershed behaves on a cell-by-cell basis, average annual distributions (1980 to 2000) of selected hydrologic responses were prepared and presented in Appendix C - These include the following:

- Simulated Average of Annual Actual Evapotranspiration,
- Simulated Average of Annual Soil Evaporation,
- Simulated Average of Annual Plant Transpiration,
- Simulated Average of Annual Groundwater Recharge,
- Simulated Average of Annual Groundwater Baseflow to Streams,
- Simulated Average of Annual Overland Flow to Streams, and
- Simulated Average Annual Snowpack.

Net precipitation (Table 5-1), including rainfall and snowfall (see Figure C-7) is greatest in upper Chuitna Watershed areas, for example, in Upper Chuitna it is 1876 mm/yr (73.6 in/yr) while in the Lower Chuitna it is only 823 mm/yr (32.4 in/yr), which is similar to the trend based on available climate data collected in 2006 (see Section 2.5.1.1). Total snow accumulation (SWE) actually increases triples from 332 to 994 mm/yr (13 to 39 in/yr) over these two watersheds as a result of decreasing temperatures with elevation and increasing precipitation.

Actual evapotranspiration (AET) generally decreases with elevation from the Lower Chuitna to Upper Chuitna (628 to 576 mm/yr, or 24.7 to 22.7 in/yr), which is similar to reported values (see Section 2.5.1.4). Figure C-1 shows that localized areas of higher and lower AET occur within each sub-watershed; the higher areas are generally associated with shallower groundwater or more consistently ponded areas during the simulation. The relatively small difference in total AET with elevation, compared to precipitation and snow accumulation is attributed to the relatively high availability of near surface water throughout the watershed (i.e., high water content of peat soils, shallow groundwater levels). As a percent of average annual precipitation, this ranges from 76 to 31%, respectively. At lower elevations, AET is the dominant hydrologic process and is responsible for most of the direct loss of precipitation in the lower sub-watersheds. The remaining water flows out of the system as either baseflow or overland flow to streams (a comparably small percent flows out as groundwater to Cook Inlet). Soil evaporation and plant transpiration (Table 5-1) only make up a small portion of the AET in the Upper Chuitna (73 and 134 mm/yr of total AET 576 mm/yr), while the remaining AET is accounted for by snow sublimation and evaporation from open water bodies, snowmelt water and water intercepted by the canopy. In the Lower Chuitna, plant transpiration exceeds soil evaporation (250 and 145 mm/yr) and these make up 63% of the total AET (628 mm/yr). Therefore, soil evaporation and plant transpiration losses are greater in lower sub-watersheds (see Figure C-2 and Figure C-3). Average daily AET varies smoothly throughout the year, similar to changes in air-temperature, with lowest values

during the winter (< 1 mm/day) and highest values during June (>8 mm/day). At lower elevations, AET values are higher during all months, except June.

Overland flows (OL Bou) across sub-watershed boundaries should not occur, because the boundaries are defined based on topographic divides. However, the resolution of the digital topography is limited and some flows do occur across these boundaries, though it is small (i.e., 1 to 11% on the lower Table 5-1). Overland flows are highest in the Upper Chuitna (551 mm/yr, or 21.7 in/yr, or 29% of annual precipitation) and lowest in the Lower Chuitna (6 mm/yr, or 0.2 in/yr, or 1% of annual precipitation). They are highest in the Upper Chuitna because of the increased topographic slopes (see Section 2.3) and lower permeability soils (see Section 2.4.3). Spatial distribution of simulated average annual overland flow to rivers on a cell basis (see Figure C-6) show higher flows in the upper watersheds, effectively where lower soil permeability is specified (Figure 2-9) in the model.

Groundwater flow across sub-watershed boundaries was not expected to be zero, especially given the overall topographic slope over the Chuitna Watershed, from Capps Plateau towards Cook Inlet. The model simulates flows across these boundaries from 1 to 11% of annual precipitation (Subsurf). Although baseflows are also highest in Upper Chuitna (669 mm/yr, or 26.2 in/yr) and lowest in Lower Chuitna (59 mm/yr, or 2.3 in/yr), as a percent of annual precipitation, the Middle Chuitna shows 44%, while the Upper Chuitna shows only 36% and the Lower Chuitna shows 7%. The spatial distribution of average annual baseflows (see Figure C-5) also shows higher values in upper watershed areas, but also on upgradient (i.e., north/northwestern) sides of drainages. Despite the watershed-scale resolution of the integrated model, these results are supported by similar observations of spring flows occurring preferentially on north/northwestern sides of drainages studied by Oasis (2010), for example on Lone Creek and streams 2003 and 2004.

It is not surprising that spatial trends in simulated sub-watershed groundwater recharge are similar to those for baseflow, since once recharged, the groundwater system discharges most of this inflow back out to streams as baseflows. The highest recharge occurs in the Upper Chuitna (722 mm/yr, or 28.4 in/yr) and lowest occurs in the Lower Chuitna (149 mm/yr, or 5.9 in/yr). The higher baseflows correlate to higher recharge, but in lower areas, more groundwater is removed to the atmosphere prior to discharging as baseflow due to the much higher AET, especially from plant transpiration. Average annual spatial distribution of recharge (see Figure C-4) varies significantly within each sub-watershed area. Negative recharge values indicate areas where groundwater on average, discharges (i.e., via AET or to the ground surface in non stream areas) more than is recharged. Although this spatial variability doesn't reflect the temporal (or seasonal) variations in recharge, where it may be positive part of the time, the discharge areas generally occur in steeper uphill sides of drainages, or on the north/northwest sides of drainages due to the overall slope of the Chuitna Watershed from northwest to southeast into Cook Inlet.

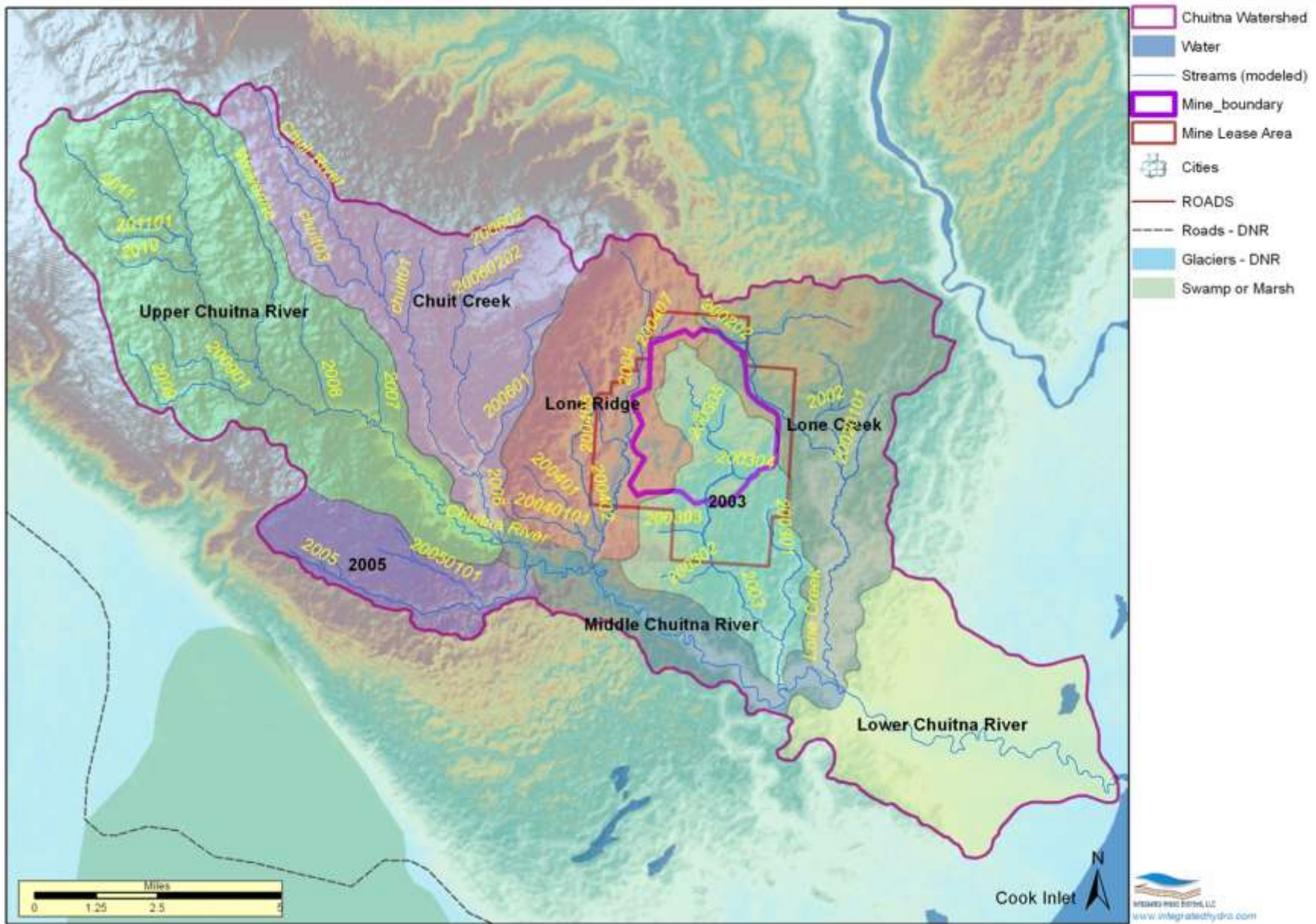


Figure 5-6. Sub-watershed Water Balance Areas

Table 5-1. Summary of Average Annual Water Balance Components - Basecase

Net Water Balance (mm/m²)

Flow Component	Middle Chuitna	Lower Chuitna	Lone Creek	Stream 2004	Upper Chuitna	Chuit Creek	Stream 2003	Stream 2005	Entire Watershed
Net Precipitation	-1088	-823	-1065	-1377	-1876	-1668	-1110	-1522	-1393
Canopy ThroughFall	926	692	902	1187	1644	1452	944	1314	1203
Evapotranspiration	642	628	652	621	576	590	643	613	613
TOTAL Snow (swe)	-483	-332	-469	-657	-994	-843	-496	-747	-679
OL Bou.Inflow	-34	-2	-31	-16	-17	-61	-35	-11	0
OL Bou.Outflow	15	60	44	102	85	90	12	171	47
Overland Flow to River	50	6	63	235	551	523	26	339	278
SubSurf.Bou.Inflow	119	17	62	33	14	29	72	22	0
SubSurf.Bou.Outflow	46	29	20	91	16	21	112	37	3
Baseflow to River	480	59	370	372	669	525	415	386	436
Soil Infiltration	-809	-564	-782	-817	-931	-796	-855	-750	-802
Soil Evaporation	130	145	135	99	73	91	136	100	108
Plant Transpiration	254	250	248	197	134	171	260	183	200
Groundwater Recharge	415	149	382	514	722	530	443	464	485
Total Error	0	0	0	0	0	0	0	0	0
Baseflow+OL to River	530	64	433	606	1220	1048	440	725	714

Flow as a Percent of Net Sub-Watershed Precipitation

Flow Component	Middle Chuitna	Lower Chuitna	Lone Creek	Stream 2004	Upper Chuitna	Chuit Creek	Stream 2003	Stream 2005	Entire Watershed
Canopy ThroughFall	-85%	-84%	-85%	-86%	-88%	-87%	-85%	-86%	-86%
Evapotranspiration	-59%	-76%	-61%	-45%	-31%	-35%	-58%	-40%	-44%
TOTAL Snow (swe)	44%	40%	44%	48%	53%	51%	45%	49%	49%
OL Bou.Inflow	3%	0%	3%	1%	1%	4%	3%	1%	0%
OL Bou.Outflow	-1%	-7%	-4%	-7%	-5%	-5%	-1%	-11%	-3%
Overland Flow to River	-5%	-1%	-6%	-17%	-29%	-31%	-2%	-22%	-20%
SubSurf.Bou.Inflow	-11%	-2%	-6%	-2%	-1%	-2%	-6%	-1%	0%
SubSurf.Bou.Outflow	-4%	-3%	-2%	-7%	-1%	-1%	-10%	-2%	0%
Baseflow to River	-44%	-7%	-35%	-27%	-36%	-31%	-37%	-25%	-31%
Soil Infiltration	74%	69%	73%	59%	50%	48%	77%	49%	58%
Soil Evaporation	-12%	-18%	-13%	-7%	-4%	-5%	-12%	-7%	-8%
Plant Transpiration	-23%	-30%	-23%	-14%	-7%	-10%	-23%	-12%	-14%
Groundwater Recharge	-38%	-18%	-36%	-37%	-38%	-32%	-40%	-31%	-35%
Baseflow+OL to River	-49%	-8%	-41%	-44%	-65%	-63%	-40%	-48%	-51%
Baseflow % of River Q	91%	91%	85%	61%	55%	50%	94%	53%	61%

6.0 Future Scenario Simulations

Future model simulation scenarios are described in this section. Definition of the scenarios is described first in Section 6.1 and results of the future scenario simulations are described in Section 6.2.

6.1 Definition of Future Scenarios

Five climate change scenarios were defined for the end of the 21st century (2080-2099) to bracket projected high and low air temperature and precipitation changes (4 scenarios) and to estimate a single mid-level change scenario (Figure 6-1). The 2080-2099 period was selected to estimate the maximum range of hydrologic impacts (changes would be less for earlier periods) and to allow enough time for the proposed mine reclamation configuration to reach a pre-mining condition (i.e., vegetation fully established, stabilization of residual mine dewatering). The baseline (Basecase) was derived from 3-hourly time-series air temperature and precipitation data for 1980 to 2000 from the North American Regional Reanalysis dataset. Future climate scenarios were based on averaged results from 21 global climate models for greenhouse gas emissions under a “moderate” emissions scenario (A1B; Figure 6-2), as tabulated in the Intergovernmental Panel on Climate Change Fourth Assessment for Alaska (IPCC, 2007, Figure E04). According to the averaged model results, for the Chuitna River watershed, predicted changes in air temperature and precipitation will be greatest in winter months (December through February) and lowest in either Fall (September through November) or summer (June through August). Because increases in precipitation relative to increases in temperature are variable in global climate predictions, five future climate scenarios were defined for the hydrologic model. This accounts for the possibility in a scenario, for example, where increases in precipitation relative to temperature are high, streamflow increases, whereas it might decrease for the case where temperature increase is high compared to the increase in precipitation.

Evapotranspiration (AET) is another critical external climate variable, which depends on both air temperature and precipitation that strongly influences watershed response to climate change. Increased future air temperature affects hydrology in two ways; increased snowmelt through convective air heating (sensible heat) and warmer rain-on-snow, and increased water loss via AET. In the integrated hydrologic model, AET is calculated as a function of soil and plant properties and external climate variables, such as net short- and long-wave solar radiation, wind speed, vapor pressure, precipitation and air temperatures which are incorporated into a reference evapotranspiration (RET) value that is then used to estimate plant transpiration and evaporation from the plant canopy, surface soil, surface water and snow. Because the RET is a function of both air temperature and precipitation, which both vary with elevation, spatially-distributed values of RET were adjusted to account for climate changes in temperature and precipitation. RET was calculated using the FAO-56 Penman-Monteith equation with the REFET code (Allen, 2000)

A variety of methods exist to ‘downscale’ global climate model results to the local Chuitna Watershed hydrologic model. We chose the ‘delta method (Hamlet et al, 2010)’, because it was simple to implement and preserves the sequence of weather and natural climate variability in the

baseline 1980 to 2000 time period. Though this method does not account for changes in the intensity or frequency of events, it is not expected to significantly affect predicted changes to system hydrology over seasonal and annual time frames. For future temperature changes, we add the predicted change in temperature (delta T on Figure 6-1) to the seasonally corresponding 3-hour value in the historical baseline NARR data. For precipitation, we increased the historical baseline by the percent shown (delta %P).

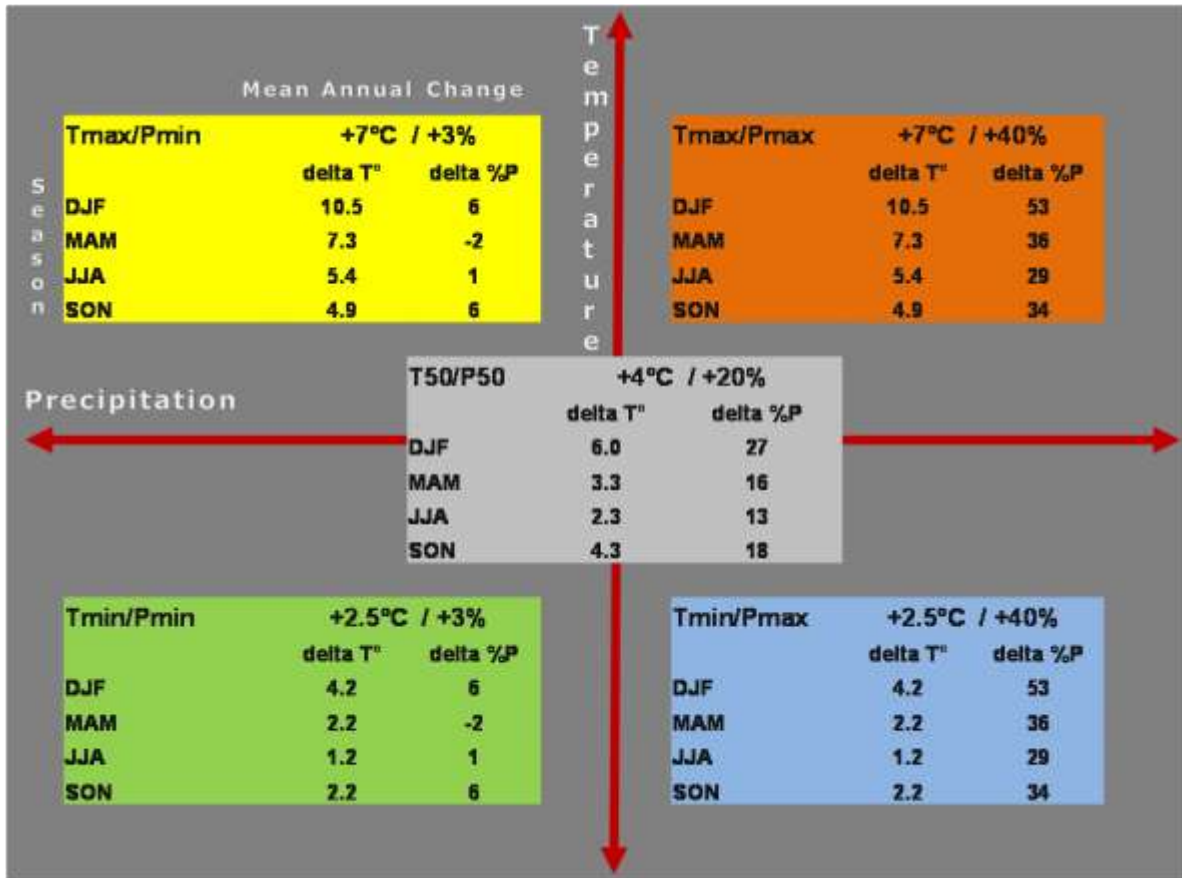


Figure 6-1. Climate Change Scenarios for 2080-2099 for Alaska (Christensen et al, 2007)

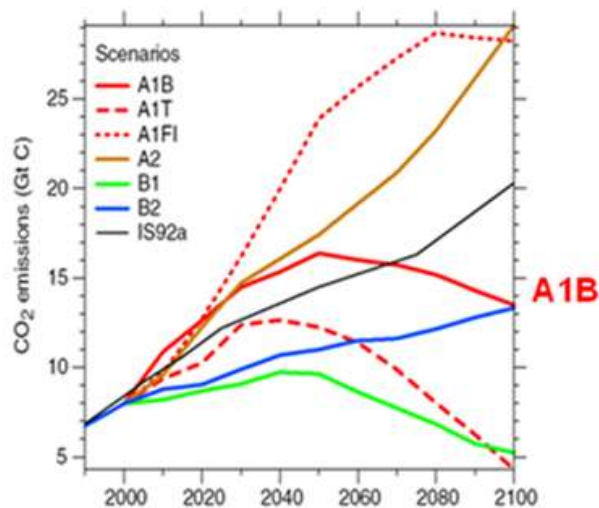


Figure 6-2. The A1B scenario refers to a future where global population peaks mid-century, there is rapid economic growth and a balanced portfolio of energy technologies is rapidly adopted that includes fossil fuels and high efficiency technologies. (Climate Impacts Group, 2009)

6.2 Results of Future Scenario Simulations

Results of the climate change, mine reclamation and combined climate change and reclamation scenarios are described in this section.

- Results are described as changes in hydrology relative to the Basecase simulation from 1980 to 2000 (see Section 5.3).
- Simulated changes in system hydrology are also shown as net changes lumped over the entire 20 year sequence (-1 year to reach stable hydrodynamic state) for the entire watershed.
- To help illustrate how the system hydrology changes both spatially and at various time-scales (within the 20-year time period), simulated results relative to the Basecase are also shown at different spatial and temporal resolutions (i.e., grid-scale to sub-watersheds, and seasonal to sub-daily, respectively) for the following output.
 - Snowpack/snowmelt
 - Unsaturated Zone
 - Groundwater Recharge
 - Evapotranspiration
 - Unsaturated zone moisture distributions
 - Saturated Zone
 - Baseflow to Stream
 - Surface Flows
 - Overland flow to Stream
 - Stream flow

The ratio of change in temperature to precipitation is important.

6.2.1.1 Changes in Snowpack

In the present-day system, precipitation reaches the ground surface or vegetation canopy as either rainfall during warmer months or snowfall during colder months. In all future climate scenarios, increasing air temperatures decreases total snowpack and melt snow snowmelt earlier in the spring. Although snowmelt occurs earlier, the actual snowpack is melt off of the snowpack is partially offset by the increased precipitation specified in winter for all scenarios.

Historically, the snowpack in the Chuitna Watershed has been greatest in the upper reaches and lowest near the coast (see Figure C-7). Figure 6-3 shows the Basecase average snow depth averaged by day from 1980 to 2000 (the black line on the three graphs) for three different locations within the Chuitna Watershed indicated on the upper right plan-view map. Depending on location, snow depths increase relatively smoothly from mid-October, peak in early April (Lower Chuitna) to mid-May (Upper Chuitna) and then melt-out by about mid-May (Lower Chuitna) to late June (Upper Chuitna). In the upper Chuitna Watershed, the maximum Snow Water Equivalent (SWE) approaches 1000 mm, while in the lower watershed it is less than 200 mm. The spatial variation is primarily due to orographic effects on temperature and precipitation.

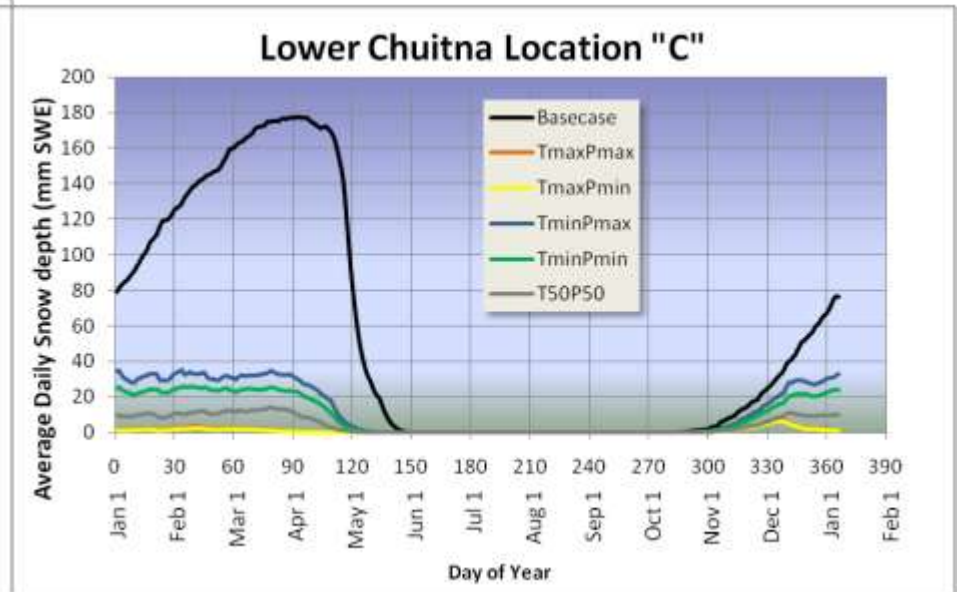
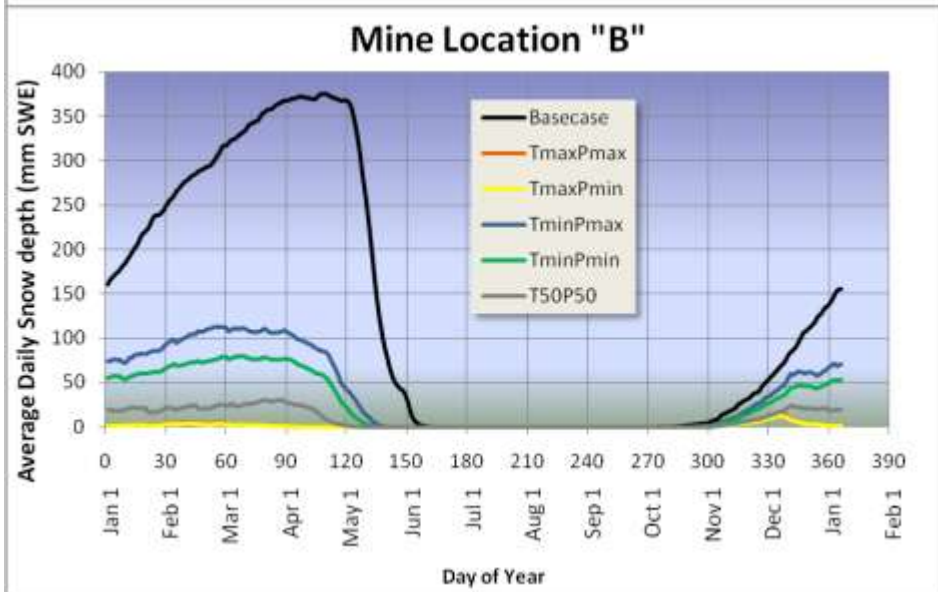
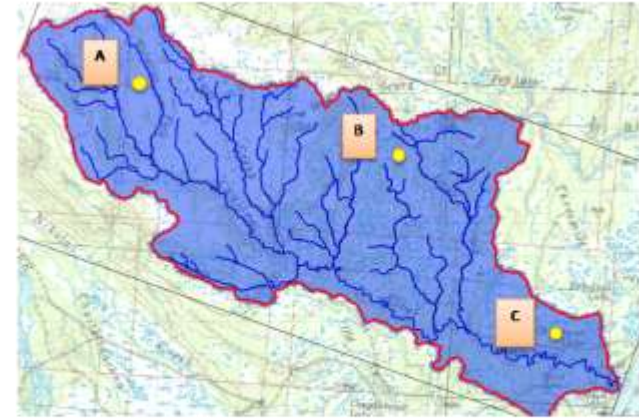
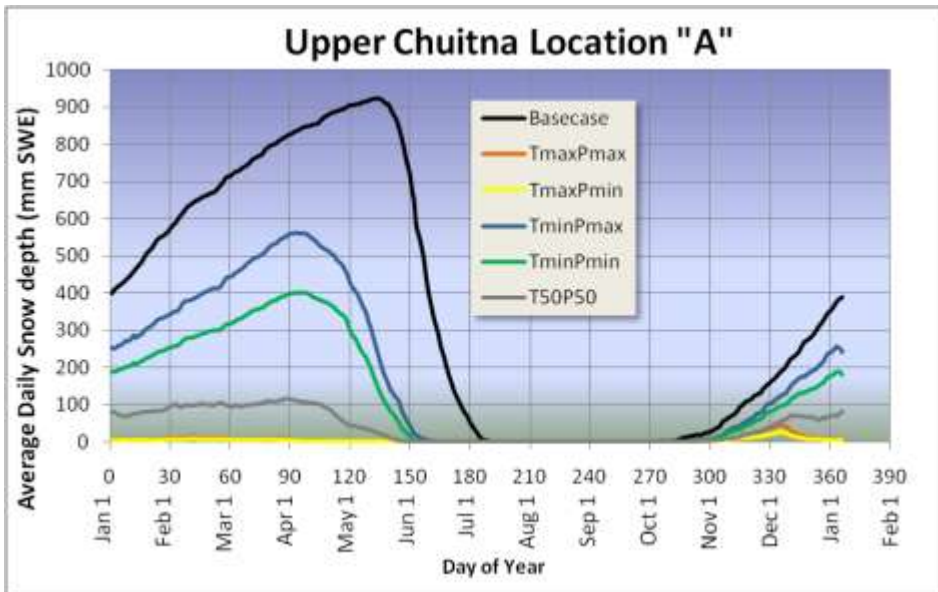


Figure 6-3. Simulated Average Daily Snow Depth (mm SWE). Elevations are 15 m, 216 m and 512 m for A, B and C Points.

In all future scenarios, average annual snowpack decreases and snowmelt increases (Figure 6-3). The decrease in snowpack relative to the historical baseline is greatest at lower elevations where annual snowpacks are lower and temperatures are higher, indicating that melting thresholds are reached sooner at lower elevations. The difference in change in snowpacks relative to the historical is least for the Tmin/Pmax scenario (-4% Upper Chuitna; -35% Lower Chuitna) and greatest for the Tmax/Pmin scenario (-88% Upper Chuitna; -92% Lower Chuitna). As elevations within the watershed decrease, snow depths stay more constant in time, rather than smoothly increasing to a peak.

Scenarios with the greatest temperature increase (Tmax) virtually eliminate the continuous baseline winter snowpack. In these scenarios snow accumulates in a series of smaller snowpacks that melt-out every few weeks (see Figure 6-4 for simulated snowpack every 2 days). In scenarios where temperatures increase the least (Tmin), inter-annual variability of winter snowpack increases. In some years the snowpack reduction is more pronounced and similar to the Tmax scenario, while in other years it is similar to, or exceeds historic baseline conditions.

Another significant change predicted by our model is that the start and end of snowpack also change due to the climate changes. The start of snowpack is delayed in most years and for all scenarios between 1 to 2 weeks and ends sooner by about 1 to 3 months on average (Figure 6-5), depending on the elevation and scenario. At lower elevations, melt-out occurs sooner, but the number of days reduced is less than upper elevations. Tmax scenarios reduce melt-out most, by about 75 to 100 days (or to late February to mid- to late-March), while the reduction is about 30 to 40 days for Tmin scenarios.. Snowpack is reduced by 40 to 65 days for the T50/P50 scenario.

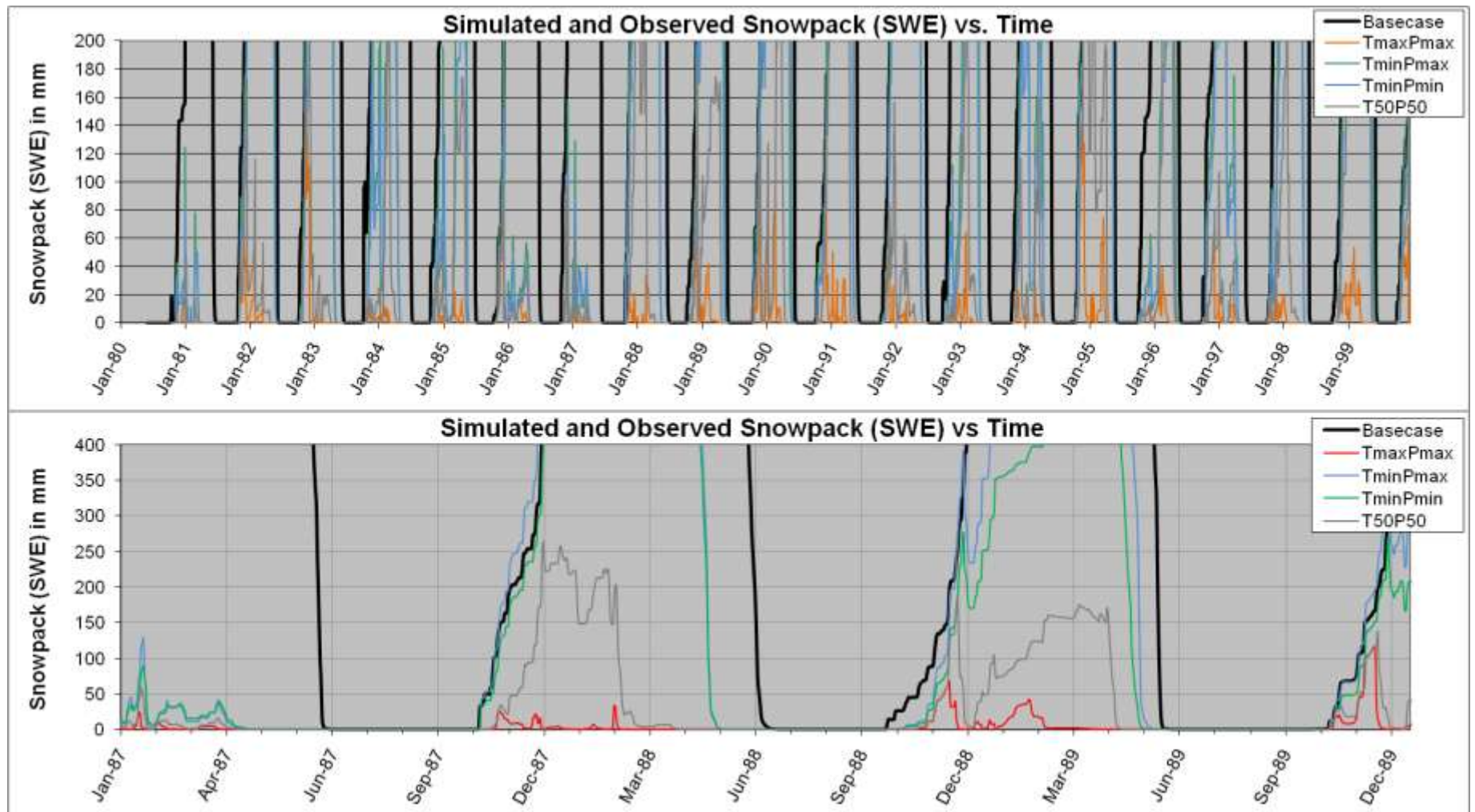


Figure 6-4. Simulated Baseline Snowpack (every 2 days). The TmaxPmin case is not shown, but shows less snowpack than the TmaxPmax case (red).

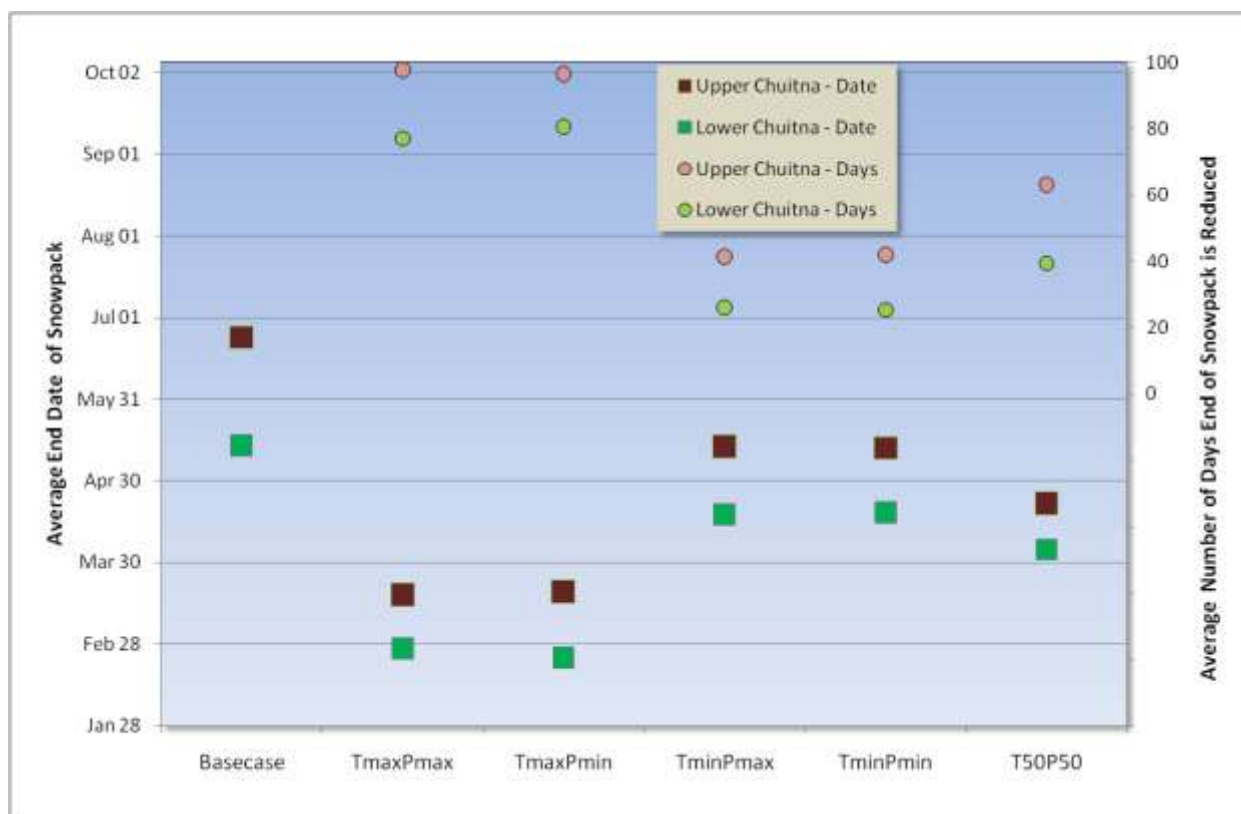


Figure 6-5. Change in Average End Date and Reduction in Days of Snowpack

6.2.1.2 Changes in the Unsaturated Zone

Soil Moisture Content:

The soil moisture content at any moment in time or point within the model is quite variable because it depends on a number of spatially-variable factors such as type of vegetation, soils, groundwater depths, snowmelt, surface topography and climate. Despite this complexity, Basecase model results show that soil moisture content varies most in surface soils (Figure 6-6) because of the direct net effect of precipitation, snowmelt, soil evaporation and plant transpiration. The variations decrease rapidly with depth as the effects of the surface processes diminish. Depending on the location, surface soils saturate during spring snowmelt (June for the Upper Chuitna area “A” and May for the Mine area “B”), de-saturate during the summer (early-August for Upper Chuitna area “A” and late June for Mine area “B”) and then re-saturate during fall rains by September.

Future climate effects on surface soil moisture contents are significant and mostly related to the dramatic shift in snowmelt (see Figure 6-6). Surface soil moisture contents for all scenarios are higher than the Basecase from November through about the end of March due to increased snowmelt caused by increased winter temperatures. From March to mid-summer, moisture contents decrease, then increase to October. The timing of minimum summer soil moisture content shifts from late-June at the mine location (“B”), to about mid- to early-June (2 to 4 weeks) and from late-July in Upper Chuitna (“A”) to early- to late-June (1 to 2 months). In

addition, surface soil moisture contents decrease more for the Upper Chuitna location. The deviation of soil moisture content from baseline conditions is also greater in the Upper Chuitna area, which suggests upper watershed soils are more sensitive to climate changes. One reason for this may be because lower soil permeability in upper watersheds causes lower and slower rates of infiltration, which increases soil moisture loss via evapotranspiration. Soil moisture content decreases most for the TmaxPmin case because the increase in precipitation is insufficient to offset the increased “drying” effect caused by increased AET due to increased temperatures. Soil moisture content decreases least in the TminPmax case because the increase in precipitation is highest relative to the increase in temperature.

The climate changes imposed on the model cause less change in soil moisture content with increasing depth (Figure 6-7). For example, at a depth of 1 meter, simulated soil moisture contents at the Mine location (“B”) for future scenarios increase only slightly (i.e., ~0.05) from September to mid-April for all scenarios, and then decrease slightly for the other months (i.e., ~0.02). In the Upper Chuitna (“A”), soil moisture contents increase similar amounts from October to about June. The changes in shallow soil moisture contents may cause increased stress on vegetation, which may in turn exacerbate current problems like wetland drying, spruce bark beetle (there may be other insect problems like green alder sawfly), or forest fires.

Actual Evapotranspiration (AET):

As shown on Figure 6-8, average monthly simulated AET, compared to other hydrologic flows for the Basecase in the Upper and Lower Chuitna sub-watersheds peaks in June (~100 to 150 mm/month) and declines to low values in colder months (~ 5 mm/month). Although AET is actually higher in the Upper Chuitna, relative to monthly precipitation, AET is much greater in the Lower Chuitna. This is important in evaluation of climate changes to AET.

Model predictions show that actual evapotranspiration (AET; Figure 6-9) increases most for the Tmax scenarios (29% to 58%) and least for the Tmin scenarios (10% to 17%) relative to the Basecase. Effectively, this means that with greater inputs of precipitation into the system, greater AET will occur with increasing air temperatures. Results from the TmaxPmin scenario show the greatest spatial variability in changes in AET relative to the Basecase across the watershed (i.e., 23%), or an increase of 52% in the Upper Chuitna and an increase of 29% in the Lower Chuitna. The TminPmin case shows the least spatial variability in changes relative to the Basecase (4%). This suggests that in cases where precipitation decreases and air temperatures increase, AET will be more pronounced in upper watersheds. Much of this is due to increased precipitation in higher elevations relative to lower areas, which increases the amount of evapotranspiration in upper areas relative to the Basecase (Figure 6-8). When evaluated by month, AET increases most during the colder months (i.e., TmaxPmax scenario), or by about 48 times in December in the Upper Chuitna (Figure 6-10). These values will likely increase as vegetation adjusts to the warmer, moister climate.

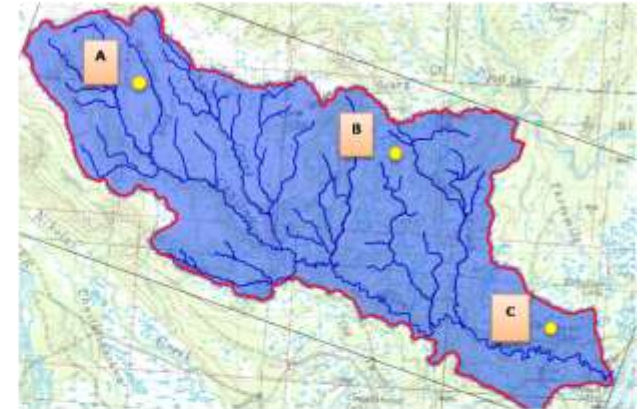
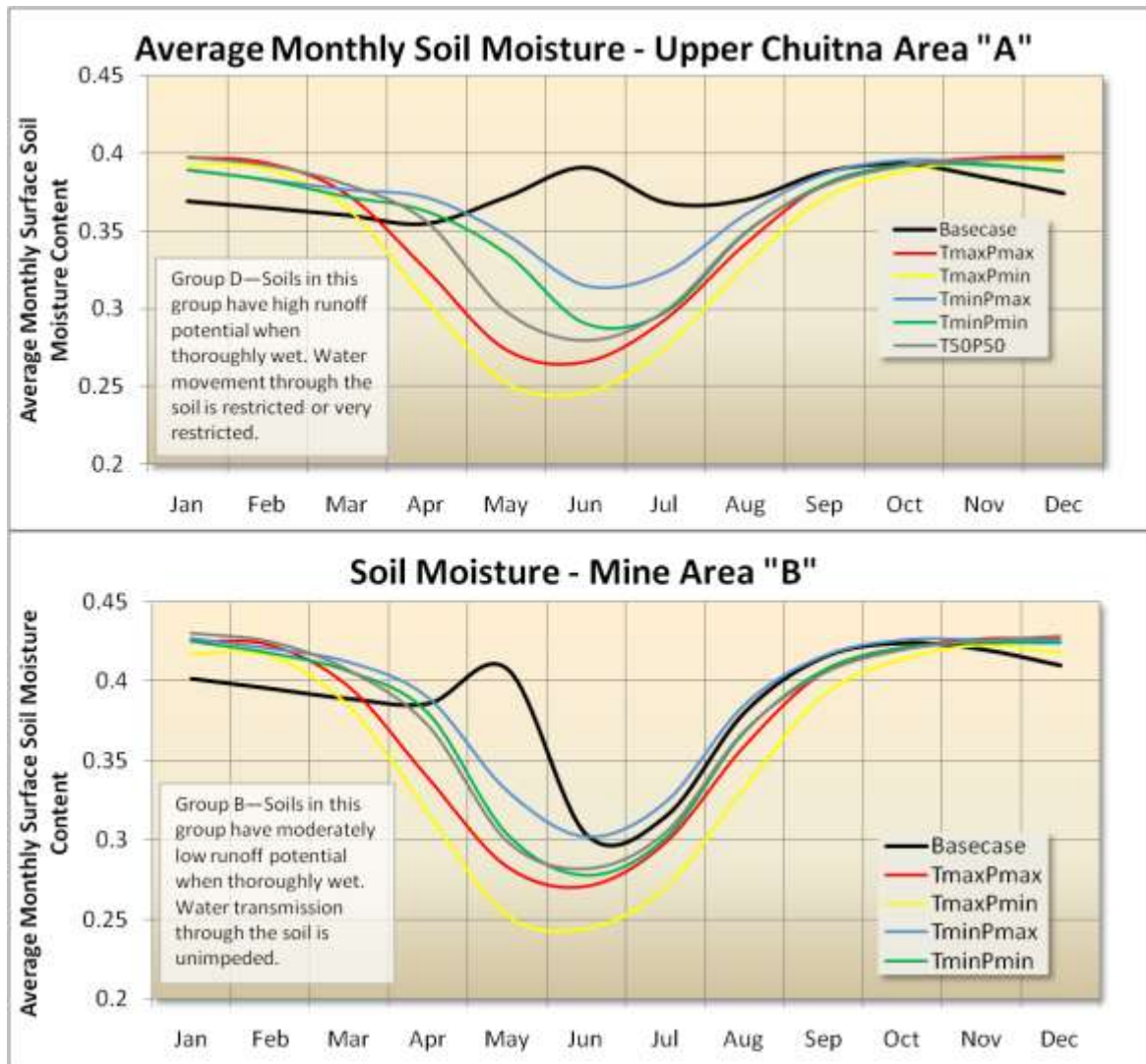


Figure 6-6. Simulated Average Monthly Surface (Top 5 cm) Soil Moisture for Mine and Upper Chuitna Areas.

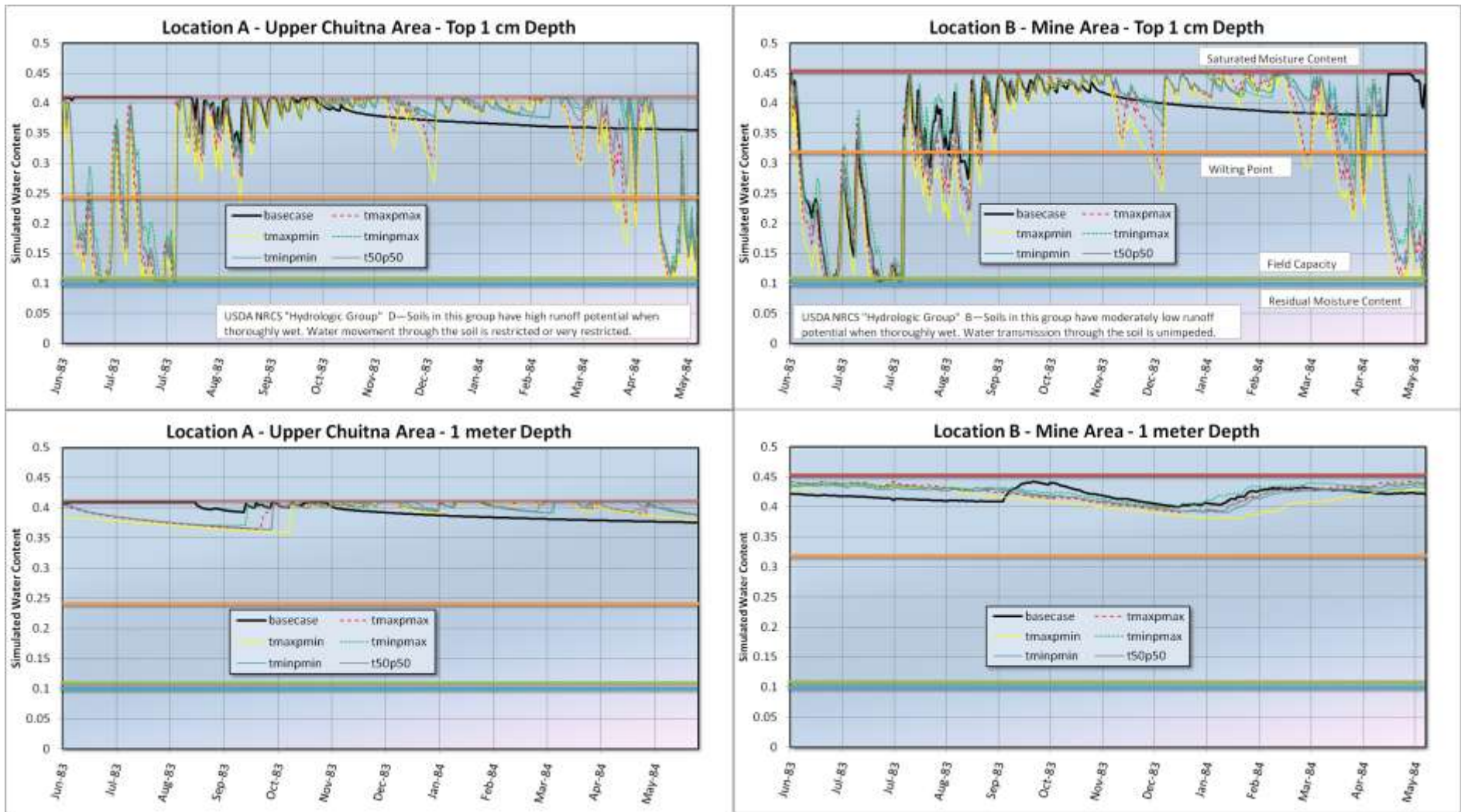


Figure 6-7. Simulated Soil Moisture at 1 cm and 1 m depth at Locations A and B (previous figure).

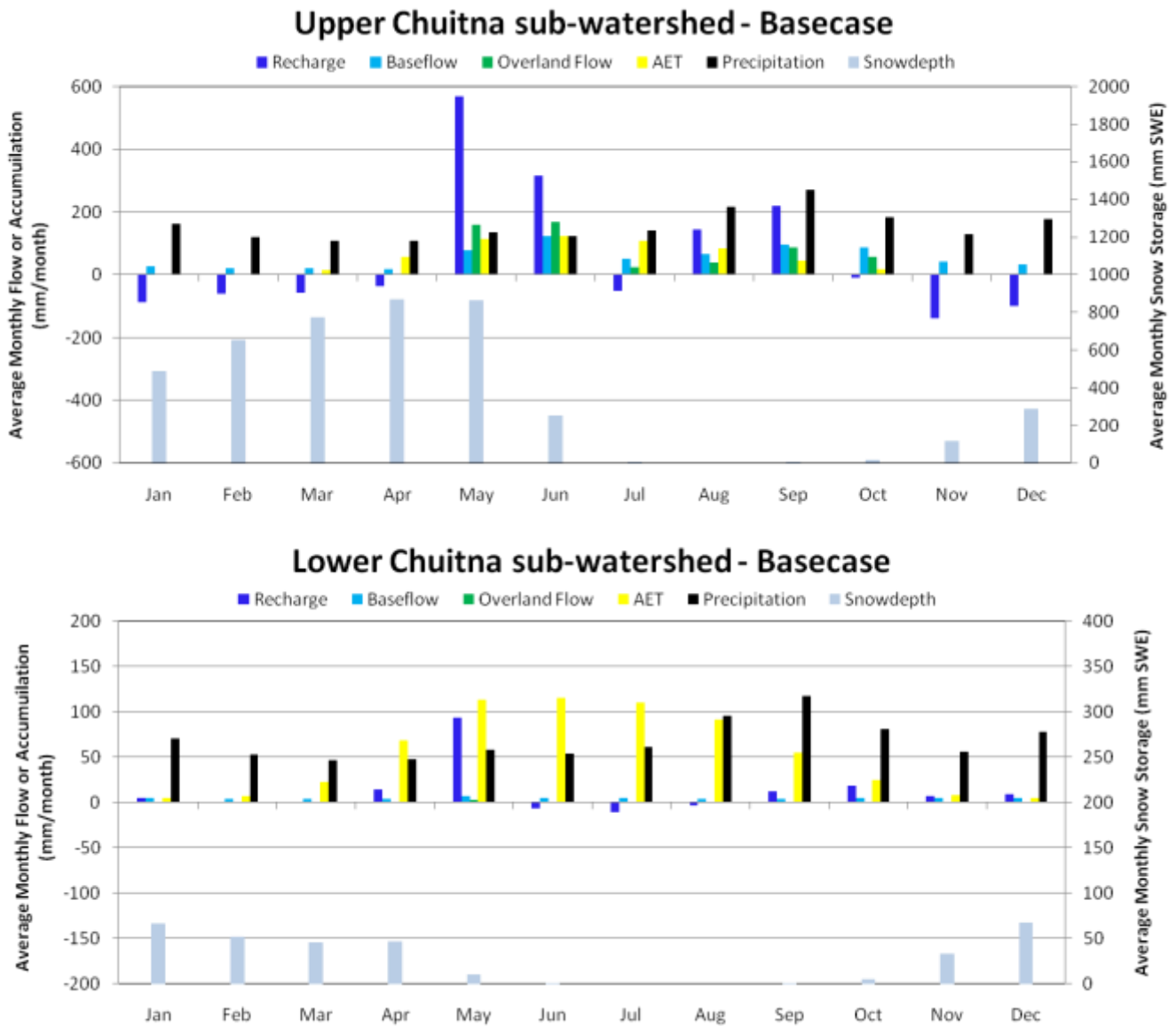


Figure 6-8. Average monthly Flow or Accumulation (Recharge, Baseflow, Overland flow, AET, Precipitation and Snow Storage) for Upper and Lower Chuitna sub-watersheds.

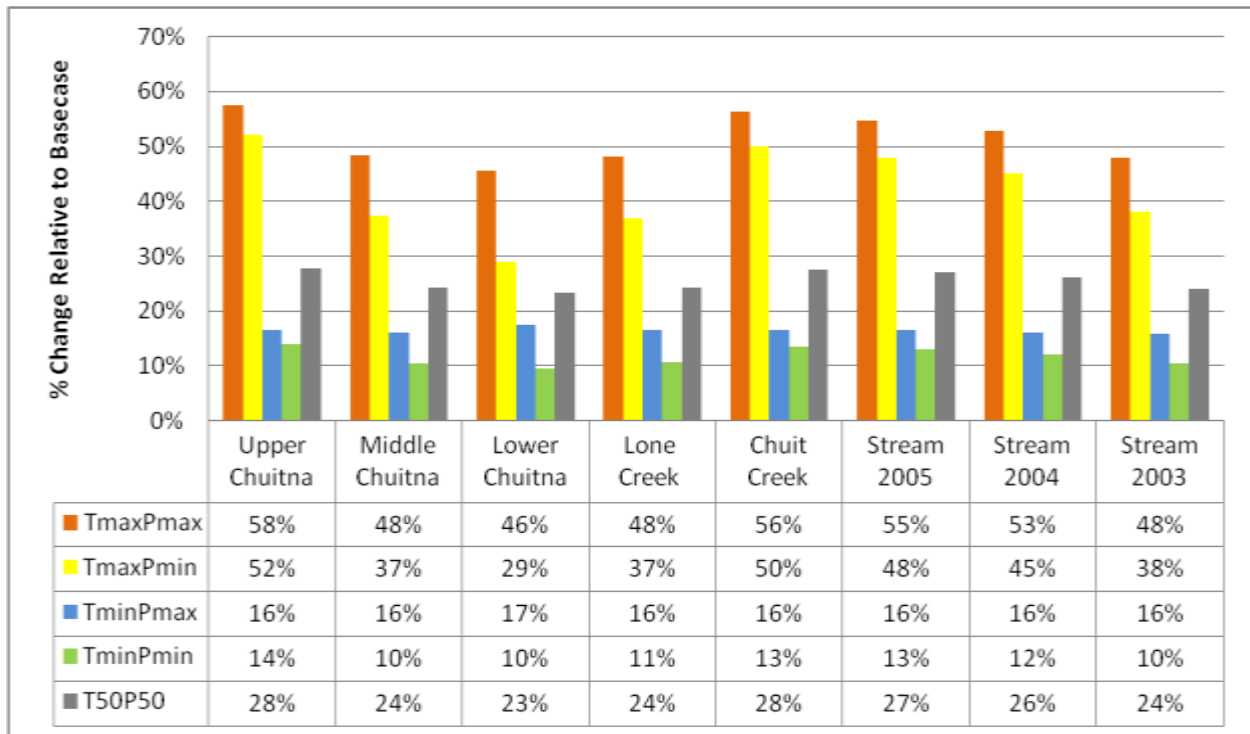


Figure 6-9. Simulated percent change in mean annual Actual Evapotranspiration (AET) for five climate change scenarios relative to the historical baseline, by sub-watershed.

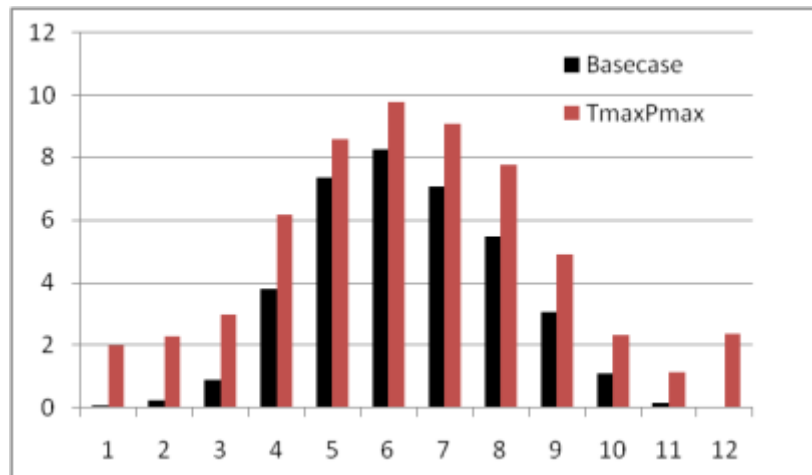


Figure 6-10. Average Daily AET by month for the Basecase (1980 to 2000) and TmaxPmax Scenario (2080 to 2100) for the Upper Chuitna sub-watershed. Units are mm/d on vertical axis and months on lower axis, starting with January.

6.2.1.3 Changes in the Saturated Zone

Groundwater Recharge and Baseflow to Streams:

Changes to groundwater recharge relative to the Basecase by sub-watershed are summarized on Figure 6-11. For most scenarios, the climate changes increase the amount of groundwater recharge. However recharge rates decrease for both Pmin cases at lower elevations, which suggests that a threshold is reached somewhere at mid-watershed elevations, where enough precipitation is added that recharge increases despite the increased evapotranspiration. The TminPmax case emphasizes this point, where recharge increases 33% to 104%. Although recharge increases 104% in the lower Chuitna watershed, net recharge is substantially lower than in the Upper Chuitna watershed (i.e., Lower Chuitna is 149 mm/yr, or ~6 in/yr and Upper Chuitna is ~722 mm/yr or ~28 in /yr, respectively).

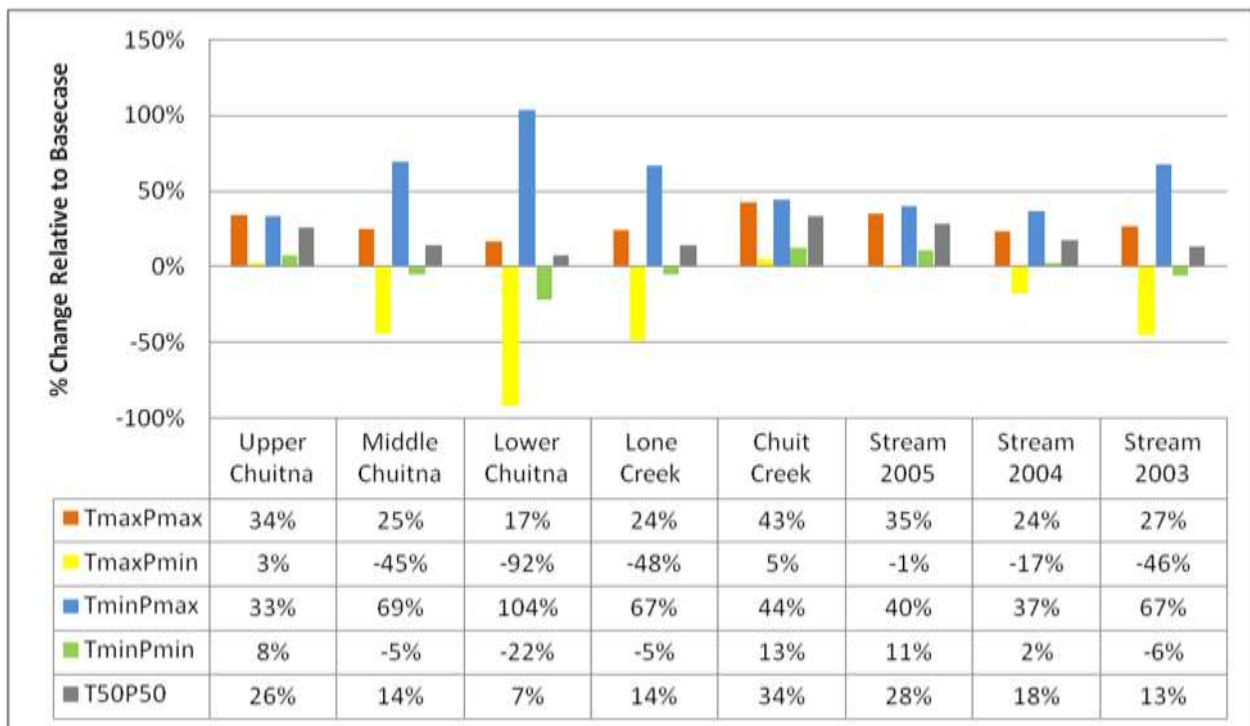


Figure 6-11. Change in Groundwater Recharge Relative to the Basecase

For the Lower Chuitna sub-watershed, the average monthly baseline recharge rates are all positive except from June to August, when AET is high (lower plot; Figure 6-8). Simulated average monthly baseline recharge rates for the Upper Chuitna (upper plot; Figure 6-8), are positive during May-June and then during August-September in response to snowmelt and fall rains, respectively. All other months are negative, indicating that groundwater storage in upper reaches decreases during this period. In contrast, for the Upper Chuitna, recharge actually increases for the majority of climate change scenarios during most months, except May to June, which reflects the shift in snowmelt to early months (Figure 6-5). Large increases are shown for all scenarios in October, but historical recharge in the Upper Chuitna sub-watershed is low during this time period. Similar changes are predicted in the Lower Chuitna, though all

scenarios show negative recharge from May to August and notably increased positive recharge from January to March as a result of increased rainfall versus snowfall at lower elevations.

Simulated Basecase baseflows by month are shown for both the Upper and Lower Chuitna sub-watersheds Figure 6-8. Baseflows are highest during and immediately following the snowmelt and fall rain periods (May through September), which is similar to the change in monthly recharge rates. However, the baseflows are lower, but all positive. Baseflows are lowest in April (winter baseflows) because this period corresponding recharge rates have continuously decreased from November through April due to the increasing snowpack (Figure 6-3).

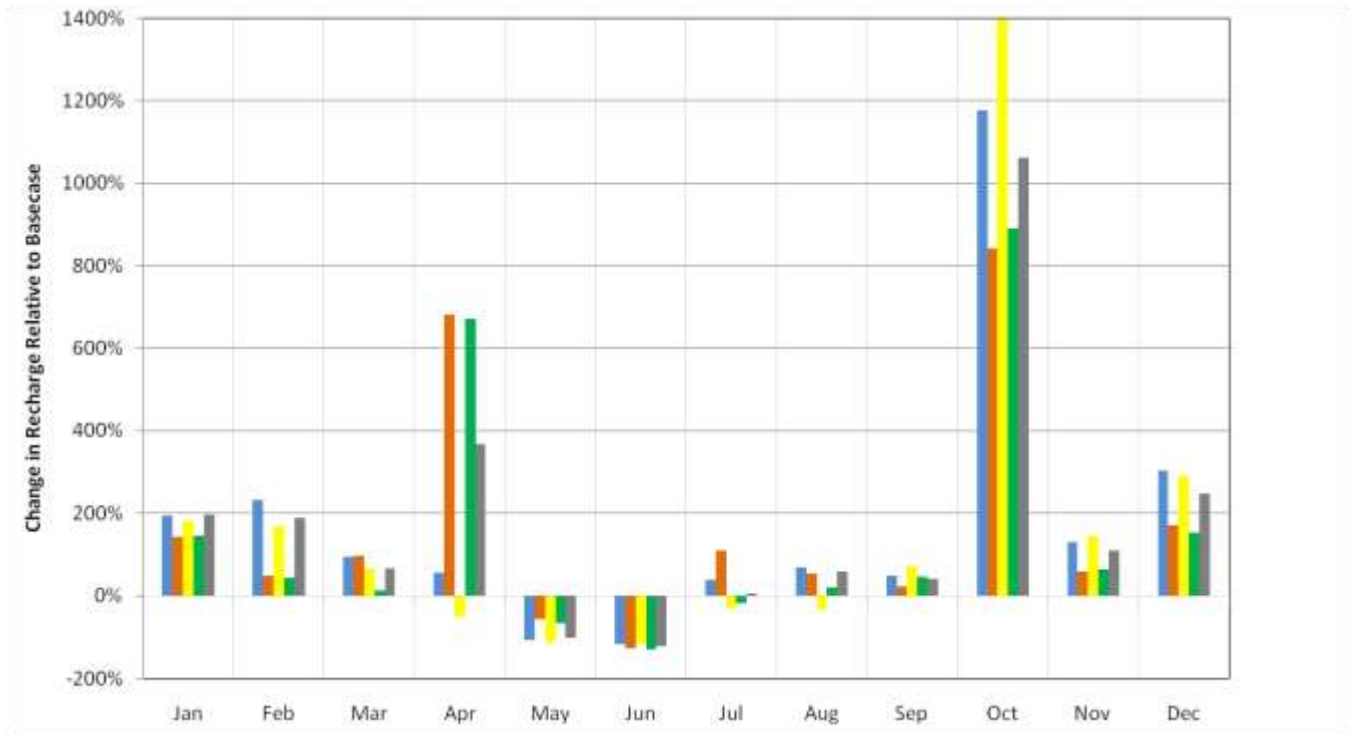


Figure 6-12. Upper Chuitna sub-watershed average monthly change in Recharge for climate scenarios on lower plot. Average Monthly Baseflow Rates (mm/month) for climate scenarios (colored) and Basecase Recharge (black) on upper plot.

Changes in the groundwater baseflow contribution to streamflow by sub-watershed are summarized on Figure 6-13. As in the calibrated model (Section 5.3.2), changes in groundwater baseflow are similar to changes in recharge relative to the Basecase. This is because, once infiltrating water enters the groundwater system, little ‘saturated zone’ water is actually lost via evapotranspiration to the atmosphere because groundwater depths are generally less than the ~ 1 meter root depth. As a result, effects of climate change on baseflows are similar to those on recharge. All scenarios except the Pmin scenarios in lower elevations cause an increase in baseflow. The Pmin scenarios in mid- to lower-elevation watersheds cause a decrease in baseflow.

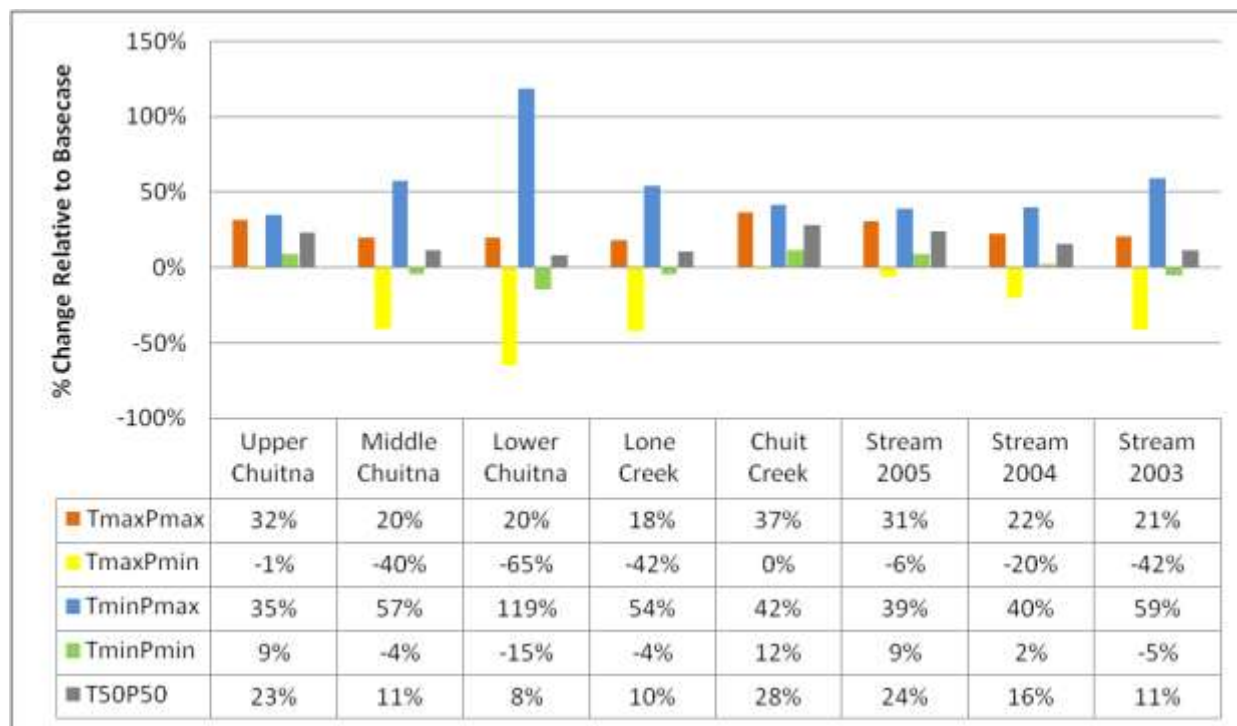


Figure 6-13. Change in Groundwater Baseflow to Streams Relative to the Basecase

6.2.1.4 Changes in Surface Flows

Overland Flow:

In the Basecase model simulations, overland flow to streams is generated from cells adjacent to the streams. On a monthly basis, overland flows follow a similar trend as baseflows (see Figure 6-8), where flows are highest during spring melt and fall runoff and low for other periods. Results also show that 10 to 100 times the amount of overland flow is generated in the upper sub-watersheds like the Upper Chuitna and Chuit Creek sub-watersheds than in lower sub-watersheds such as the Lower Chuitna or Stream 2003 (see Table 5-1). This is due to the combination of lower permeability of soils in the upper half of the Chuitna Watershed, increased precipitation and steeper topography. Similarly, the percent of annual precipitation as overland flow to streams ranges from 1% (lower elevations) to 31% (upper elevations). Overland flow to streams as a percent of total streamflow ranges from 6% (Stream 2003) to 50% (Chuit Creek). The overland flow percentage in Stream 2003 is likely higher due to a bias in calibrated streamflow attributed to limited accuracy of the topography which limits explicitly simulating smaller surface water drainages apparent in higher resolution hard-copy topography in mining reports. Increasing grid resolution to less than 200 m may also increase the overland flow percentages somewhat as near stream overland areas are better simulated. Despite this, modeling results suggest the majority of streamflow is derived from baseflow rather than overland flow.

Changes in overland flow contributions to streamflow for the climate change scenarios are summarized on Figure 6-14. Changes in overland flow are sensitive to the changes in both precipitation and temperature. For both Pmax cases, overland flow increases in all sub-watersheds, and decreases for Pmin cases for Pmin cases. Increases are greatest for the

TminPmax case (471%) and smallest for the T50P50 case (< 10% increase). This indicates that when enough precipitation is added to the system (i.e., Pmax), both overland flow and baseflow increase, and when too little is added (Pmin), even the smaller increases in temperature cause decreases in both of these. The relative change in overland flow (either increase or decrease) is amplified in lower sub-watersheds because historical flows are low compared to flows in upper areas. As a result, even small changes can lead to larger relative climate impacts compared to higher elevations. On a monthly basis, overland flows increase during fall periods and former snowpack months (November through April), but decline from May through July due to the earlier melt-out.

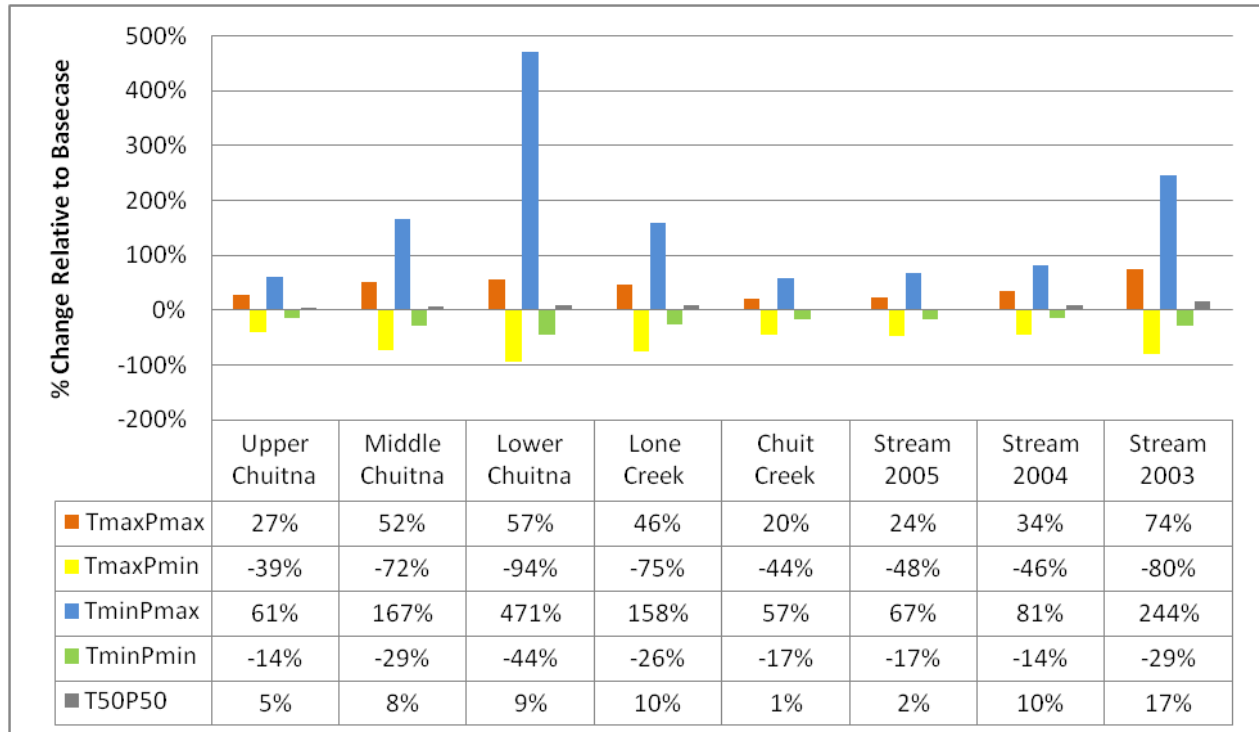


Figure 6-14. Change in Overland Flow to Streams Relative to the Basecase

Streamflow:

Basecase simulations capture the key characteristics of streamflow within the watershed, such as winter baseflows, the rapid flow ascensions (days) and slow recessions (weeks), peak flows and volumes (see Section 5.3.1). Characteristics such as the seasonal occurrence of baseflows and ascension/recession in response to spring snowmelt and fall rains are similar for different sub-watersheds, but differ in the timing and magnitude of changes. For example, in all gages, streamflow decreases smoothly during winter, increases rapidly during spring snow melt, and then slowly recedes through summer until fall rains increase groundwater recharge and flows increase again. The differences in the timing and magnitude are due to differences in precipitation and temperature with elevation and differences in overland flow and baseflow in sub-watersheds as described above.

Climate changes cause both increases (to 76%) and decreases (to -38%) in streamflow based on the ratio of increases in temperature to precipitation. For example, on an annual basis, when changes in streamflow from several key gage locations are averaged by scenario, streamflow increases for the Pmax and P50 climate change scenarios, but decreases for the Pmin scenarios (upper plot on Figure 6-15). This is similar to the response in overland flow (Figure 6-14) and baseflow (Figure 6-13) and demonstrates that the uncertainty in global climate models translates into uncertainty in whether net annual streamflow increases or decreases.

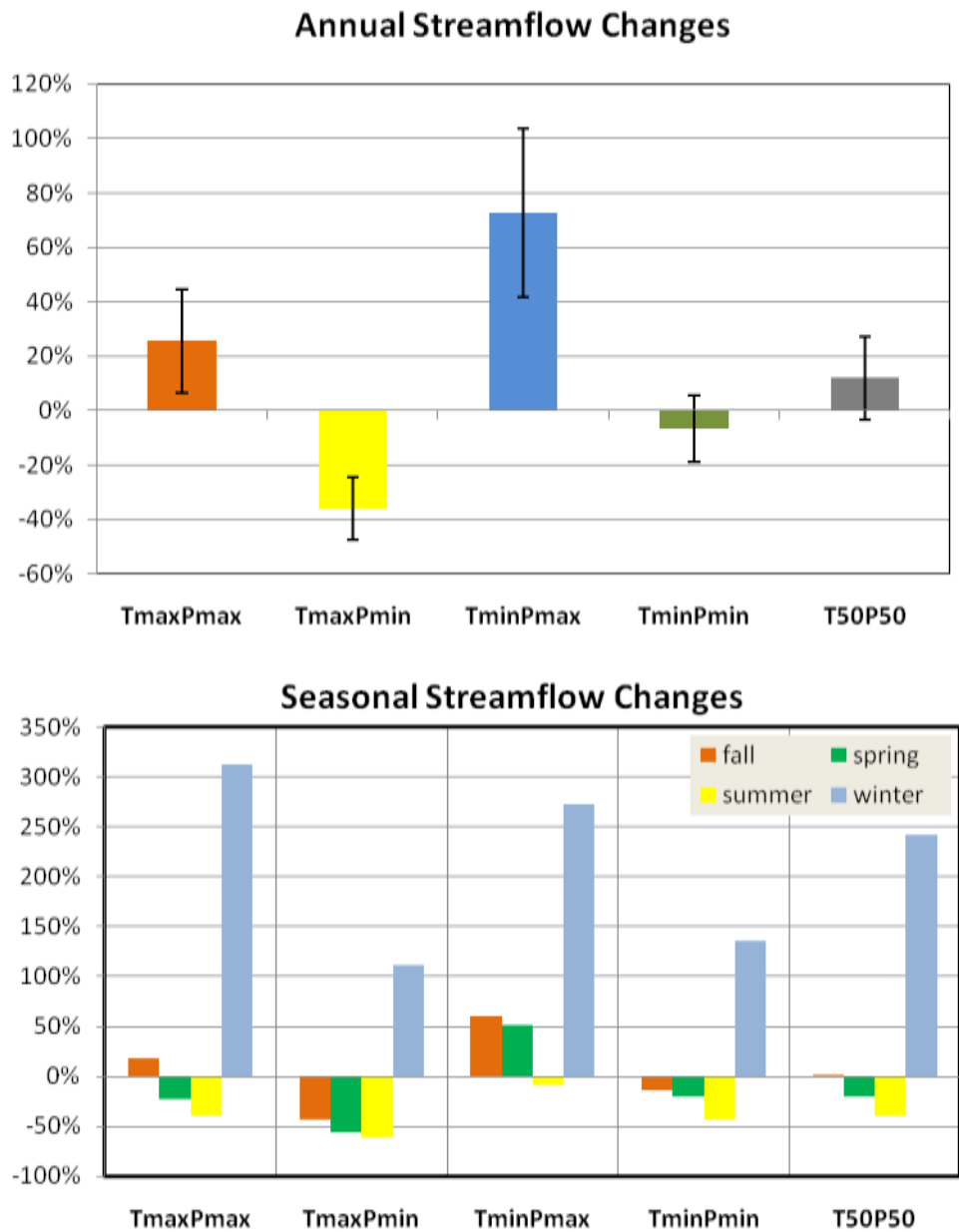


Figure 6-15. Annual and Seasonal Changes in Streamflow Relative to the Basecase.

When summarized by season (lower plot, Figure 6-15) model results convey a clearer sense of the distribution of hydrologic changes over time. For example, in all scenarios, winter streamflow increases (from 105% to over 300%) and summer streamflow decreases (5% to 60%). The dramatic change in winter streamflow is caused by the shift towards earlier and greater snowmelt (Figure 6-3 and Figure 6-5), which increases both overland flow and baseflow (Figure 6-14). This is consistent with similar changes in overland flow and baseflow. However in fall, streamflow either increases (Pmax) or decreases (P50 and Pmin) and in spring streamflow only increases scenario TminPmax, suggesting that unless precipitation increases enough, streamflow decreases.

Simulated average monthly streamflow based on 2-hour simulated flows (Figure 6-16) shows how individual climate change scenarios deviate from the Basecase flow at a key stream gage (gage 230) in Lower Chuitna. In the Basecase, precipitation is stored as snow from November through April. During this period streamflow smoothly declines (black line), in response to declines in baseflow which reflect the continuous but declining supply of groundwater storage in the shallow fluvio-glacial aquifer. Streamflow increases during spring melt and fall rains and is low during July due to increased evapotranspiration and low rainfall. In contrast, streamflow in all scenarios increases dramatically from the Basecase during the former winter snowpack period (November to April) due to the significant changes in snowmelt (Figure 6-3) and peaks during December. All scenarios peak in fall (September-October), but increase (Pmax) or decrease (Pmin) relative to the Basecase. Interestingly, the Tmin scenarios show a third annual streamflow period develops that is similar to the historical spring peak, but they occur earlier (Apr-May instead of May-June) and are smaller. None of the climate scenarios generate average monthly streamflow as high as the Basecase spring streamflow event. The lowest baseflow occurs in July for all scenarios, rather than around April.

Spatial changes in streamflow by sub-watershed and by season summarized on (Figure 6-17) further illustrate how climate changes impact streamflow in different areas of the entire Chuitna Watershed. For example, although nearly all scenarios show streamflow increases in winter and decreases in summer, the magnitudes in individual sub-watersheds is much larger than indicated in either the annual or seasonal plots on Figure 6-15. This is important because it points out that summarizing hydrologic impacts at coarse spatial/temporal scales tends to average out, or decrease the local-scale changes. Summer flows decrease most for the TmaxPmin case, but decrease up to 77% (rather than 60% seasonally or 38% annually). Winter flows decrease most, for all scenarios in the upper watersheds (i.e., Chuit Creek and Upper Chuitna), ranging from 275% to nearly 640%. In addition, there are exceptions to this increase, for example in Lone Creek (2002) and Stream 2003 sub-watersheds, which actually show a decrease. Finally, depending on the sub-watershed and specific climate scenario, a greater uncertainty exists in streamflow actually increasing or decreasing in fall and spring.

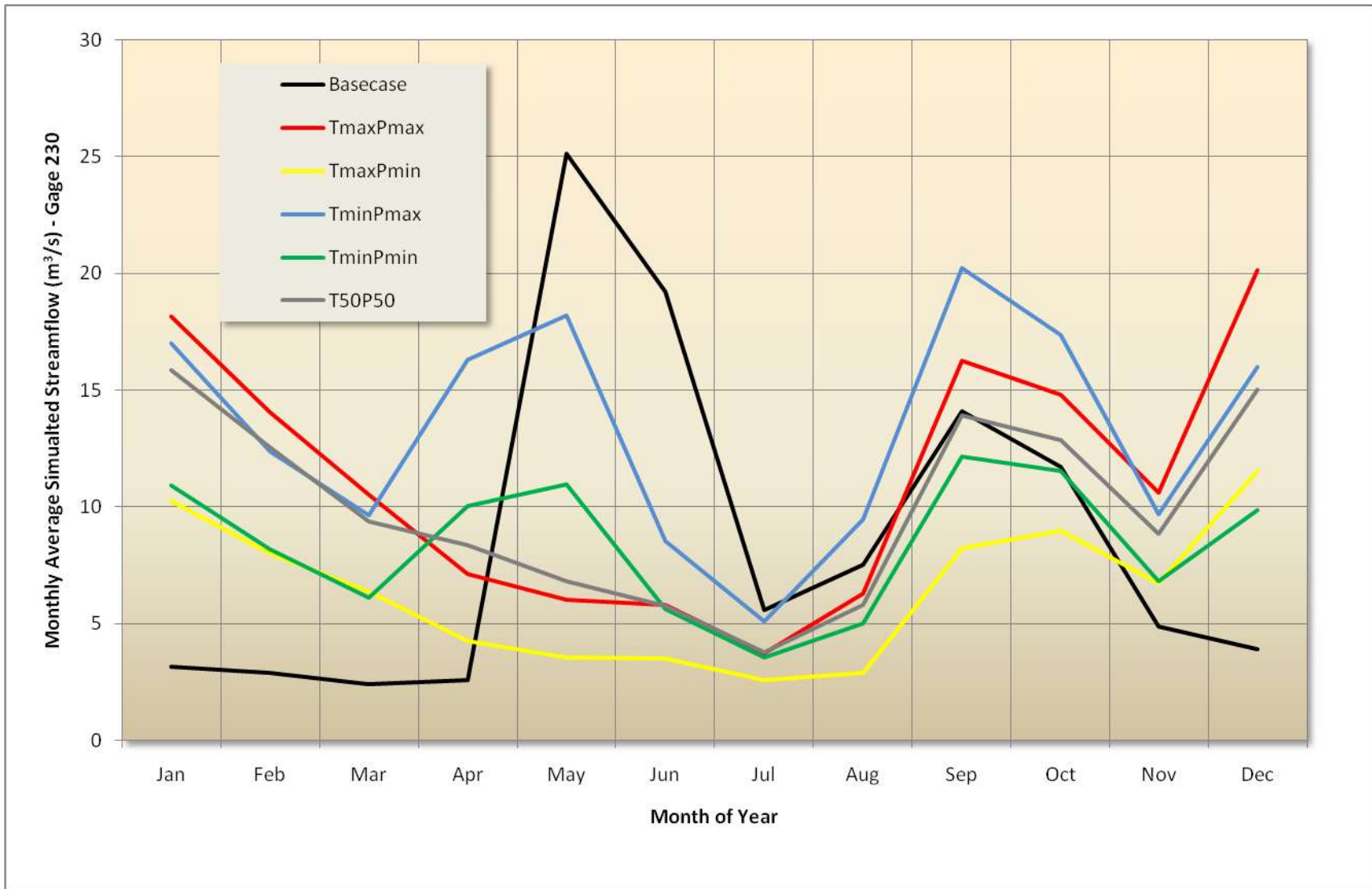


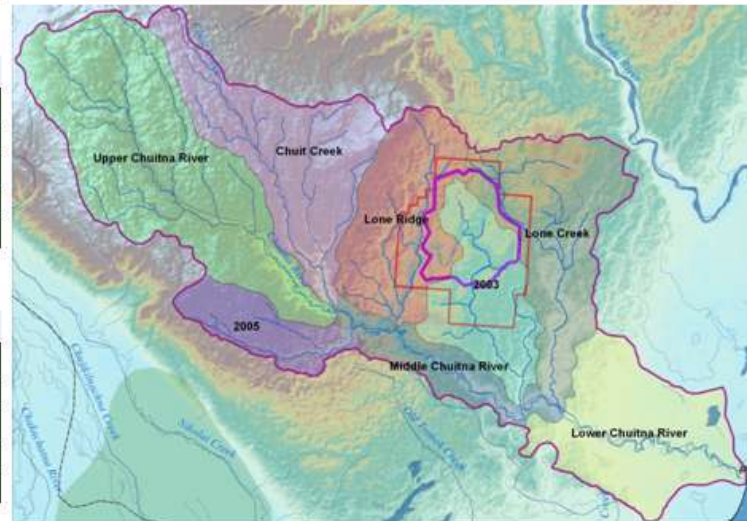
Figure 6-16. Average Monthly Streamflow based on simulated flows every 2 hours at Gage 230 in Lower Chuitna.

Chuit Creek	fall	spring	summer	winter
TmaxPmax	43%	-38%	-51%	638%
TmaxPmin	-16%	-60%	-73%	365%
TminPmin	5%	-23%	-58%	312%
TminPmax	54%	23%	-28%	493%
T50P50	22%	-36%	-53%	522%

Lone Ridge	fall	spring	summer	winter
TmaxPmax	26%	-37%	-43%	363%
TmaxPmin	-40%	-61%	-64%	146%
TminPmin	-10%	-29%	-46%	178%
TminPmax	56%	14%	-13%	324%
T50P50	4%	-36%	-44%	284%

2003	fall	spring	summer	winter
TmaxPmax	3%	6%	-28%	173%
TmaxPmin	-60%	-55%	-59%	-19%
TminPmin	-30%	-21%	-40%	43%
TminPmax	64%	59%	-7%	228%
T50P50	-12%	1%	-28%	122%

Upper Chuitna	fall	spring	summer	winter
TmaxPmax	44%	-11%	-58%	629%
TmaxPmin	-8%	-42%	-77%	370%
TminPmin	7%	13%	-62%	275%
TminPmax	50%	76%	-37%	436%
T50P50	24%	-5%	-60%	495%



Lone Creek	fall	spring	summer	winter
TmaxPmax	7%	-9%	-23%	170%
TmaxPmin	-58%	-60%	-57%	-7%
TminPmin	-20%	-18%	-28%	65%
TminPmax	61%	45%	4%	226%
T50P50	-7%	-9%	-22%	125%

2005	fall	spring	summer	winter
TmaxPmax	35%	-42%	-45%	477%
TmaxPmin	-28%	-63%	-67%	248%
TminPmin	-2%	-31%	-51%	241%
TminPmax	55%	10%	-16%	395%
T50P50	15%	-40%	-46%	390%

Lower Chuitna	fall	spring	summer	winter
TmaxPmax	35%	-21%	-50%	417%
TmaxPmin	-23%	-53%	-72%	194%
TminPmin	-1%	-11%	-56%	186%
TminPmax	54%	47%	-27%	353%
T50P50	16%	-19%	-52%	327%

Middle Chuitna	fall	spring	summer	winter
TmaxPmax	38%	-23%	-53%	478%
TmaxPmin	-19%	-52%	-73%	242%
TminPmin	1%	-10%	-58%	216%
TminPmax	53%	45%	-30%	381%
T50P50	18%	-20%	-54%	378%

Decrease in streamflow

Increase in Streamflow

Figure 6-17. Simulated Average Seasonal Change in Streamflow Relative to the Basecase by Sub-Watershed.

7.0 Summary and Conclusions

The main objective of this study was to evaluate the range of hydrologic impacts within the Chuitna Watershed due to a range of future climate changes predicted by global climate models using an integrated hydrologic modeling tool. Another objective was to develop an approach where these types of integrated hydrologic modeling tools can be used to assess climate change and land-use modification impacts on other hydrologic systems throughout Alaska.

The first objective was met by performing the following steps:

- a) Collected and reviewed available data, reports, modeling, GIS info (Section 2.1),
- b) Synthesized data into a comprehensive GIS/database, using a single coordinate system (Section and 2.2),
- c) Characterized different datasets, developed interpretations (Section 2.3 through 2.6),
- d) Developed several conceptual flow models for system processes (Section 3.0)
- e) Developed numerical model of system (Section 4.0),
- f) Calibrated the flow model to available system response data (Section 5.0) and
- g) Simulated future climate change scenarios, evaluated output (6.0).

The second objective was effectively met through documentation in this report, which systematically outlines key steps used to identify key data, characterize and conceptual flows within the surface and subsurface flow systems and develop, calibrate and apply fully integrated hydrologic models to evaluate effects of climate change on system hydrology.

Key conclusions developed from results of this study include the following:

- 1) Although a reasonable calibration of the integrated hydrologic model to available data was accomplished in this study, uncertainties in climate data, model structure (i.e., geologic framework, aquifers etc), parameter values and conceptualization of flows across the entire Chuitna Watershed are significant and affect the accuracy of the calibration and future predictions. The long run-times and complexity of the fully integrated model did not permit performing a detailed uncertainty analysis, but results are believed to be reasonable for purpose of estimating approximate flow conditions within the historical system, and future changes in flows within the system given the range of specified climate changes.
- 2) Simulated hydrologic changes in streamflow in winter and summer are more certain during spring and fall. Winter streamflow increases due to the increased snowmelt during the winter, and summer streamflow decreases due to increased temperatures which cause increased actual evapotranspiration. Depending on the climate scenario considered, or the relative increase in precipitation to air temperature, streamflow during spring and fall may either increase or decrease. As a result, predicted changes during spring and fall are more uncertain than winter and summer.

- 3) Differences in Basecase and future scenario climate changes over the extent of the Chuitna Watershed (from Upper to Lower Chuitna) are largely due to spatial distributions of precipitation, temperature and RET (orographic), and significant breaks in soils and vegetation that occur approximately in the middle of the Chuitna Watershed.
- 4) Projected effects of climate change on specific hydrologic components include the following:
 - Snowpack:
 - Snowpack is projected to melt out 75 to 100 days earlier for Tmax cases (by late February to mid-March), and about 20 to 40 days for the Tmin cases.
 - For Tmax cases, snowpack is projected to melt out intermittently throughout the winter, in contrast to the historically continuous snowpack (November into June).
 - For Tmin cases, the inter-annual variability in snowpack is projected to increase. In some years it may be reduced as projected for the Tmax scenarios, but in other years it may be similar to Basecase conditions or even exceed the maximum historical snowpack.
 - Soil moisture:
 - Soil moisture is projected to change most in the shallow surface soils as a result of increases in both soil evaporation and plant transpiration. Changes decrease with depth, but are still shifted in time to occur earlier in the spring and later in fall.
 - Early melt-off and increased snowmelt during early spring increases soil moisture from February to March relative to the baseline conditions. Soil moisture in all future scenarios decreases significantly during the summer months, due to increased AET and the early melt-off of snowpack.
 - AET:
 - AET is projected to increase in all scenarios and in all months, but more for the Tmax cases (29% to 58%) and less for the Tmin scenarios (10% to 17%).
 - Relative to the Basecase, AET is projected to increase more in upper watersheds, because more shallow water is available due to greater precipitation in higher elevations combined with lower soil permeability.
 - Recharge:
 - For most scenarios, groundwater recharge is projected to increase, but is variable. Over the baseline period, projected changes generally range from -50 % to +50% by sub-watershed, and from -92% to 104% in the Lower Chuitna. On a monthly basis projected recharge increased most in April (~400% to 600%) and October (~600% to >1200%) and decreased most in May and June (~150%). Recharge rates decrease for both Pmin cases, but only at lower elevations under the Pmax scenarios (-22% for TminPmax). This suggests that a threshold is reached somewhere mid-watershed, where

enough precipitation is added that recharge increases despite the increased evapotranspiration.

- Baseflow:
 - Projected change in baseflows are similar to changes in recharge because, once infiltrating water enters the groundwater system, little ‘saturated zone’ water is actually lost via evapotranspiration to the atmosphere because depths to groundwater generally exceed the ~ 1 meter root depth specified in the model.
- Overland flow:
 - The magnitude of projected change in overland flow is greater relative to the Basecase than the recharge or baseflow.
 - Overland flow is projected to increase in all sub-watersheds for the Pmax cases, and decrease for the Pmin cases.
 - Projected flows increase most for the TminPmax case (471%) and decrease most for the TmaxPmin case (-94%). Both of these occur in the Lower Chuitna, while upper watersheds show less variability. This suggests overland flow in lower watersheds is more sensitive to changes in climate.
 - Flows are projected to change the least for the T50P50 case.
- Streamflow:
 - On an *annual basis*, climate change could cause streamflow to either increase (to 76%) or decrease (to -38%), based on the ratio of increases in temperature to precipitation.
 - On a *seasonal basis*, winter streamflow is projected to increase (from 105% to over 300%) and summer streamflow is projected to decrease (5% to 60%). The notable change in winter streamflow is caused by the shift towards earlier and greater snowmelt, which increases both overland flow and baseflow.
 - Across all scenarios, streamflow is projected to increase and peak in December during the former winter snowpack period (November to April) due to increases in temperature. Further, streamflow is projected to continue to peak in fall (September-October), but may increase (Pmax) or decrease (Pmin) relative to the Basecase. The Tmin scenarios are the only ones to project a streamflow period similar to the historical spring peak, but which may occur earlier (Apr-May instead of May-June) and may be smaller.
 - None of the climate scenarios project average monthly streamflow as high as the Basecase spring streamflow event. The lowest baseflow occurs in July for all scenarios, rather than around April in the Basecase.
 - Simulated streamflow summarized by sub-watersheds and for different seasons show the maximum change occurs in summer (-77%) in the Upper Chuitna for the TmaxPmin case. In contrast, the maximum decrease in streamflow based on seasonal and annual spatial averages is -60% or -38%, respectively. Winter flows are projected to decrease most in the upper

watersheds (i.e., Chuit Creek and Upper Chuitna), ranging from -275% to nearly -640% across all climate change scenarios. In addition, Lone Creek (2002) and Stream 2003 sub-watersheds are also projected to decrease during winter.

8.0 References

Allen, R.G., L.S. Pereira, D. Raes, and M. Smith. 1998. Crop Evapotranspiration: Guidelines for computing crop water requirements. Irrigation and Drainage Paper 56, Food and Agriculture Organization of the United Nations, Rome, 300 p.

Anderson, M.G., Burt, T.P. (editors) 1990. Process Studies in Hillslope Hydrology. published 1990 by John Wiley & Sons Ltd.

Anderson, M.P., and Woessner, W.W., 1992, Applied groundwater modeling: San Diego, Ca., Academic Press.

ASTM D 5979 – 96 (Reapproved 2002) - American Society for Testing and Materials, Standard Guide for Conceptualization and Characterization of Ground-Water Systems

ASTM D 5981 – 96 (Reapproved 2002) - American Society for Testing and Materials, Standard Guide for Calibrating a Ground-Water Flow Model Application

Blasone, R.S., Madsen, H., Rosbjerg, D. 2007. Parameter estimation in distributed hydrological modeling: comparison of global and local optimization techniques. Nordic Hydrology Vol 38 No 4–5 pp 451–476 q IWA Publishing

Borden, C., Delaney, D., Ying, Q., Kobor, J., Guy, B., 2010. A Modeling Approach To Evaluating The Impacts Of Climate Change And Mountain Pine Beetle Infestation On Water Resources In The Okanagan Basin, British Columbia. Presented at the Western Snow Conference 2010.

Camp Dresser & McGee. 2001. Evaluation of Integrated Surface Water and Groundwater Modeling Tools.

Chow, V. T. 1959. Open channel hydraulics. New York: McGraw-Hill.

Chow, V.T., Maidment, D.R., Mays, L.W. 1988. Applied Hydrology. McGraw-Hill.

Christensen, J.H., B. Hewitson, A. Busuioc, A. Chen, X. Gao, I. Held, R. Jones, R.K. Kolli, W.-T. Kwon, R. Laprise, V. Magaña Rueda, L. Mearns, C.G. Menéndez, J. Räisänen, A. Rinke, A. Sarr and P. Whetton, 2007: Regional Climate Projections. In: Climate Change 2007: The Physical Science Basis. Contribution of Working Group I to the Fourth Assessment Report of the Intergovernmental Panel on Climate Change [Solomon, S., D. Qin, M. Manning, Z. Chen, M. Marquis, K.B. Averyt, M. Tignor and H.L. Miller (eds.)]. Cambridge University Press, Cambridge, United Kingdom and New York, NY, USA.

Fang, H., Liang S., Townshend, T.R., Dickinson, R.E., 2008. Spatially and temporally continuous LAI data sets based on an integrated filtering method: Examples from North America. *Remote Sensing of Environment* 112 (2008) 75–93.

Finzel, E.S., Gillis, R.J., Ridgway, K.A., and LePain, D.L. 2009. Preliminary Evaluation of Basin Margin Exhumation and Provenance of Cenozoic Strata, Chuitna and Beluga Rivers Area, Cook Inlet Forearc Basin, Alaska. State of Alaska, Department of Natural Resources, Division of Geological & Geophysical Surveys. Preliminary Interpretive Report 2009-4.

Flores, Romeo M., Stricker, Gary D., Stiles, Robert B. (1995). Tidal Influence on Deposition and Quality of Coals in the Miocene Tyonek Formation, Beluga Coal Field Upper Cook Inlet, Alaska. In Dumoulin, J.A., and Gray, J.E., eds., *Geologic studies in Alaska by the Geological Survey, 1995: U.S. Geological Survey Professional Paper 1574*, p.

Flores, Romeo M., Stricker, Gary D., Kinney, Scott A. (2004). Alaska Coal Geology, Resources, and Coalbed Methane potential. U.S. Geological Survey DDS-77.

Graham, C.B., Woods, R.A., McDonnell, J.J. 2010 in press. Hillslope threshold response to rainfall: (1) A field based forensic approach

Graham, C.B., McDonnell, J.J. 2010 in press. Hillslope threshold response to rainfall: (2) Development and use of a macroscale model

Graham, D.N. and M. B. Butts (2005) Flexible, integrated watershed modelling with MIKE SHE. In *Watershed Models*, Eds. V.P. Singh & D.K. Frevert Pages 245-272, CRC Press. ISBN: 0849336090.

Gray, D. M., and Prowse, T. D. 1992. “Snow and Floating Ice,” in *Handbook of Hydrology*, D. R. Maidment, ed., McGraw-Hill, Inc., New York: 7.1-7.58.

Hackett, S.W., 1976, Regional gravity survey of Beluga Basin and adjacent area, Cook Inlet region, southcentral Alaska: Alaska Division of Geological & Geophysical Surveys Alaska Open-File Report 100, 41 p.

Hackett, S.W., 1977, Gravity survey of Beluga Basin and adjacent area, Cook Inlet region, southcentral Alaska, 31 p., 3 sheets, scale 1:528,000.

HDR Alaska, Inc., 2008. Chuitna Coal Project Wetland Functional Assessment. Prepared for Mine Engineers, Inc., March 5, 2008.

Hill, M.C., 1998, Methods and guidelines for effective model calibration: U.S. Geological Survey Water Resources Investigations Report 98-4005, 90 p.

Homer, C., C. Huang, L. Yang, B. Wylie and M. Coan, 2004. Development of a 2001 national land cover database for the United States. *Photogrammetric Engineering and Remote Sensing* Vol.70,No.7,pp 829-840

Illangasekare, T.H., Prucha, R.H., and DHI. 2001a. MIKE SHE Code Verification and Validation for Rocky Flats Environmental Technology Site Site-Wide Water Balance Model. for Kaiser-Hill, Inc. September, 2001.

Illangasekare, T.H., Prucha, R.H., and DHI. 2001b. MIKE SHE Code Verification and Validation for RFETS Site-wide Water Balance Model. for Kaiser-Hill, Inc.

James, A.I., K. Hatfield, and W.D. Graham. 2000. Review of Integrated Surface Water/Ground Water Computer Models. Special Publication SJ2000-SP8. St. Johns River Water Management District.

Kaiser-Hill (K-H). 2002. Site-Wide Water Balance Model Report for the Rocky Flats Environmental Technology Site. May.

Kimley-Horne Consultants, 2002. Central and Southern Florida Project Comprehensive Everglades Restoration Plan B.2 Hydraulics Final Model Evaluation Report EAA Storage Reservoirs – Phase 1. Coordination with USACE (Jacksonville District) and South Florida Water Management District.

Kirchner, J.W., 2003. A double paradox in catchment hydrology and geochemistry. *Hydrol. Process.* 17, 871–874 (2003).

Kirkby, M.J., ed. 1978. Hillslope hydrology. New York: John Wiley and Sons. 389 p.

Klein E, Berg EE, Dial R. 2005. Wetland drying and succession across the Kenai Peninsula Lowlands, south-central Alaska. *Can. J. For. Res.* 35(8): 1931-1941

Klein E, Berg EE, Dial R. 2011. Reply to comment by Gracz on “Wetland drying and succession across the Kenai Peninsula Lowlands, south-central Alaska”. *Canadian Journal of Forest Research*, 2011, 41:(2) 429-433.

Koehler, K.D. and Reger, R.D., Reconnaissance Evaluation of the Lake Clark Fault, Tyonek Area, Alaska. State of Alaska, Department of Natural Resources, Division of Geological & Geophysical Surveys. Preliminary Interpretive Report 2011-1.

Kolm, K. E., Conceptualization and Characterization of Hydrologic Systems: International Ground-Water Modeling Center Technical Report 93-01, Colorado School of Mines, Golden, CO, 1993.

Kristensen, K. J. and S.E. Jensen, 1975. A model for estimating actual evapotranspiration from potential evapotranspiration. *Royal Veterinary and Agricultural University, Nordic Hydrology* 6, pp. 170-188

Leij, F.J., Alves, W.J., van Genuchten, M, Williams, J.R., 1996. The UNSODA Unsaturated Soil Hydraulic Database User's Manual Version 1.0. U.S. Salinity Laboratory U.S. Department of Agriculture, Agricultural Research Service Riverside, California 92507.

Letts, M.G., Roulet, N.T., Comer, N.T., Skarupa, N.R., Verseghy, D.L. 2000. Parameterization of Peatland Hydraulic Properties for the Canadian Land Surface Scheme. *ATMOSPHERE-OCEAN* 38 (1) 2000, 141–160.

McDonnell, J.J. 2003. Where does water go when it rains? Moving beyond the variable source area concept of rainfall-runoff response. *Hydrol. Process.* 17, 1869–1875 (2003).

McGuire, K. J., and J. J. McDonnell (2010), Hydrological connectivity of hillslopes and streams: Characteristic time scales and nonlinearities, *Water Resour. Res.*, 46, W10543, doi:10.1029/2010WR009341.

McVehil-Monnett Associates, Inc., 2006. Site Climatology for the Chuitna Coal Project. Prepared for: Mine Engineers, Inc. Cheyenne, Wyoming.

Newman, J. E. and C. I. Branton. 1972. Annual Water Balance and Agricultural Development in Alaska. *Ecology*, Vol. 53, no. 3, pages 513-519.

Neuman, S. P. and Weirenga, P. J.. 2003. A comprehensive strategy of hydrogeologic modelling and uncertainty analysis for nuclear facilities and sites, NUREG/CR-6805.

Oasis Environmental Inc. (Oasis) 2010. Investigation of Seeps and Hydrologic Exchange between Surface Waters and the Hyporheic Zone for Selected Sections of Streams 2002 and 2004. Draft Rev. 5 dated February 2, 2010.

Odum, J., Yehle, Y., Schmoll, H., Garon, C., Er, G. and Dearborn, L., 1988. Lithological, Geotechnical Properties Analysis, and Geophysical Log Interpretation of U.S. Geological Survey Drill Holes 1C-79, 2C-80, CW 81-2, and CE 82-1, Tyonek Formation, Upper Cook Inlet Region, Alaska. Prepared in cooperation with the State of Alaska Department of Natural Resources. U.S. GEOLOGICAL SURVEY BULLETIN 1835.

PacRim, 2011. Chuitna Coal Project 2011 Supplemental Well Program Draft Field Summary Report. July.

Prucha, R.H. 2002. A Conceptual and Modeling Framework for Investigating Recharge in Arid/Semi-Arid Environments. Ph.D. Dissertation. Department of Civil Engineering, University of Colorado, Boulder, Colorado.

Prucha, R.H., Leppi, J., McAfee, S., Loya, W., 2011. Integrated Hydrologic Effects Of Climate Change In The Chuitna Watershed, Alaska.

Riordan, B., P. Verbyla, and A. D. McGuire. 2006. Shrinking Ponds in Sub-Arctic Alaska based on 1950-2002 Remotely Sensed Images. *J. Geophys Res.*, Vol. 111, G04002, DO: 10.1029/2005JG000150.

Riverside Technology, inc. (Riverside) 2010. Chuitna Coal Project Groundwater Baseline Report –Draft: 1982 through January 2010. April 2010.

Riverside Technology, inc. (Riverside) 2009. Chuitna Coal Project Surface Water Component Baseline Report – Final Draft: 1982 through September 2008. Revised June 2009.

Riverside Technology, inc. (Riverside) 2007. Chuitna Coal Project Hydrology Component Baseline Report: Historical Data Summary. Revised March 2007.

Sutinen, R., Äikää2, O., Piekkari1, M., Hänninen, P., 2009. Snowmelt Infiltration Through Partially Frozen Soil in Finnish Lapland. *Geophysica* (2009), 45(1–2), 27–39.

Swenson, Bob. Alaska Gas Exploration Potential in the Cook Inlet. Alaska Division of Geological and Geophysical Surveys. Presentation October 15, 2007.

U.S. Army Corps of Engineers (1998) Engineering and Design—Runoff from Snowmelt. Engineering Manual 1110-2-1406.

Vrugt, J. A., C. G. H. Diks, H. V. Gupta, W. Bouten, and J. M. Verstraten (2005), Improved treatment of uncertainty in hydrologic modeling: Combining the strengths of global optimization and data assimilation, *Water Resour. Res.*, 41, W01017, doi:10.1029/2004WR003059.

Wilson, F., Hults, C., Schmoll, H., Haeussler, P., Schmidt, J., Yehle, L. and Labay, K., 2009. Preliminary Geologic Map of the Cook Inlet Region, Alaska Including parts of the Talkeetna, Talkeetna Mountains, Tyonek, Anchorage, Lake Clark, Kenai, Seward, Iliamna, Seldovia, Mount Katmai, and Afognak 1:250,000-scale quadrangles. USGS Open-File Report 2009-1108.

Appendix A - USDA National Resources Conservation Service (Soils Dataset Download Information).

Example B Hydrologic group	Top Depth (in)	Bot Depth (in)	Texture	Ksat	Ksatlow micron/s	Ksathigh micron/s
<i>Puntilla silt loam (7 to 20% slope)</i> Hydrologic group B, Runoff class: medimum	0	6	slight decom plant material	high	1.40E-05	4.20E-05
	6	12	silt loam	mod high	4.23E-06	1.41E-05
	12	42	silt loam	mod high	4.23E-06	1.41E-05
	42	60	gravelly silt loam	mod high	1.41E-06	4.23E-06
<i>Strandline-Kroto-Chichantna complex, 1 to 20 percent slopes</i> <i>Kroto (30%) Hydrologic group: B, runoff class: medium</i>	0	3	mod decom plant material	high	1.40E-05	4.20E-05
	3	5	silt loam	mod high	4.23E-06	1.41E-05
	5	22	silt loam	mod high	4.23E-06	1.41E-05
	22	60	gravelly silt loam	mod high	1.41E-06	4.23E-06
<i>Strandline (30%) Hydrologic group: B, runoff class: medium</i>	0	2	mod decom plant material	high	1.40E-05	4.20E-05
	2	7	silt loam	mod high	4.23E-06	1.41E-05
	7	31	silt loam	mod high	4.23E-06	1.41E-05
	31	60	gravelly silt loam	mod high	1.41E-06	4.23E-06
<i>Chichantna (25%) Hydrologic group: D, runoff class: very high</i>	0	6	Peat	high	4.23E-05	1.41E-04
	6	28	Stratified mucky peat to silt loam	mod high	4.23E-05	1.41E-04
	28	35	loam	mod high	4.23E-06	1.41E-05
	35	60	muck	mod high	4.23E-05	1.41E-04
<i>Nancy-Kashwitna complex 0 to 2% slopes</i> <i>Nancy Soils Hydrologic group: B, runoff class: low</i>	0	1	mod decom plant material	high	1.40E-05	4.20E-05
	1	4	silt loam	mod high	4.23E-06	1.41E-05
	4	25	silt loam	mod high	4.23E-06	1.41E-05
	25	60	very cobbly sand	high	4.23E-05	1.41E-04
<i>Kashwitna Soils</i> Hydrologic group: B, runoff class: low	0	3	slightly decom plant material	high	1.40E-05	4.20E-05
	3	5	silt loam	mod high	4.23E-06	1.41E-05
	5	21	silt loam	mod high	4.23E-06	1.41E-05
	21	60	very cobbly sand	high	4.23E-05	1.41E-04

Example B Hydrologic group	Top Depth (in)	Bot Depth (in)	Texture	Ksat	Ksatlow micron/s	Ksathigh micron/s
Example C Hydrologic group - Kliskon silt loam, 2 to 12 % slopes						
<i>Kliskon Soils 90% of group,</i>	0	3	mod decom plant material	high	1.40E-05	4.20E-05
Hydrologic group C, Runoff class: medium	3	5	silt loam	mod high	4.23E-06	1.41E-05
	5	22	silt loam	mod high	4.23E-06	1.41E-05
	22	60	gravelly loam	mod high	1.41E-06	4.23E-06
Example D Hydrologic group - Chuit-Nakochna-Chichantna complex 2 to 7% slope						
<i>Chuit Soils 45% of group</i>	0	3	slight decom plant material	high	1.40E-05	4.20E-05
	3	12	silt loam	mod high	4.23E-06	1.41E-05
	12	36	silt loam	mod high	4.23E-06	1.41E-05
	36	60	gravelly silt loam	mod high	1.41E-06	4.23E-06
<i>Nakochna Soils (25% of group)</i>	0	2	slight decom plant material	high	1.40E-05	4.20E-05
Hydrologic group: D, Runoff class: very high	2	5	silt loam	mod high	4.23E-06	1.41E-05
	5	19	silt loam	mod high	4.23E-06	1.41E-05
	19	60	Unweathered Bedrock	mod high	0.00E+00	1.00E-08
<i>Chichantna Soils (20%)</i>	0	6	Peat	high	4.23E-05	1.41E-04
Hydrologic group: D, Runoff class: very high	6	28	Stratified mucky peat-silt loam	high	4.23E-05	1.41E-04
	28	35	loam	mod high	4.23E-06	1.41E-05
	35	60	muck	high	4.23E-05	1.41E-04

Appendix B - Long-term Monthly NARR Precipitation Data Comparison to Available Site Data

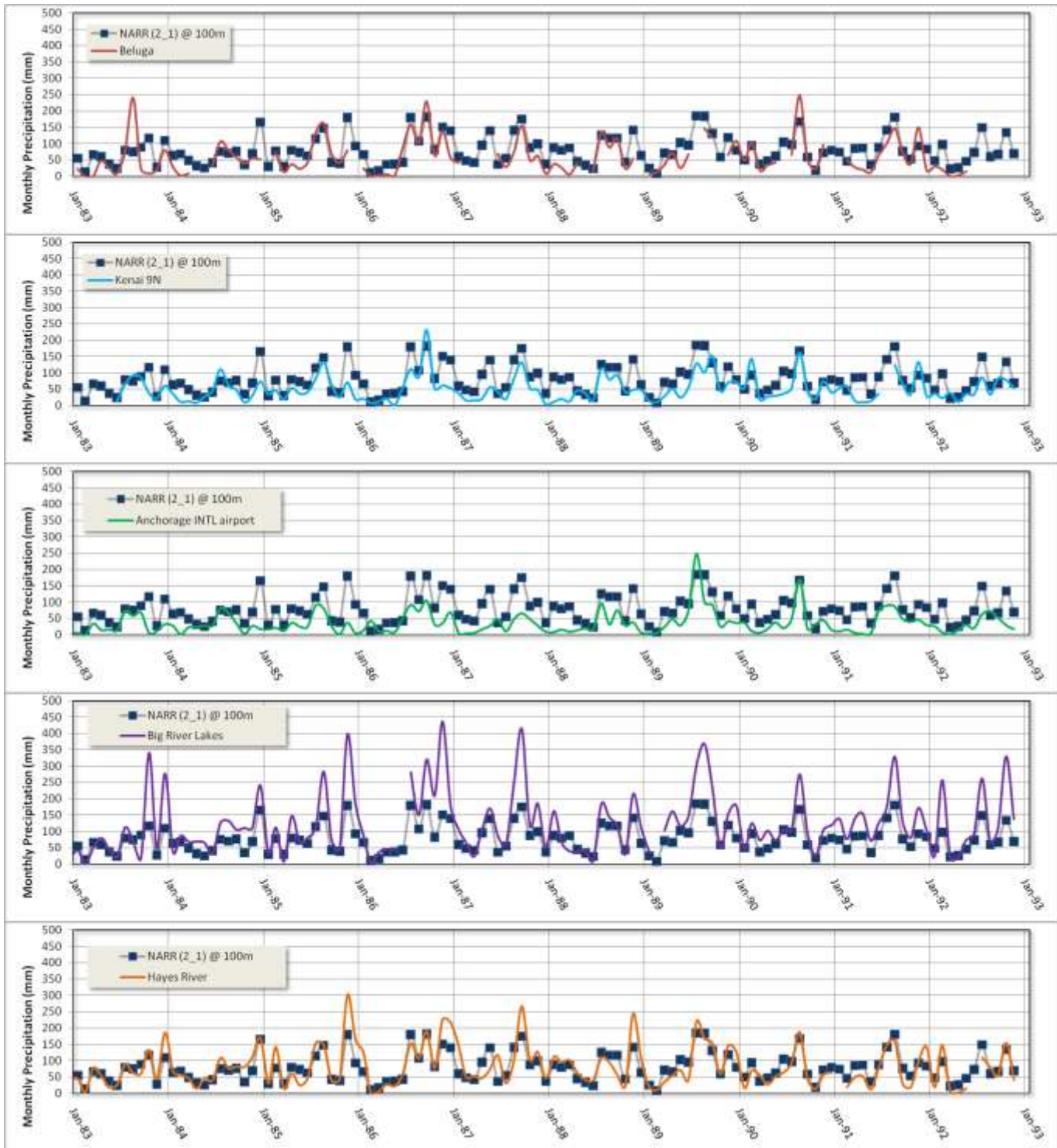


Figure B-1. Comparison of NARR data to Local Data.

Appendix C - **Additional Hydrologic Response of Basecase Model**

Simulated Average of Annual Actual Evapotranspiration (1980 to 2000)

Simulated Average of Annual Soil Evaporation (1980 to 2000)

Simulated Average of Annual Plant Transpiration (1980 to 2000)

Simulated Average of Annual Groundwater Recharge (1980 to 2000)

Simulated Average of Annual Groundwater Baseflow to Streams (1980 to 2000)

Simulated Average of Annual Overland Flow to Streams (1980 to 2000)

Simulated Average Annual Snowpack (1980 to 2000).

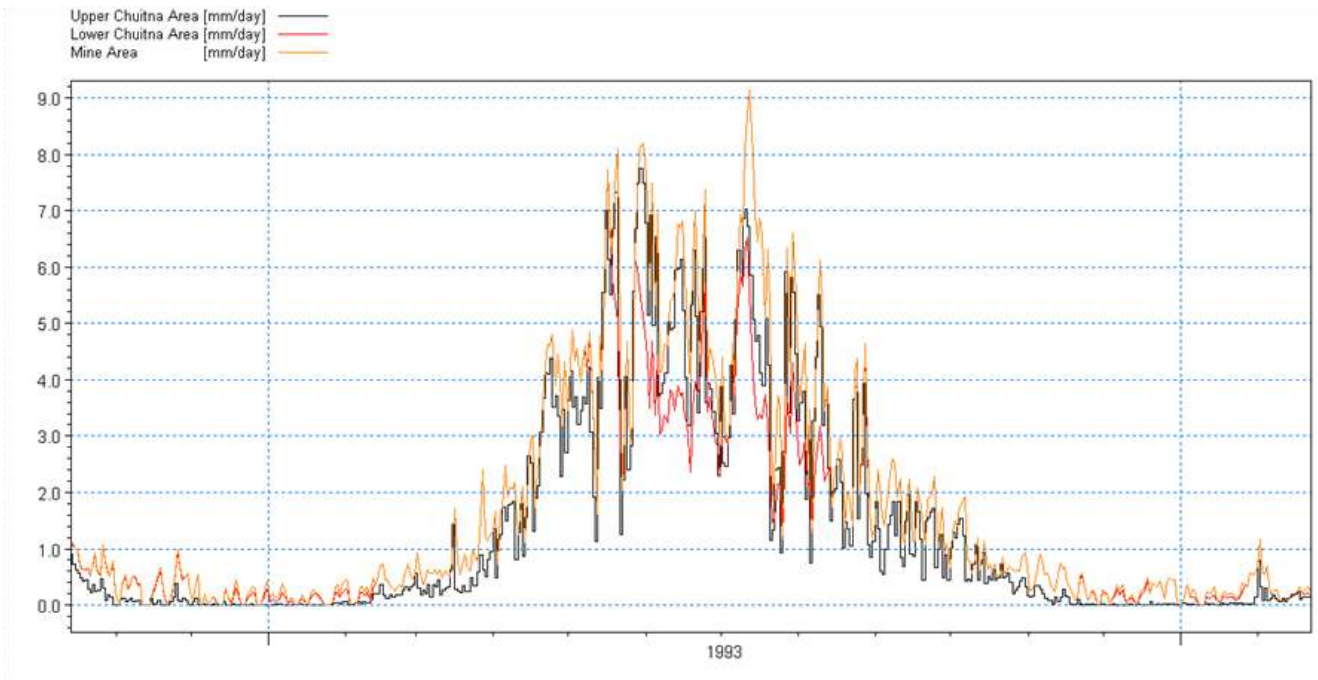
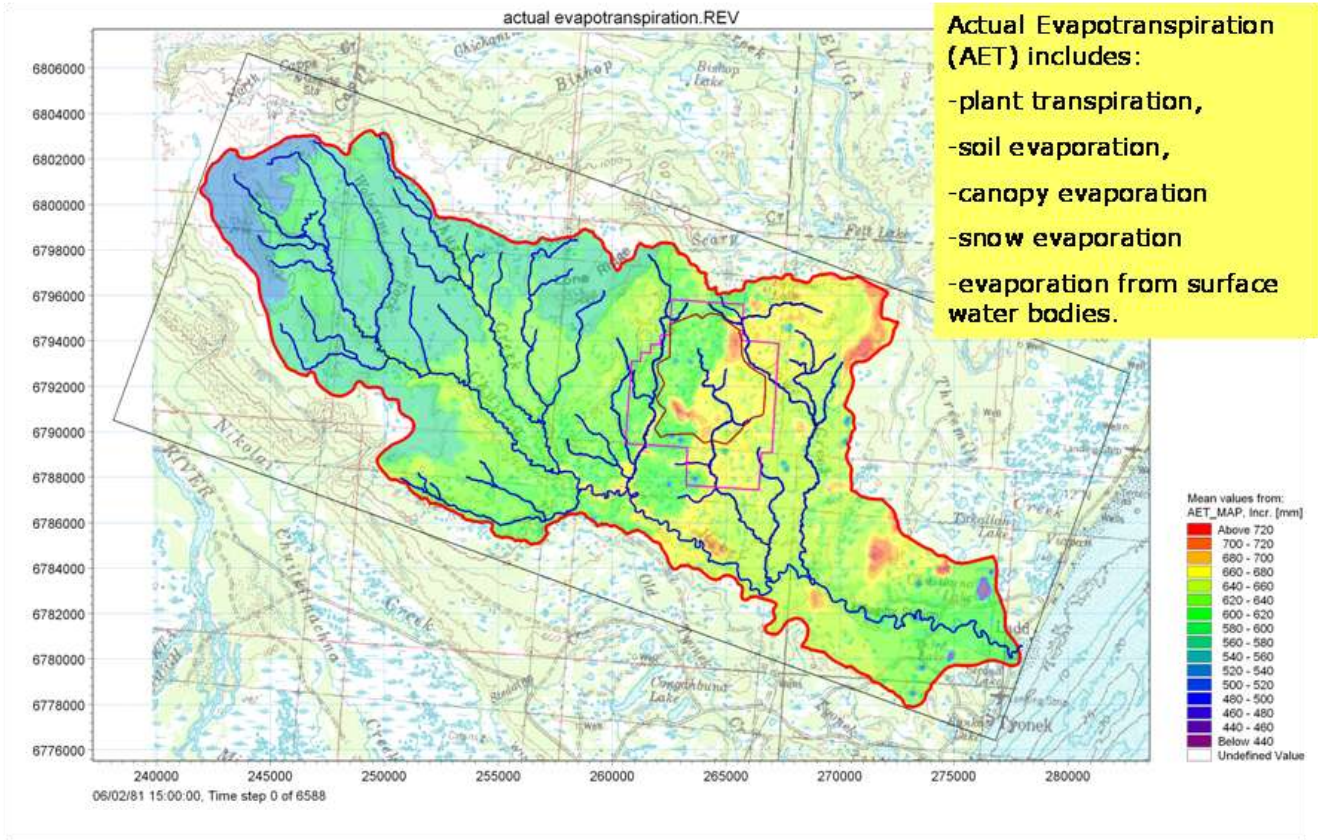


Figure C-1. Simulated Average of Annual Actual Evapotranspiration - 1980 to 2000 (mm/yr).

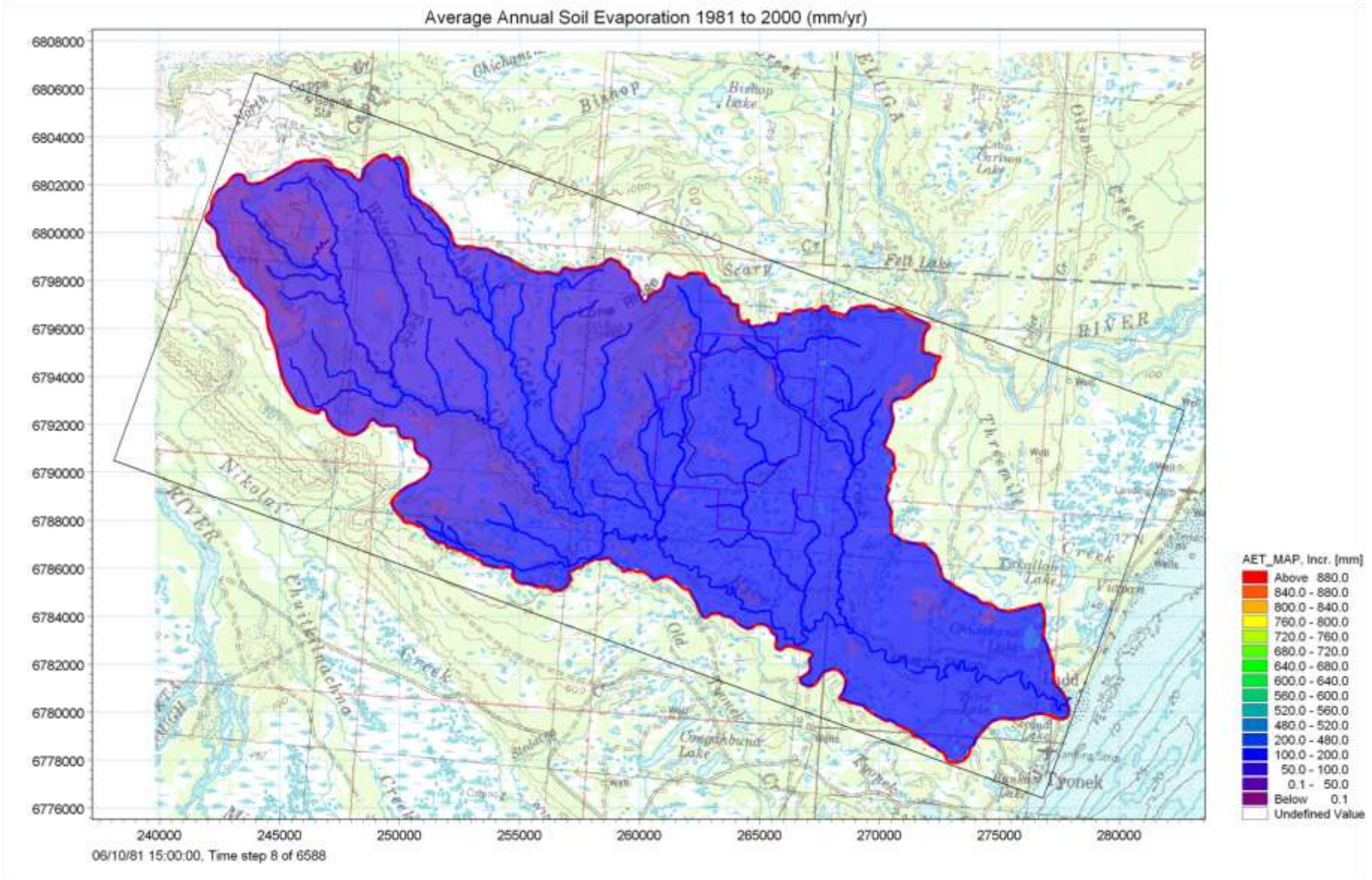


Figure C-2. Simulated Average of Annual Soil Evaporation - 1980 to 2000 (mm/yr).

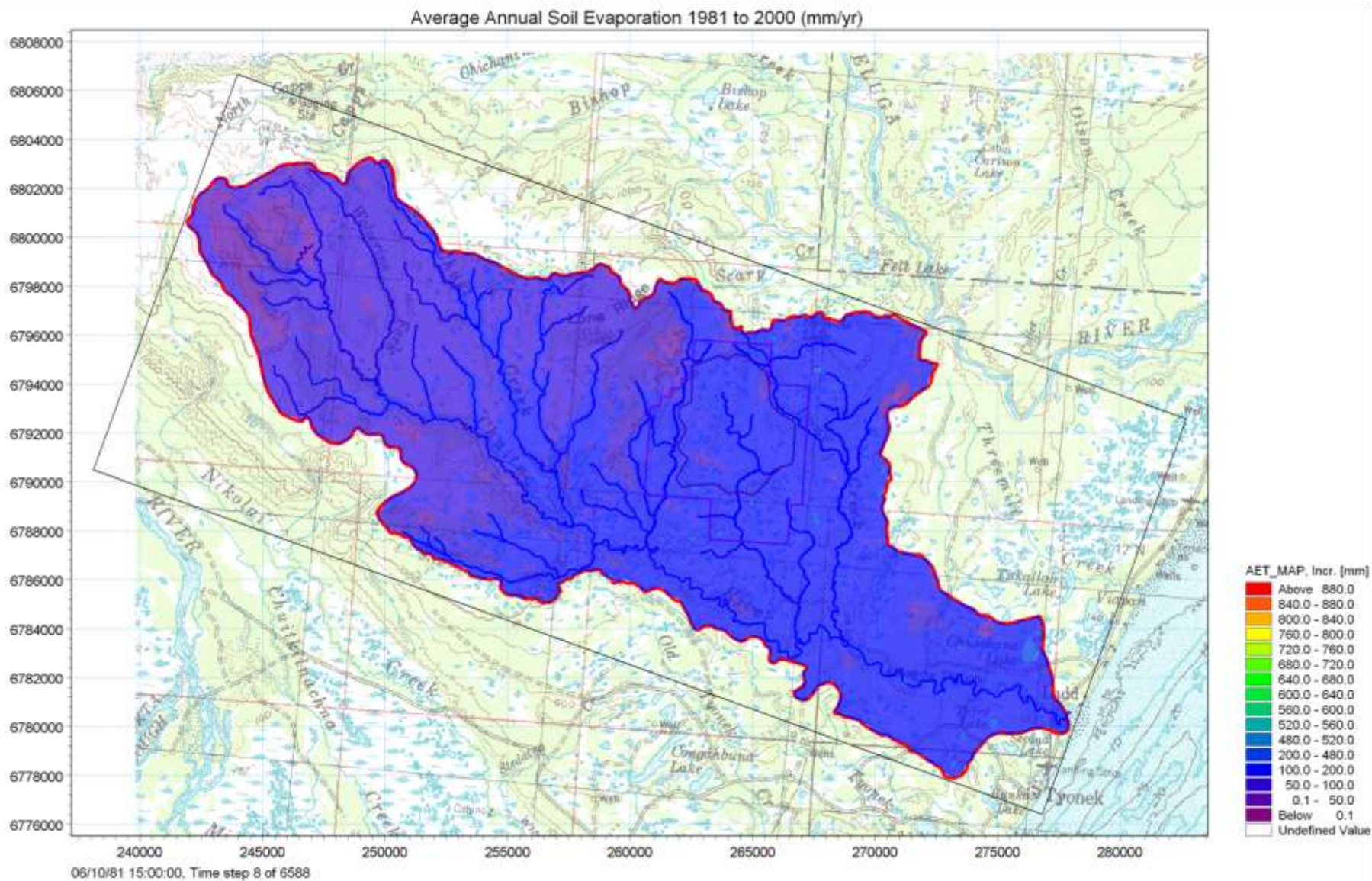


Figure C-3. Simulated Average of Annual Plant Transpiration - 1980 to 2000 (mm/yr).

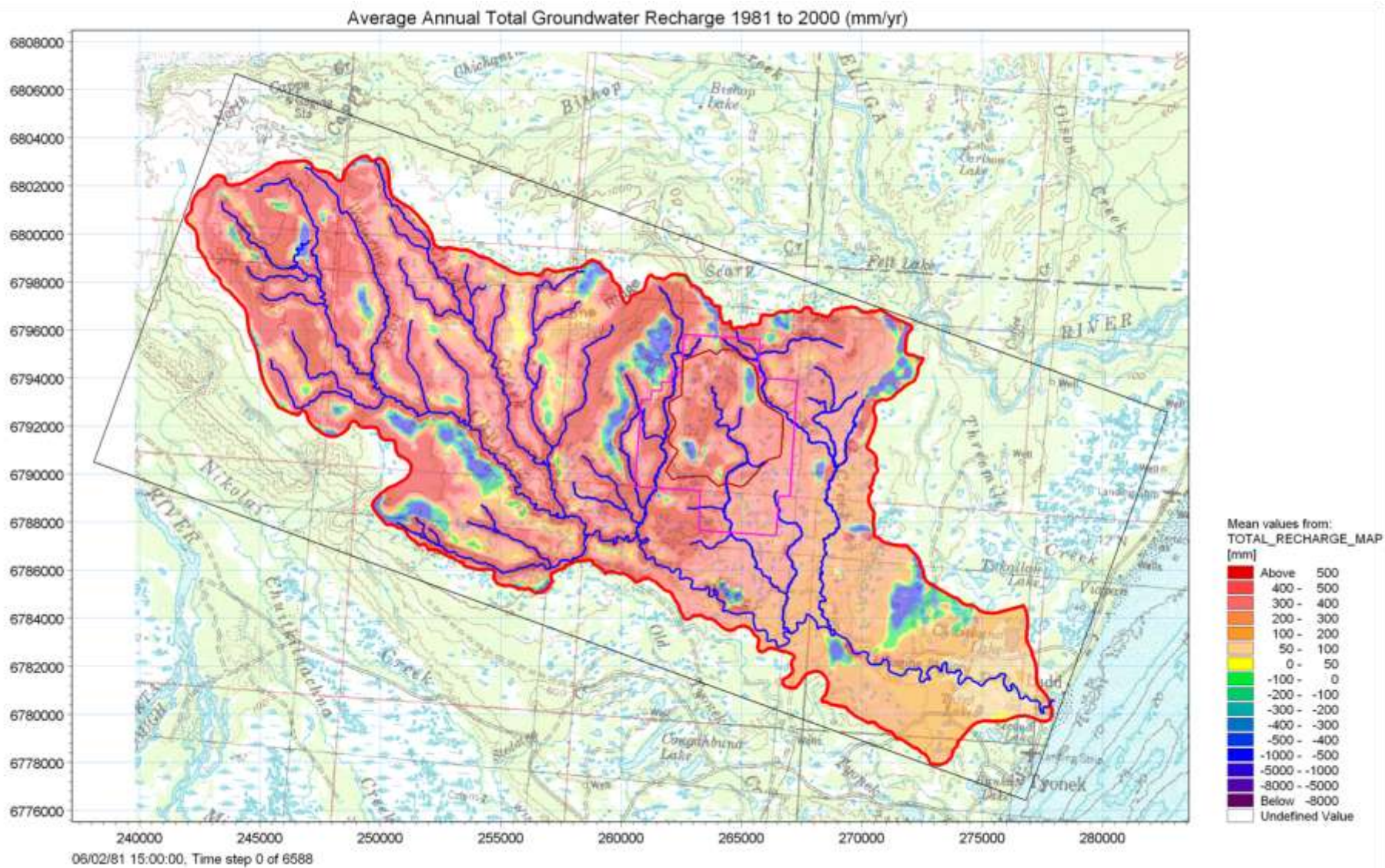


Figure C-4. Simulated Average of Annual Groundwater Recharge - 1980 to 2000 (mm/yr).

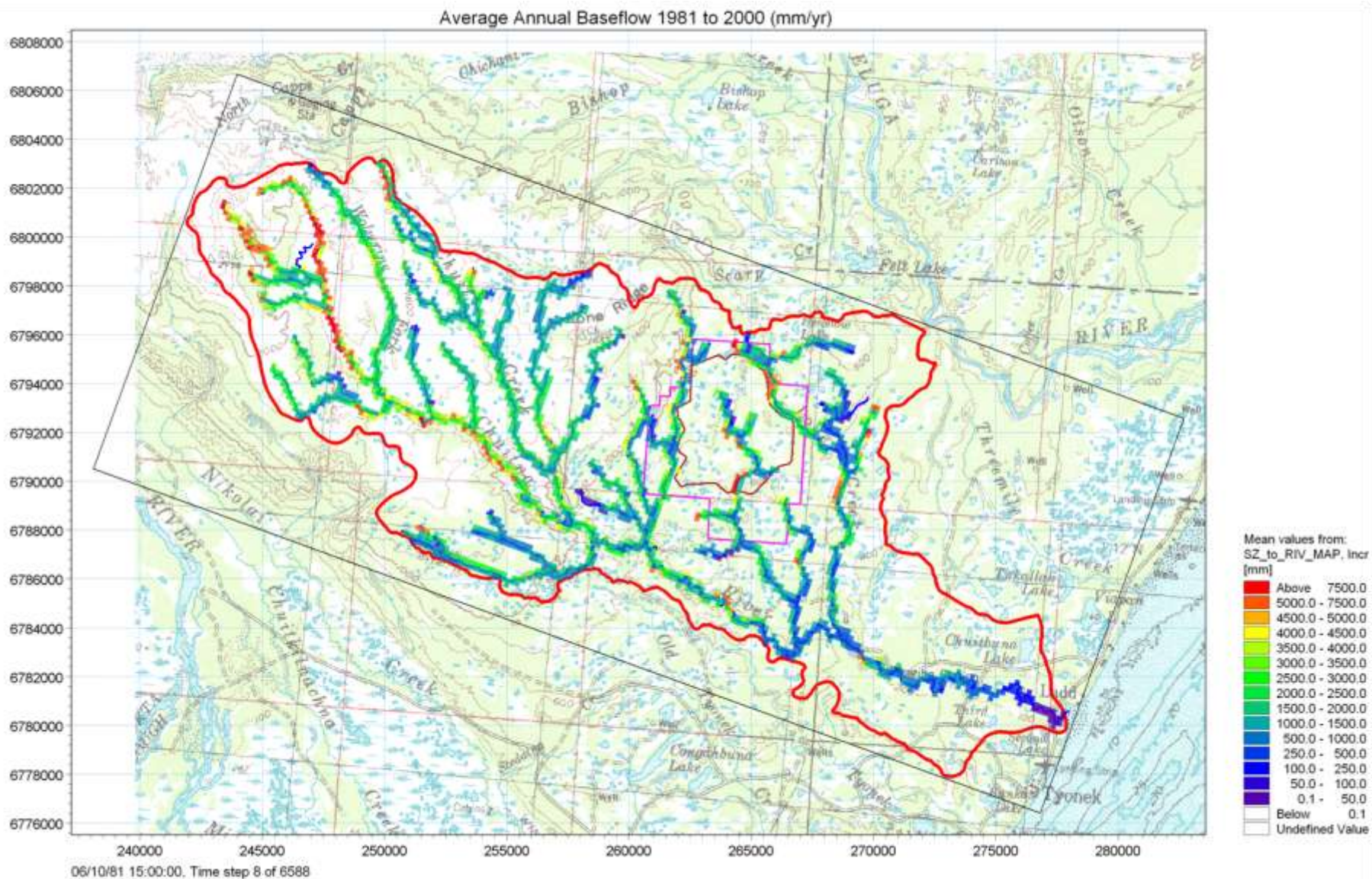


Figure C-5. Simulated Average of Annual Groundwater Baseflow (mm/yr) to Streams (1980 to 2000)

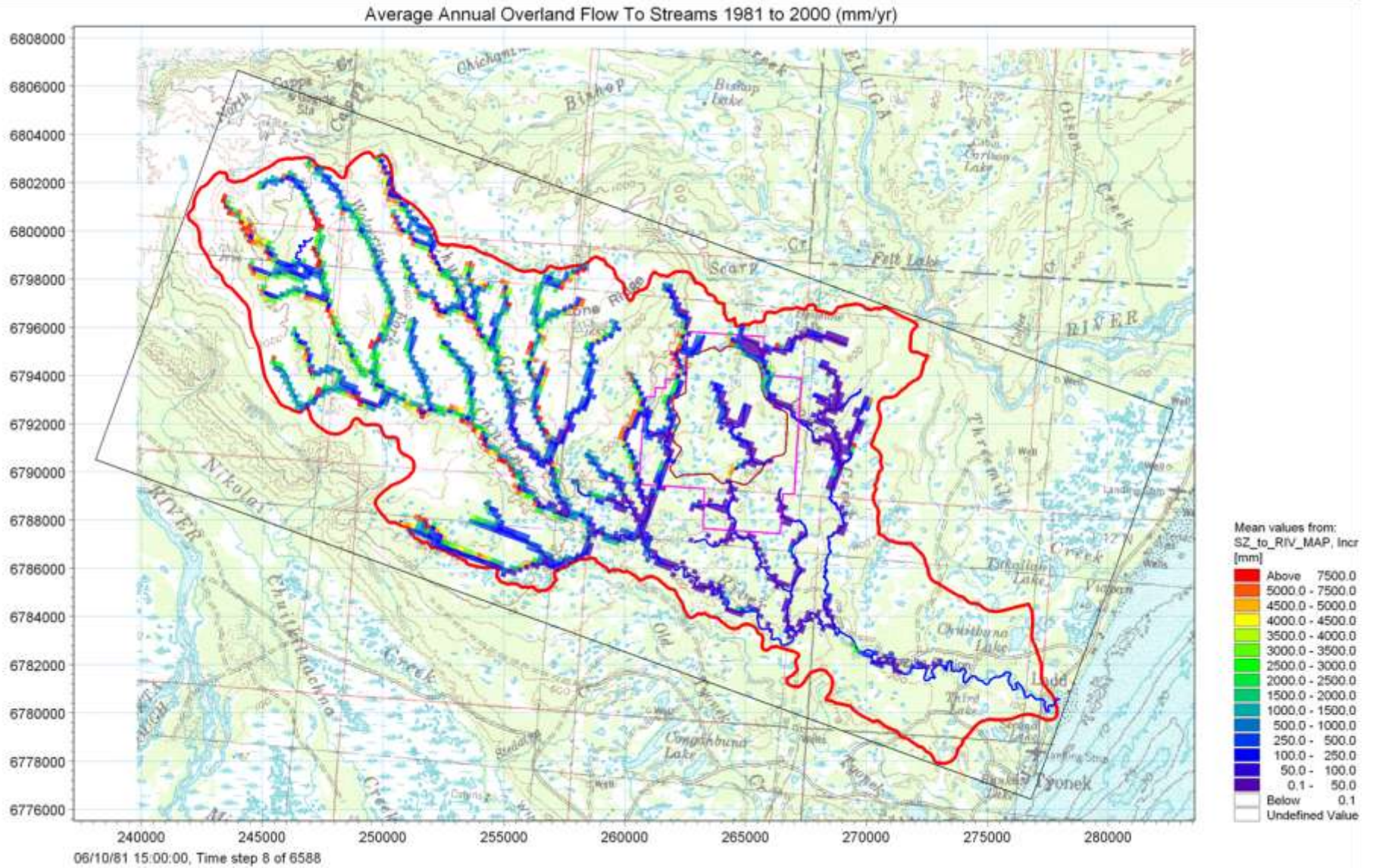


Figure C-6. Simulated Average of Annual Overland Flow (mm/yr) to Streams (1980 to 2000)

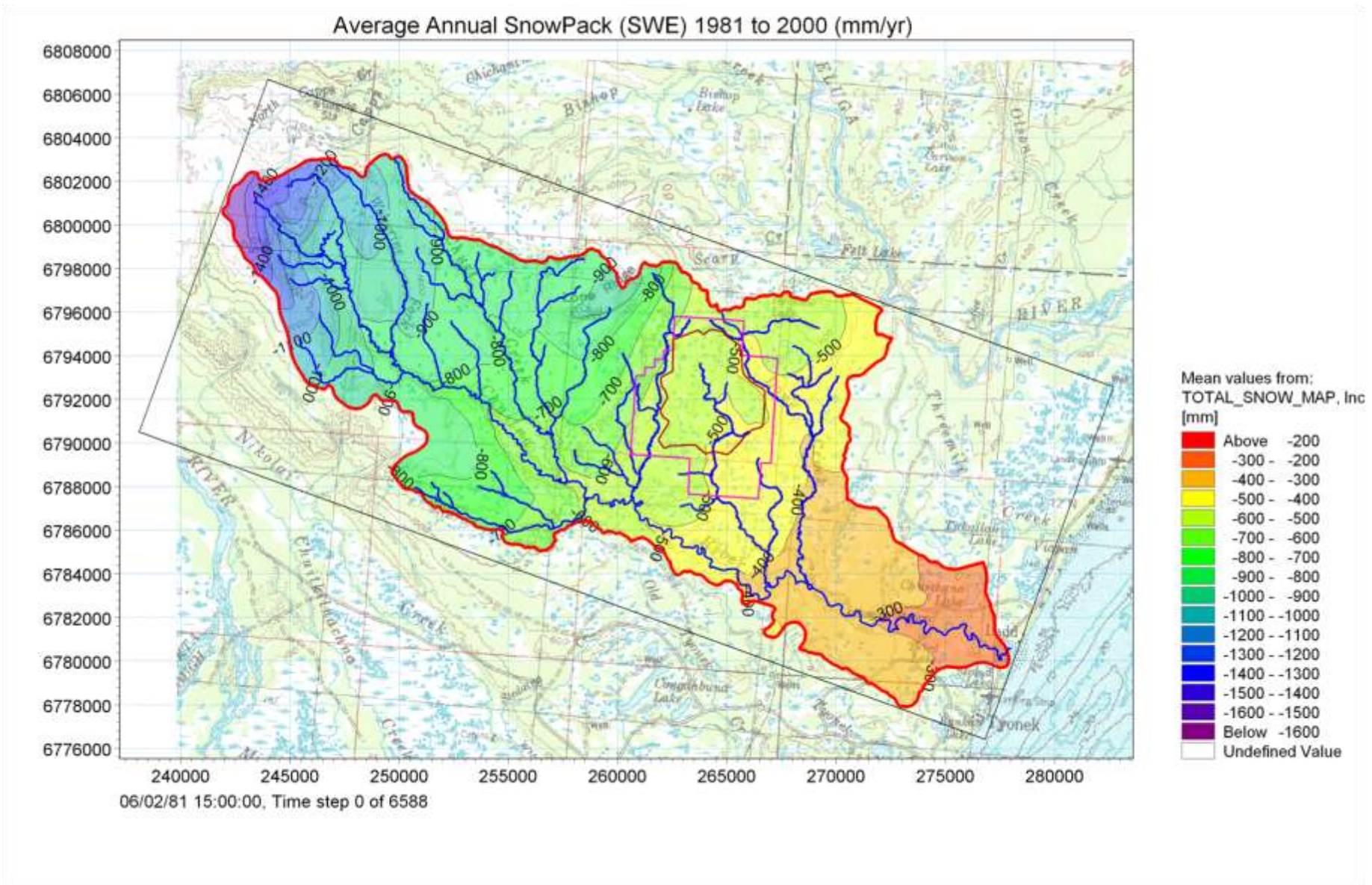


Figure C-7. **Simulated Average Annual Snowpack (mm/yr).** Negative values are sign convention in MIKE SHE.